Evaluating the use of SfM (Structure from Motion) as a tool for monitoring post-restoration fluvial dynamics

John Hart

MPhil Candidature

ESF
Llywodraeth Cymru
Welsh Government
Ewrop & Chymru: Buddsoddi yn eich dyfodol
Cronfa Gymdeithasol Ewrop
Europe & Wales: Investing in your future
European Social Fund

kess
Ysgoloriaethau Sgiliau Economi Gwybodaeth
Knowledge Economy Skills Scholarships

Acknowledgements

I would like to thank a number of people who have helped with this project. As my main supervisor throughout the project, Dr Richard Williams has helped immensely with the technical workflows presented and helped improve my GIS understanding through various components of this study. He has also led on the fieldwork element in all three UAV surveys and guided data collection from a morphological sense. I would also like to thank KESS who funded my MPhil scholarship which enabled me to carry out this study. Prof. Stephen Tooth has provided further guidance from a writing perspective by reading draft material and suggesting further edits to be made. WaterCo have also provided me with an introduction to hydraulic modelling, while the help of the WCRT (West Cumbria Rivers Trust) in giving information on the pre-restoration site and joining our fieldwork campaigns was of great benefit. Lastly, my family and my girlfriend have been invaluable in their support to me while writing and producing this thesis. I would like to thank all of these people from the bottom of my heart, I will be forever grateful to all of you. Thank you.

Abstract

River restoration has become increasingly important as drivers such as the Water Framework Directive (WFD) aim to promote a culture of "healthy" and balanced river systems. There is a need to monitor these schemes to learn from past mistakes and provide adequate knowledge transfer between all stakeholders. Identifying and promoting new and novel techniques which can aid this knowledge transfer and monitoring of restoration schemes over a variety of spatial and temporal scales is significant for future applications. A platform to collect imagery, Unmanned Aerial Vehicles (UAVs) and a technique to process them Structure from Motion (SfM) is evaluated to assess how the workflows presented can be used in a restoration monitoring capacity along the Whit Beck, Cumbria. Three UAV surveys (October 2014, March 2015 and July 2015) were carried out and initial results suggest that higher image overlaps and increased number of targets result in better quality Digital Elevation Models (DEMs). DEMs were built using the optimum conditions discussed, and bathymetric correction was carried out using a refraction correction technique on wetted areas. A DEM of difference (DoD) technique was used to map patterns of erosion and deposition using two SfM DEMs from two differing surveys, while hydraulic modelling of the DEM allowed geomorphic units to be mapped. SfM offers a low cost, high point density approach with comparable spatial-temporal dynamics to Terrestrial Laser Scanning (TLS) datasets. However, a number of limitations, most notably vegetation penetration and shallow bathymetry have been noted. The approach does however have great potential if these drawbacks can be improved and can also be used as a tool for communicating geomorphology to a wider audience.

List of Contents

Chapter 4: Parameter Analysis, TLS comparisons and Bathymetry

Chapter 5: DoDs and Hydraulic Modelling

Chapter 6: Discussion

Chapter 7: Conclusions and Future Perspectives

Appendices

List of Tables

List of Figures

List of Acronyms

aDcp - acoustic Doppler current profiler

ALS - Airborne LiDAR scanning

AOD - Above Ordinance Datum

CAA - Civil Aviation Authority

CEH - Centre for Ecology and Hydrology

CWA - Clean Water Act

DEM - Digital Elevation model

DoD - DEM of difference

DTM - Digital Terrain Model

GCD (toolbox) - Geomorphic Change Detection

GCP - Ground Control Point

LWD - Large Woody Debris

MAE - Mean Absolute Error

MBS - Multi beam solar

MLD - Minimum Level of Detection

MLS - Mobile Laser Scanning

OS - Ordinance Survey

PRR - Project Recovery Plan (New Zealand)

RMSE - Root Mean Squared Error

rtkGPS - real time kinetic Geographical positioning system

SBS - Single Beam solar

SfM - Structure from Motion

SIFT – Scale Invariant Feature Transform

STDEV - Standard Deviation

TLS - Terrestrial Laser Scanning

UAV - Unmanned Aerial Vehicle

WFD - Water Framework Directive

Chapter 1: Introduction and Context

1.1 Introduction

River restoration has emerged to incorporate a number of different activities which aim to improve and reinstate river processes and controls. It is becoming an increasingly popular term in the river management literature and a variety of techniques, applied over different spatial scales, are being utilized to achieve a number of potential benefits (Jahnig et al. 2011; Smith et al. 2014a). The relative success of efforts to manage and restore fluvial systems is dependent upon many variables, from local to international levels (Morandi et al. 2014). Many drivers of restoration can be identified and with the implementation of legislation such as the Water Framework Directive (WFD) in Europe and the Clean Water Act (CWA) in the United States, the importance of understanding how different rivers respond to restoration and learning from past mistakes is becoming increasingly important. The transfer of knowledge is seen as vital to drive a cycle of constant river restoration improvements. A holistic approach which encompasses many pockets of society (academia, environmental consultants, land owners, businesses) is required to maximise the potential of future restoration schemes by increased knowledge transfer, cooperation and collaboration (Smith et al. 2014a).

Implementing new methods for river monitoring and mapping can increase our knowledge about the processes controlling and determining the state of fluvial systems on both spatial and temporal scales. A platform to collect images (Unmanned Aerial Vehicles) and a technique to process images to produce topographic data (Structure from Motion) provide unique and novel ways to acquire knowledge that can be used to monitor post restoration morphodynamics. This knowledge can better our understanding of key fluvial characteristics which can in turn improve future river restoration efforts (Rinaldi et al. 2011; Smith et al. 2014a). The promotion

and use of new techniques within the geomorphic community (restoration practitioners) may allow better criteria for river management success to be designed (Morandi et al. 2014).

The main aim of this study is to examine and evaluate the use of UAVs, while collecting adequate data to be used in SfM workflows to monitor river system development. The monitoring of post-restoration morphology will be at the Whit Beck site (West Cumbria, UK). This section will firstly define the term river restoration, while acknowledge that the term can be applied and used in a variety of different fields and encompass varying techniques (Section 1.2). The need for valid monitoring procedures will then be discussed, while lastly the aims and objectives of this thesis will be presented (Section 1.5).

1.2 River Restoration Definition

River restoration is a term applied to many different techniques which aim to reinstate a river corridor towards its "natural" state (Beechie et al. 2010). The definition in itself is subjective and deterministic depending on individual variables and characteristics. Each restoration project is dependent on the specific objectives that relate to the particular environment under investigation. This provides a wide range of differing meanings that can be incorporated within the larger "restoration" notion. Although the idea of improving a river that has been degraded may seem relatively straightforward, it is vital to recognise that river restoration will signify different restoration strategies depending on the context it is being used within (Wilcock 2012). The term river restoration has become increasingly used throughout the last 40 years (Figure 1.1). The use of the term has increased since 1990 and the term is becoming increasingly used within the scientific community. The term is used and applied by academics, industries and the general public and thus the exact definition of the practice will differ accordingly depending on who and when it is used (Wilcock 2012). This is emphasised by the use of differing terms as indicated in Figure 1.1. The term may be used more widely within scientific literature;

however, this may not necessarily translate to more projects on the ground. The use of all the terms related to river restoration has increased rapidly since 1990, but different terms such as "river rehabilitation" and "stream enhancement" have also been used that all relate to river restoration notion as a whole. These terms have been used in differing scenarios under different environmental pressures and within and between different groups of people. Although the term "river restoration" is useful, it can be easy to ignore the fact that the definition is defined and dependable upon the individual variables which determine a project.

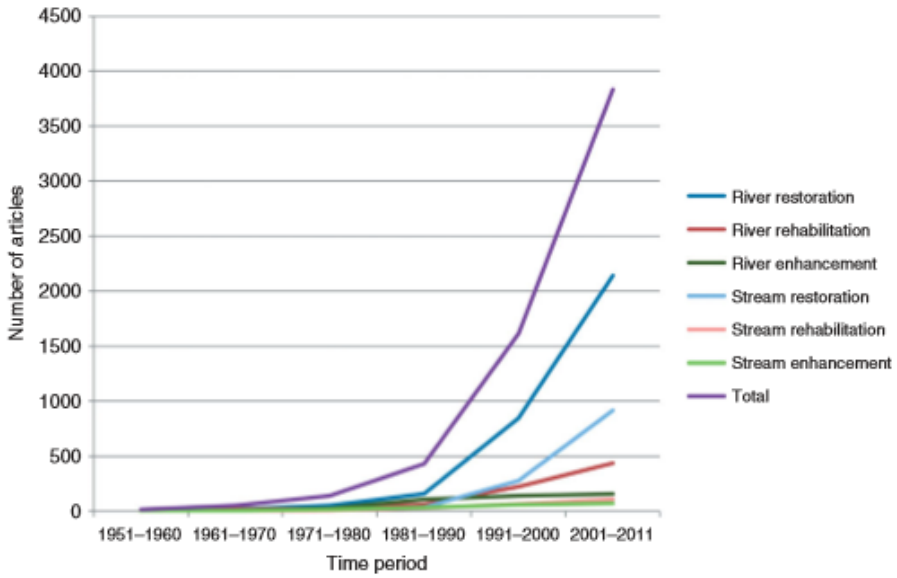

Figure 1.1: The use of terms within scientific literature. The figure highlights the increased use and links to river restoration work since 1990. It also emphasises the differing terms that can be used which relate to the broad concept of river restoration. Figure adapted from Smith et al. (2014b) using searches from Google Scholar.

Monitoring of river restoration schemes is not a new idea and small spatial studies were completed in the late 1970s and early 1980s. Leeks et al. (1988) present an example from the Afon Trannon in mid-Wales. They concluded that understanding lessons from past restoration measures was important in providing the basis for further development. This principle of learning from past schemes was established within these early papers and continues to be a key

idea which underpins development within the discipline. River restoration in the 1990s was seen as building upon a current state and improving the river habitat from a current point. Today, it has been recognised that rivers are complex and ever changing, meaning it is very difficult to suggest rivers are static (Cairns 1991; Dufour and Piegay 2009). Restoration efforts now aim to reinstall processes that promote a "healthy system" that is always adjusting and evolving (Dufour and Piegay 2009). This however in some cases is context specific, especially in constrained urban stretches (Chin and Gregory 2005). Although the term is discussed throughout this thesis in a coherent manner, an understanding of the range of differing meanings connected to the term must be incorporated and acknowledged into the wider fluvial geomorphological community (Morandi et al. 2014).

1.3 Importance of Monitoring

Figure 1.2 shows a range of techniques that can be applied to monitor river restoration (England et al. 2008). These methods will vary depending on the type of restoration that has taken place, the relative risk associated with the condition of the fluvial system, and the scale of the system or area under investigation. There is, however, uncertainty associated with the monitoring of restoration schemes. One key component of adequate monitoring is the need for valid and true baseline data which shows the river in an "unchanged" state (Smith et al. 2014a). If initial baseline data is poor or unreliable, it is difficult to attain the degree to which the fluvial system has altered, meaning it is difficult to establish a firm set of criteria which allows subsequent project appraisal. In other words, you cannot determine how effective the measures put in place were if you have a poor understanding of the initial baseline data (England et al. 2008). A holistic understanding that incorporates all spatial and temporal scales under investigation is required for a full appreciation of project achievement (Lave 2014).

Smith et al. (2014a) argues that the analysis and evaluation of current data from river restoration sites is of great importance in supporting future restoration schemes. Long term records of fluvial and ecological systems can give information about system resilience on local levels and knowledge from past schemes can be useful in the implementation of future schemes (Large et al. 2007). Monitoring has a big part to play in developing our knowledge of fluvial dynamics. The lessons learned from past restoration schemes can be used to help develop criteria for river restoration success. Continuous monitoring can provide baseline datasets which show how rivers have adjusted to a particular intervention and how they are likely to change in the future (Woolsey et al. 2007) (Smith et al. 2014a).

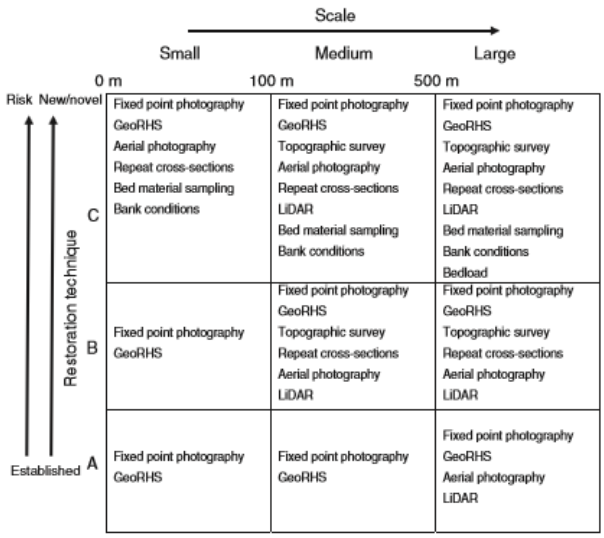

Figure 1.2: Different geomorphic technequies that can be applied to monitor river restoration schemes over varying spatial scales. Figure from England et al. (2008).

Understanding and evaluating the relative successes and weaknesses of past restoration efforts is critical to improve the design of contemporary restoration projects (Smith et al. 2014a). Since the morphology of restoration schemes determines the mosaic of habitats that are created, and strongly influences flow dynamics and flood water storage, gaining insight into morphological adjustment of restoration schemes is particularly important. There is thus a growing need to monitor the morphological evolution of restoration schemes to investigate their sensitivity to

adjustment. In particular, there is a need to evaluate methods that will enable repeat surveys of restoration schemes in an effective and affordable manner. There is also a requirement to critically evaluate how data from SfM surveys can be used as an input to more holistic assessment of river restoration.

Table 1.1 shows a comparison of techniques and their associated characteristics. SfM offers high resolution topographic data at relative ease and at lower cost when compared to other topographical techniques (Passalaqua et al. 2015). SfM has the advantage of being utilised over a relatively large spatial extent (0.1-100 km^2) in comparison with other techniques (ALS, MLS, TLS and rtkGPS). Although TLS and rtkGPS have smaller spatial extents, they offer more accurate data, especially when compared to MLS. SfM offers comparable accuracy to ALS and MLS surveys and higher point densities than ALS data. The downside to SfM appears to be the fact that it cannot penetrate vegetation which may reduce its applicability in certain environments. Similar to ALS and rtkGPS data, shallow bathymetry can be used with SfM data.

SfM data compares adequately when examined alongside other geomatics techniques. The spatial extent to which surveys can be undertaken and the relatively high point density (and associated accuracy) can be seen as advantages of the workflow. Nevertheless, the applicability of the technique for differing environmental settings and characteristics does need to be questioned. The applicability of SfM in a monitoring morphodynamics capacity will be assessed in this thesis. It is hoped that future studies will be able to use this knowledge in examining whether SfM can be utilised for other similar geomorphic enquires.

Table 1.1: A comparison of different geomatics techniques using data discussed in Passalaqua et al. (2015). *ALS (Airborne LiDAR); MLS (Mobile Laser Scanner); TLS (Terrestrial Laser Scanner); rtkGPS (real time kinematic GPS) and SfM (Structure from motion).

Method	Spatial extent (km^2)	Point density (pts/m^2)	Best accuracy (m)	Vegetation penetration	Shallow bathymetry
ALS	10 – 100s	1-30	0.05 – 0.2	Yes	Yes
MLS	1 - 100	100 - 10,000	0.05	Yes	no
TLS	0.1 - 10	1000 – 100,000	0.002-0.01	Yes	no
rtkGPS	0.1 - 10	1 -10	0.002-0.01	Yes	yes
SfM	0.1 - 100	1 – 1000	0.02-0.2	No	indirectly, yes

1.4 Aims and Objectives

The main aim of this research was to evaluate the use and applicability of UAV and SfM technology in a post-restoration river environment. This would be done by acquiring a dataset that will be used to quantify the morphological evolution of the Whit Beck restoration scheme in Cumbria.

The main objectives are as follows:

- To apply SfM techniques using imagery captured from a UAV
- To compare the outputs associated with the SfM with appropriate TLS data
- To calculate bed levels from the SfM data and produce bathymetrically corrected DEMs
- To use DoD techniques to map patterns of erosion and deposition
- To assess if SfM outputs can be used within hydraulic modelling framework
- To evaluate the techniques applied and evaluate the applicability of UAV and SfM technology to the monitoring of river restoration, and thus the potential for further use by the wider geomorphic community and socially as a tool for communicating geomorphology

1.5 Conclusion

This chapter has provided an introduction to river restoration. The use of the term and its different drivers have been discussed. The importance of monitoring has been acknowledged, while a quick comparison between SfM and other techniques has been completed. At this current time, SfM compares adequately with other geomatics techniques, but advantages and drawbacks are apparent. Among various objectives, an emphasis will be placed on evaluating the use of SfM.

Chapter 2: Literature Review

2.1 Introduction

This chapter provides an introduction to the SfM concept and then discusses the current use of the technique within the geomorphic community. Areas of limited knowledge are highlighted and further research in these fields are required to fully establish best practice guidelines.

2.2 What is Structure from Motion (SfM)?

SfM offers an alternative approach to acquiring survey points compared to other contemporary geomatics techniques such as TLS, ALS and Rtk-GPS. (James and Robson 2012; Fonstad et al. 2013). The potential for using SfM in the geosciences is particularly strong because it is relatively low cost and software provides an automated processing workflow. The basic principle of SfM is aligned to photogrammetry studies; a number of overlapping digital images are taken which are then processed to develop a DEM of the area under investigation (Westoby et al. 2012). Although the technique is relatively new from a geomorphic perspective, it has been used in computer science and other disciplines for longer (Snavely et al. 2008). Many geomorphological disciplines (including fluvial geomorphology) have already used this technique to varying degrees of success and they are discussed in depth in Section 2.2.

SfM reconstructs topography by "matching" reference points in a conjugate manner from images which are taken from different locations and from differing angles (Snavely et al. 2008). SfM is based around image correlating algorithms which were first developed by Lucas and Kanade (1981). These algorithms are critical to the success of the SfM process (Woodget et al. 2014). Knowledge of camera positions is not needed and thus imagery from a variety of differing scales, angles and contexts can be used to accurately map areas of interest (Rosnell

and Honkavaara 2012). GPS positioning can also accelerate the process of image matching (Snavely et al. 2006; Snavely et al. 2008).

The use of SfM to collect appropriate data, to infer different river processes could allow the complex geometry of rivers systems to be monitored and assessed further. This helps promote more sophisticated technologies within river science as new techniques offer the opportunity for accurate topographical datasets to be developed. These techniques offer the opportunity to survey systems at regular intervals in order to quantify their dynamism. Appropriate timing of repeat surveys can then be used to quantify temporal and spatial variation in morphological change, and to infer process (Vericat et al. 2014; Woodget et al. 2014). UAV image acquisition allows regular data acquisition which can help map and locate differing river processes. This variation within river systems, particularly at "hyperspatial" resolutions needs to be investigated and analysed in detail, to ensure fluvial geomorphology and other topographic relations are developed and defined accordingly (Woodget et al. 2014). Additionally, understanding and quantifying the topography of submerged regions in fluvial systems has been difficult as adequate techniques have not been available to accurately "map" these regions. SfM offers the potential that submerged areas, where water is clear and the bed can be seen on imagery, can be reconstructed in DEMs, as refraction correction techniques allow spatial errors to be reduced (Woodget et al. 2014). There is still, however, a large amount of uncertainty associated with this and more research is needed in order to establish the controls of error formation in relation to the overall SfM process (James and Robson 2012). Other errors such as inadequate referencing make finding the cause of errors difficult, particularly in computer software packages, such as Agisoft Photoscan (Vericat et al. 2009; Fonstad et al. 2013). The absence of a formulated technique that removes non-linear deformations in the built DEM has been highlighted and is seen as a current drawback (Fonstad et al. 2013).

2.3 SfM in the Geosciences

Although the technique has now been accepted into the wider geomorphological framework in relation to image capturing and DEM generation (Smith and Vericat 2015), the process of SfM gaining validity and attention from the geomorphic community has been gradual when compared with computer science investigations (Snavely et al. 2008; Woodget et al. 2014). The first published paper that used SfM within geomorphology was James and Robson (2012) who investigated three distinctly different geomorphic scales. A coastal cliff, a volcanic crater and geological sample were all examined, ensuring study of a large range of spatial areas (of between 0.1 and 1600 m in length) (James and Robson 2012). The errors for the three distinct areas can be seen in Table 2.1. Errors ranged between 110 um and 1.0 m between the geological sample and volcanic crater suggesting the spatial extent under investigation greatly influences the effectiveness of the technique. Table 2.1 shows some of the key information from this study and shows a range of different factors which could have been responsible for influencing SfM outputs reported. Factors such as the number of images, data collection technique and flying altitude can all be seen to influence the data produced during the SfM process (Woodget et al. 2014). More recent studies have tried to gain more insight into the "optimum" conditions required for best quality SfM datasets and thus DEM and DTM production. Table 2.1 shows a range of recent SfM studies. Woodget et al. (2014) were one of the first studies to use SfM, specifically in a fluvial topographic manner. Images were collected using a DragonFlyer X6 quadcopter and a Lumix 10.1-megapixel camera, while DEMs were generated using AgiSoft PhotoScan software (similar to the software used in this study). The main conclusions from this study were that submerged areas were associated with greater errors, mainly due to refraction issues associated with the air-water interface.

Table 2.1: A summary of past geomorphic SfM studies.

Reference	UAV	Camera	Camera resolution	Flying Height (m) (If applicable)	Focal length (mm)	Image overlap estimate (%)	Study	Error Analysis (m)	Processing Software	Comments
Woodget et al. (2014)	Dragonflyer X6 Quadcopter	Panasonic Lumix DMC-LX3	10.1-megapixel camera.	25-30	5	80	River Arrow and Coledale Beck (UK)	Mean error / m: May 2013; June 2013; August 2013; July 2013 (Coledale Beck) Exposed areas: 0.005; 0.004; 0.044; 0.111 Submerged areas: 0.089; 0.053; 0.064; 0.016 Submerged (refraction correction technique): 0.053; 0.008; 0.023; 0.029	Photoscan, DEM validation based on Orthophoto construction.	Ground control targets used. Images were selected based on image quality. Agisoft Photoscan software was used.
Fonstad et al. (2013)	Helium-filled blimp (Allsopp Skyshot Helikite) GeoXH GPS unit for reference points, LiDAR data using Optech 2050 system	A480 Canon Compact camera	10.0-megapixel camera.	Average 40 (between 70-10)	10		Pedernales Falls State Park, Texas (USA)	Average axis SfM – GPS errors X: 0.03; Y: 0.05; Z: 0.07 SfM –LiDAR errors: Average individual distance between SfM and LiDAR points – 0.27 Mean difference – 0.60 Regression analysis showed 97% variance explanation. A 1:1 ratio/100% would suggest all points matched.		304 photographs were used. A comparison of techniques was incorporated into this study. SfM, LIDAR and GPS were all utilized. More images required. Issues associated with: • How many ground points needed? • Angle/height of flight • Procedure • Texture practicality

										• Practicality in differing environments
Tamminga et al. (2014)	Aeryon Scout Quadcopter	Photo 3S camera		100	8.4	80	Elbow River, Alberta (Canada)	Mean errors: Exposed areas – 0.08 m Submerged areas – 0.11 m	EnsoMOSAIC	45 ground control points used, 297 geo referenced check points incorporated into study. Eight flight lines used to construct DEM. Submerged DEM correction took place.
Javernick et al. (2014)	Robinson R22 helicopter Trimble R8 GNSS system (GPS)	Canon camera.	10.1-megapixel camera	600 and 800	28 (18-55)	60-70	Ahuriri River (New Zealand)	Mean error under different environmental characteristics Planar: 0.04 Elevation: 0.10 Non-vegetated: 0.10	AgiSoft PhotoScan	95 ground control points used over a 100 m grid.
James and Robson (2012)	Micro-light (tourist) aircraft	Canon E0S D60 camera			20			Mean error Geological sample: 0.000110 Coastal cliff: 0.036 Volcanic crater: 0.1	VMS (Vision Measurement Software)	133 images
Lucieer et al. (2013)	OktoKopter	Canon 550D DSCR camera		40	18	80-90	Home Hill Landslide, Tasmania (Australia)	Mean error / RMSE Horizontal accuracy: 0.061 / 0.074 Vertical accuracy: 0.006 / 0.062	Agisoft Photoscan	39 GCPs used
Smith and Vericat (2015)	Ground based imagery; Hexacopter	Panasonic DMC-TZ65	Both 10 megapixel cameras.	Substantial range (47 m for 2013	4 and 5	Significant	Upper River Cinca, Ebro Basin (Spain)	Total station (TS) validation of SfM mean errors (m)	AgiSoft Photoscan	Validation with TS and TLS datasets

<table>
<tr>
<td></td>
<td>DJU F550 and gyrocopter</td>
<td>and Ricoh CX5</td>
<td></td>
<td>dataset and targeted altitude flights in 2014)</td>
<td></td>
<td></td>
<td></td>
<td>
<table>
<tr><td>Plot scale</td><td>0.008</td><td>-0.002</td><td>0.004</td><td>-0.003</td></tr>
<tr><td>Small catchment scale</td><td>-0.003</td><td>0.027</td><td>0.018</td><td>- 0.020</td></tr>
<tr><td>Landscape scale</td><td>0.012</td><td>-0.014</td><td></td><td></td></tr>
<tr><td colspan="5">Terrestrial Laser Scanner (TLS) validation of SfM mean errors (m)</td></tr>
<tr><td>Plot scale</td><td>0.006</td><td>0.000</td><td>0.003</td><td>0.000</td></tr>
<tr><td>Small catchment scale</td><td>0.023</td><td>0.022</td><td>-0.048</td><td>-0.133</td></tr>
</table>
</td>
<td></td>
<td>Errors smaller at the plot scale.
SfM favours quickly changing environments

Likely to be of significant importance in the future, specifically landscape scale DEMs.</td>
</tr>
<tr>
<td>Westoby et al. (2012)</td>
<td>Ground based imagery</td>
<td></td>
<td></td>
<td></td>
<td>10</td>
<td>80</td>
<td>Three distinct geomorphic environments: Constitution Hill, Aberystwyth (UK); Dig Tsho moraine complex, Khumbu Himal (Nepal) and Cwm Cau, Snowdonia (UK)</td>
<td>
<table>
<tr><td colspan="4">Transformation residuals (m)</td></tr>
<tr><td></td><td>X</td><td>Y</td><td>Z</td></tr>
<tr><td>Constitution Hill</td><td>0.196
0.076
0.016</td><td>0.156
0.064
0.072</td><td>0.020
0.035
0.005</td></tr>
<tr><td>Dig Tsho</td><td>1.002
0.630
1.015</td><td>1.158
0.694
0.482</td><td>2.917
3.241
4.653</td></tr>
<tr><td>Cwm Cau</td><td>0.538
1.411</td><td>0.117
0.205</td><td>0.164
0.679</td></tr>
</table>
</td>
<td></td>
<td>Good analysis of limitations</td>
</tr>
<tr>
<td>Piermattei et al. (2015)</td>
<td>Ground based imagery</td>
<td>Nikon D5100 and Canon 5D Mark III, for October and September surveys respectably.</td>
<td>16 and 22</td>
<td></td>
<td>15 and 28</td>
<td></td>
<td>Montasio Occidentale Glacier (Italy)</td>
<td>
<table>
<tr><td></td><td>October 2012</td><td>September 2013</td></tr>
<tr><td>Mean X</td><td>0.531</td><td>0.516</td></tr>
<tr><td>Mean Y</td><td>0.441</td><td>0.403</td></tr>
<tr><td>Mean Z</td><td>0.271</td><td>0.351</td></tr>
<tr><td>Mean total</td><td>0.742</td><td>0.743</td></tr>
</table>
</td>
<td>Agisoft Photoscan</td>
<td>Two surveys completed in October 2012 and September 2013.

35 images for the October 2012 survey. 347 images for the September 2013 survey.</td>
</tr>
</table>

This error was also proportional to depth, with deeper areas associated with a larger degree of error. Tamminga et al. (2014) also found that submerged areas were more vulnerable to larger errors with exposed and submerged parts having errors of 0.08 and 0.11 m respectively. Despite this, local characteristics such as tree cover and shade were also seen to be important and a large amount of variation was seen between differing areas in both of the study areas investigated, specifically in wetter areas (Woodget et al. 2014; Tamminga et al. 2014). Tree cover makes the image matching process more difficult as it is harder to pair corresponding coherent reference points together. Shade and glare are also issues as they make the validation of true elevations within image processing software harder (Snavely et al. 2008). As shown in Table 2.1, when a refraction correction technique is applied to submerged areas, errors do seem to decease substantially. Despite this, many submerged areas had elevations that were over predicted and the refraction technique was found to be inferior in shallower streams (>0.2 m) (Woodget et al. 2014). This may have implications when investigating the Whit Beck scheme as the Coledale Beck in Cumbria shares a similar geomorphic and hydrological background to the area under investigation.

Table 2.2: Data collection values from James and Robson (2012).

	Geological sample	Coastal cliff	Volcanic crater
Sample size / m	0.1	50	1600
Equipment cost in US dollars	1000-10,000		
Data collection time	20 mins	10 mins	2 x 30 min flights
Number of images	92	143	89

James and Robson (2012) investigated the applicability of SfM to differing spatial scales (Table 2.2). Woodget et al. (2014) also found that variables such as flying height (which correlates closely with image resolution) and image overlap are integral in the production of valid and

reliable DEMs. Figure 2.1 shows a diagram which illustrates the connections between differing variables in this process. The importance of acceptable point clouds is also vital and errors with the construction of these were also found to be an issue in AgiSoft Photoscan. The "black-box" characteristic of Photoscan is also unhelpful as it is virtually impossible to isolate individual sources of error (Woodget et al. 2014). Other errors such as "dome like deformation" have also been attributable to image viewing angle and flying altitude (James and Robson 2014). James and Robson (2014) provide a comprehensive analysis of the effect camera calibration has on error propagation. The use of camera calibration within software such as Agisoft Photoscan can lead to dome-like deformation occurring if only downward-looking images are acquired during an aerial survey, promoting associated error increases. They provide a list to minimise the effect of dome-like deformation, including when best to use camera calibration adjustments, and they examine why understanding the relationship between deformation and radical distortion is of major importance in promoting best possible use to eliminate this type of error (James and Robson 2014). More work is required to understand these differing variables and the deterministic effects they have on one another, and an appreciation of the needs of the investigation is also required to fully understand and develop the techniques needed in order to attain appropriate data. There are a lot of unknowns associated with this technique and Woodget et al. (2014) suggest that improving knowledge relating to unknown values and variables (such as slope) will help develop our understanding of SfM.

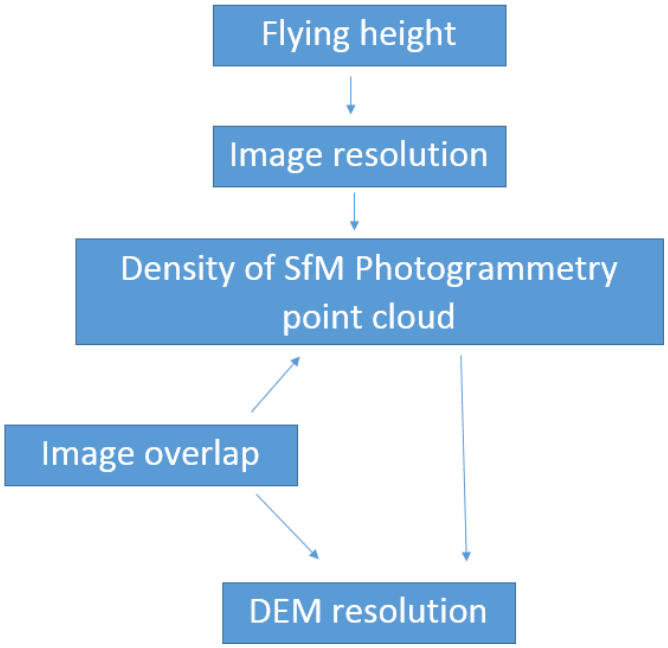

Figure 2.1: The importance of flying height and image overlap in final DEM generation. Figure adapted from Woodget et al. (2014).

Fonstad et al. (2013) found that compared to LiDAR, the SfM technique provided results with a similar accuracy and precision, while acknowledging SfM was easier to use. Table 2.3 shows the associated error of both SfM and LiDAR techniques in the X, Y and Z axes. SfM had lower errors associated with the X and Z coordinates, while LiDAR was more reliable within the Y axis. There is a large difference observed along the Z axis where errors for the LiDAR technique were seven times that of proportional errors using the SfM technique (Fonstad et al. 2013). Similar to other studies, they also found that there were significant uncertainties associated with the technique (Table 2.1). Smaller spatial areas were also found to be more favourable for DEM generation. This was associated with low image texture resulting in the formation of inappropriate point clouds, specifically in deeper areas of the channel. Fonstad et al. (2013) concluded that the validity of DEMs produced under these conditions needs to be questioned and analysed further. A drawback of the SfM technique is the absence of a procedure to correct non-linear deformations (Fonstad et al. 2013; Woodget et al. 2014; Vericat et al. 2014).

Table 2.3: The associated errors between SfM and LiDAR in the X, Y and Z axes (Fonstad et al. 2013).

Error axis	SfM error (m)	LiDAR error (m)
X	-0.03	-0.04
Y	0.05	-0.03
Z	0.07	0.51

Further analysis has taken place which investigates the controls of an effective Ground Control Point (GCP) network. There are many questions about how the characteristics of a GCP network influence the type of data generated, and thus the subsequent DEM produced. Uncertainty surrounding the number, density, orientation and style of targets have all been highlighted and further work is required to understand the deterministic influences of varying variables (Javernick et al. 2014). The overriding opinion at this current time suggests that the effectiveness of the GCP network is dependent on firstly establishing the true needs and characteristics of the investigation. This will vary over differing spatial and temporal scales and will undoubtedly be different depending on local characteristics associated with specific study locations. Research however suggests a higher density of GCPs has been correlated with higher resolution point clouds, leading to more sophisticated DEM production. Further studies have suggested that GCP errors are increased in periphery regions of images where overlap is reduced (Lucieer et al. 2013).

Table 2.4: The main advantages and disadvantages of SfM.

Advantages	Disadvantages
Provides high resolution and accurate DEM's that are comparable to similar methods e.g. LiDAR	Issues with submerged areas and refraction
Little training needed (practical or computational)	Lot of unknowns and uncertainties that need to be investigated.
Low cost	Correction methods needed for submerged regions in some cases
Relatively easy to use software e.g. Photoscan	Applicability – spatial and temporal
High vertical accuracy, good efficiency and operational flexibility (see Tamminga et al. 2014)	Applicability to different environmental settings

The main advantages and disadvantages of SfM are summarised in Table 2.4. The most critical and significant factor is that the technique offers high resolution DEM generation that can be used in a range of applications (Gomez-Gutierrez et al. 2014; Piermattei et al. 2015). A good example that highlights the effectiveness of the SfM workflows is presented by Westoby et al. (2012). SfM also offers a low cost approach, and little experience in using the methods is required (Hugenholtz et al. 2013). Despite this, there are also negatives associated with SfM. As discussed above, errors are exacerbated in submerged areas due to refraction errors. These errors can be reduced significantly with the use of correction techniques; but, there are still uncertainties associated with the scale and frequency of such faults. Also, high turbidity may obscure a channel bed entirely resulting in a supplementary survey being required. Many variables need to be investigated further as their relative importance in some cases has still not been identified. As examples, vegetation influences and turbidity of water can be highlighted as factors which are still associated with large amounts of uncertainty (Tamminga et al. 2014).

A range of studies have concluded that the SfM technique can have great benefit for mapping fluvial processes and forms. A variety of spatial scales can be assessed and with the appropriate correction techniques, errors can be minimised accordingly. Issues surrounding submerged topography and periphery areas have been discussed, while the importance of variables such

as flying height and image overlap can be vital in producing reliable point clouds, which can then be processed into acceptable and valid DEMs. Existing approaches such as LiDAR and TLS do not always allow variability over a range of differing spatial scales to be acknowledged (Woodget et al. 2014). SfM allows a new and dynamic approach to mapping topography to be utilized, but the unknowns and uncertainties associated with the technique need to be analysed and incorporated into future studies.

More recent investigations have attempted to assess how different spatial scales will influence DEM quality. Smith and Vericat (2015) examined the use of SfM under three distinct scales (plot scale, small catchment scale, and landscape scale) and their results can be seen in Table 2.1 and Figure 2.2. Figure 2.2 highlights the very small errors associated with the plot scale DEMs which suggest the use of SfM is very applicable to monitor small-scale topographical change. Errors substantially increase when a catchment or landscape scale are examined. Small spatial areas (of around 0.1 m^2) can be associated with lower mean error values, while larger spatial scales (such as small catchment and landscape scales) can be seen to have larger average errors associated with both validation using TS (Total station) and TLS (Terrestrial Laser Scanner). This suggests that smaller spatial scales are more appropriate for the use of SfM. Smith and Vericat (2015) conclude that SfM validation shows a reduction in error values at lower spatial extents. Furthermore, it is suggested that SfM should be principally used in environments with a large degree of change, such as fluvial systems or soil monitoring (as was the focus of their paper). This assertion would seem to be supported by error results from Piermattei et al. (2015) who used SfM to monitor the Montasio Occidentale Glacier (Italy) in October 2012 and September 2013. Mean errors for this study across all axes seem to be substantially higher than errors reported by Smith and Vericat (2015). This may be because a large spatial area was investigated. Furthermore, the rate at which glacial processes occur can be of a longer timeframe than that of soil moisture or fluvial processes. This would suggest the

use of SfM for glacial topographic relations may be less effective, than for studies on smaller spatial scales. The smallest error reported by Piermattei et al. (2015) was 0.271 m (mean error in z axis October 2012); this is considerably larger than any results from Smith and Vericat (2015). Therefore, an appreciation of spatial scale is suggested to be of major importance in providing an adequate methodology to promote best quality DEM generation through SfM. Determining the "optimum" spatial scale for SfM is likely to be challenging as it will be different for differing geomorphic environments. The frequency and magnitude of geomorphic processes occurring will ultimately influence the temporal period to which surveys are collected, but it is important to accept that this is likely in itself to influence SfM outputs. More investigations to determine the most effective spatial and temporal extents, under contrasting geomorphic environments are required in the future.

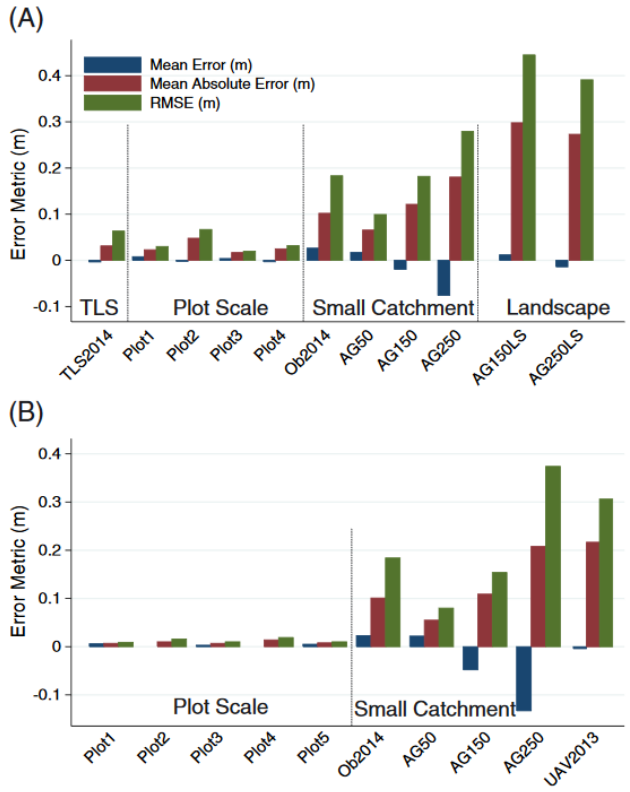

Figure 2.2: The mean error, mean absolute error and root mean squared error (all in m) for different spatial scales as reported by Smith and Vericat (2015). Figure A relates to the validation by TS (Total station); while Figure B relates to validation of SfM with TLS (Terrestrial Laser Scanner) datasets. Figure from Smith and Vericat (2015).

2.4 Clarifying the Unknowns

The above review shows that the amount of literature on SfM has increased considerably within the last 4-5 years and principal research now aims to find the "optimum" workflows for particular survey requirements. The precision and accuracy of DEM outputs is heavily reliable upon the data being input into the image processing software and determining the most effective way of using UAVs and SfM together remains of key importance in developing the technology. There is a need for more research on the mechanisms which promote a reduction in errors (horizontal and vertical) by exploring and explaining what control differing variables (such as image overlap) has to the specific building of orthophotos and DEMs. Errors have been seen to change substantially when different spatial extents are investigated (see Smith and Vericat 2015 for a recent review) and more investigations are required to fully examine this issue. This study hopes to assess how suitable SfM can be when mapping topographic change from a river restoration and river dynamics perspective and thus hopes to add some information which will determine how suitable the workflow can be for other similar projects. This will be achieved by exploring the variables outlined above. Determining the effectiveness of SfM remains of major importance from a geomorphology perspective as if accurate and reliable DEMs of similar errors to TLS and LiDAR can be achieved, a new and novel methodology for topographic mapping and modelling can gain further interest from a range of different scientific communities. Questions remain over the extent of spatial coverage using SfM, with a lack of comparable results to that of TLS or LiDAR over larger spatial scales apparent (sub-catchment, landscape level).

2.5 Conclusion

To summarise, SfM has been used in many different geomorphic investigations over a variety of different spatial and temporal scales. There are a number of advantages and disadvantages to the process, but ensuring a valid and high quality DEM is crucial in further data processing techniques. Improvements can be made by firstly establishing the unknowns associated with new approaches and secondly, targeting studies and investigations within the highlighted issues (to determine best suitability for practice).

A number of uncertainties about the SfM technique have been highlighted, including the importance and effect of different variables. Image overlap, oblique imagery, number of targets, spacing of these targets and flying altitude can all be shown to affect SfM outputs. More information is required to determine the best possible criteria required for suitable outputs (DEM/orthophoto generation). The methodology used in this study hopes to gain valuable knowledge about how certain variables influence the quality of the SfM product. In a broader sense, this investigation hopes to contribute results which help to determine the environmental settings to which SfM can be used most effectively by assessing its applicability from a river restoration and fluvial geomorphology perspective. The methodology outlined in the next chapter aims to gather more knowledge about the key variables influencing the quality of SfM outputs and questions whether results can be compared to comparable TLS outputs on a sub-catchment scale.

Chapter 3: Study Site and Methodology

3.1 Introduction

The study site for this project was the Whit Beck restoration scheme in the Derwent catchment, West Cumbria. The aim of this restoration scheme was to increase biological productivity within a section of river that had poor ecological status and thus failed to meet the requirements of the WFD. This scheme was completed in August 2014. The original channel was straight and thus re-meandering of the river aimed to increase habitat diversity by increasing the length by a factor of 4 to approximately 1200 m (Environment Agency, West Cumbria Rivers Trust 2016). Prior to restoration, the old Whit Beck channel was failing the WFD ecological requirements and the creation of pool riffle sequences was aimed at increasing biological productivity within the stretch of river.

3.1.1 Regional Landscape Setting – Cumbria

Figure 3.1 shows a geological map of the same area using OneGeology mapping software. Figure 3.2 highlights the location of Figure 3.1 within the UK. The geological characteristics of Cumbria are very variable with differing bedrock types and structures present throughout the county. Areas of northern Cumbria and the far west coast are compromised predominantly of Triassic bedrock (Figure 3.1). The central area of Cumbria can be separated into 4 distinct geological units. The northern central area is made up of Middle Jurassic bedrock (Light blue); this encompasses towns such as Keswick and Cockermouth (Figure 3.2). Areas of Meso-Variscan bedrock can also be located in "pockets" around the central area of Cumbria. The largest area of Meso-Variscan bedrock is situated around 3-4 km inland. The large majority of central Cumbria has a bedrock group classed as "Volcanism other than Cenozoic". This stretches southwards until Ambleside and eastwards towards the M6 motorway (Figure 3.1). Most geological bedrock south of Ambleside consists of Cretaceous and Cenozoic bedrock. This encompasses Windermere and continues southwards towards Kendal. The majority of the north west of England consists of Cretaceous and Cenozoic bedrock, apart from areas of the western coast where Triassic bedrock can be seen, specifically around Liverpool reaching north as far as Fleetwood. See McMillian (2002) for a good overview of the Quaternary processes which shaped the Cumbrian landscape.

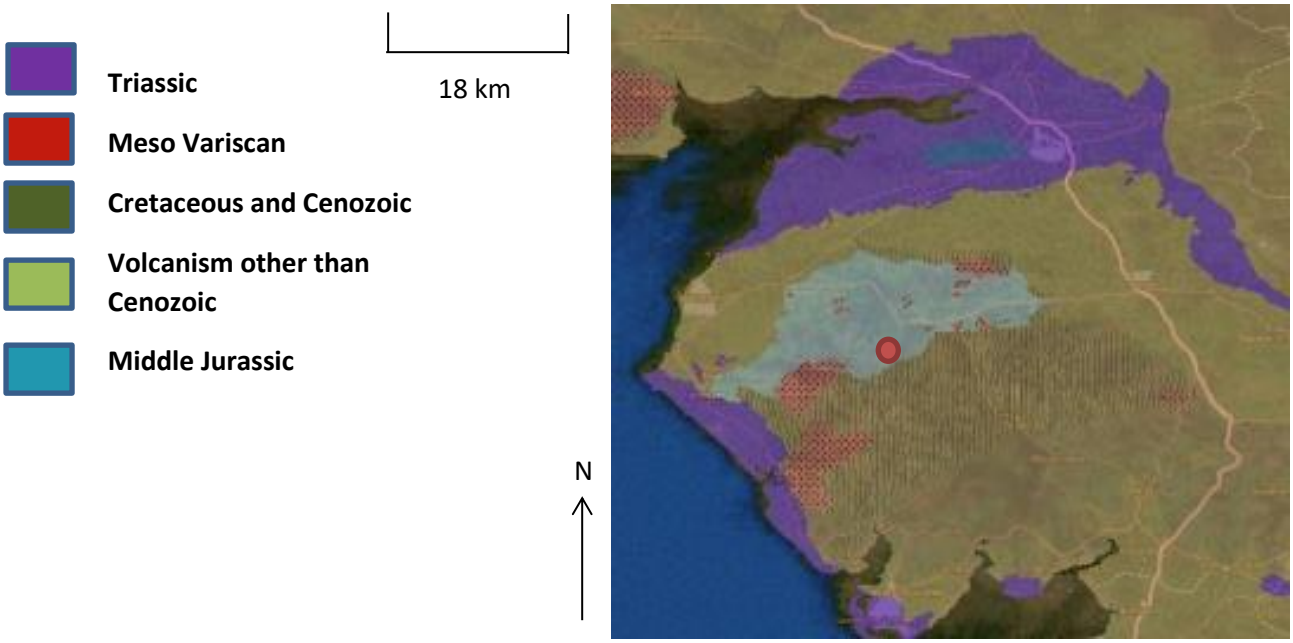

Figure 3.1: A geological map of Cumbria. Data used was adapted from OneGeology (2016) using 1GE BGS 1M Surface Geologic Unit and Europe GISEurope 1: 1.5M Bedrock age. The orange line represents the M6 motorway, while the red dot shows the location of the Whit Beck site.

Figure 3.2: A OS Map of Northern England with Cumbria shown in the green box and the study site shown with the red dot. Data from Digimap (2016) ©.

Figure 3.3a shows average rainfall (precipitation) data per month for Cumbria over the last 20 years. Rainfall is highest in October with an average value of 109 mm. Winter months (December, January, and February) generally have higher than average rainfall with values ranging from 93 to 105 mm. Average rainfall values generally decrease as you move from the winter months into summer. Figure 3.3b also shows the number of average rainfall days associated with Cumbria. This shows a similar general trend to the values discussed for average rainfall. January, October and November have the highest average number of wet days with a value of 22. The months of February, March and December all have higher than average values (around 21 days).

Frontal rainfall accounts for the majority of precipitation within Cumbria, especially during the winter months (Neal and Phillips 2011). The dominant wind direction is south-westerly which brings mild and unsettled weather in the winter and cool and overcast conditions in the summer months. During the summer months, with a southerly wind direction, warm land temperatures can also lead to localised convectional thunderstorms and rainfall (Barry and Chorley 2009). Topographical (orographical) rainfall can also occur at higher elevations. See Neal and Phillips (2011) for a detailed analysis of rainfall types and associated annual variability between them. A discussion on rainfall comparisons between the Derwent and Eden catchments is provided in Appendix I. Predicted increases in future rainfall, induced primarily by a warming climate, would suggest the monitoring of restoration schemes will become more significant as an increased number of forcing events (which promote geomorphic change/flood risk) are seen.

A

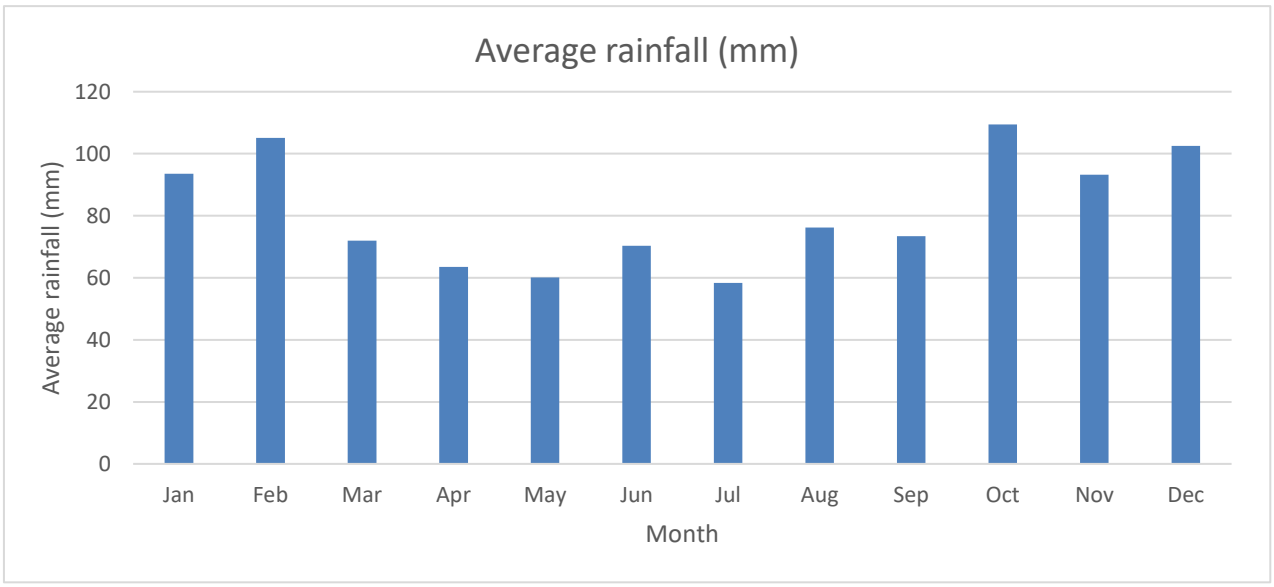

B

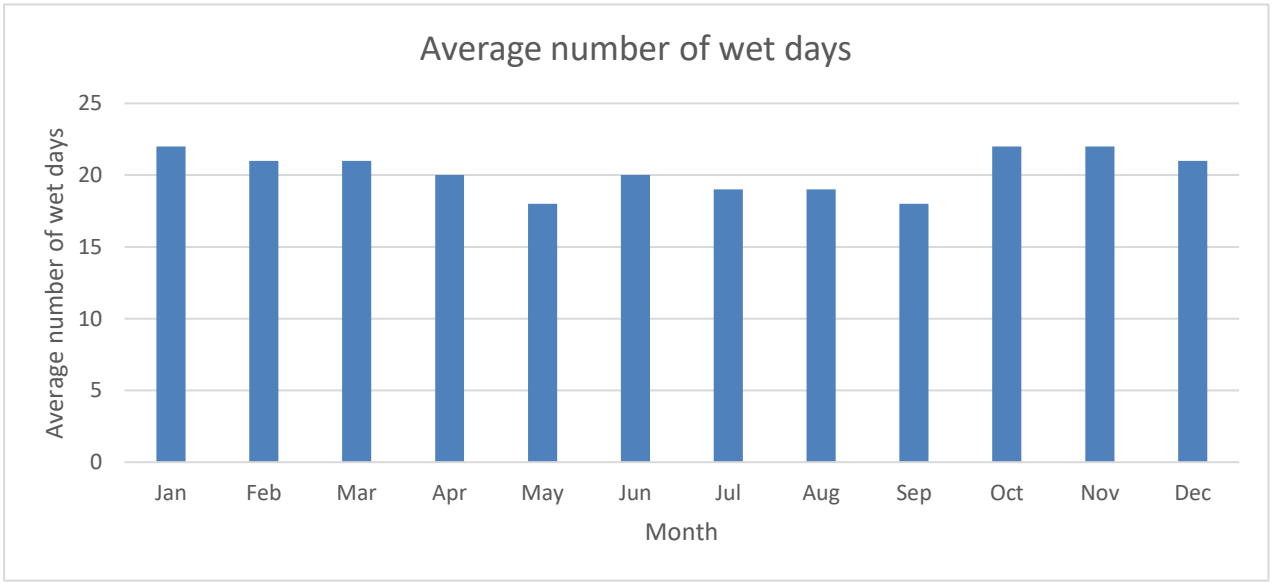

Figure 3.3: A. The average rainfall (in mm) for Cumbria monthly. Values averaged across sites in Cumbria over a 20-year period. B. The average number of rainfall days per month in Cumbria. Values obtained from World Weather (2016).

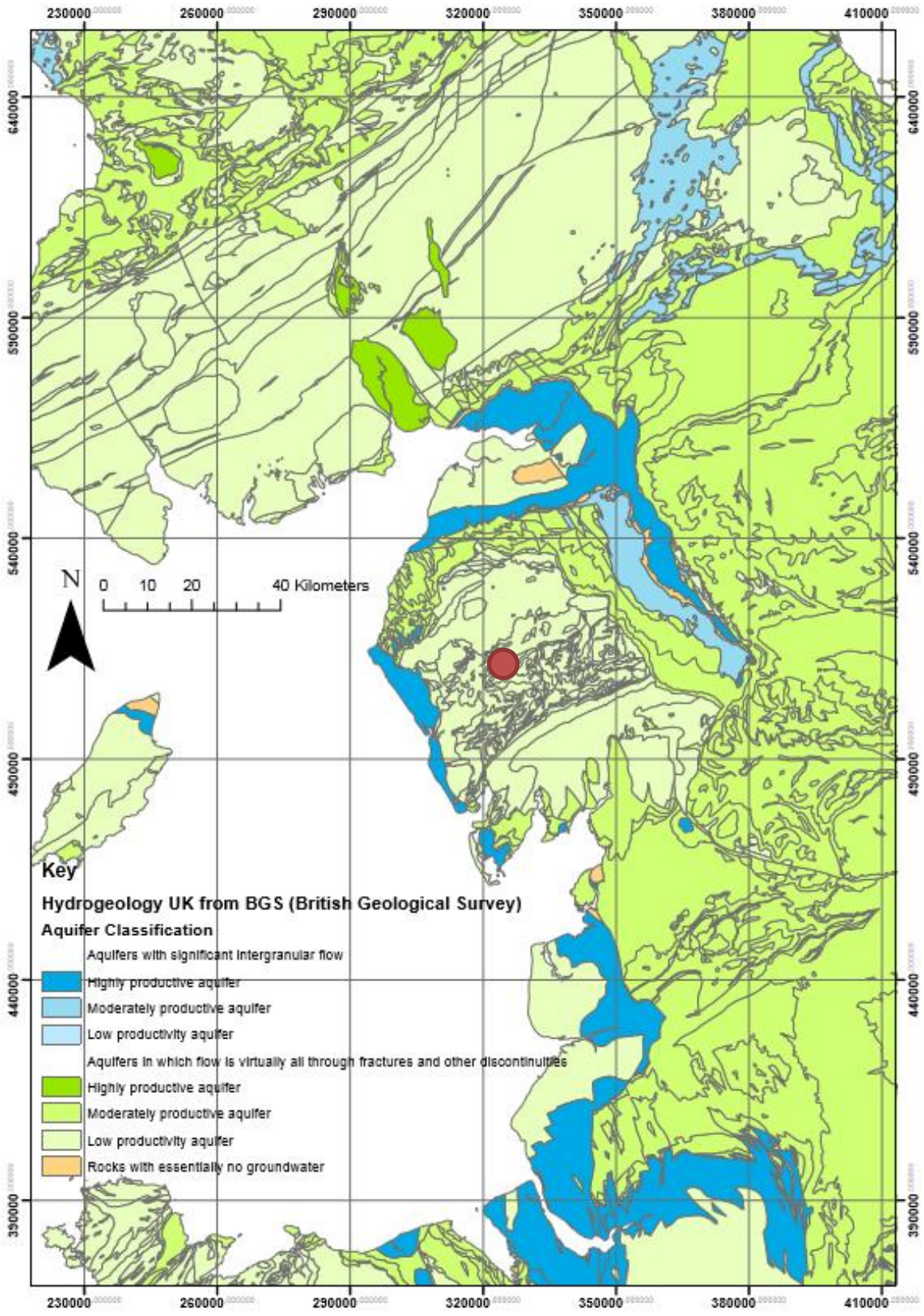

Figure 3.4: The aquifer classification for Cumbria. Data from the British Geological Survey (BGS) (2016). Whit Beck is shown with the red dot.

Figure 3.4 shows the aquifer arrangement within Cumbria. The majority of the inland area of the county is characterised by unproductive aquifers. Both study locations (Whit Beck and Barnskew) have similar aquifers of this type. The west coast of Cumbria is made up of a very productive aquifer, unlike central areas which has a significant intergranular flow through both macro and micro-pore structures. The far north of the county has moderately productive aquifers that stretch towards the north west and arc around the central part of Cumbria.

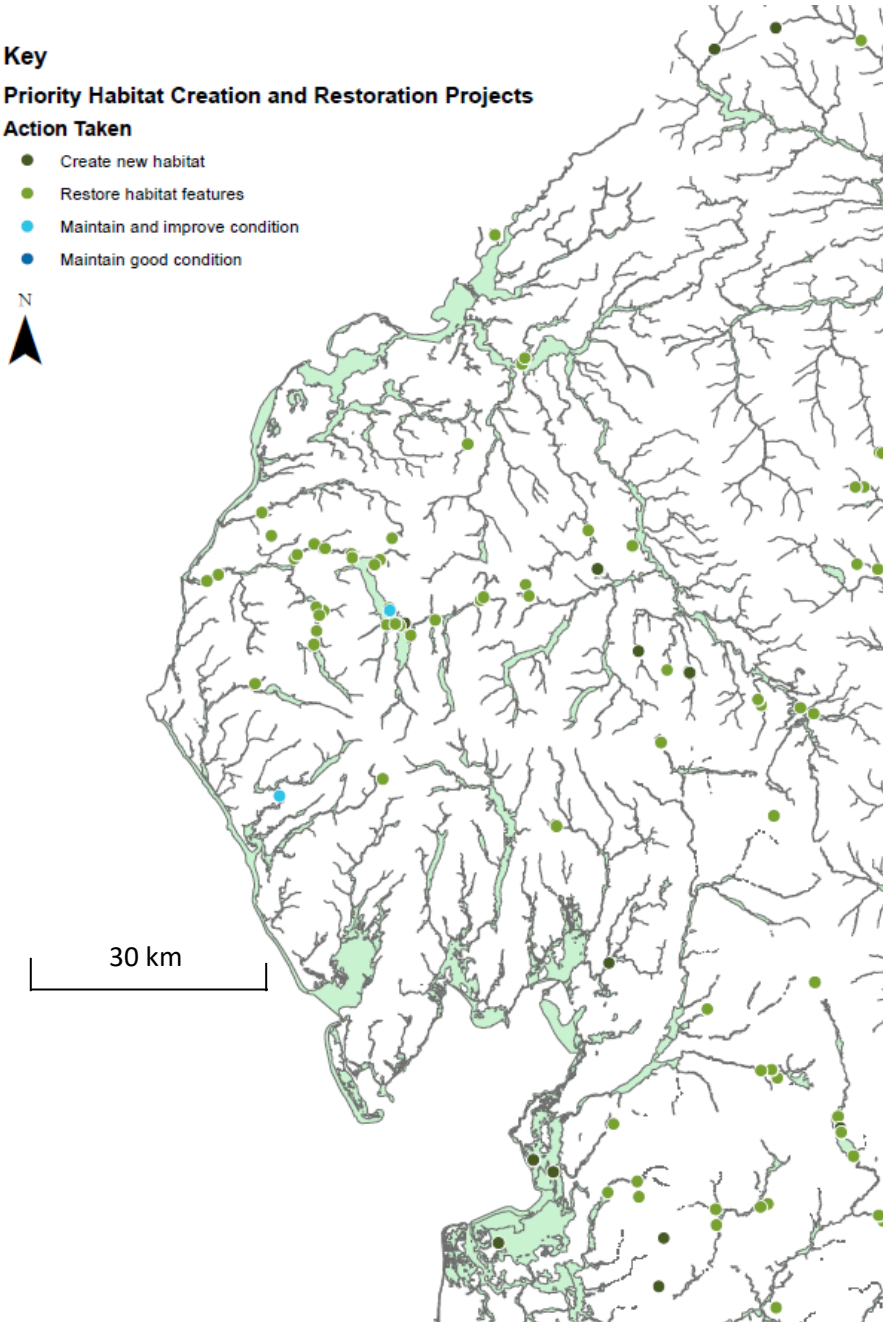

Figure 3.5: The habitat creation and restoration projects carried out in Cumbria. Map from Environment Agency (2016).

As discussed throughout Chapter 1, river restoration efforts have increased throughout the UK and Europe over the last 15-20 years for a variety of reasons. The north west of England, similar to much of the UK, has seen a number of different restoration efforts which combine differing drivers of river restoration (such as flood mitigation and improving biological relations) become more widespread during recent years. Figure 3.5 shows the number of restoration projects within Cumbria using data provided by the Environment Agency (2016). Out of the 87 projects on this map, the vast majority relate to restoring habitat features. 14 restoration projects within the area aim to have created a new habitat, while 2 maintain and improve the current condition of the system.

3.2 Basic Information on Restoration Scheme

3.2.1 Whit Beck

The Whit Beck discharges into the River Cocker and is part of the Derwent catchment in West Cumbria. The WCRT (West Cumbria Rivers Trust) was responsible for managing the restoration scheme. The original Whit Beck channel was straight and ran for a distance of approximately 350 meters (Figure 3.6). The new channel was created to become an active meandering channel which would create new ecological habitats along the stretch of the river, while ensuring hydrological efficiency was maintained. The length of the new channel is approximately 1200 meters meaning channel length has increased by a factor of around 4. The inclusion and creation of a pool-riffle sequence along this new section was also seen as important in sustaining local biological habitats. The new channel size (cross sectional area) was created to accommodate 7 m^2 (Figure 3.7) in upper sections of the Whit Beck, and 9.5 m^2 in the lower sections (West Cumbria Rivers Trust 2016).

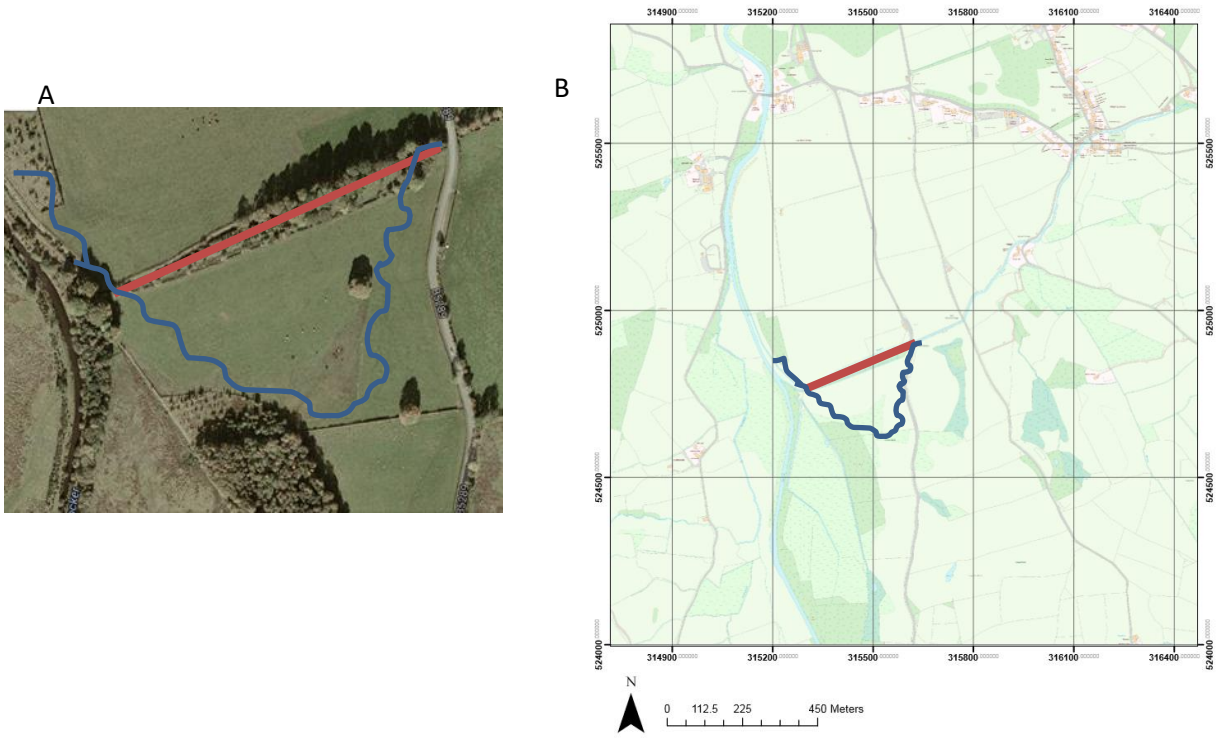

Figure 3.6: A. An aerial image of the Whit Beck site. Image adapted from GoogleEarth (2016) ©. B. A map of the immediate area. Image adapted from DigiMap (2016) ©. The red lines represent the original straight, walled channel, while the blue lines represent the new meandering section. Both images are pre-restoration.

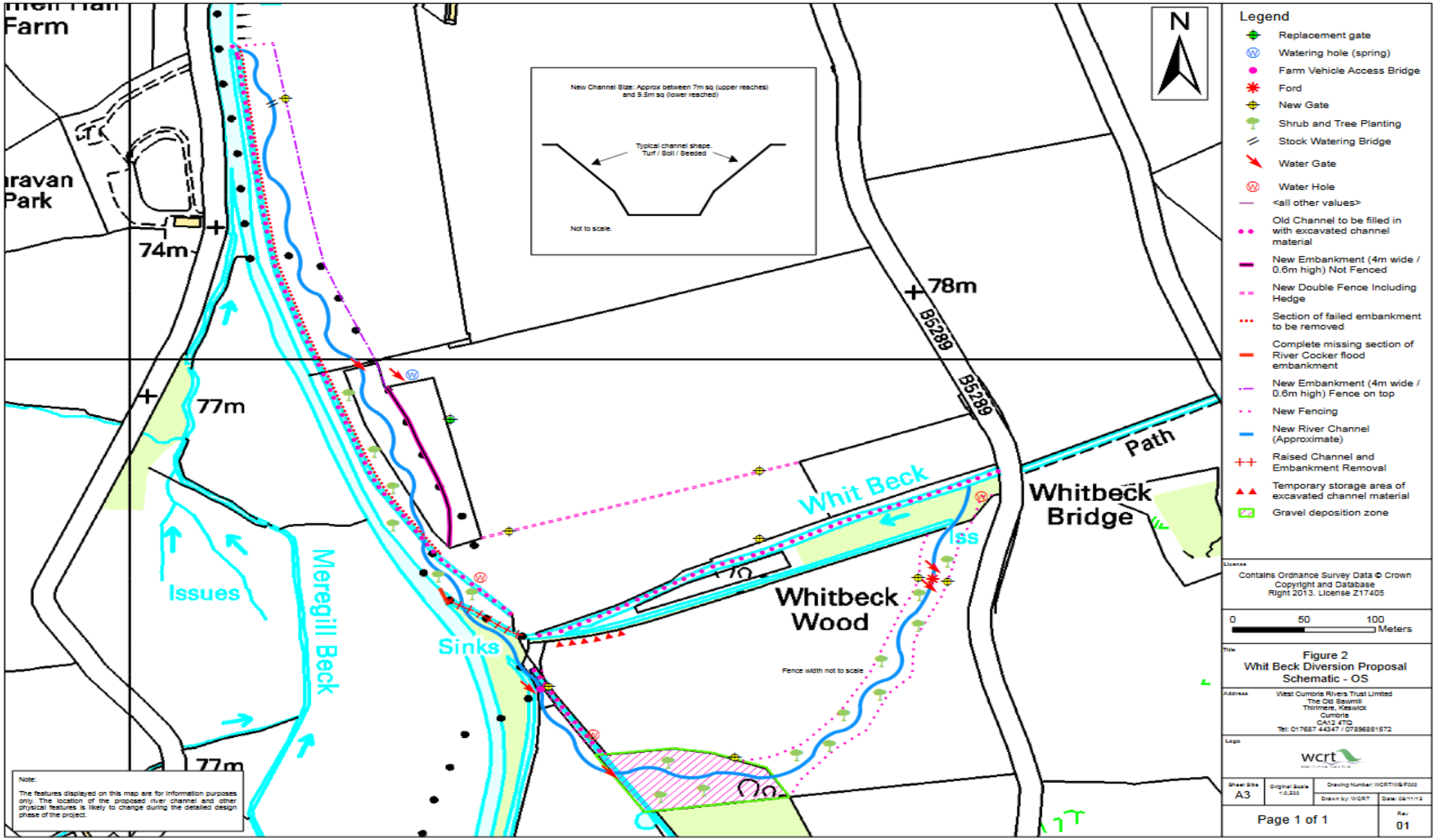

Figure 3.7: A diagram showing the changes made at Whit Beck. Diagram from WCRT (2016)

3.2.1.1 Topography

The topography of the immediate area around the restoration site is shown in Figure 3.8 using an OS DEM 5 m resolution. The Whit Beck restoration scheme is situated near a confluence with the River Cocker and thus has a relatively low land elevation in comparison to the surrounding areas. The majority of the site is characterised by an elevation of below 50m (red lines) and elevations increase in both an easterly and westerly direction. Higher elevations can be seen in the upstream section above the Whit Beck site. Significantly higher elevations of above 200 m can be seen towards the north west, south west and east of the site.

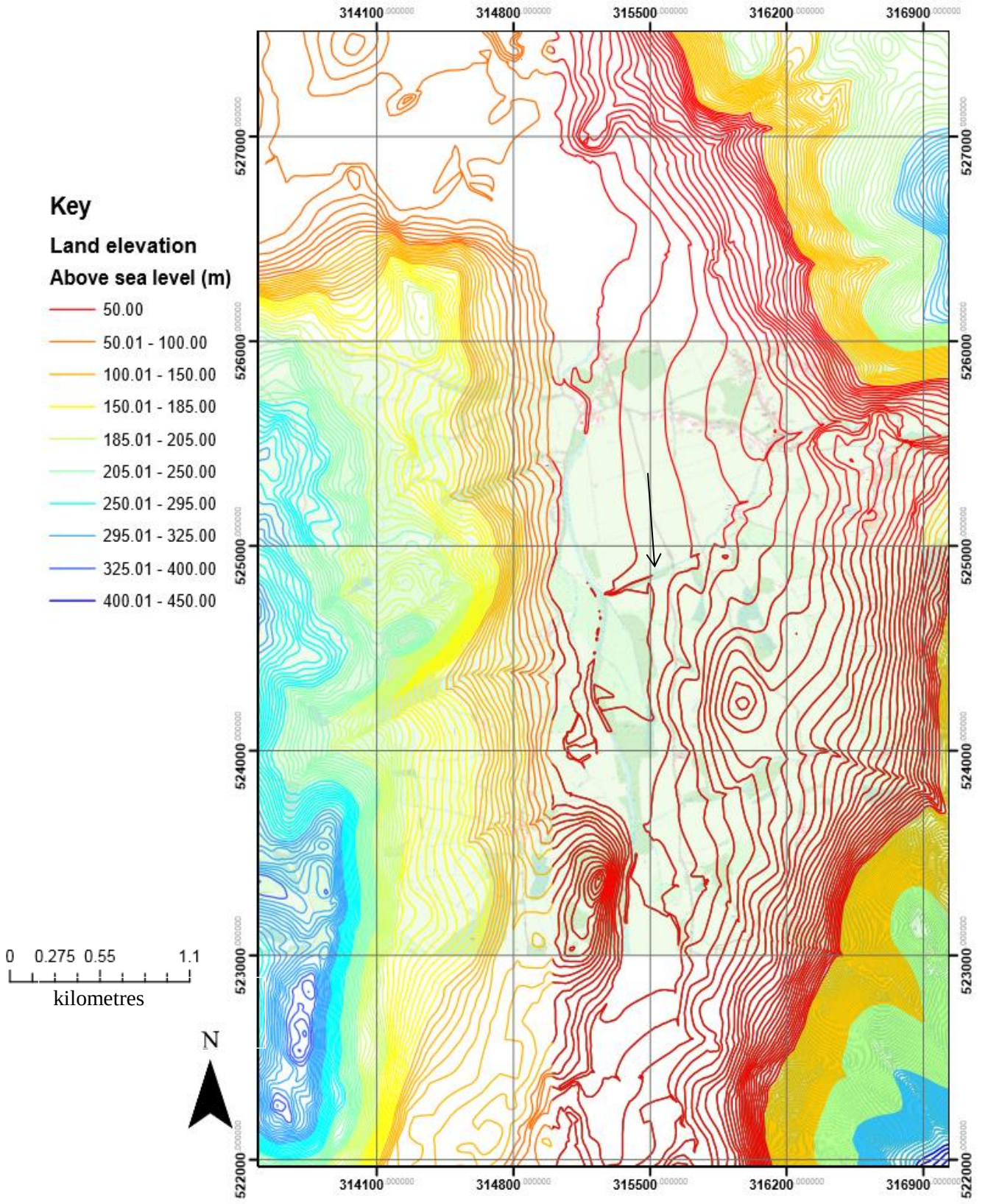

Figure 3.8: An OS (Ordinance survey) 5 m DEM of the Whit Beck area. Data adapted from Digimap (2016) ©. The location of the original channel is shown.

3.2.1.2 Geology

The bedrock geology of West Cumbria is diverse and a range of different bedrock types can be found at Whit Beck. The majority of the wider catchment area is made up of either mudstone or siltstone; while the immediate underlying bedrock around the restoration site is considered kirk stile Fomration (mixes of mudstone and sandstone). Areas of Siluro - Devonian rocks can also be associated with the cachment. The bedrock geology can be important in promoting or controling a range of fluvial processes such as infiltration rates, groundwater, throughflow and thus an appreciation of the effect different bedrock material may have is important. A summary of the bedrock geology of the immediate area around the Whit Beck site can be seen in Figure 3.9. Fault lines are also shown. A number of fault lines run across the study site in a east -west orientation. This may influence the groundwater dynamics on a smaller spatial scale and promote overland flow and saturation of ground, espcially at lower elevations. No apparent influence however can be aknowledged on site.

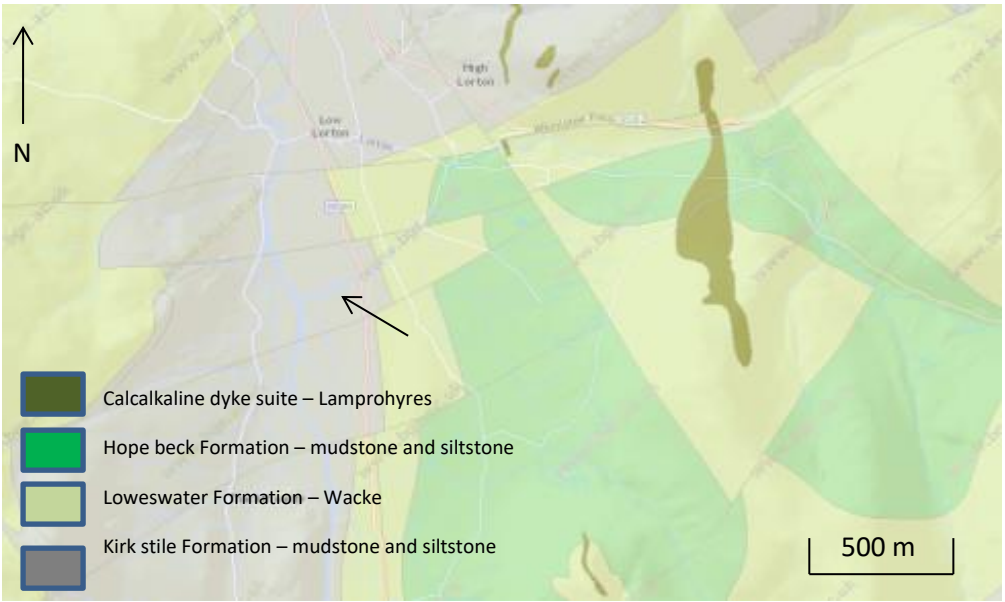

Figure 3.9: Geology of the Whit Beck area. Data from British Geological Survey (BGS) (2016). The original Whit Beck channel is shown.

3.2.1.3 River Flooding Risk

Flood risk and flood mitigation is one of the most important drivers in river restoration efforts and schemes across the UK (Smith et al. 2014b; Grabowski et al. 2014). The inundation risk from river flooding can be summarised in Figure 3.10. It is important to note that these flooding potentials were reported before the construction of the new channel. The effects restoration will have on flood alleveation within the local area must be evaluated before new schemes and proposals are put forward for planning. The field directly to the north of the original channel had a higher probability of flooding compared to the location of the new channel. Flood risk along the River Cocker is also shown on the diagram, with areas of the lower section of the Whit Beck (new channel) located within this flood risk zone.

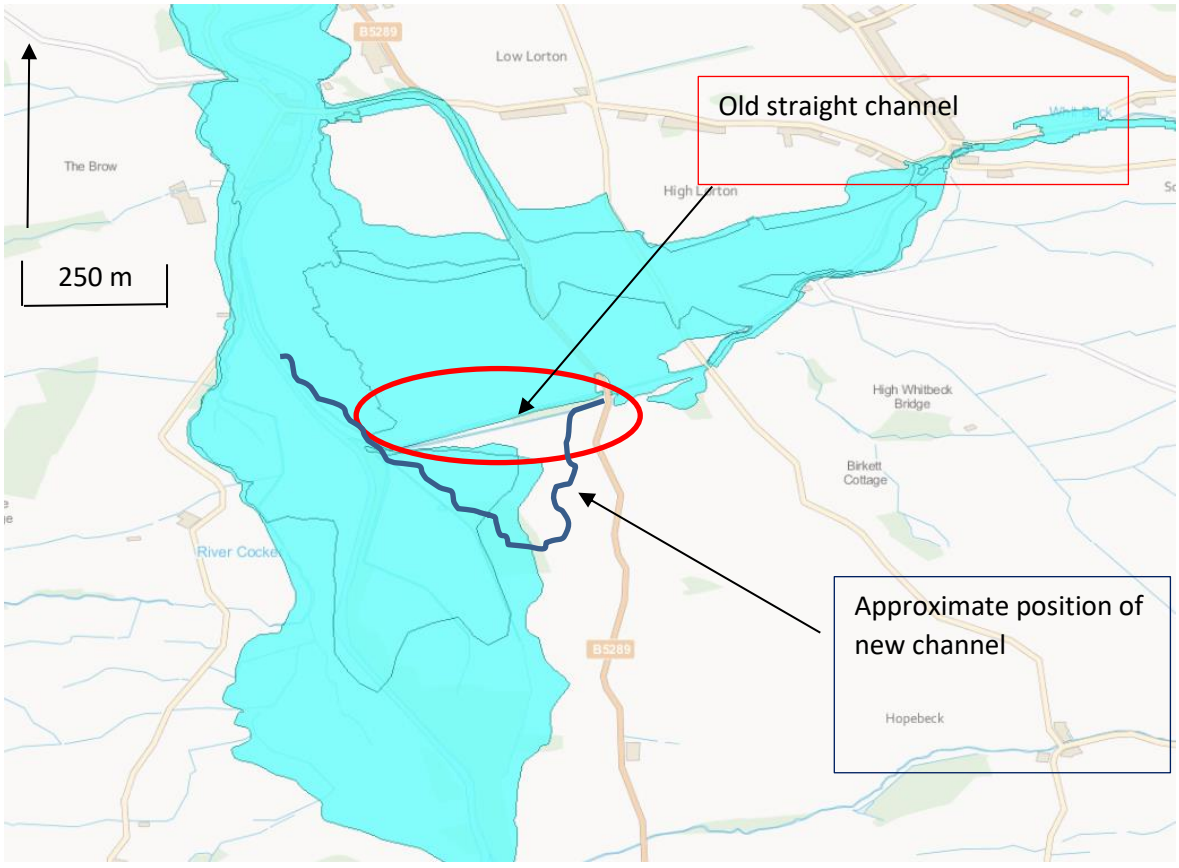

Figure 3.10: Flooding risk at Whit Beck, using data from the Environement Agency (2016). The area shown (light blue) is the area at risk of flooding up to 1 in 1000 year event (0.1%). All data pre-restoration in August 2014.

3.2.1.4 Groundwater Conditions

Groundwater hydrology and the underlying geology can play an important role in determining the hydrological relations through a catchment on a reach, sub-catchment and landscape scale. Figure 3.11 summaries the groundwater level at Furness Abbey in West Cumbria (nearest groundwater site with available data to the Whit Beck site) between the years of 1973 and 1995. As expected, oscillations can be seen between the summer and winter months. Mean annual rainfall at Furness Abbey is 1027 mm. The values discussed may have little relevance to the groundwater levels today and levels are likely to differ spatially, meaning this dataset is unlikely to give a fair reflection of groundwater conditions at Whit Beck. However, the Figure highlights the importance of different seasons in promoting differing groundwater conditions that will influence hydrological behaviour at the study site.

Groundwater levels are also likely to alter significantly temporally, specifically during high rainfall or discharge events during prolonged periods. Predicted models for future flow suggest the likelihood is that groundwater levels may increase by 0.5 m on average across the year (Figure 3.12). Larger differences are expected in late summer and early autumn with some predictions suggesting groundwater levels at Furness Abbey may be around 1 m higher in 5-10 years. It is suggested that this would be due to increased precipitation within the local area. Proportional increases in flood risk would be expected if these scenarios proved to be correct.

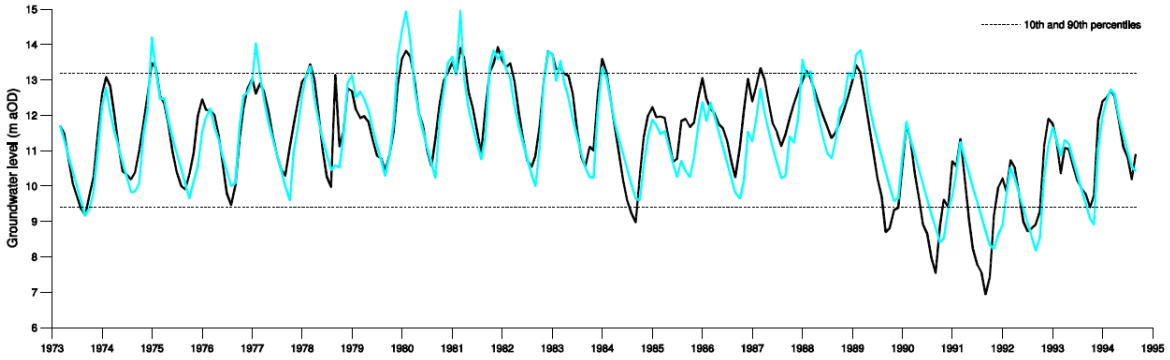

Figure 3.11: Groundwater flow at Furness Abbey (West Cumbria). Observed data is shown by the black line, while simulated data is shown by the blue line. Data from Catchment Fact sheets, sourced from the British Geological Survey (BGS) (2016). Please see BGS link for full details.

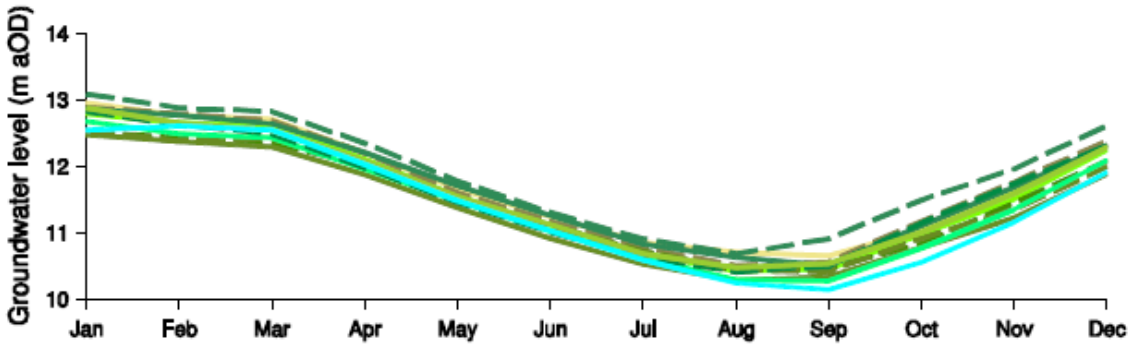

Figure 3.12: Predicted groundwater flow at Furness Abbey (West Cumbria). Observed data is shown by the blue line, while future flow data (10 years) is shown by the green lines. Differing green lines relate to different environmental parameter values, all relating to a warmer and wetter climate in 2026. See BGS link for specific details. Data from Catchment Fact sheets, sourced from the British Geological Survey (BGS) (2016).

3.2.1.5 Land Cover

The area around the site has a range of different land classifications as outlined by the land cover map (CEH 2007). The majority of the area can be classified as improved grassland. This is grassland that could be used for agricultural purposes. The fields towards both the north and south of the old and new channel are classed as improved grassland. Towards the confluence with the River Cocker, a greater proportion of broadleaved, mixed and yew woodland can be seen that run parallel with the River Cocker moving upstream. The land cover of the Whit Beck can be seen in Figure 3.13, while the relative percentages of different types of land cover can be viewed in Table 3.1. A small area of neutral grassland can be seen towards the far south east section of the restoration site. For the immediate area and upstream section, around 55% of land can be classified as improved grassland. A fair proportion (12%) of rough grassland can be seen in pockets around the sub-catchment. Broadleaved and horticultural land cover make up about 10 and 8 % respectively.

Table 3.1: Land cover percentages for Whit Beck (Figure 3.13).

Land cover	%
Improved grassland	55
Rough grassland	12
Broadleaved, mixed and yew woodland	10
Arable and Horticulture	8
Acid grassland	8
Neutral grassland	7

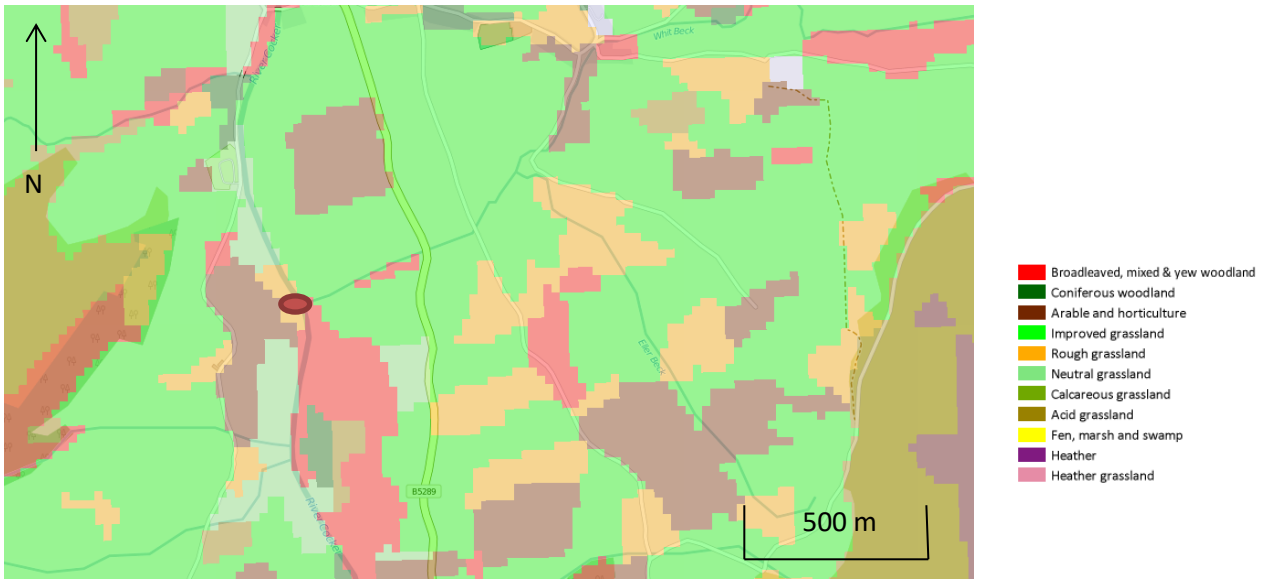

Figure 3.13: Land use classifications for Whit Beck using Land use map (2007) from Centre for Ecology and Hydrology (CEH) (2007). The red circle shows the location of the where the old channel disscharged into the River Cocker.

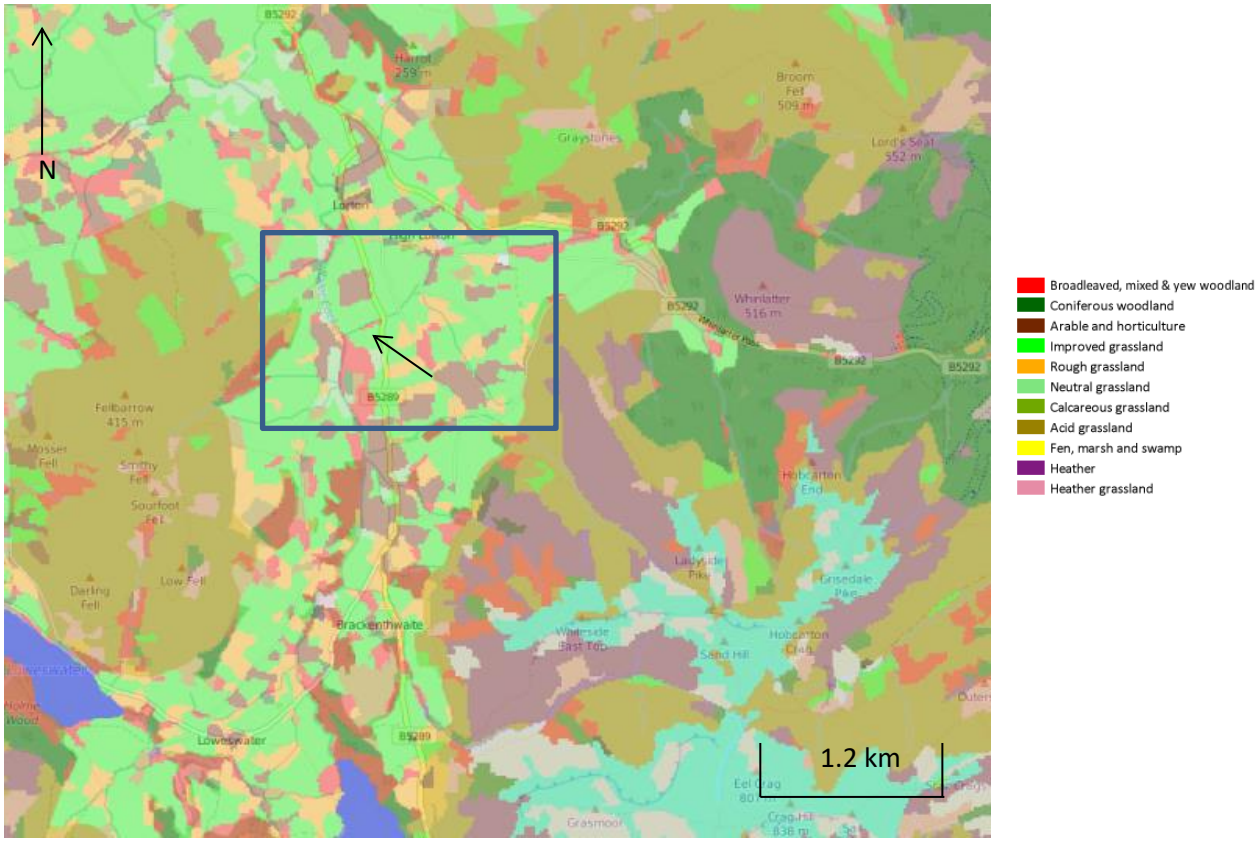

Figure 3.14: Land use classifications for the wider catchment using Land use map (2007) from Centre for Ecology and Hydrology (CEH) (2007). Whit Beck is shown. The location of Figure 3.13 is shown within the blue box.

The wider Derwent catchment has a range of different land classifications as shown in Figure 3.14. Unlike the immediate Whit Beck sub-catchment, the land use is not predominately improved grassland (light green). Large areas of acid grassland can be noted, specifically towards the west in high topographical areas. Large areas of acid grassland coincide with higher elevations towards the north west and south east of the Whit Beck site also. Lower areas (closer to Whit Beck) can be characterised by improved grassland and broadleaved, mixed and yew woodland. Areas of heather are also more apparent at higher topographic elevations. A large area of coniferous woodland is immediately east of the site, once elevations start to increase.

Methodology

3.3 Fieldwork Campaigns

A variety of different techniques are used in this thesis in order to evaluate the use of SfM technology in monitoring the restoration scheme examined. A discussion of the techniques used is presented and flowcharts are used to show specific procedures used for the data analysis presented. After outlining the fieldwork campaigns (Section 3.3), the use of Photoscan and the formation of DEMs is first examined (Section 3.4), which is followed by a dialogue on the techniques used in the TLS, bathymetric, DoD and modelling (Sections 3.5-3.8).

Three visits to Cumbria were undertaken with data collection taking place in October 2014, March 2015 and July 2015. The purpose of this was to enable a fair representation of channel development to be thoroughly documented and analysed along Whit Beck. This would also allow monitoring of the morphodynamics of the channel during the first year since restoration. Table 3.2 shows information on the surveys undertaken. For all subsequent geomorphic analysis, the focus was on change between the upstream end of the Whit Beck and the 1st bridge. The October 2014 SfM survey mapped only until this point, whereas the March 2015 and July 2015 surveys mapped the channel up until the confluence with the River Cocker. Three different camera/quadcopter platforms were used to allow comparison between different techniques of image acquisition.

Table 3.2: Whit Beck fieldwork campaigns overview.

Survey	Approx. days of work	Time of Day	Approx. total number of images	Weather conds	Survey method	Total number of images	Total number of flights	Bathymetric survey/ depth measurements	TLS survey	Number of targets set out	Flight orientation	Spatial extent
October 2014	2/3	All day (dawn-dusk)	900	Changeable, sunny and showers, cold	Airscapes Imagery	1342	4	Yes	Yes	49	Upstream to downstream	Up to 1st bridge
March 2015	2	All day (dawn-dusk)	850	Changeable, some showers	DJI+ with compact camera	917	3	Yes	No	96	Upstream to downstream to 1st bridge, back to upstream end. Upstream to confluence	Up to confluence with the River Cocker
July 2015	2	All day (dawn-dusk)	1000	Warm and sunny	DJI phantom 2 with Panasonic Lumix camera	866	3	Yes	No	55	Upstream to downstream	Up to confluence with the River Cocker

3.4 SfM and UAV Workflow

3.4.1 SfM Methodology

The primary methodology used in this investigation was SfM photogrammetry. In October 2014, a company based in Cumbria called Airscapes was asked to take aerial imagery of the Whit Beck site at a cost of £280. Four flight lines were flown to give an initial understanding of how the processing of data could be used. The aim of the first field campaign was to acquire data to design the methodology of subsequent image acquisition. This would allow a better understanding of the effect that variables such as image overlap and number of targets had on the quality of the DEM produced.

A DJI Phantom+ with compact camera was used in March 2015. A DJI phantom 2 was used in July 2015 with an additional camera mount and Panasonic Lumix camera. A mount from Drone Expert was purchased for a cost of £850.The purpose of this was to hold a camera in place which could take a higher quality image of the channel under investigation. The cost of the Panasonic Lumix camera was £450.

The purpose of using these three different formats was to see if these had any influence in DEM production and formation. Comparisons between the Airscapes imagery and the DJI Phantom imagery could then be made. Data collection from October 2014, March 2015 and July 2015 would then provide an appreciation of channel change through time to be acknowledged.

For the UAV surveys, targets (consisting of 0.5 x 0.5 m plastic black sheets with yellow crosses) were used to ensure accurate referencing was undertaken. The number of targets and the spacing between them for each campaign differed. A Leica RTK GPS was used to survey the target points along the river corridor. The coordinates of these targets were then used in Photoscan to georeference the model being produced.

These images acquired were used in the image processing software Photoscan and DEMs were then produced using corresponding orthophotos and dense point clouds. An overview of this process can be seen in Section 3.4.2. Hackney and Clayton (2015) discuss the use of UAVs in a geomorphic capacity in detail.

A  B 

Figure 3.15: a. An example of the type of quadcopter used (March 2015), b. a target is shown.

3.4.1.1 SfM algorithms

SfM is becoming increasingly used within the geosciences as its applicability to a wide range of geomorphic environments is favourable for a range of differing data requirements. The general SfM workflow can be split into a number of individual sections and these are explored in more detail below. SfM was developed primarily within the Computer Science discipline and interest grew in the procedures outlined after the successful development of feature matching algorithms in the 1980s (Forstner 1986; Harris and Stephens 1988, Westoby et al. 2012).

SfM has the advantage of not needing coordinates of camera positions and thus a manual GCP network can be set-up which can allow for targets to be placed in specific locations which favour the data collector. This allows more control over the spatial extent and resolution of the survey undertaken. Images which are sharp and have a higher resolution are likely to give superior results, however computer processing time must be balanced in this regard. Environmental variables such as lighting, shade and obstacles which are moving or hide parts of the image are likely to alter the results obtained. Image collection and the GCP network need to be aligned to the needs of the survey and the environmental and geomorphic settings (Westoby et al. 2012).

The first stage of data processing (Figure 3.17) relates to finding correlating points in differing images. The SIFT (Scale Invariant Feature Transform) algorithm is used in many photogrammetry software packages and allows matching features in corresponding images to be attained (Snavely 2008). Keypoints are then identified and descriptors can then be used to allow the visualisation of matching features within a local coordinate system (i.e. before georeferencing has taken place) (Lowe 2004; Westoby et al. 2012). Figure 3.16 shows an output of the SIFT algorithm from Brown and Lowe (2007).

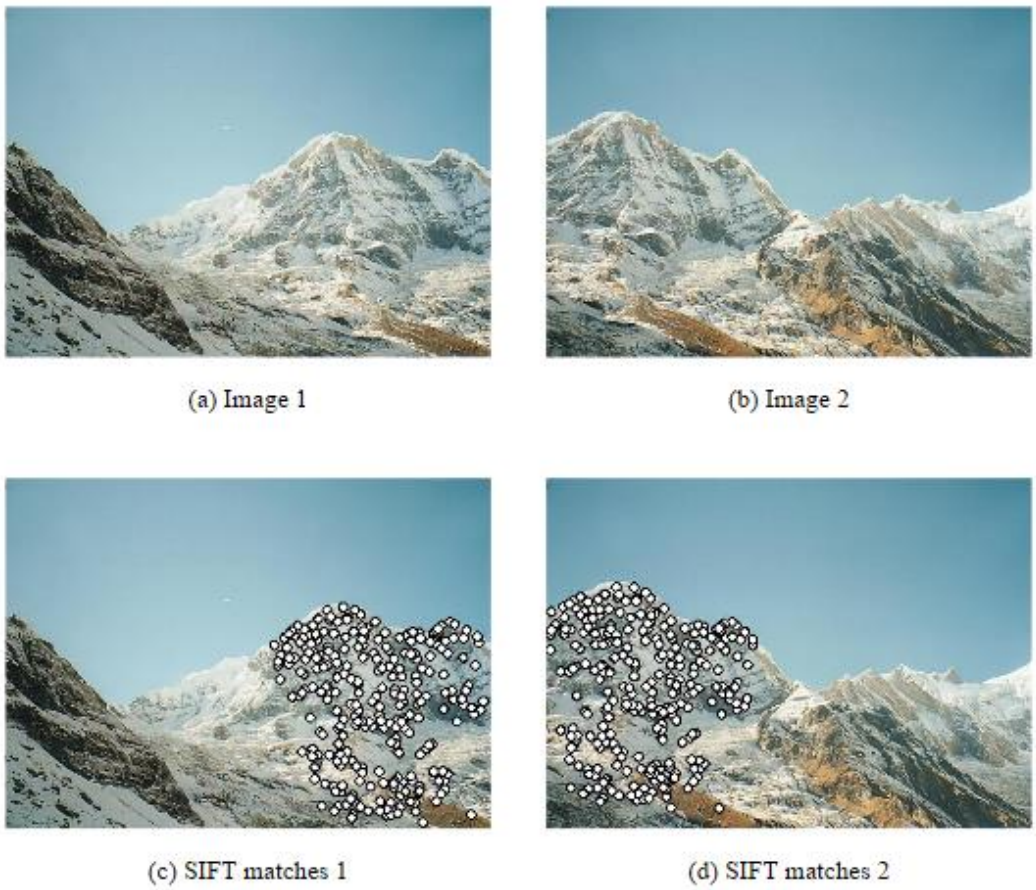

Figure 3.16: Showing outputs from a SIFT algorithm. A and b: Original images, c and d: locations of feature matches when different images are used as the reference. Image from Brown and Lowe (2007).

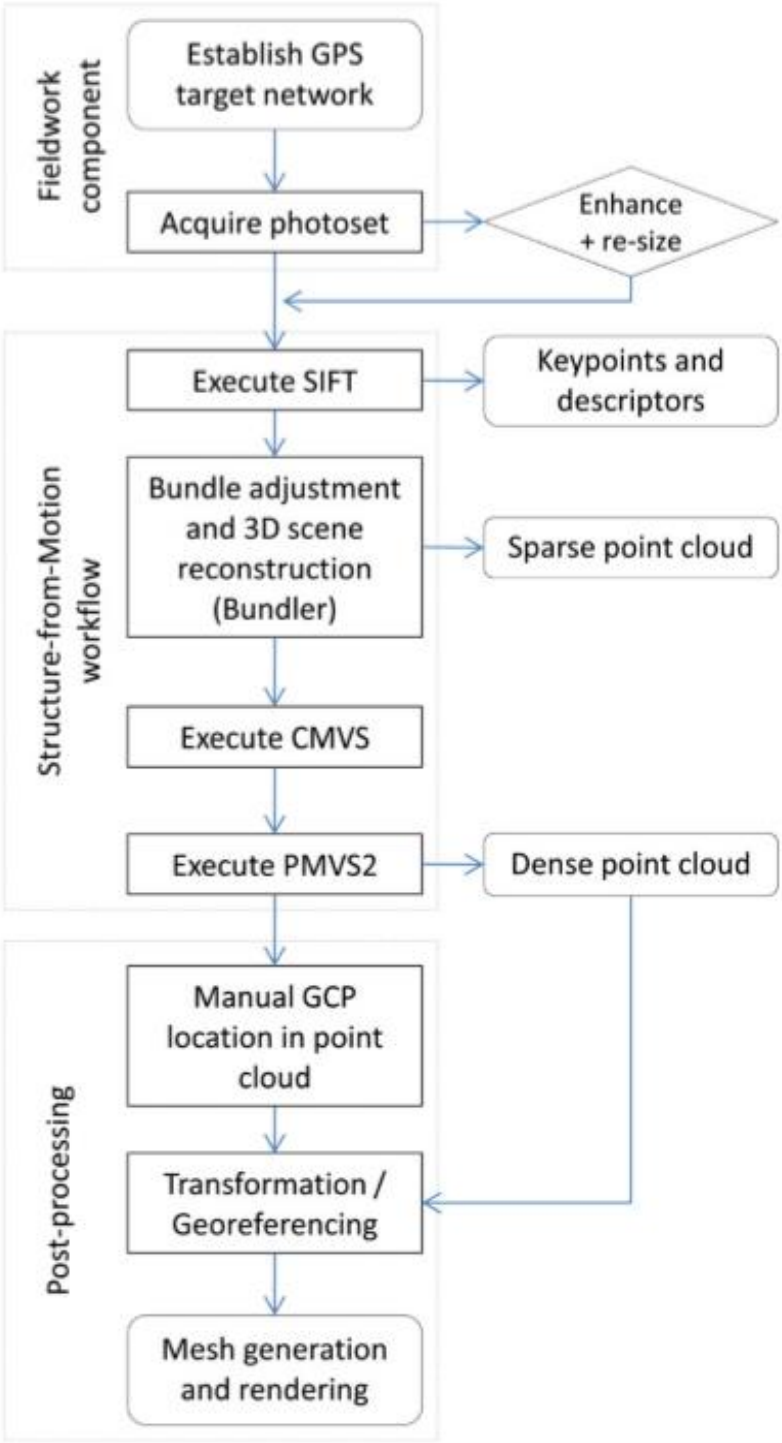

Figure 3.17: Showing an example SfM workflow from Westoby et al. (2012). See text for discussion.

The next stage involves a bundle adjustment to allow camera positions and orientations to be assigned (Lourakis and Argyros 2009). This allows the formation of a sparse cloud. A number of algorithms can be used in this step, however many SfM packages use variations of RANSAC (Random Sample Consensus) (Fischler and Bolles 1987; Arya et al. 1998). RANSAC is most widely used as it simple to apply to different codes and can be applied to data which is noisy (30% + outliers) (Schnabel et al. 2007). To produce a dense point cloud from the resulting sparse point cloud, algorithms such as CMVS (Clustering view for Multi-view stereo) and PMVS2 (Patch-based Multi-view stereo) can be used. The CMVS algorithm allows image clusters to be formed by selecting images where SfM points can be associated with objects of known reference (Furukawa et al. 2010). Figure 3.18a shows this in graphical form. This process is repeated until a required spatial extent of image clusters has been achieved (Figure 3.18b). The PMVS2 algorithm is a correlating, aggrandising and filtering technique (Furukawa and Ponce 2010). Corresponding points within differing images are correlated together and neighbouring cells which contain no data are interpolated using the patch expansion algorithm. Figure 3.18c shows the patch expansion algorithm developed by Furukawa and Ponce 2010. The interpolation and filtering steps are repeated numerous times to ensure as many points are created in empty cells as possible. There are only two conditions which do not allow data to be entered in empty neighbouring cells. Either if data has already been created within an adjacent cell or if surface depth between the two cells is of a large magnitude (Figure 3.18d) (Furukawa and Pounce 2010). Please see Furukawa and Pounce (2010) for a detailed mathematical explanation of the PMVS2 algorithm, this discussion is beyond the scope of this study.

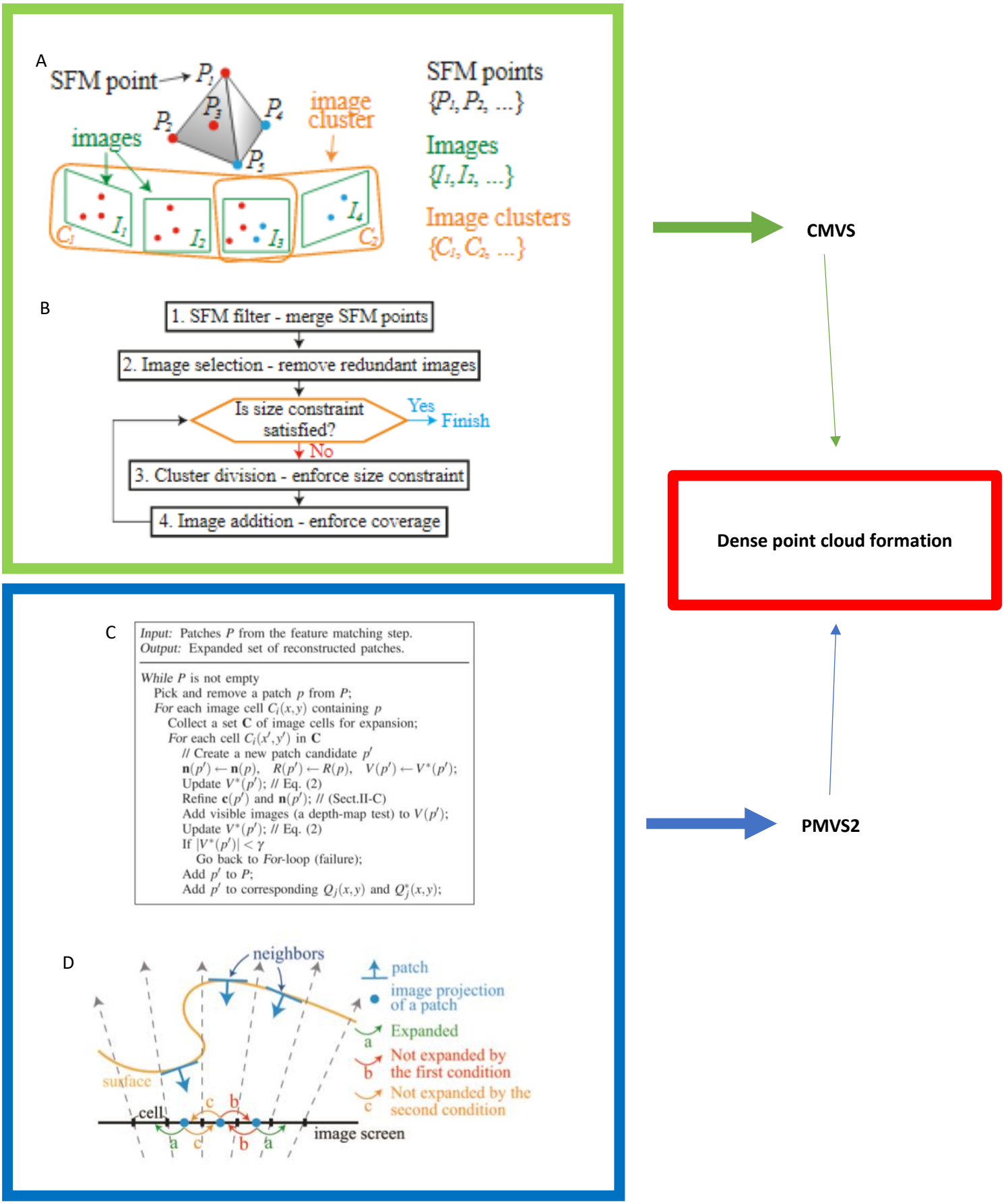

Figure 3.18 a. showing how CMVS produces image clusters. Images with similar matches are correlated together (orange boxes). B. showing a diagram representing how the process is repeated to ensure enough image clusters are produced for a given spatial extent. Figures from Furukawa et al. (2010). C. Showing the PMVS algorithm for matching patches to adjacent cells, see Furukawa and Pounce (2010) for a full mathematical explanation. D. Showing a diagram of how cells may not be interpolated. A is this diagram represents cell data calculation in the correct manner, b represents issues when neighbouring cells contain adequate data pre-algorithm and c. when differences in surface depth are too large for correct corresponding algorithm workflows. Figures from Furukawa and Pounce (2010).

The next stage is the transformation of the dense cloud into a real world coordinate system. This can be done by adding GPS data to the GCP network. Georefrencing of point cloud data is required if enviromental processes are to be measured or monitored. Mesh/DEM/DTM creation can then be carried out once the model has been sucsesfully georefrenced. The workflows discussed represent a generic procedure and differing software will use variations of the algorithms presented.

3.4.2 AgiSoft Photoscan

Once imagery was collected, photos were processed using Agisoft Photoscan. Photoscan uses coherent points from corresponding images to mesh together an area of interest, which in turn allows dense point cloud, orthophoto and DEM production. Coordinates of reference points are added to the software and a coordinate system is selected. The series of steps required to produce a DEM is shown in Figure 3.19.

The photos are loaded into the program and aligned with one another. Image overlap is important here as an increase in the number of coherent points between differing images allows for a better representation of spatial variability to be achieved (Snavely et al. 2006). Markers are then placed as reference points to enable triangulation between neighbouring images, so it is extremely important that coordinates for these points are accurate and precise. The movement of the bounding box allows the correct spatial representation and resolution to be attained, while maintaining the precise orientation required for the building of dense point clouds (Perez et al. 2013).

Matching pixels from coherent images are correlated to produce a dense point cloud of the area under investigation (James and Robson 2012). At this stage, variables such as flying height and the number of GCPs becomes significant, as the point cloud needs to be of sufficient resolution and overlap. The point clouds are then built into a mesh which aims to build up the surface of the model. Edits can be made which eliminate sources of error or outliers in the data. The data is then exported as an orthophoto and then as a DEM. A key component of the SfM process is DEM evaluation and analysis, and accuracy assessments are vital in order to distinguish if the final product is of suitable validity for the purposes it is required for (Snavely et al. 2008). A good overview of the SfM process is provided by Micheletti et al. (2015).

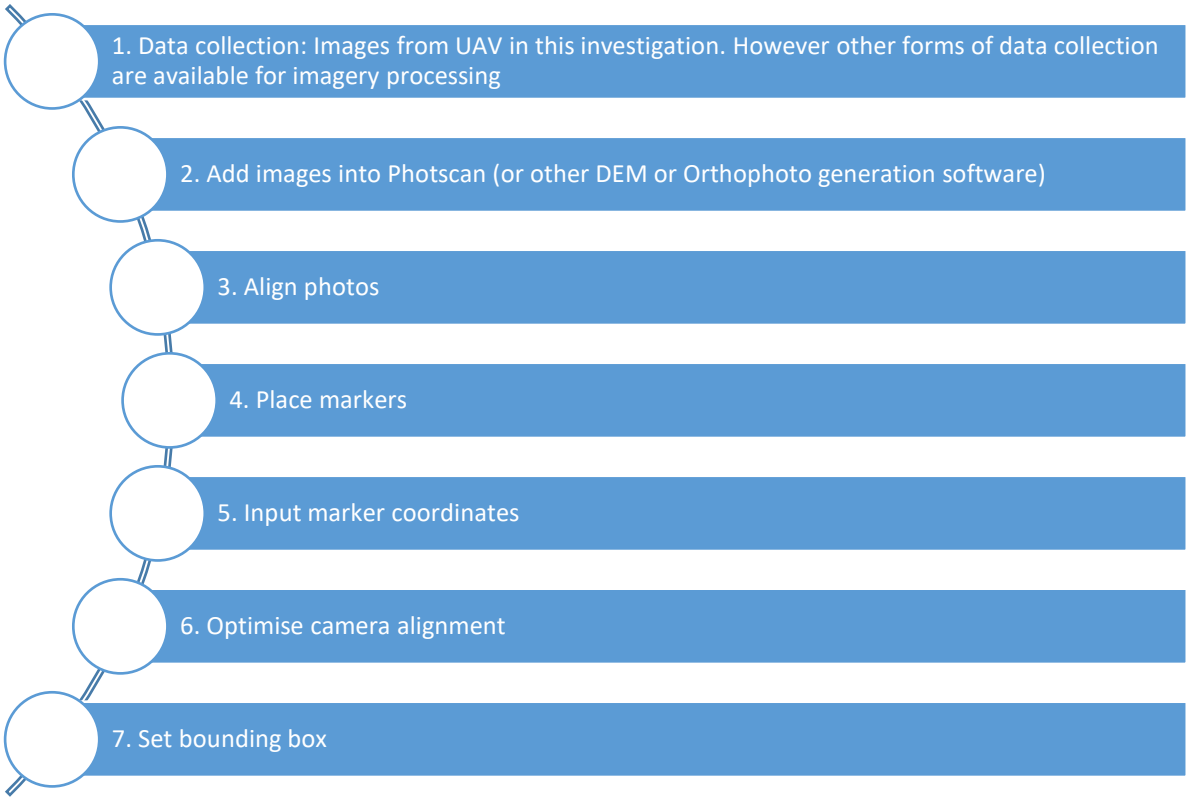

Figure 3.19: Photoscan workflow used.

The specific algorithms within Photoscan are strictly hidden and developed with programmers internally. Photoscan does however use algorithms which favour better outputs, rather than a reduction in process speed (Photoscan 2016). Table 3.3 shows the four main model formation phases and shows a description of the processes and algorithms being used. Tables 3.4 and 3.5 show the exact parameters used within Photoscan in relation to differing phases of model development. These were kept uniform throughout the model phases to ensure any DEMs produced could be adequately compared post processing.

Table 3.3: A description of the algorithms used in Photoscan. The exact details of which are not made available. The text has been taken directly from the Photoscan website (2016).

Model phase	Description	Comparisons with other algorithms
Feature matching	At the first stage PhotoScan detects points in the source photos which are stable under viewpoint and lighting variations and generates a descriptor for each point based on its local neighbourhood. These descriptors are used later to detect correspondences across the photos.	Very similar to the SIFT algorithm
Solving for camera intrinsic and extrinsic orientation parameters	PhotoScan uses a greedy algorithm to find approximate camera locations and refines them later using a bundle-adjustment algorithm.	Very similar to the Bundler algorithm
Dense surface reconstruction	At this step several processing algorithms are available. Exact, Smooth and Height-field methods are based on pair-wise depth map computation, while Fast method utilizes a multi-view approach.	
Texture mapping	At this stage PhotoScan parametrizes a surface possibly cutting it in smaller pieces, and then blends source photos to form a texture atlas.	

Table 3.4: Parameters used within Photoscan for differing phases.

Model formation stage	Parameters used
Image alignment	Accuracy: High, Pair preselection: generic, Key point limit: 40,000, Tie point limit: 10,000
Camera alignment	Measurement accuracy Camera accuracy (m):10, Camera accuracy (deg): 5, Marker accuracy: 0.0005, Scale bar accuracy: 0.0001 Image coordinate accuracy Marker accuracy (pix): 0.1, Tie point accuracy (pix): 4
Camera optimisation settings	Boxes ticked included fit f, fit cx,cy, fit k1,k2,k3 and fit p1,p2
Dense Point cloud formation	Quality: high, Depth filtering: Aggressive
Mesh formation	Surface type: Height field, Source data: dense cloud, Face count: high
Texture formation	Mapping mode: orthophoto, Blending mode: mosaic, Texture size/count: 8192 No colour correction
Orthophoto formation	Type: Geographic, Surface: DEM, Blending mode: Mosaic
DEM formation	Source data: Dense cloud, Interpolation: enabled

Table 3.5: Parameter description and justification.

Parameter	Description (taken from Agisoft Photoscan 2016 manual)	Justification of chosen value
Image alignment: Accuracy	Higher accuracy settings help to obtain more accurate camera position estimates. Lower accuracy settings can be used to get the rough camera positions in a shorter period. While at high accuracy setting, the software works with the photos of the original size, medium setting causes image downscaling by factor of 4 (2 times by each side), at low accuracy source files are downscaled by factor of 16, and lowest value means further downscaling by 4 times more. Highest accuracy setting upscale the image by factor of 4. Since tie point positions are estimated based on feature spots found on the source images, it may be meaningful to upscale a source photo to accurately localize a tie point. However, highest accuracy setting is recommended only for very sharp image data and mostly for research purposes due to the corresponding processing being quite time consuming.	The highest accuracy was chosen to ensure the most accurate camera positions where estimated.
Image alignment: pair preselection	The alignment process of large photo sets can take a long time. A significant portion of this time period is spent on matching of detected features across the photos. Image pair preselection option may speed up this process due to selection of a subset of image pairs to be matched. In the Generic preselection mode the overlapping pairs of photos are selected by matching photos using lower accuracy setting first. In the Reference preselection mode the overlapping pairs of photos are selected based on the measured camera locations (if present). For oblique imagery it is necessary to set Ground altitude value (average ground height in the same coordinate system which is set for camera coordinates data)min the Settings dialog of the Reference pane to make the preselection procedure work efficiently.	Generic setting was chosen as this has been found to be most applicable for DEM formation (see DEM construction at AgiSoft Photoscan 2016). Camera positions were also unknown.

	Ground altitude information must be accompanied with yaw, pitch, roll data for cameras. Yaw, pitch, roll data should be input in the Reference pane	
Image alignment: Key point limit	The number indicates upper limit of feature points on every image to be taken into account during current processing stage. Using zero value allows photoscan to find as many key points as possible, but it may result in a big number of less reliable points.	A limit of 40,000 was chosen as this was suggested in the Agisoft Photoscan DEM formation guidelines. This balances mesh accuracy against computational demand.
Image alignment: Tie point limit	The number indicates upper limit of matching points for every image. Using zero value doesn't apply any tie point filtering.	A limit of 10,000 was chosen as this was suggested in the Agisoft Photoscan DEM formation guidelines. This process has a significant influence over processing time and should be kept as low as possible if processing time is to be minimised.
Dense Point Cloud: quality	Specifies the desired reconstruction quality. Higher quality settings can be used to obtain more detailed and accurate geometry, but they require longer time for processing. Interpretation of the quality parameters here is similar to that of accuracy settings given in Photo Alignment section.	Highest quality settings were used to allow best possible results, despite in some cases very long processing times (over 20 hrs).
Dense Point Cloud: Depth Filtering	At the stage of dense point cloud generation reconstruction Photoscan calculates depth maps for every image. Due to some factors, like noisy or badly focused images, there can be some outliers among the points. To sort out the outliers Photoscan has several built-in filtering algorithms that answer the challenges of different projects. If there are important small details which are spatially distinguished in the scene to be reconstructed, then it is recommended to set Mild depth filtering mode, for important features not to be sorted out as outliers. This value of the parameter may also be useful for aerial projects	An aggressive option was used as this is recommended for aerial surveys over large spatial extents.

	in case the area contains poorly textured roofs, for example. If the area to be reconstructed does not contain meaningful small details, then it is reasonable to choose aggressive depth filtering mode to sort out most of the outliers. This value of the parameter normally recommended for aerial data processing, however, mild filtering may be useful in some projects as well Moderate depth filtering mode brings results that are in between the Mild and Aggressive approaches. You can experiment with the setting in case you have doubts which mode to choose. Additionally depth filtering can be disabled. But this option is not recommended as the resulting dense cloud could be extremely noisy.	
Mesh formation: Surface Type	Arbitrary surface type can be used for modelling of any kind of object. It should be selected for closed objects, such as statues, buildings, etc. It doesn't make any assumptions on the type of the object being modelled, which comes at a cost of higher memory consumption. Height field surface type is optimized for modelling of planar surfaces, such as terrains. It should be selected for aerial photography processing as it requires lower amount of memory and allows for larger data sets processing.	Height field was chosen as this surface type is most applicable to geomorphic environments.
Mesh formation: Source data	Specifies the source for the mesh generation procedure. Sparse cloud can be used for fast 3D model generation based solely on the sparse point cloud. Dense point cloud will result in longer processing time but will generate high quality output based on the previously reconstructed dense point cloud.	Dense cloud was chosen to ensure best possible outputs were achieved.
Mesh formation: Face count	Specifies the maximum number of polygons in the final mesh.	High was chosen to produce the highest number of polygons in the mesh construction phase.

	Suggested values (High, Medium, Low) are calculated based on the number of points in the previously generated dense point cloud: the ration is 1/5, 1/15, and 1/45 respectively. They present optimal number of polygons for a mesh of a corresponding level of detail. It is still possible for a user to indicate the target number of polygons in the final mesh according to their choice. It could be done through the Custom value of the Polygon count parameter. Please note that while too small number of polygons is likely to result in too rough mesh, too huge custom number (over 10 million polygons) is likely to cause model visualization problems in external software.	
Texture formation: mapping mode	In the Orthophoto mapping mode the whole object surface is textured in the orthographic projection. The Orthophoto mapping mode produces even more compact texture representation than the Adaptive orthophoto mode at the expense of texture quality in vertical regions	Orthophoto mode was chosen as this produces the best representation of texture over topographical surfaces.
Texture formation: blending mode	Selects the way how pixel values from different photos will be combined in the final texture. Mosaic implies two-step approach: it does blending of low frequency component for overlapping images to avoid seamline problem (weighted average, weight being dependent on a number of parameters including proximity of the pixel in question to the centre of the image), while high frequency component, that is in charge of picture details, is taken from a single image - the one that presents good resolution for the area of interest while the camera view is almost along the normal to the reconstructed surface in that point.	Mosaic was chosen as this gives best results when camera angle is along the normal of the reconstructed surface. It has also been found to be favourable for DEM formation (see DEM construction on Agisoft Photoscan 2016).
Texture formation: size/count	Specifies the size (width & height) of the texture atlas in pixels and determines the number of files for texture to be exported to. Exporting texture to several files allows to archive greater resolution of the final model texture, while export of high resolution texture to a single file can fail due to RAM imitations.	Value used was suggested for DEM construction.

Texture formation: colour correction	The feature is useful for processing of data sets with extreme brightness variation. However, please note that colour correction process takes up quite a long time, so it is recommended to enable the setting only for the data sets that proved to present results of poor quality.	Not chosen as results did not suggest poor accuracies would be obtained.
Orthophoto formation: Surface	Orthomosaic creation based on DEM data is especially efficient for aerial survey data processing scenarios allowing for time saving on mesh generation step. Alternatively, mesh surface type allows to create orthomosaic for less common, yet quite demanded applications, like orthomosaic generation for facades of the buildings or other models that might be not referenced at all.	DEM was used as this was suggested to be favourable.
Orthophoto formation: blending mode	Mosaic implements approach with data division into several frequency domains which are blended independently. The highest frequency component is blended along the seamline only, each further step away from the seamline resulting in a less number of domains being subject to blending. Average uses the weighted average value of all pixels from individual photos. The colour value for the pixel is taken from the photo with the camera view being almost along the normal to the reconstructed surface in that point.	Mosaic was chosen as this is the default setting and is most applicable to the environment under investigation.
DEM formation: source data	It is recommended to calculate DEM based on dense point cloud data. Preliminary elevation data results can be generated from a sparse point cloud, avoiding Build Dense Cloud step for time limitation reasons.	Dense point cloud was chosen to produce best DEM products.
DEM formation: interpolation	If interpolation mode is disabled, it leads to accurate reconstruction results since only areas corresponding to dense point cloud points are reconstructed.	Enabled was chosen as periphery areas needed to be interpolated too.

	With Enabled (default) interpolation mode will calculate DEM for all areas of the scene that are visible on at least one image. Enabled (default) setting is recommended for DEM generation.	

3.4.3 Error Validation Workflow

Error validation was also carried out to ensure error metrics reported in Photoscan were representative of the products produced (Figure 3.20). This was completed in ArcGIS. Figure 3.20 shows a workflow for this process. 10 error validation targets were used in the initial analysis presented in Section 4.2. These targets were selected randomly and different from the targets used in image processing. A DEM and orthophoto of the area was required, along with coordinates for the targets used.

Three error values were examined: MAE (Mean Absolute Error), RMSE (Root Mean Squared Error) and STDEV (Standard Deviation Error). MAE is calculated by deriving the average from a range of squared errors. A higher MAE value will represent a higher error percentage throughout the dataset. RMSE is calculated by working out the order of associated errors and correlating the multiplication of squared errors against the sum of squared errors uniformly. The standard deviation error is an indicator of how spread out the values are for a given dataset; higher values result from datasets which have a larger range of values spread around the mean. These values were calculated for the error validation targets only. These equations are shown below:

$$\mathrm{MAE} = \frac{\mathrm{SAE}}{N} = \frac{\sum_{i=1}^{N} |x_i - \hat{x}_i|}{N} \qquad RMSE = \sqrt{\overline{(f-o)^2}}$$

$\{x_i\}$ is the actual observations

$\{\hat{x}_i\}$ is the estimated or forecasted observations

SAE is the sum of the absolute errors (or deviations)

N is the number of non-missing data points

F is modelled results

O is collected results

(Spider financial 2016 and StatisticsHowTo 2016 for diagrams, see reference list)

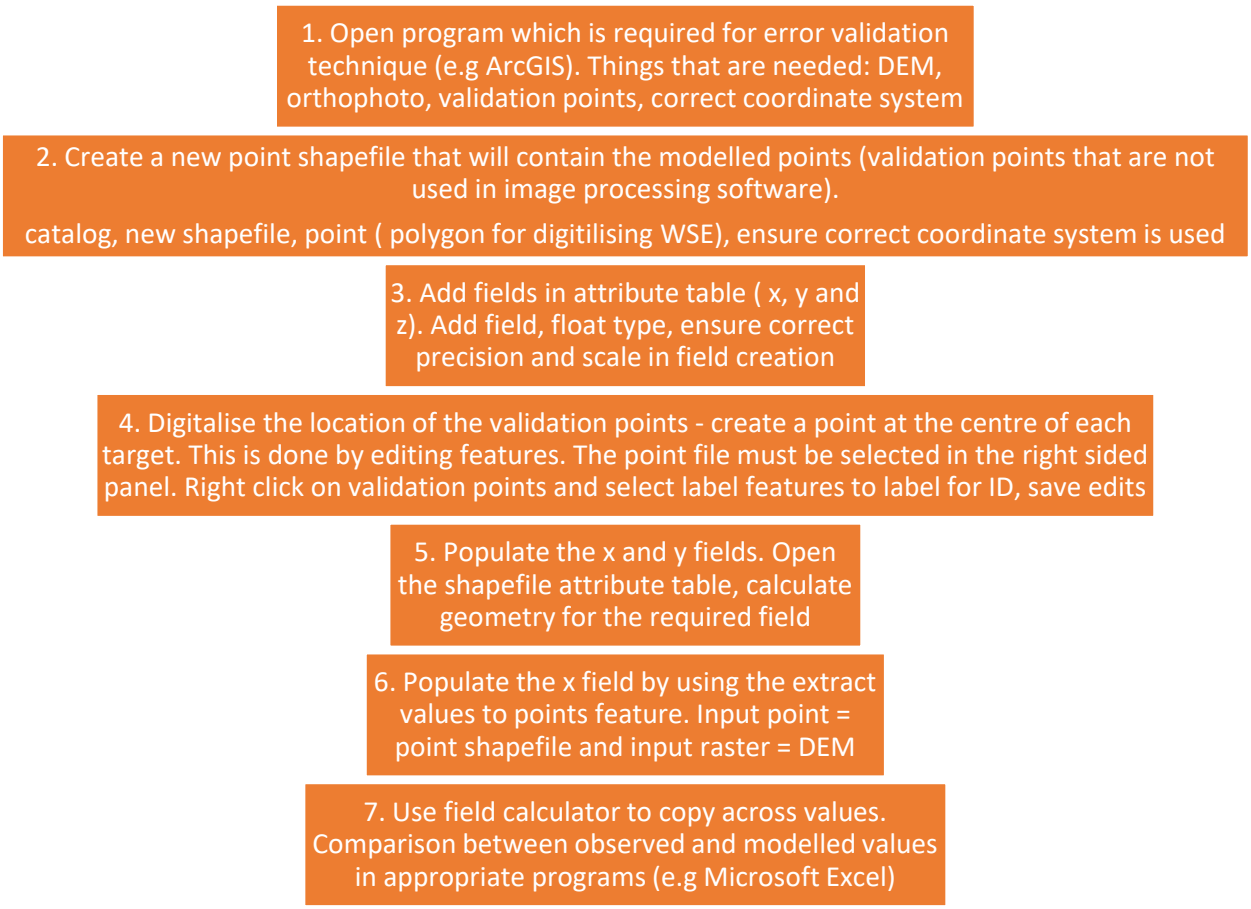

Figure 3.20: Error validation workflow in ArcGIS.

3.4.4 Parameter Analysis

Two parameters were altered in the initial testing of the October 2014 data. These were image overlap and the number of targets within Photoscan.

3.4.4.1 Image Overlap

Image overlap was altered by selecting and deselecting images in the appropriate folders used within Photoscan. Approximate image overlaps were checked using the reports generated from Photoscan (see Figure 3.22). Four approximate image overlaps were used (60, 70, 80 and 90%), while three different models were also examined. Models which started with the number one had one flight line, models which started with the number two had two flight lines, while models which started with three had three flight lines (one of which had oblique imagery of around 14°). The same number of targets were used throughout these experiments (image overlap experiments only), both for GCPs within Photoscan (30) and error validation in ArcGIS (10). Image overlap relates to each flight line; for an approximate image overlap, all flight lines were examined to ensure image overlap was near to the percentage required. It is difficult to reduce the effect of adjacent imagery when differing flight lines are close together, therefore greater image overlap may be induced if similar flight paths were taken. This has been taken into account and minimised during data processing. All flights in October 2014 were flown upstream to downstream. These images were used for initial testing of both parameters.

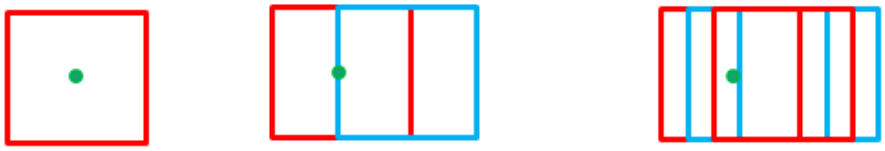

Figure 3.21: Diagram showing image overlap concept. The green dot represents a reference point of known coordinates. The first picture shows a diagram showing one image which is taken 90° to the ground level (horizontal elevation line). A 50% image overlap is presented in the centre picture where two overlapping images share a coherent point with the reference marker. The right picture shows an increased image overlap with more images sharing the coherent point as a reference marker.

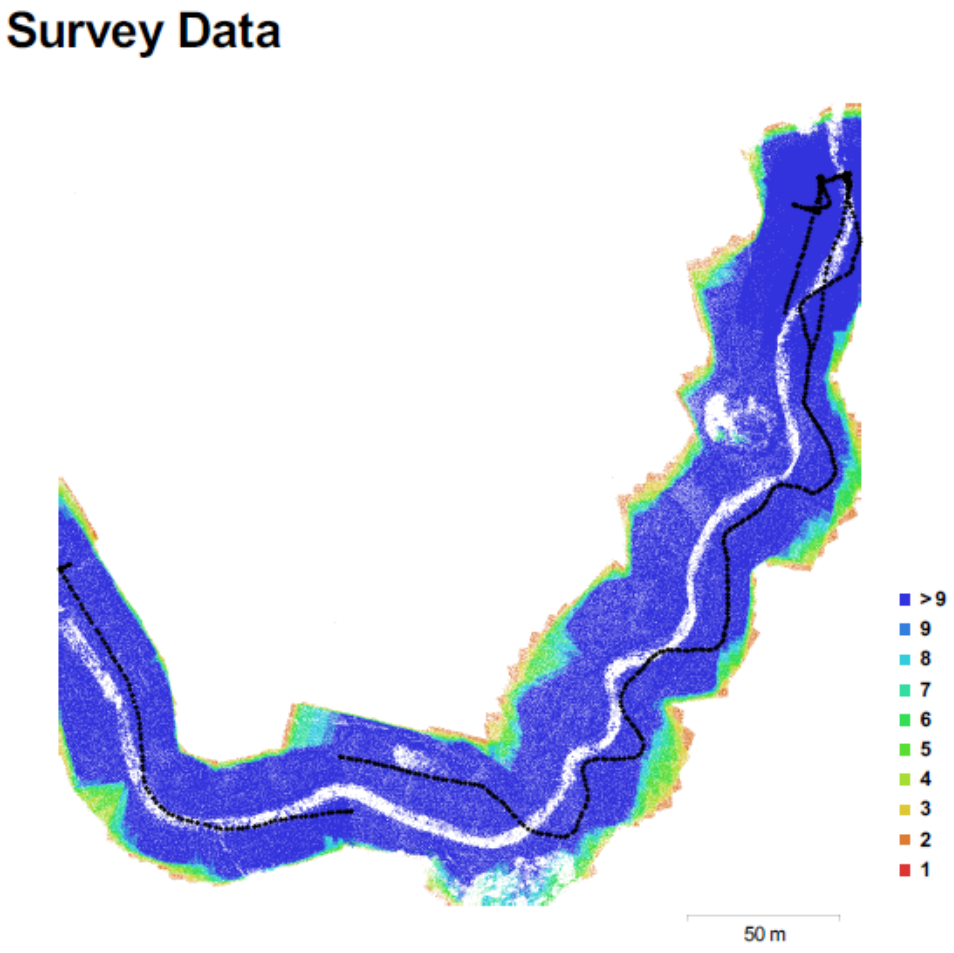

Figure 3.22: Image from report generated from Photoscan to deduce approximate image overlap. This example is from October 2014 using all images available (1 flight line). Numbers on key are the number of images which share a coherent point.

3.4.4.2 Number of Targets

The number of targets used in the Photoscan model was also investigated using the initial data from October 2014. Figure 3.23 shows how targets were arranged for the October 2014 survey. Targets were placed to ensure a complete range of elevations had a georeferenced point. Targets were placed near channel bars and edges, and on channel banks. All experiments used models which had three flight lines and a high image overlap (>90%). Targets were reduced in multiples of three (e.g. 33/30/27/24/21), but 10 error validation targets were still used for all experiments. Validation points were chosen in a random manner, where coordinate GPS points had been taken. A model which used two flight lines and oblique imagery (similar to model 3 within the image overlap experiments) was used and the same spatial area was investigated to ensure validity. All models used October 2014 imagery (same as image overlap experiments) and had a 90% image overlap, as this was found to be the best image overlap value generally in promoting best quality products.

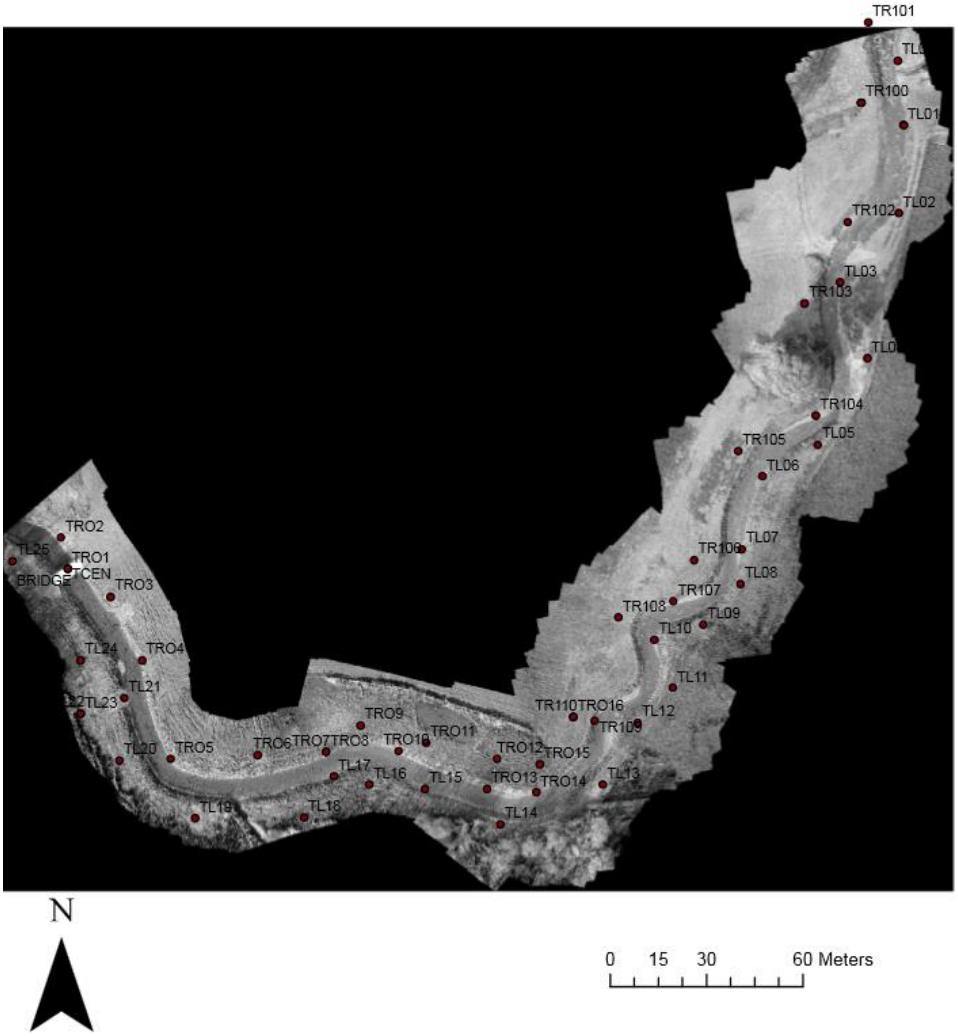

Figure 3.23: Targets used in the October 2014 experiments.

3.4.4.3 March 2015 and July 2015 Data

After initial parameter analysis, best quality DEM products were built using the information gained from the image overlap and target analysis experiments. Details of data collection for March 2015 and July 2015 can be seen in Table 3.2.

3.5 TLS and Cyclone

TLS was also used to compare outputs with the SfM results. A Leica 6100 Geosystems laser scanner was used and data was collected by triangulating corresponding reference points and progressing along the channel in a coherent manner. Each base station had three reference points that radiated from the central "recording" source. The mean error across the complete October 2014 TLS dataset was 0.0018 m. Moving objects, the weather and surface water reflection along with many other variables can all affect the quality of results and were acknowledged and steps were taken to ensure that their influence was minimised during the scanning process. Figure 3.24 shows the scanner used at Whit Beck, while Figure 3.25 shows how targets are placed in a triangular nature to allow a wide spatial extent of the whole area under investigation.

Eleven scan stations were used in the October 2014 TLS dataset, with the original point cloud containing over twenty-four million points. After manual editing, this was reduced to just over seventeen million points. The GIS software cyclone was used to edit the TLS outputs. Cyclone is made by Leica Geosystems and allows 3D point cloud production and analysis. The software costs around £500 a year for a licence and the scanner itself costs approximately £50,000. A TLS dataset for August 2014 was also used that incorporated the entire restoration scheme; this dataset had 29 scan stations. See Smith (2015) for a detailed overview of this technique.

Figure 3.24: TLS hardware used in this investigation along the Whit Beck.

Figure 3.25: Showing how targets are set out when a TLS scan is being carried out to ensure a wide spatial representation. The main scanner is shown in the centre circle, while two targets are shown on the left and right side. The third target was situated 50 m downstream of the arrow on the left side bank (looking upstream).

The TLS data was then converted into a raster file using ArcGIS, a workflow for this technique is presented in Figure 3.26. This raster was then compared to the SfM outputs using the raster calculator function in the program. Two SfM October 2014 products were compared with the October 2014 TLS data. A SfM DEM made using one flight line (model starting with 1) and three flight lines (model starting with three) were compared. A high image overlap was used (>90%) and 33 targets were used in Photoscan.

Further comparisons with the August 2014 TLS dataset were also made. Firstly, a TLS-TLS comparison was undertaken to assess channel change between these two surveys. Comparisons between the August 2014 TLS data and the two SfM October 2014 products (using one and three flight lines) were then investigated and compared with the earlier TLS-TLS comparison.

All TLS comparisons were carried out with the wetted channel area shaded out, as TLS cannot penetrate water. Therefore, this analysis was seen as an indicator of how SfM compared to the TLS datasets.

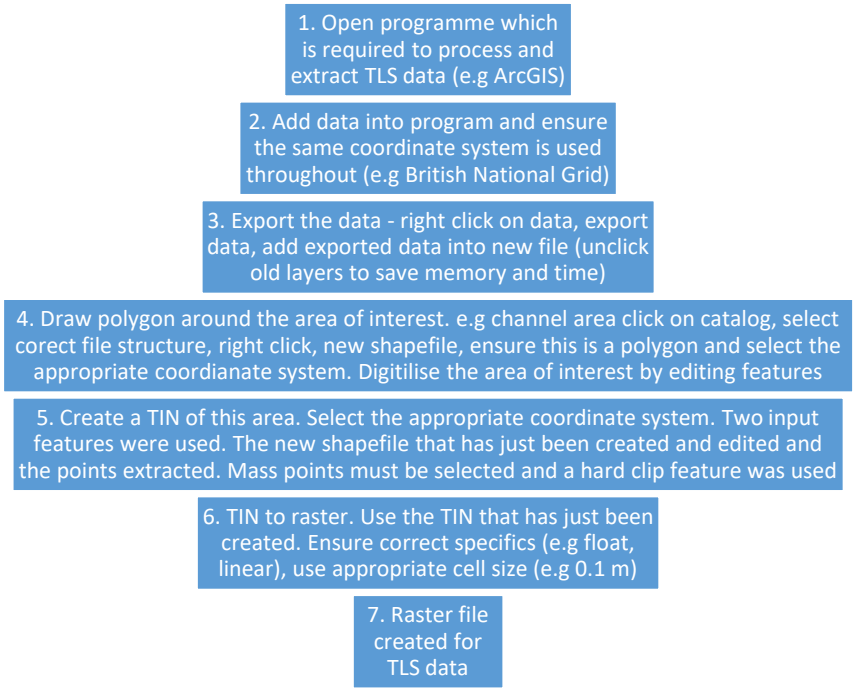

Figure 3.26: Workflow for TLS raster formation.

3.6 Bathymetric Analysis

Bed levels were derived using the technique shown in Figure 3.27 in ArcGIS. SfM alone produces datasets which do not represent wetted areas well and thus to view channel change accurately, this procedure was undertaken. This technique has been used in previous studies (e.g Woodget et al. 2014) with errors found to range between 0.02 and 0.09 m. This was the magnitude of error aimed for in this analysis. Depths inferred were compared with measured depths in the field (using raster calculator for the z field) with the assumption that shallower areas would to be less favourable to this technique. Measured depths were randomly taken in a downstream direction and georeferenced by means of rtk-GPS.

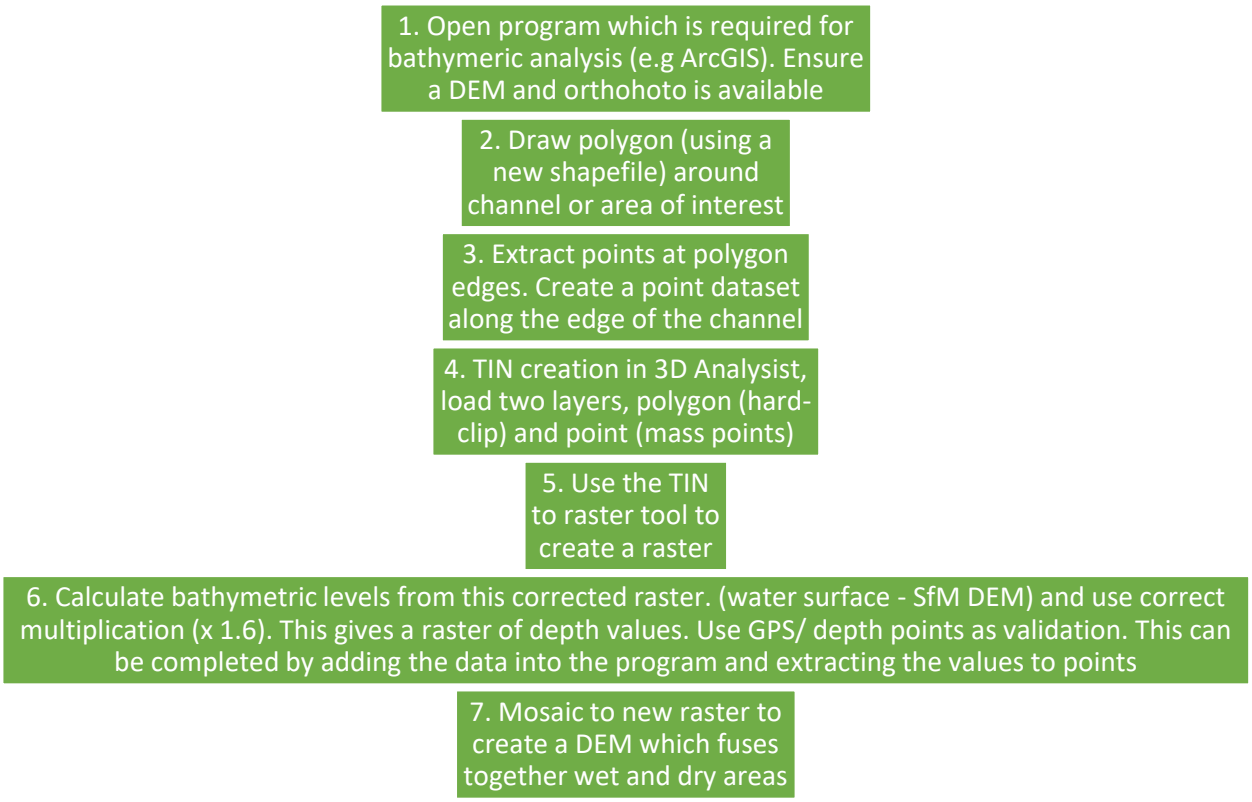

Figure 3.27: Bathymetric analysis workflow. Depth points (measured) were added and compared to the depths derived from this technique.

3.6.1 Mosaicking Wet and Dry Areas

Wet and dry areas were mosaicked together to produce a corrected DEM which was then used in the subsequent analysis (Figure 3.28). A cell size of 0.01 m was used for all products (October 2014, March 2015 and July 2015) and the raster was created using a 32_bit_float cell type in ArcGIS.

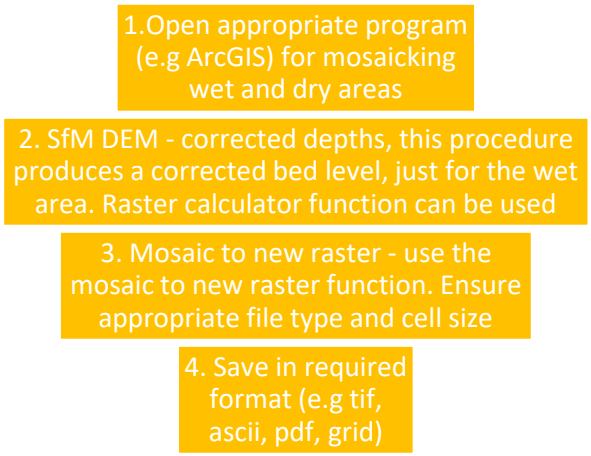

Figure 3.28: Mosaicking workflow.

3.7 DEMs of Difference Methodology

A technique which allows geomorphic differences between surveys to be mapped was undertaken. Corrected DEMs were used and Figure 3.30 shows a workflow for this technique. This was completed by using an additional extension in ArcGIS. The Geomorphic Change detection (GCD) toolbox (Table 3.6 and Figure 3.29) was used to measure change between the October 2014 and July 2015 surveys. These two surveys were chosen as they allowed net morphological change across the entire monitoring period to be attained. An appropriate cell size (0.01 m) and horizontal decimal position (1) was used. Williams (2012) provides a detailed discussion of the use of DoD analysis.

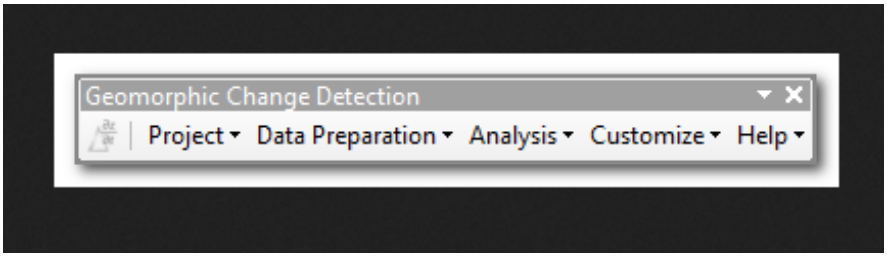

Figure 3.29: Geomorphic Change Detection main menu. Figure from GCD (2016).

Table 3.6: Abilities that can be carried out by the Geomorphic Change Detection Toolbox.

Menu	Options available	Description
Project	New GCD project Open GCD project Close GCD project GCD project explorer Project properties GCD report	General workflow buttons
Data preparation	Clean raster Create bounding polygon Add DEM survey to explorer ToPCAT	Tools available for data preparation before analysis
Analysis	Uncertainty Analysis Roughness Analysis Geomorphic Change Detection	Data analysis available

First, an initial DoD was used to assess morphological change on wet and dry areas using no Minimum Level of Detection (MLD). Different MLDs were then used to assess larger changes in the October 2014 and July 2015 DEMs. MLDs of 0.05 m, 0.20 m, 0.50 m and 1.00 m were examined which allowed a better understanding of the changes seen over the monitoring period.

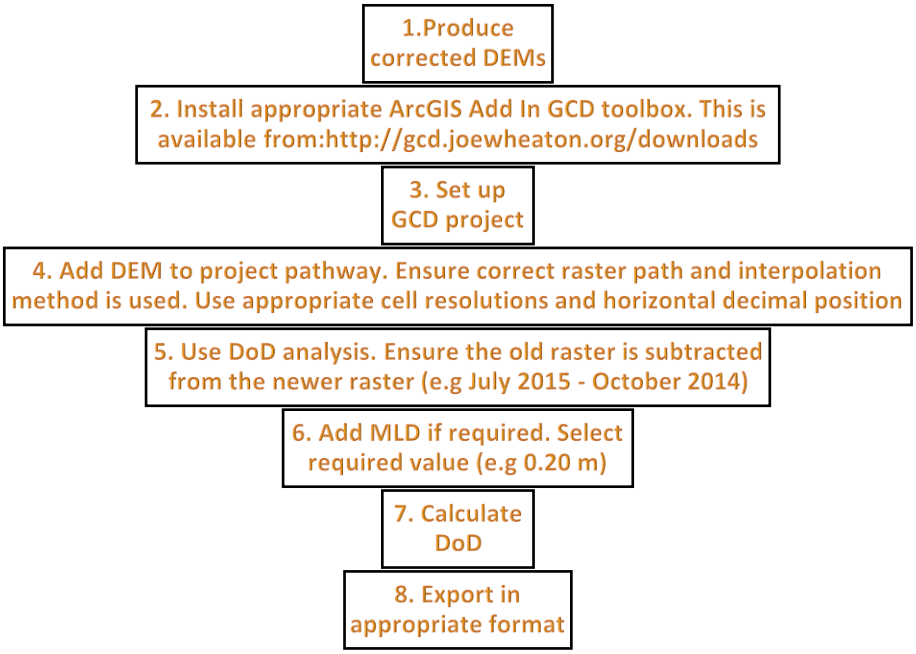

Figure 3.30: DoD workflow.

3.8 Flood Modeller Modelling (formerly called ISIS 2D modelling)

Flood Modeller hydraulic modelling software was also used to map geomorphic units. Rasters were converted to ASCII format to be usable within the Flood Modeller software. Table 3.7 shows some of the parameters used in this modelling, while Figure 3.31 shows a workflow for the 2D modelling. Modelling was initially carried out on the October 2014 data. Further modelling using the July 2015 outputs was undertaken to assess how geomorphic units varied. All models were run to a steady state and results were exported to produce mapped products.

The software developed by CH2M allows differing flood scenarios to be mapped along areas of interest. 1D and 2D modelling can be carried out and the software used for this investigation along the Whit Beck; allowed up to 100,000 2D ADI, TVD and FAST cells to be incorporated into the modelling program (if required). This allows a range of spatial and temporal scales to be examined. Flood Modeller can also be used for a number of different applications including 1D and 2D floodplain modelling, floodplain mapping, flood forecasting and peak values, dam breach analysis, blockage designs and environmental checks (Flood Modeller 2016).

Figure 3.32 shows the peak flows from the Environment Agency (2013) modelling report on the Whit Beck. Peak flows for a return period of 2 years range between 8 -13 m^3/s. The aim of the modelling was to replicate baseflow conditions along the section of river. Although, the report uses the old channel for modelling, it is the only data available and was used to help select input flows into the model. For this analysis, it was assumed baseflow was approximately one sixth to one eighth of a two-year return period. Total flows of 1,2,4 and 6 m^3/s were selected and used as input values into the model.

Table 3.7: Parameters used in the Flood Modeller modelling.

Parameter	Value	Description (from Flood Modeller Manual)	Justification
Simulation length (hours)	1	The modelled simulation length	This simulation length was chosen as it gave an adequate precision and did not require long waiting times (less than 2 hours)
Grid size (m^2)	0.2 x 0.2	The size of each cell within the model (wet and dry areas)	This was decided by balancing time requirements and modelling accuracy
Time step (seconds)	1	The minimum time interval for modelled data	This was decided by balancing time requirements and modelling accuracy
Roughness value (Manning's)	0.05	The roughness value given to the modelled area.	This was the default figure suggested by Flood Modeller for DEM modelling
Upstream boundary (Total flow m^3/s)	1,2,4 and 6	The input upstream boundary flow	These values were chosen by using the data from the River Cocker at Low Lorton and Whit Beck at High Lorton modelling report (Environment Agency 2013). Peak flows range from between 8-13 m^3/s for a 2-year return period. Please note this report was on the old Whit Beck channel
Downstream boundary (normalised depth / m)	0.05	The downstream output flow	This was suggested to keep the model running at a steady state
Number of cells used	68461	The number of cells within the spatial extent modelled (wetted area)	The exact value was not chosen, however the study aimed to provide around 60,000 cells per simulation. This was chosen in regard to modelling accuracy and time requirements
Memory usage (per simulation) (MB)	671	The data used for each simulation (average)	The exact vale was not chosen; however, the aim of the study was to reduce computer time requirements when possible
Solver Scheme	ADI	The solver scheme used to model the area under investigation.	The ADI solver was suggested in the Flood Modeller manual as best for DEM modelling at the Whit Beck

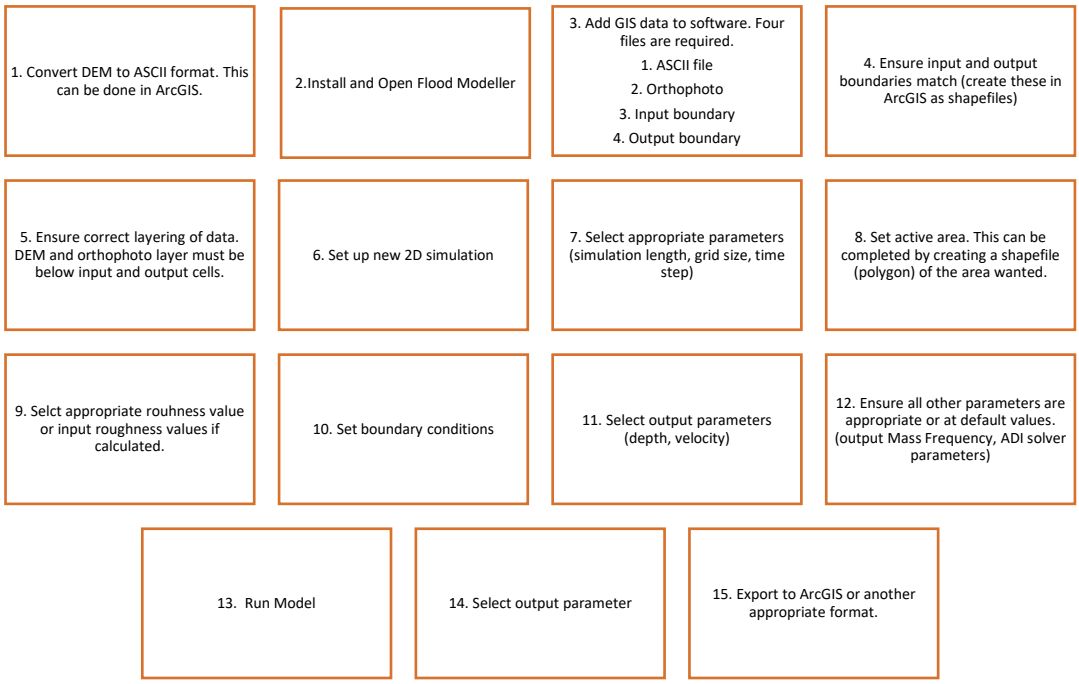

Figure 3.31: Flood Modeller workflow.

	Whit Beck Peak Flows (m^3/s)		
Return period (years)	2008 study	2012 study	This study
2	8.3	12.9	12.0
5	10.8	16.6	15.5
10	12.4	19.6	18.0
50	16.7	26.7	24.5
75	18.8	30.8	26.4
100	22.0	35.8	27.9
1,000	32.9	52.2	47.2

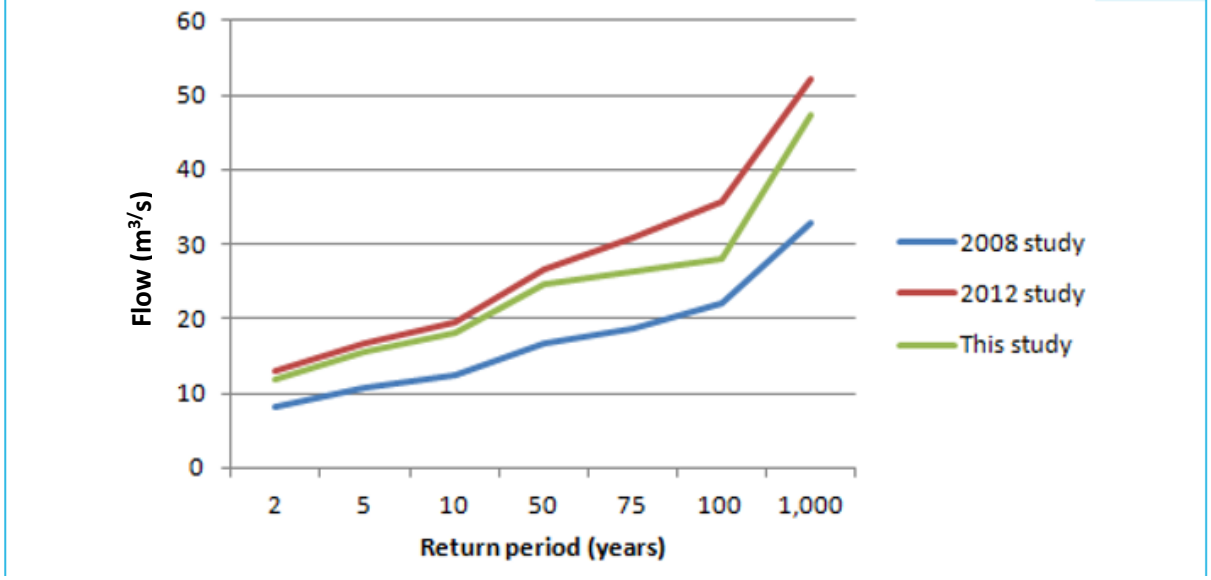

Figure 3.32: Data from the River Cocker at Low Lorton and Whit Beck at High Lorton – modelling report (Environment Agency 2013). Peak flows range from between 8-13 m^3/s for a 2-year return period. Please note this report was on the old Whit Beck channel.

3.9 Study Justification

This project is significant as it aims to evaluate the use of SfM as a tool for the monitoring of morphological evolution of one river restoration scheme (Whit Beck, West Cumbria) over a considerable temporal (10 month) and spatial scale (hundreds of meters). A clear set of criteria will be established to enable an evaluation of whether restoration schemes can to be monitored effectively using a low cost approach. An overview of the feedback mechanism that enables constant improvement in restoration schemes is shown in Figure 3.33. This is underpinned by gaining detailed and appropriate knowledge of catchment-scale processes which then can be acknowledged and incorporated into future projects. It is also important to realise that river evolution and system development can happen on a variety of interconnecting levels. This project will be using novel techniques and it is hoped that the results shown will be used to guide further restoration modelling studies. Restoration monitoring has been acknowledged as an integral and important factor in providing growth within the area of fluvial sciences and understanding how restoration schemes are likely to evolve in the future is of major importance.

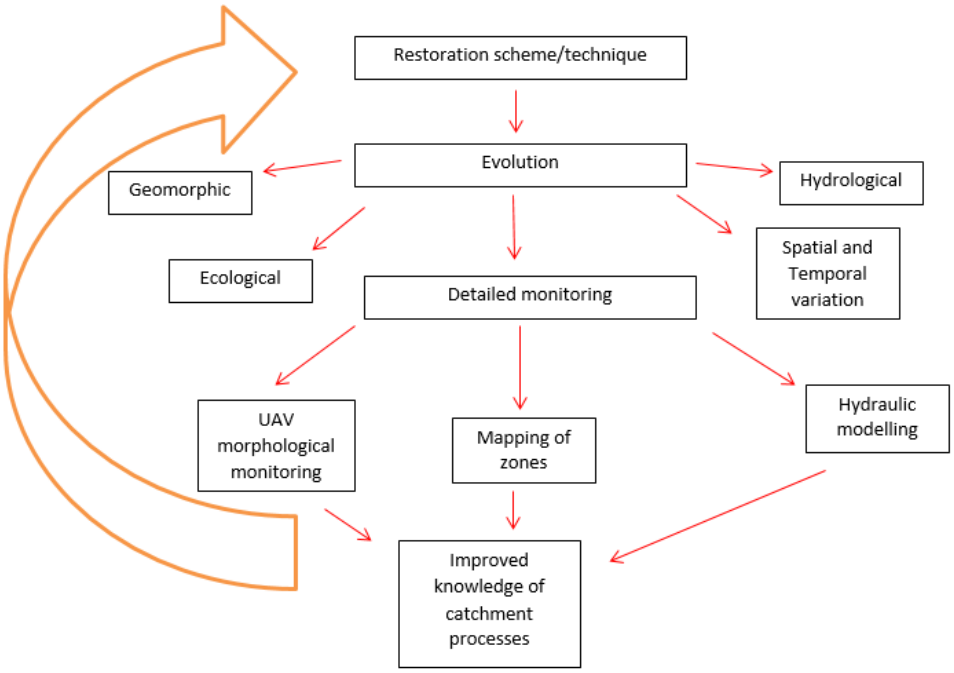

Figure 3.33: Showing how an improved knowledge of catchment-scale processes can be gained and fed back into improving future restoration schemes.

3.9.1 Why was the Whit Beck chosen?

The site was chosen as it is an area of specific interest within Cumbria and the wider river restoration community. Whit Beck was chosen to evaluate the use of UAV (Unmanned Aerial Vehicles) surveys as it allowed the technology to be adequately tested and examined efficiently over a 10-month period. The main focus of this thesis is on the evaluation of the workflows presented, rather than the morphological evolution at the Whit Beck site.

The site is a pioneering restoration scheme within the UK and have had a lot of regional and national attention (see links to BBC (2014) and ITV (2016)) due to the strategies employed at the site and the possible advantages to both biological and hydrological relations within the area. Finally, the project links to the WFD (Water Framework Directive) and highlight the growing importance that this has as a primary and direct driver of river restoration within the

UK. The original straight channel failed the WFD ecological status and this was seen as an important driver in implementing the strategies developed on site.

3.10 Conclusion

An overview of the Whit Beck restoration site was discussed. A range of environmental characteristics were examined including topography, geology, flood risk, groundwater conditions and land use. A range of techniques have been described which were used in this thesis to evaluate the use of the SfM technology in a monitoring of river restoration capacity. Workflows have been presented which show detailed steps in the methods used and these can act as a guideline for repeat data acquisition. By using a range of appropriate methods, a detailed evaluation of the SfM procedures could be attained.

Chapter 4: Parameter Analysis, TLS Comparisons and Bathymetry

4.1 Introduction

This results chapter consists of three components. First, an analysis of image overlap and target numbers is presented, to establish the characteristics of improved orthophoto and DEM production and to determine how subsequent data can be used most effectively in further data processing (Section 4.2). The products created are then compared to TLS outputs from August 2014 and October 2014 in order to evaluate the two different techniques (Section 4.3). Lastly, bathymetric correction is carried out in order to map bed levels across the SfM DEM (Section 4.4).

4.2 Parameter Analysis

4.2.1 Image Overlap

Image overlap investigations were carried out to determine the optimum percentage overlap required to induce best quality products from the SfM workflow. The specifics of these investigations were outlined in Sections 3.4.2, 3.4.3 and 3.4.4. The purpose of these experiments was to enable a better understanding of the parameters which control DEM and orthophoto production to subsequently produce best quality outputs for all campaigns investigated along the Whit Beck.

4.2.1.1 Ground Control Point Errors

A DEM showing the output produced for the 90% overlap using three flight lines can be seen in Figure 4.1. A corresponding orthophoto of this area is shown in Figure 4.2. Model 1 shows that errors were lowest when a 90% image overlap was used (Figure 4.3a). Mean errors of 0.006 m (x), -0.002 m (y) and -0.003 m were calculated for model 1 (90% image overlap). Highest errors for 60 and 70% image overlap were seen in the z field with values of 0.024 m and 0.037 m respectively.

Unlike models 1 and 3, results for model 2 show varied error values which show no clear pattern (Figure 4.3b). High z mean values can be observed for image overlaps of 60, 70 and 90%. The lowest combined error reported was for an image overlap of 80% where error values were 0.007 m (x), - 0.016 m (y) and 0.008 m (z).

The introduction of oblique imagery seems to produce datasets with lower error values across all image overlaps and throughout all three axes. Model 3 shows errors which are lower than any reported in both models 1 and 2 (Figure 4.3c), (apart from model 2 80% image overlap). An image overlap of 90% has the lowest combined error, however little difference can be

observed throughout the experiments with model 3. Errors in the y field seem large compared to corresponding x and z errors with values ranging from 0.018 m to -0.023 m. An image overlap of 90% is associated with the lowest errors in the x and z field.

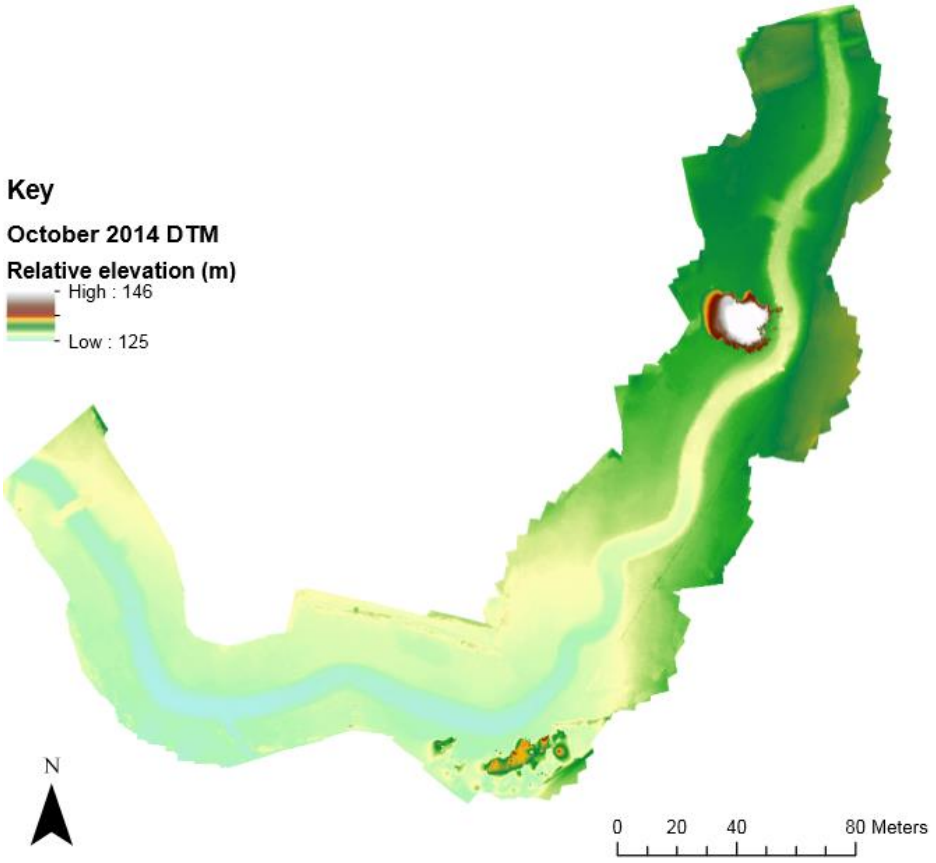

Figure 4.1: A DEM of Whit Beck for October 2014 using three flight lines (including oblique imagery) at a 90% image overlap.

Figure 4.2: An orthophoto of the October 2014 SfM dataset using three flight lines (including oblique imagery) with a 90% image overlap.

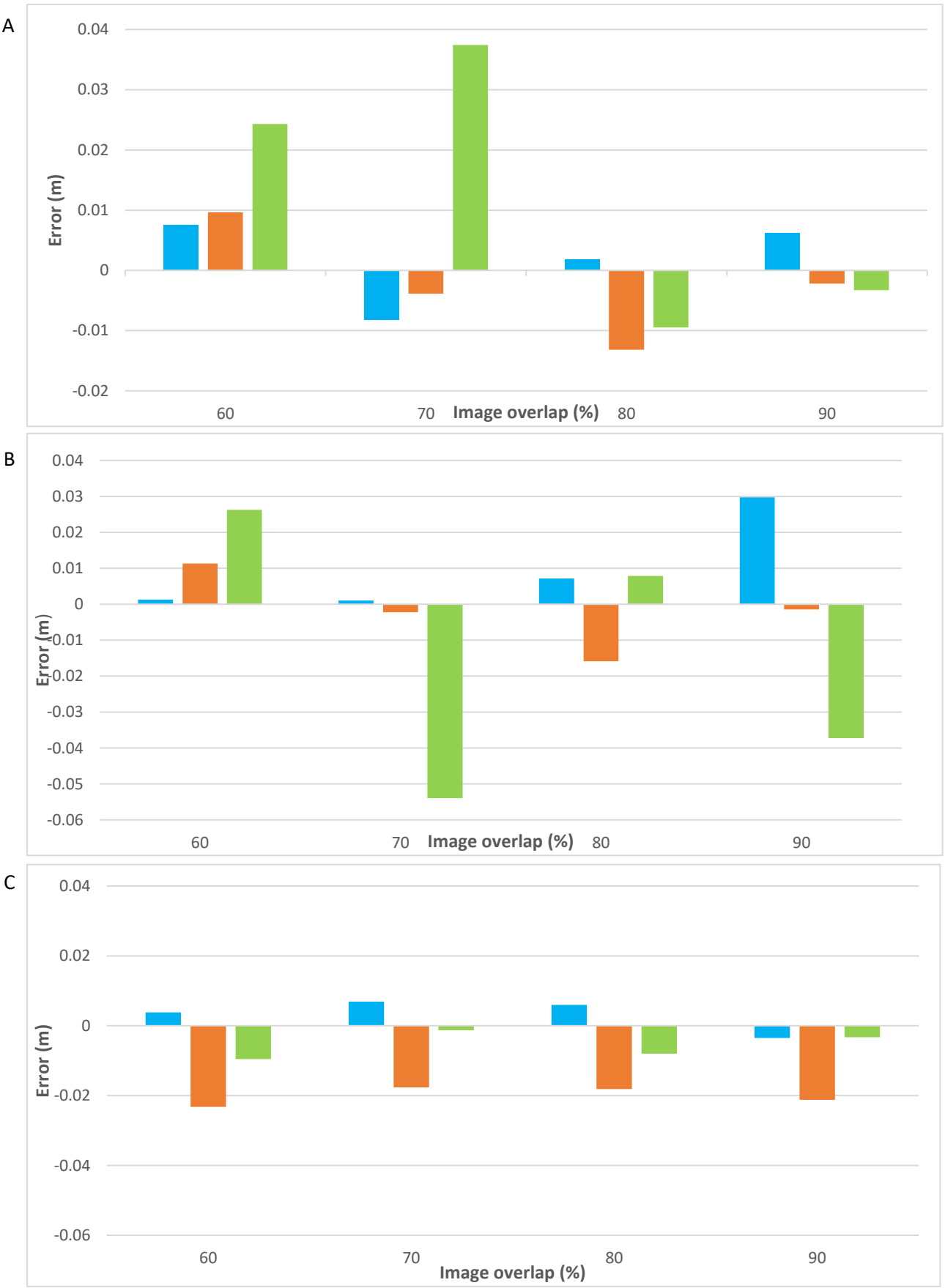

Figure 4.3: Errors at different image overlaps for a. model 1, using one flight line; b. model 2, using two flight lines and c. model 3, using three flight lines. The x, y and z axes are shown in blue, orange and green respectively.

In summary, the results indicate that the addition of oblique imagery into the dataset reduces error values across all image overlaps, despite the relatively large errors in the y axis as compared to the x and z axis. An increased image overlap is likely to reduce errors in all three fields as highlighted by the error statistics associated with model 1 (90%) values, model 2 (80%) values and model 3 (90%) values. Based on the results, models with a high image overlap of 90% were used in the subsequent data processing, while the inclusion of oblique imagery was also seen as important in promoting a reduction in errors in all fields. A table showing all error values for all image overlap tests is shown in Appendix II.

4.2.1.2 Check Point Errors

Further error analysis was carried out on the image overlap experiments to assess the reliability of any conclusions made. Details of this error validation process can be seen in Section 3.4.3. Figures 4.4a, 4.4b and 4.4c shows the results for MAE, RMSE and standard deviation error respectively.

Figure 4.4a indicates that lower MAE values tend to be associated with higher image overlaps for all three models under investigations (little variation seen with model 3 results). The lowest errors were seen with model 3 (three flight lines, including oblique imagery), while larger errors were seen with higher image overlaps for models 1 and 2 respectively. A similar trend can be observed when RMSE is analysed for differing image overlaps and models (Figure 4.4b). Higher image overlaps have lower RMSE values as a general trend, however specifically for model 3, RMSE values for a 70 and 80% image overlap are lower than the corresponding value for a 90% image overlap. The highest RMSE value obtained was for model 2, 60% image overlap. Lower standard deviations can be associated with higher image overlaps, specifically for models 1 and 2 (Figure 4.4c). Model 3 has similar standard deviations throughout the four image overlaps investigated, which suggest that the error values are closer together than other model results. The largest standard deviation values were found with lower image overlaps (60 and 70%) with models 1 and 2.

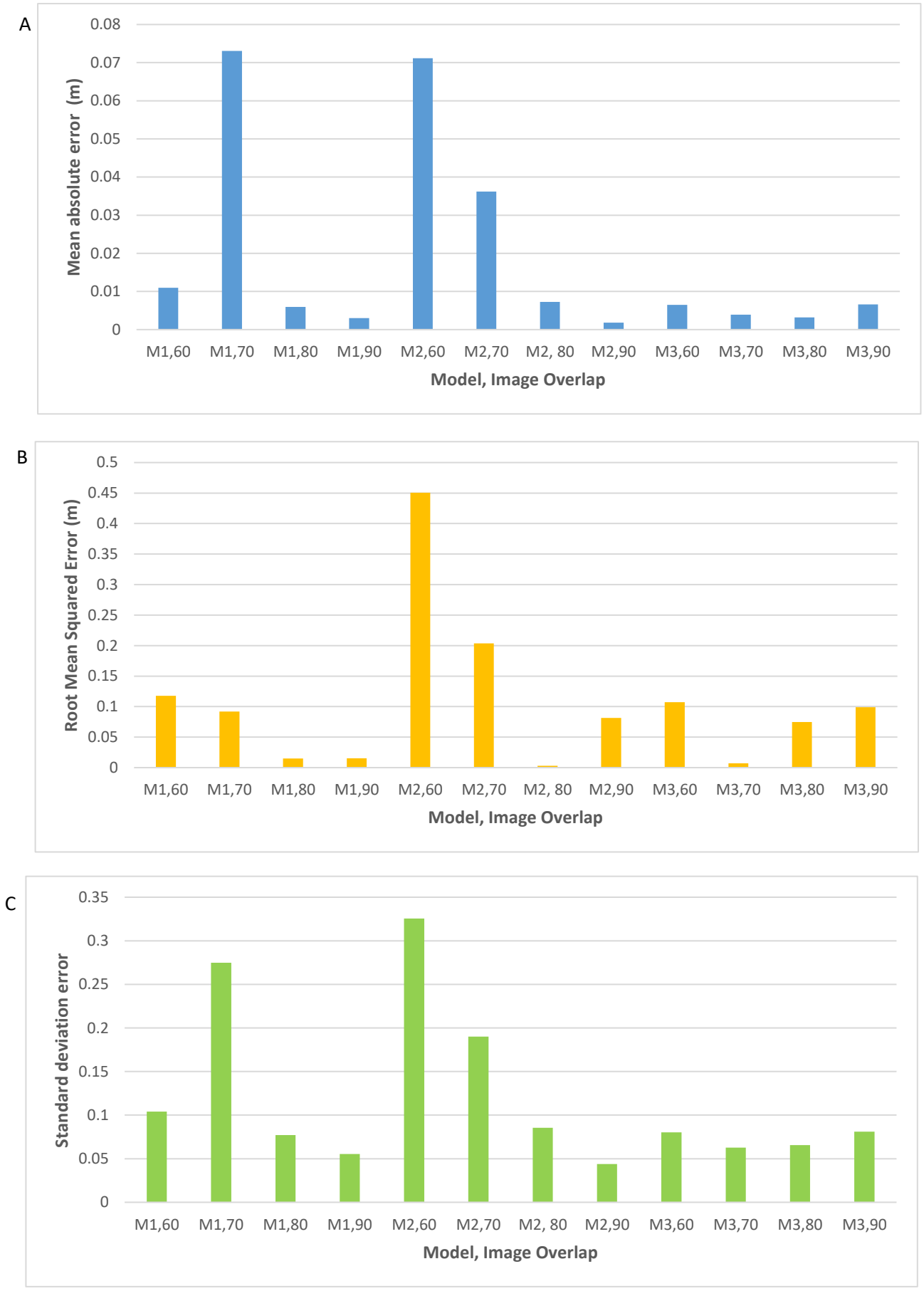

Figure 4.4: MAE, RMSE and Standard deviation for the image overlap tests. a. MAE, b. RMSE and c. standard deviation. M1, M2 and M3 represent models 1, 2 and 3 respectively.

4.2.1.3 Summary – Image Overlap

The experiments suggest that higher image overlaps result in lower error values throughout the dataset (x, y and z field). Lower error values are seen when higher image overlaps of 80 - 90% are used and thus this represents the best possible conditions for DEM and orthophoto production. The presence of oblique imagery within model 3 also results in a reduction in errors compared to other models (models 1 and 2), and can be seen as an advantage in the production of better quality outputs.

4.2.2 Target Analysis

The second parameter that was investigated was the influence of number of targets on orthophoto and DEM quality. As discussed, (Section 3.4.2), data was processed using the highest quality settings within Photoscan to ensure the best possible error results. Error validation was also carried out (Section 4.2.2.2).

4.2.2.1 Ground Control Point Errors

Models with a larger number of targets induce a reduction in mean errors (Figure 4.5). 33 targets had the lowest combined error with values of 0.005 m (x), 0.018 m (y) and 0.014 m (z). A gradual reduction in errors can be seen in both the x and y axis errors as the number of targets within a model increases. Although lower combined errors can be associated with increased number of targets (33), lower z axis values can be observed for models with fewer targets (15, 18, 21 and 24). These error values range from 0.005 m to 0.007 m.

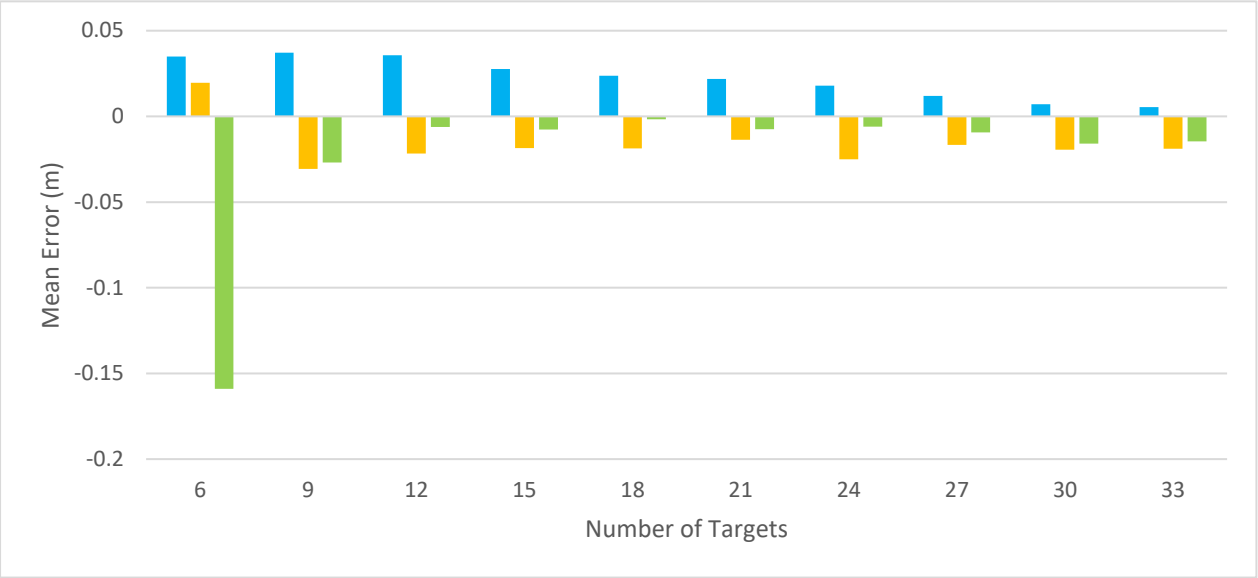

Figure 4.5: Mean errors when differing number of targets are used. The x, y and z axes are shown in blue, orange and green respectively.

The results show that mean error reduces as the number of targets within the model increases. Nevertheless, variation can be seen, specifically in the z field. It is suggested that to ensure best possible outputs, a large number of targets should be used. The results strongly support the notion that an increased number of targets is likely to have a positive influence over output quality.

4.2.2.2 Check Point Errors

Further error analysis was carried out on the target experiments to assess the reliability of any conclusions made. Three error values were examined; MAE (Mean Absolute Error), RMSE (Root Mean Squared Error) and STDEV (Standard Deviation Error) (Figures 4.6a – c). A table showing all target analysis errors can be seen in Appendix II.

MAE was seen to be more uniform when more targets were used for data processing (Figure 4.6a). Error values seem constant between models 15 to 33 with similar MAE values calculated. The model with 21 targets had the lowest MAE value with a figure of 0.0036 m. RMSE shows that a model with 21 targets has the lowest error statistic (Figure 4.6b). This goes against initial notion that an increased number of targets within a model will result in lower error values across the three axes. Models with 30 and 33 targets had higher RMSE values than corresponding models with 24 and 27 targets. Standard deviation is uniform throughout all target analysis carried out, except at lower target numbers (especially 6 and 9) (Figure 4.6c).

A

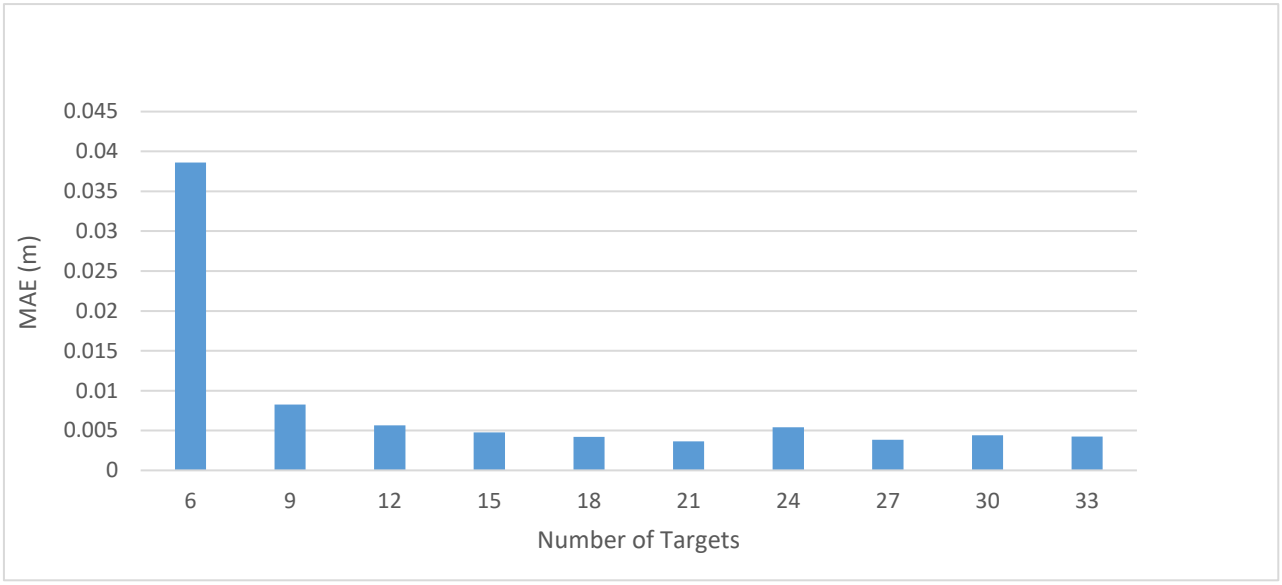

B

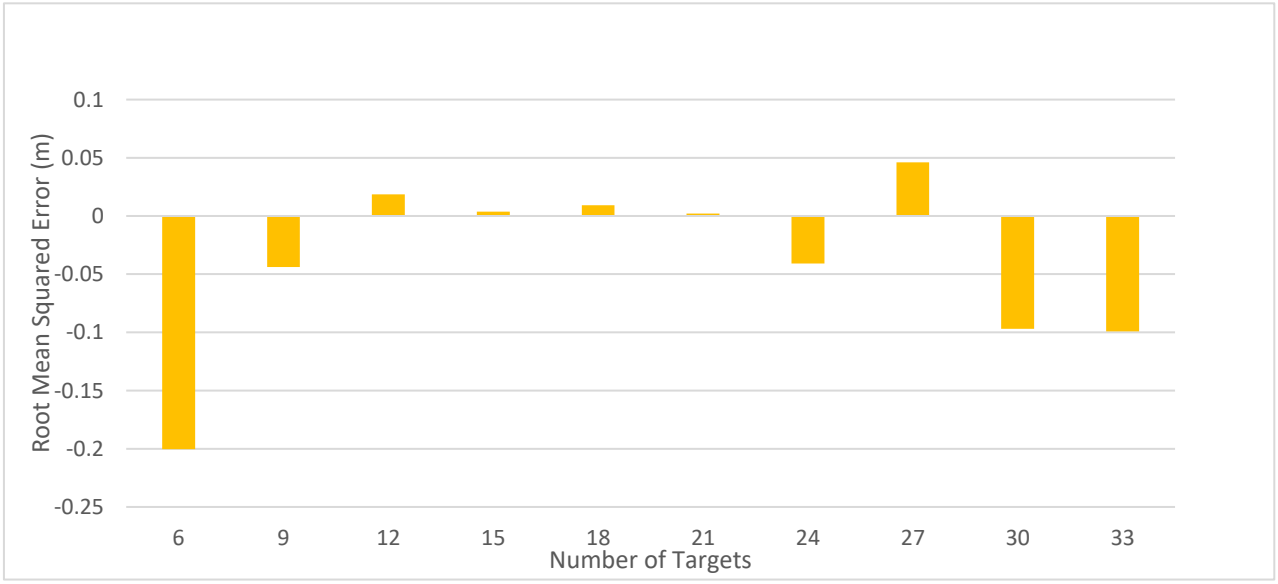

C

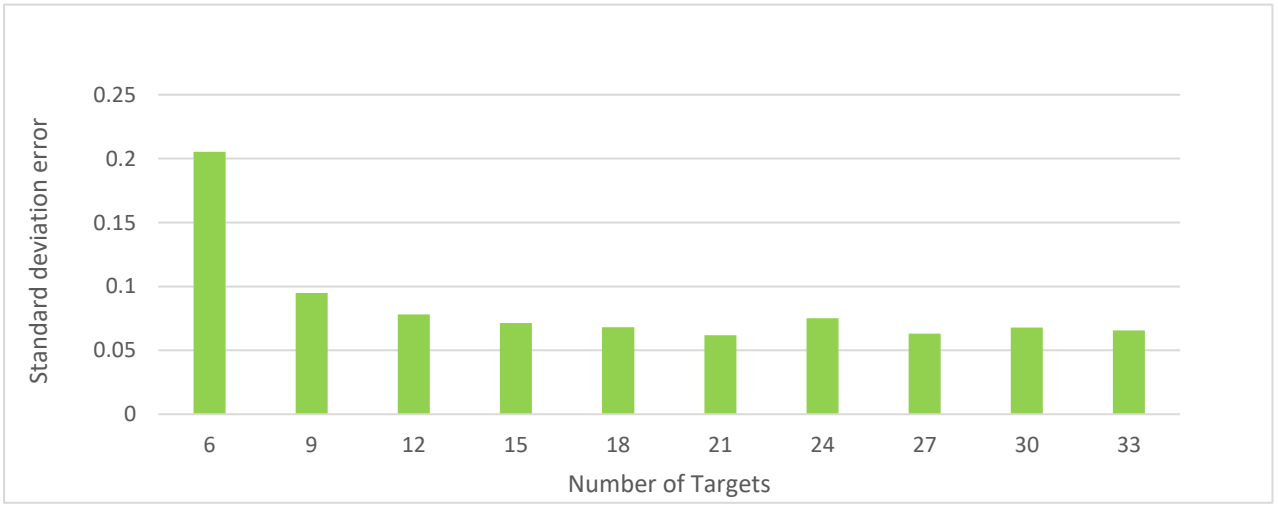

Figure 4.6: a. MAE (Mean Absolute Error), b. RMSE (Root Mean Squared Error) and c. STDEV (Standard deviation error) for target analysis tests.

4.2.2.3 Summary-Target Analysis

The target experiments have provided an insight into how the number of targets influence output quality. Results suggest an increased number of targets within a model can significantly reduce error values in all fields (x, y and z), but variation within the z field can be noted. Highest error values can be associated with models which have fewer targets within them. A higher probability of reduced errors exists when using more targets within a model. Error validation would suggest that a model with 33 targets will produce best quality orthophoto and DEM production resulting in fewer errors being propagated into subsequent datasets and processing. However, variability can also be acknowledged, specifically with the RMSE values.

4.2.2.4 Image Overlap and Target Analysis Conclusions

The image overlap and target experiments suggest that to increase the probability of best quality outputs, a high image overlap should be utilised in conjunction with a high number of targets. The presence of more than one flight line can also be seen as an advantage, while oblique imagery has been seen to reduce errors significantly (model 3, 90% image overlap).

In the subsequent analysis, this knowledge has been used to construct the best possible products to best represent the processes and features under investigation. In the following sections, a brief overview of the datasets for October 2014, March 2015 and July 2015 are provided. All data is for Whit Beck and shows the same spatial areas as discussed throughout earlier analysis.

4.2.3 March 2015 and July 2015 Data

To build the best quality March 2015 and July 2015 SfM products. a 90% image overlap was used for mesh construction, and as many flight paths as possible (and oblique imagery) were incoparated into the data processing. A discussion is presented on the March 2015 and July 2015 data and for comparison, the same spatial area as the October 2014 dataset is used to allow bed level and DoD analysis. All products were made using the same resolutions (0.01 m) and target configurations as October 2014 to allow adequate comparisons to be made.

4.2.3.1 DEMs

Figures 4.7 and 4.8 show DEMs and orthophotos of the March 2015 and July 2015 data. Errors are presented in Figure 4.9. A table showing all error values is shown in Appendix II. The lowest (mean) combined errors were seen in July 2015 with values of -0.00312 m, -0.00364 m and -0.00572 m for the x, y and z fields respectively (Ground Control points). The highest combined errors were seen in the March 2015 dataset (Figure 4.9). Y axis fields had the highest errors on average across the three surveys, but the z field was highest for the July 2015 data.

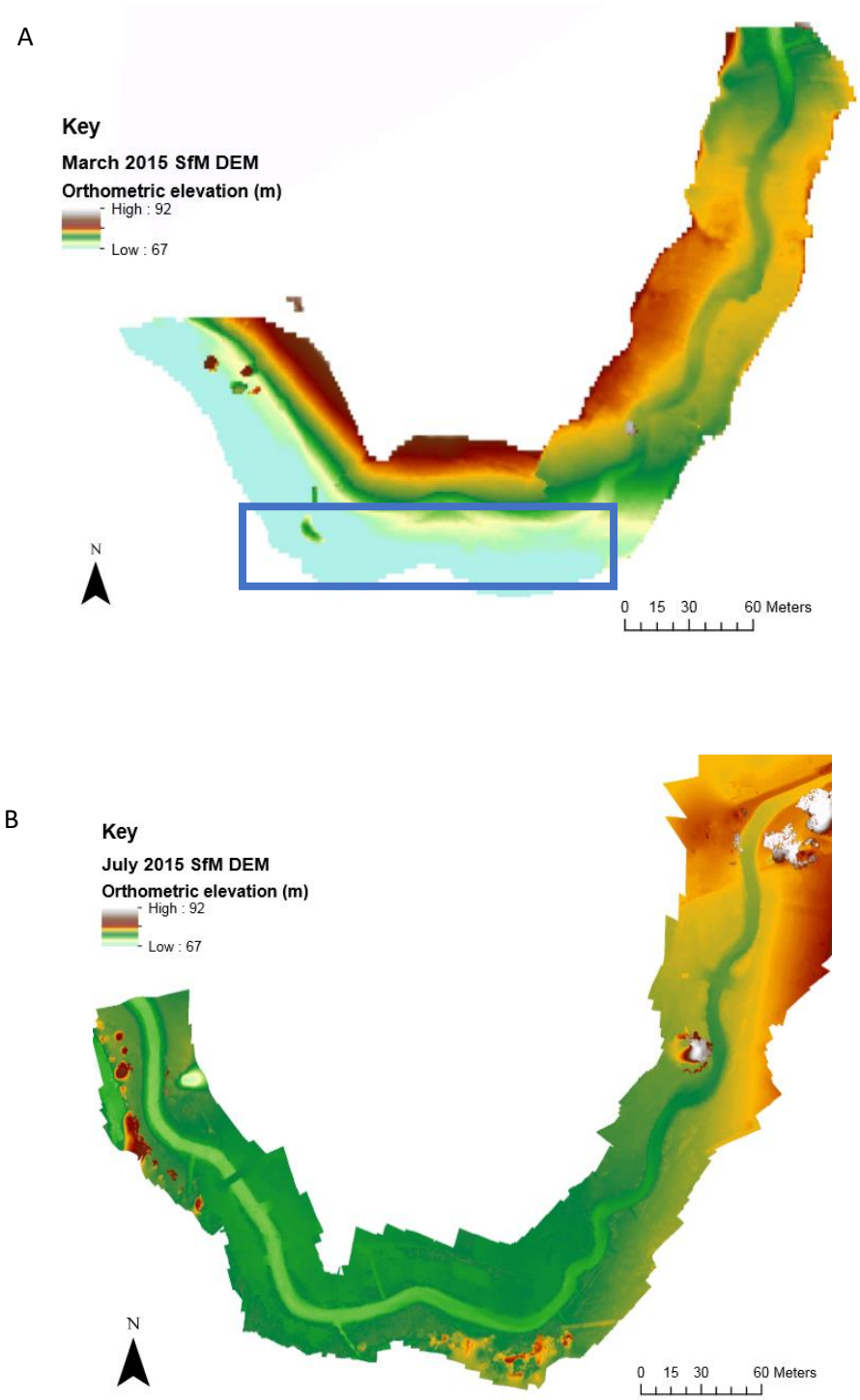

Figure 4.7: DEMs for a. March 2015 and b. July 2015. Scale has been enlarged to make viewing clearer, same scale for both figures. The blue box shows an area of the March 2015 DEM which shows elevation values which are not in agreement with the other DEMs (October 2014 and July 2015), shade and tree cover are given as possible reasons for this. No DoD calculations were carried out using the March 2015 data as a result. This blue box is also shown in Figure 4.8a.

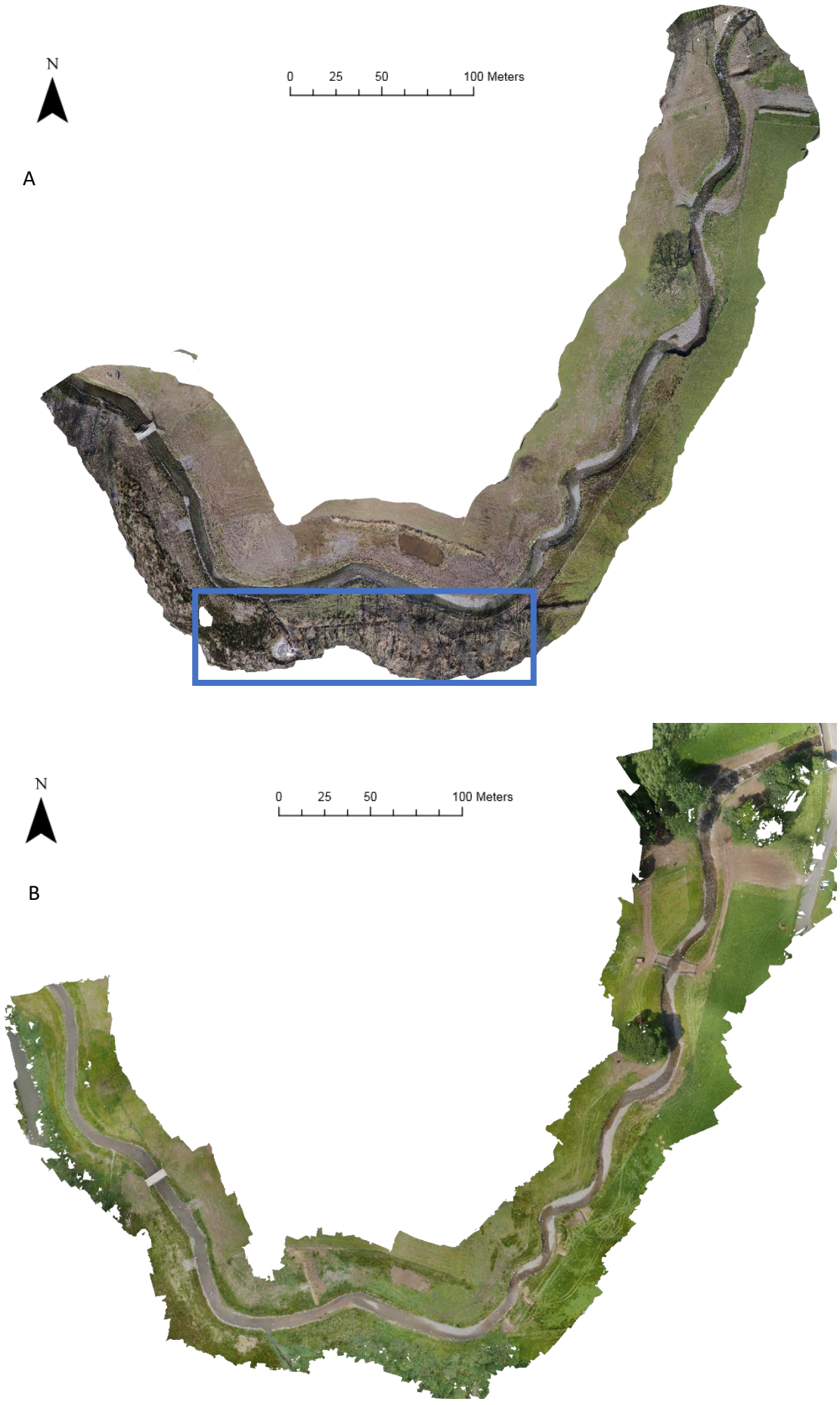

Figure 4.8: Orthophoto for a. March 2015 and b. July 2015.

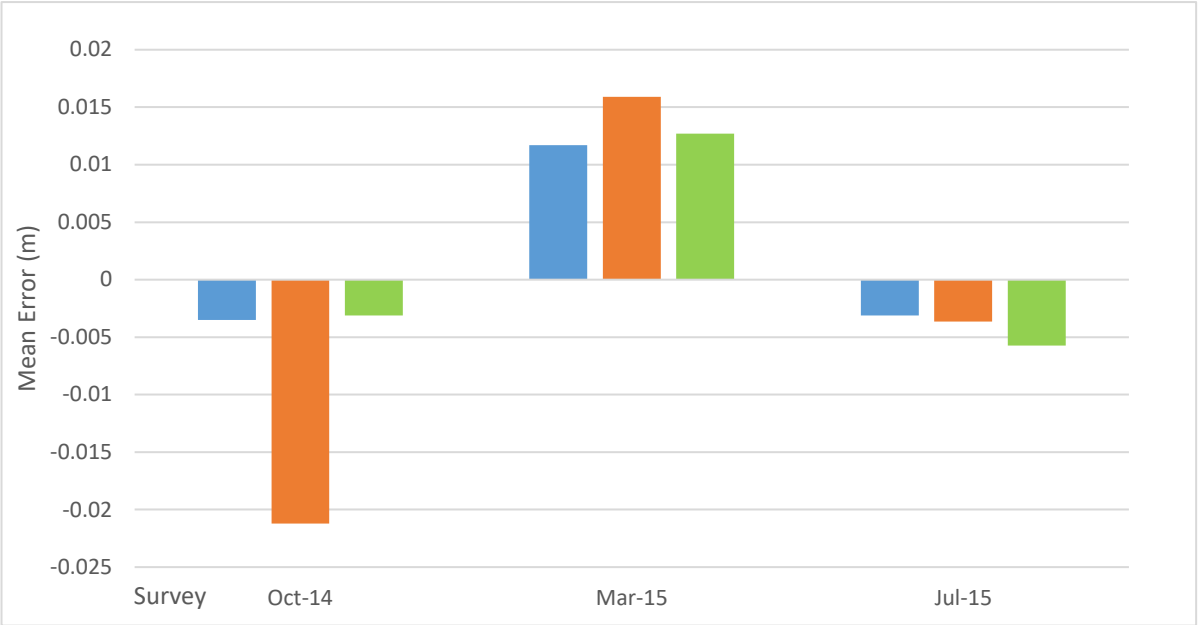

Figure 4.9: Mean errors in the x, y and x field for the three surveys. The x, y and z fields are shown in blue, orange and green respectively. Values are Ground Control points with no error validation. All had the same number of targets and a high image overlap.

4.2.3.2 Summary

Further data processing outputs for March 2015 and July 2015 are presented and compare adequately in quality with October 2014 data. July 2015 had the lowest combined errors across all three fields, while March 2015 had the highest combined errors seen. By examining the orthophotos, geomorphic variation throughout the temporal period under investigation is apparent across the monitored area.

4.3 TLS Comparisons

To assess the errors in the SfM data across a spatially extensive area, a comparison with TLS data was carried out. This would allow a fair assessment of the SfM data to be attained and thus determine the effectiveness of the technique against data of a known vertical error quality.

4.3.1 TLS Data

TLS data from August 2014 and October 2014 were used in the subsequent discussion. Details regarding the error characteristics of these data can be seen in Section 3.5. First, a comparison of the October 2014 TLS dataset was carried out against October 2014 SfM products. Earlier experiments concluded that a high image overlap produced a reduction in error values in all three fields (x, y and z) and thus two SfM products (both October 2014) were compared with the TLS data.

A SfM DEM which had a 90% image overlap and the inclusion of three flight lines (including oblique imagery) was used. This was created using 33 targets and was measured using the error validation technique outlined in Section 3.4.3. A second SfM DEM was also compared which used only one flight line, but otherwise used optimum conditions (33 targets were also used with this model and a 90% image overlap was used). Errors were of the same magnitude as reported in earlier discussion. The purpose of using two SfM outputs was to assess the importance of additional flight lines and oblique imagery. It is also important to acknowledge that all TLS data used for comparisons consisted of z minimum values.

In addition, data from August 2014 were also investigated to allow further analysis of the effectiveness of SfM outputs against TLS data. A comparison of August 2014 and October 2014 TLS data was first completed to assess channel change over this time period. The SfM products were then compared to the August 2014 TLS data to assess what differences were

observed and how these related to the changes seen when the two TLS datasets were compared. As discussed in the methodology section, October comparisons between TLS and SfM were carried out using the raw raster (using ellipsoidal elevations). TLS cannot penetrate through water and thus only dry areas were compared. Similarly, vegetation cannot be penetrated using SfM and thus these areas were omitted from the analysis.

4.3.2 October 2014 TLS and SfM Outputs

Figure 4.10a shows the October 2014 TLS data output for the area under investigation. The same spatial area as investigated in the earlier experiments was analysed. The difference between this October 2014 TLS data and two differing SfM outputs is shown in Figure 4.10b and 4.10c. The first SfM output used three flight lines from the October 2014 SfM dataset and had an image overlap of 90%. The mean difference between the two sets of data is 0.041 m. These errors are averaged across the full extent (excluding wetted area) and thus need to be examined with a degree of caution. The second SfM was used as a comparison and only used one flight line. The mean difference between this SfM output and the October 2014 TLS data was 0.043 m. The two comparisons show similar features and difference values throughout the dry area. The majority of the immediate channel bank area is characterised by small differences as indicated by the white colour (Figure 4.10). A similar level of difference can be seen when both SfM outputs are compared and this suggests that they are both of adequate quality to compare with the October TLS dataset.

A

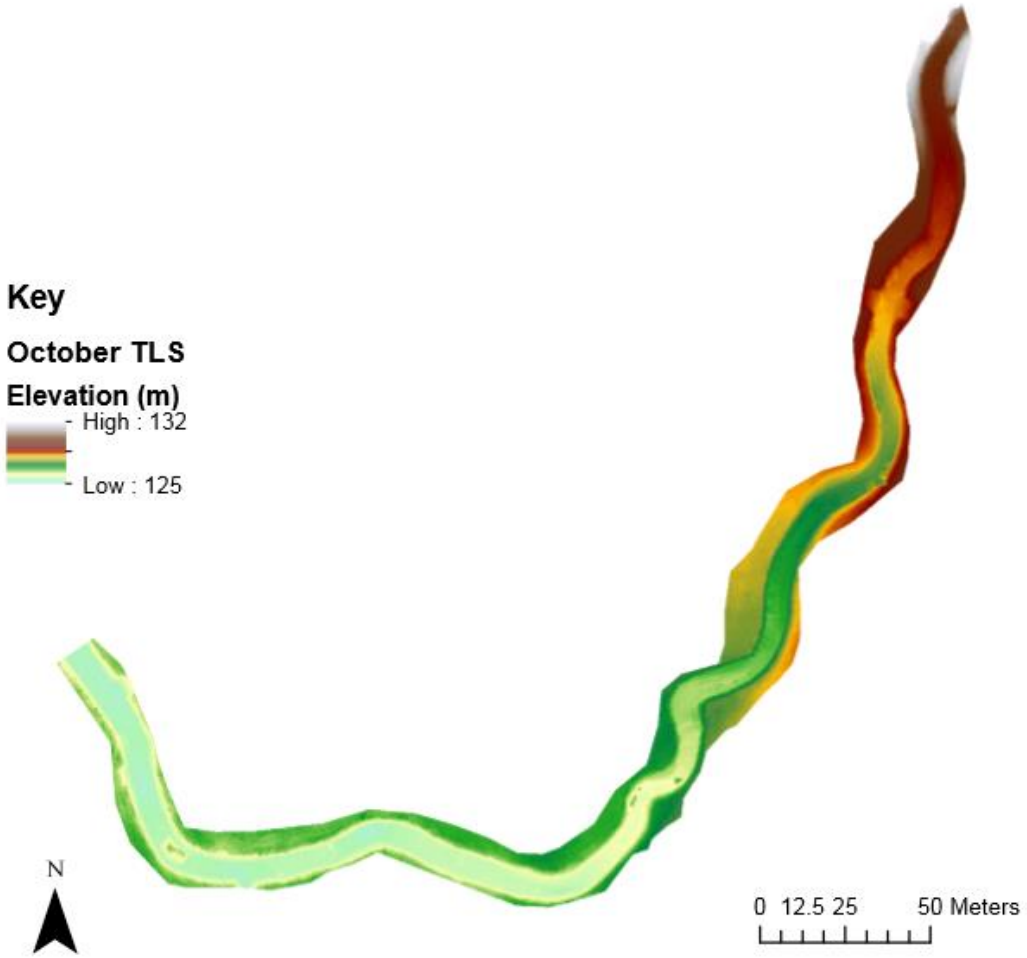
Key
October TLS
Elevation (m)
High : 132
Low : 125
N
0 12.5 25 50 Meters

B

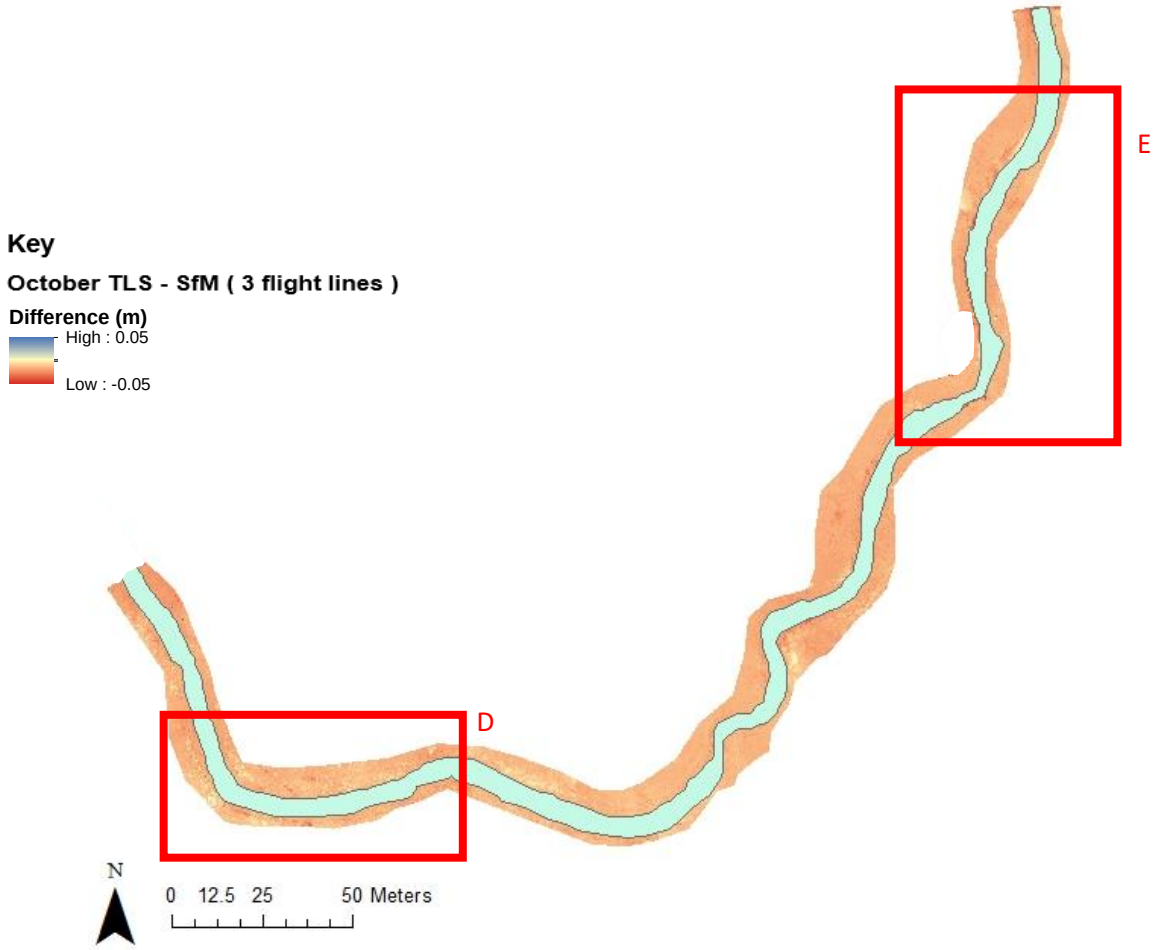
Key
October TLS - SfM (3 flight lines)
Difference (m)
High : 0.05
Low : -0.05
D
E
N
0 12.5 25 50 Meters

C

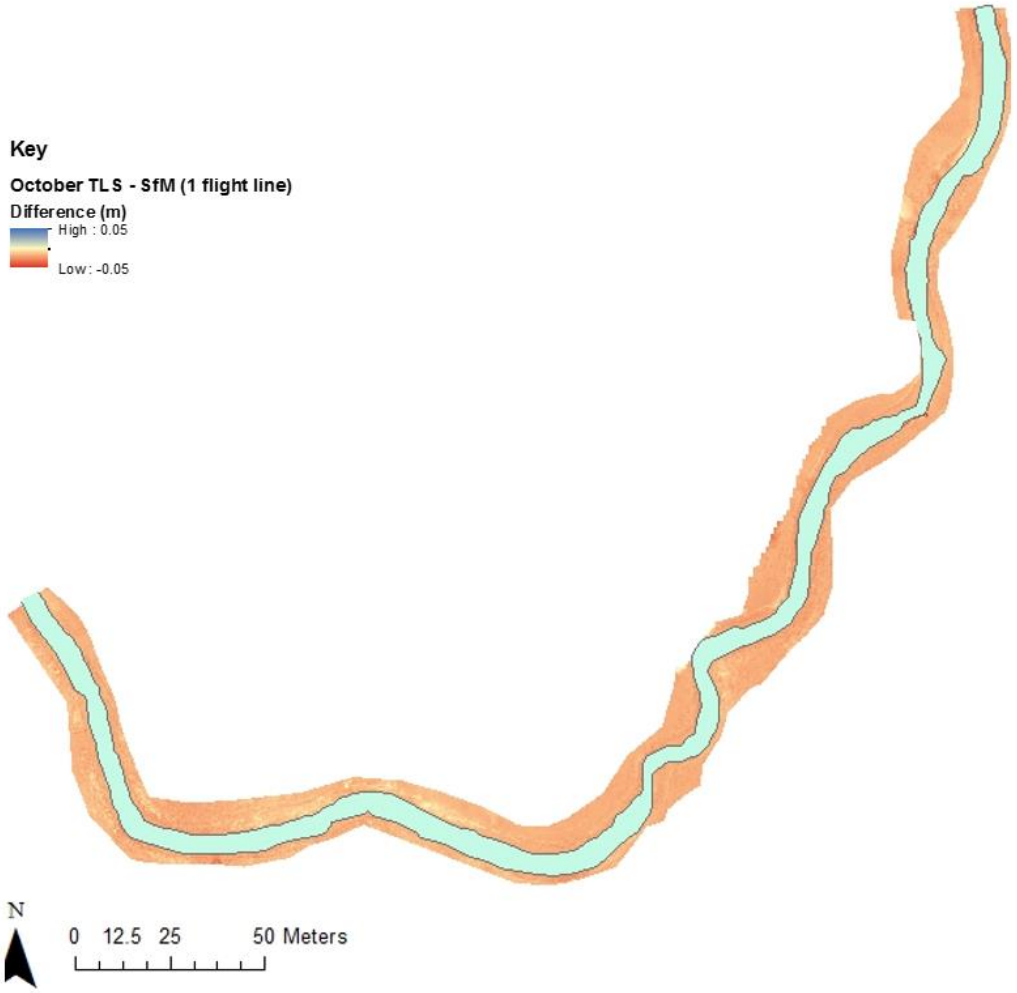
Key
October TLS - SfM (1 flight line)
Difference (m)
High : 0.05
Low : -0.05
N
0 12.5 25 50 Meters

D

E

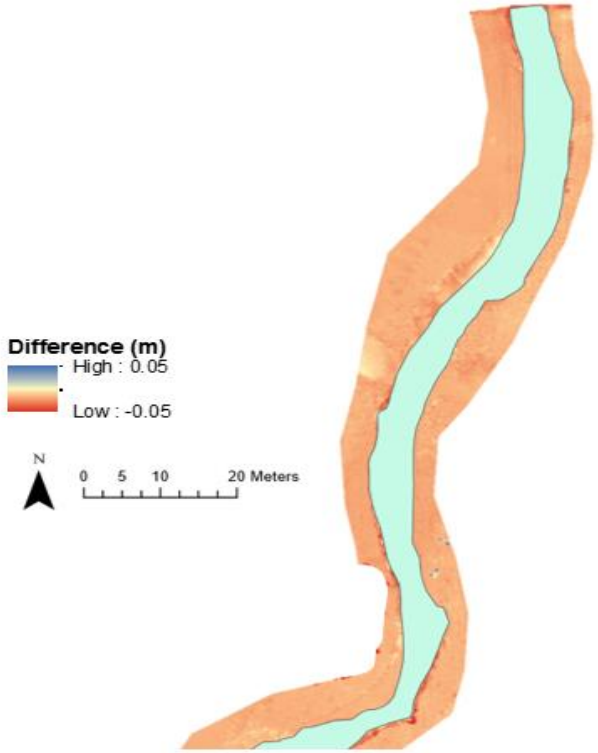

Figure 4.10: Differences observed between October 2014 TLS data and SfM outputs. a. October 2014 TLS data, b. comparison with SfM three flight lines and c. comparison with SfM one flight line (both 90% image overlap) and using optimum conditions as discussed in Section 4.2. Wetted area shaded out. D and E are close ups of the comparison in B.

4.3.3 Comparisons with the August 2014 TLS Data

To further assess the quality of the SfM data, comparisons with an August 2014 TLS dataset were made. The same spatial area that was investigated throughout the parameter analysis and earlier comparisons was examined.

Figure 4.11a shows a comparison between the August (TLS) 2014 and October 2014 TLS data. This analysis was carried out using the raster calculator and shows the earlier raster (October 2014) minus the older raster (August 2014). A large range of positive and negative differences can be observed throughout (Figure 4.11a). The mean difference is + 0.048 m (across the full spatial extent), which is relatively low, however this does not take into account the large range of positive and negative changes observed.

The comparisons with the SfM outputs can be seen in Figures 4.11b and 4.11c respectively. Similar values across all August TLS comparisons can be seen, suggesting the SfM data is of high enough quality to accurately match the comparisons made with just TLS data alone. The average differences seen for the two SfM comparisons were + 0.0518 m (three flights) and + 0.0517 m (one flight). Some of the similarities between the comparisons made can be seen (Figure 4.11a).

A

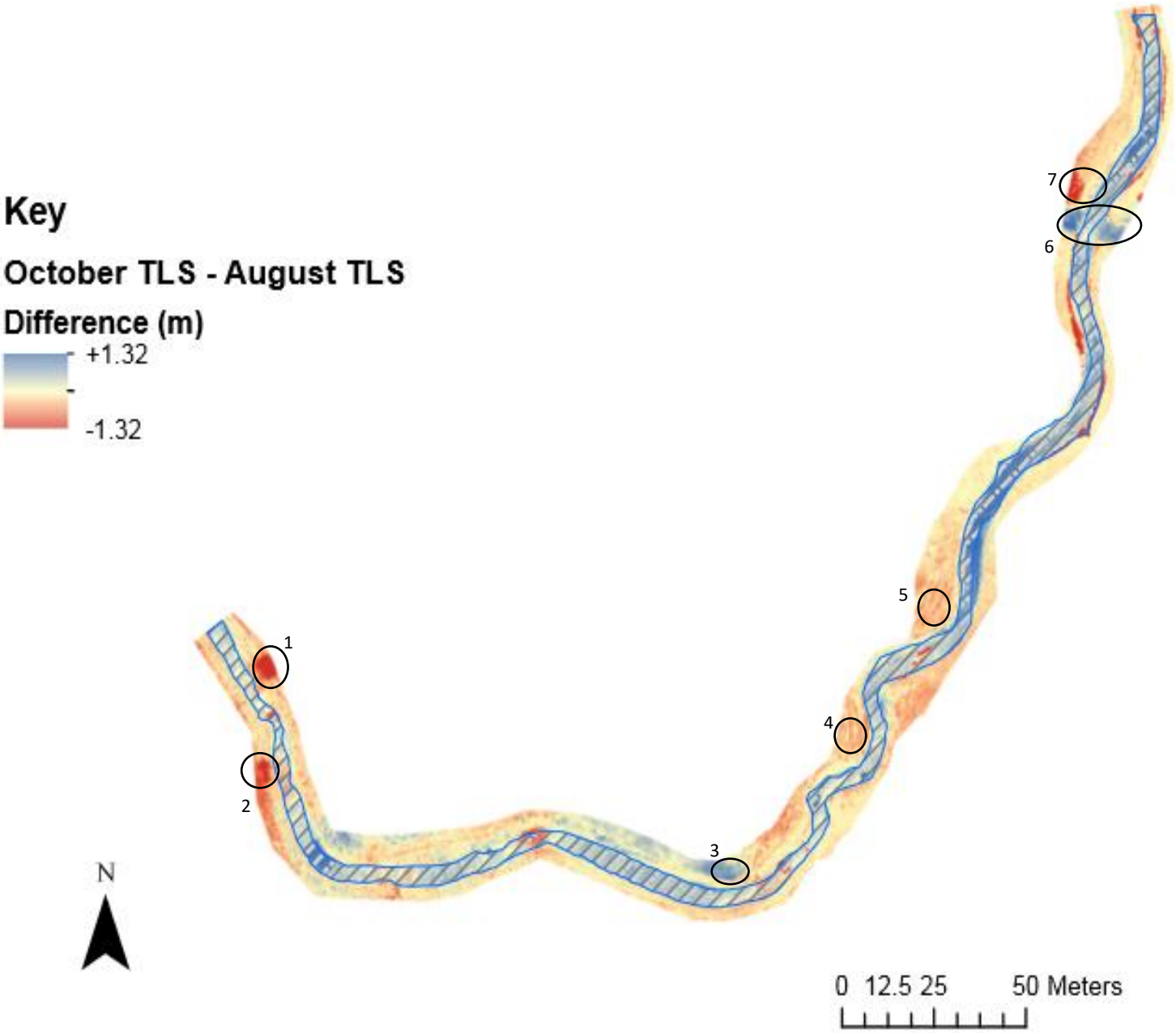
Key
October TLS - August TLS
Difference (m)
+1.32
-1.32
1
2
3
4
5
6
7
N
0 12.5 25 50 Meters

B

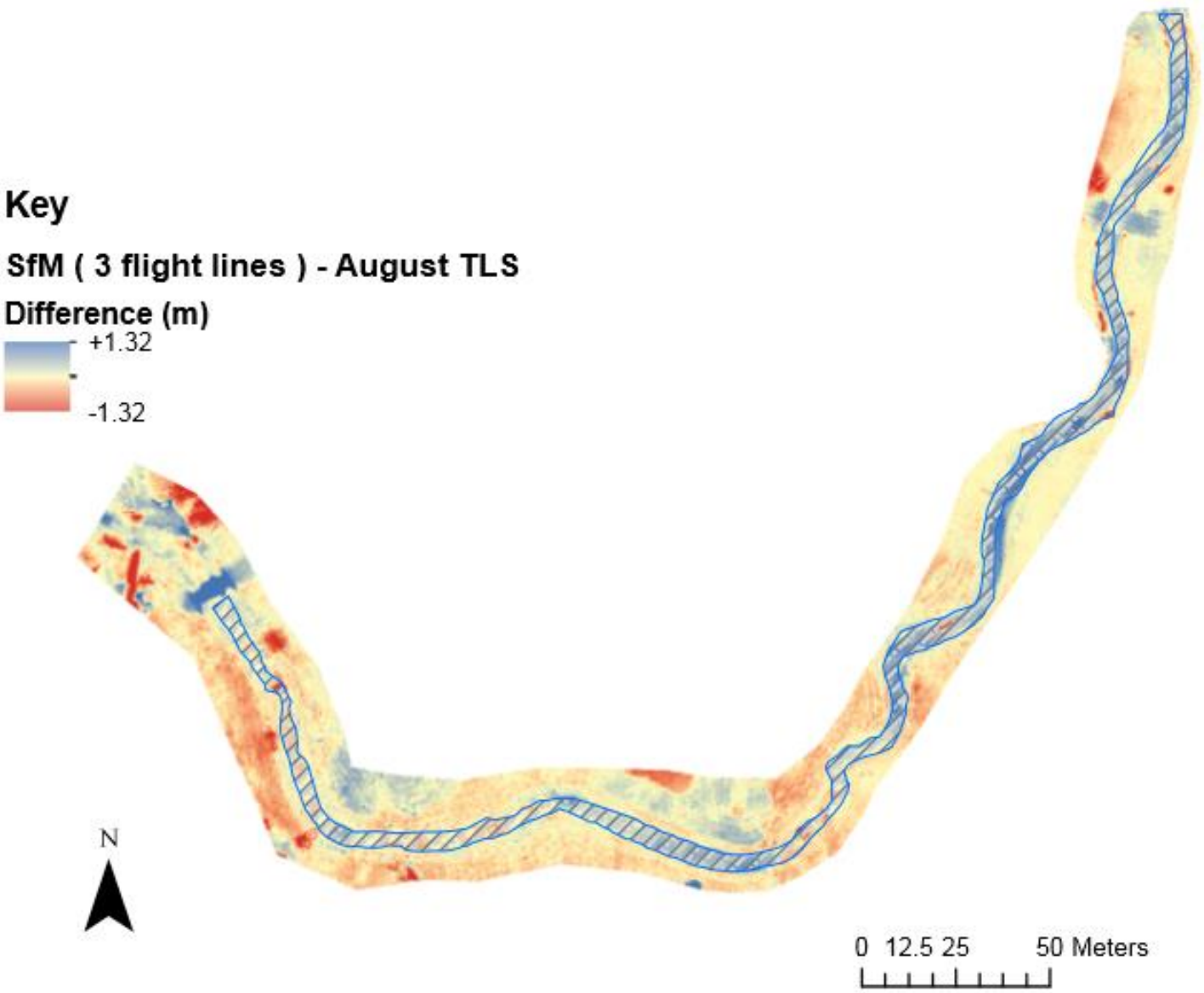
Key
SfM (3 flight lines) - August TLS
Difference (m)
+1.32
-1.32
N
0 12.5 25 50 Meters

C

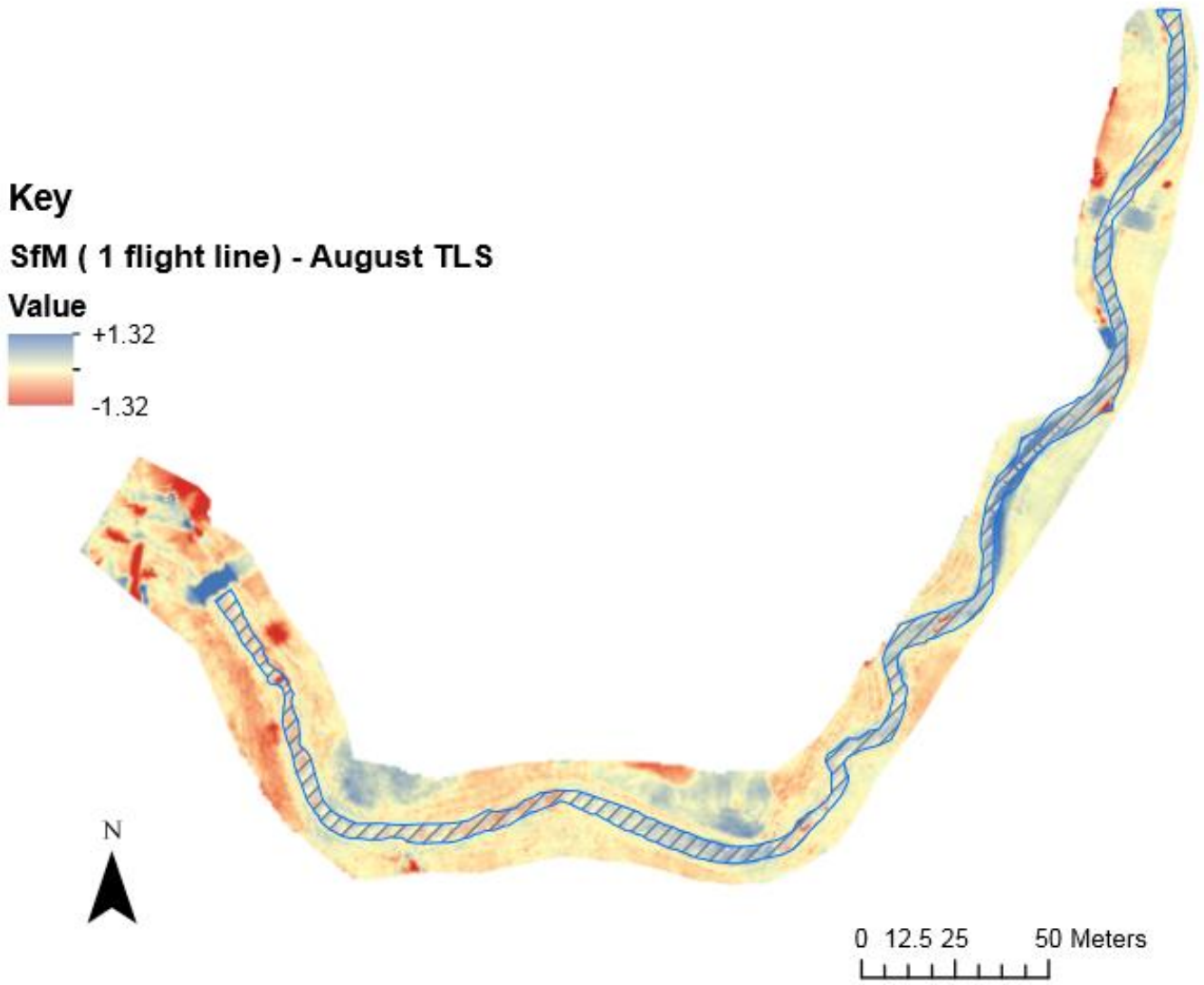

Figure 4.11: August 2014 TLS comparisons with a. October 2014 TLS, b. SfM three flight lines and c. SfM one flight line. Black circles indicate some of the similarities seen in all three comparisons. Wetted area shaded out.

4.3.4 Summary

SfM and TLS comparisons have been made to determine the validity of the SfM outputs in relation to data of a known error value. SfM data compare adequately with TLS data for the majority of the area under investigation. Limited differences between the comparisons between three flight lines and one flight line can be seen which suggests even data which has not been constructed using "optimum" conditions (as discussed and analysed in Section 4.2) can be of sufficient quality to compare with TLS outputs. The average difference observed between the October 2014 TLS and SfM data was around 0.04 m. These errors are across the full extent (excluding wetted area) and thus need to be examined with a degree of caution. The comparisons with the August 2014 TLS data further suggest that the SfM data are of reliable quality as they are very similar to associated October 2014 TLS comparisons for both datasets (three and one flight lines used).

4.4 Bed Level Correction

A refraction correction technique was used to determine bed levels which is described in detail in Section 3.6. The resulting bed level data was then used in the subsequent DoD analysis and hydraulic modelling outputs. Bed level correction was carried out on three surveys (October 2014, March 2015 and July 2015). The same spatial extent was investigated for each survey using the optimum criteria discussed in earlier sections. The purpose of correcting the wetted area was to examine how varied depth was between the three surveys and to establish error values between corrected and measured depths.

4.4.1 Bathymetric Data

4.4.1.1 October 2014 Data

The refraction correction technique allowed submerged areas to be mapped, thus allowing an appreciation of bed level changes throughout the three surveys to be attained. Figure 4.12a shows the depths acquired for the October 2014 SfM data. A relatively deep area can be associated with the upstream section of Whit Beck, while other pool areas have been highlighted on the figure. A shallower section can be noted after the near 90° meander with depths typically of around 0.2 and 0.4 m. A deeper section is observed before the bridge where depths reach a maximum of 0.7 m (Figure 4.12a).

4.4.1.2 March 2015 Data

In comparison with the October 2014 data, the March 2015 data (Figure 4.12b) shows that the river was deeper on average, which correlates with measured depths in the field (Section 4.4.3). The majority of channel area featured depths of between 0.5 and 0.7 m.

4.4.1.3 July 2015 Data

The July 2015 bed level analysis suggests depths during this period were the lowest seen during monitoring (Figure 4.12c). This correlates with measured depths in the field and is what would be expected as precipitation levels tend to be lower during the summer months. Average depths within the shallower regions (upstream section and after the near 90° meander) were approximately 0.3 m, with deeper (pool) areas having depths which range from 0.6 to 0.7 m.

4.4.1.4 Banding Issue

All three depth charts shown in Figure 4.12 have areas of depth banding which may highlight errors within the respective datasets. It is difficult to attribute these bands to signal (real depth change) or noise (error formation) and thus an appreciation of this uncertainty within the data presented is required. These bands may be due to glare, shadow effects or tree cover and may be unrepresentative of actual depth variation.

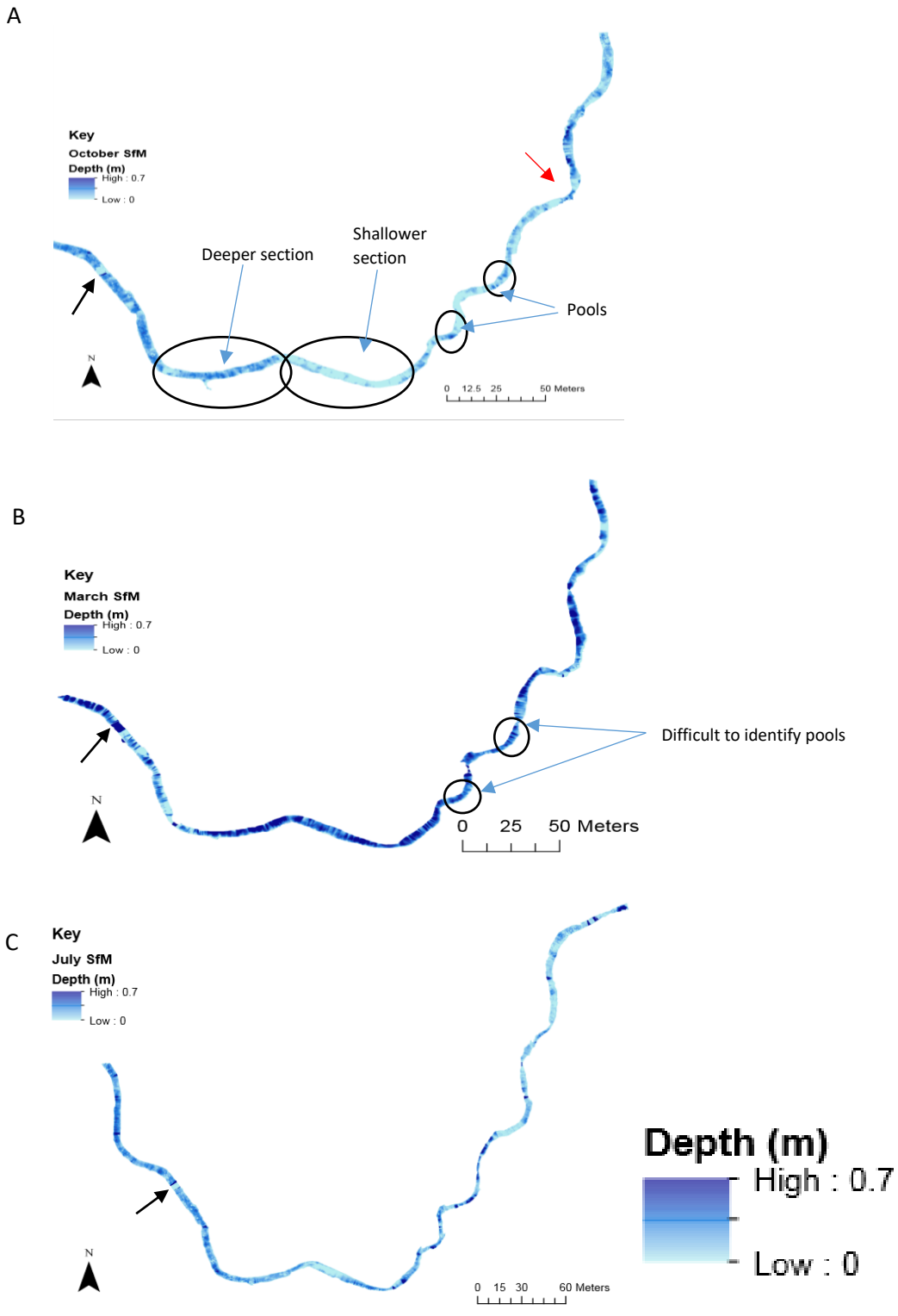

Figure 4.12: Depths derived from the refraction correction technique for a. October 2014; b. March 2015 and c. July 2015. The black arrows indicate the location of the bridge. The red arrow shows the location of the tree for the discussion in the next section (Section 4.4.2). Scale has been enlarged to make viewing clearer, same depth scale for all figures.

4.4.2 Geomorphic / Depth Variation

By analysing the three surveys, an area of relatively large magnitude changes can be mapped. Figure 4.13 shows this area in detail, and highlights that some river systems (specifically newly formed reaches, or reaches close to thresholds within the system) can be very dynamic, even over relatively small spatial and short temporal scales. Data from October 2014, March 2015 and July 2015 indicate that channel change throughout the scheme was occurring at varying rates (See Section 5.2.1). The majority of the lower section of the scheme can be characterised as having little adjustment (for small to medium sized forcing events), while the upper section of the new channel experienced frequent changes in patterns of erosion and deposition. Figure 4.13 also shows some banding of depth data which may be due to errors from glare, shadow effects or tree cover. This may cause depths to be poorly represented.

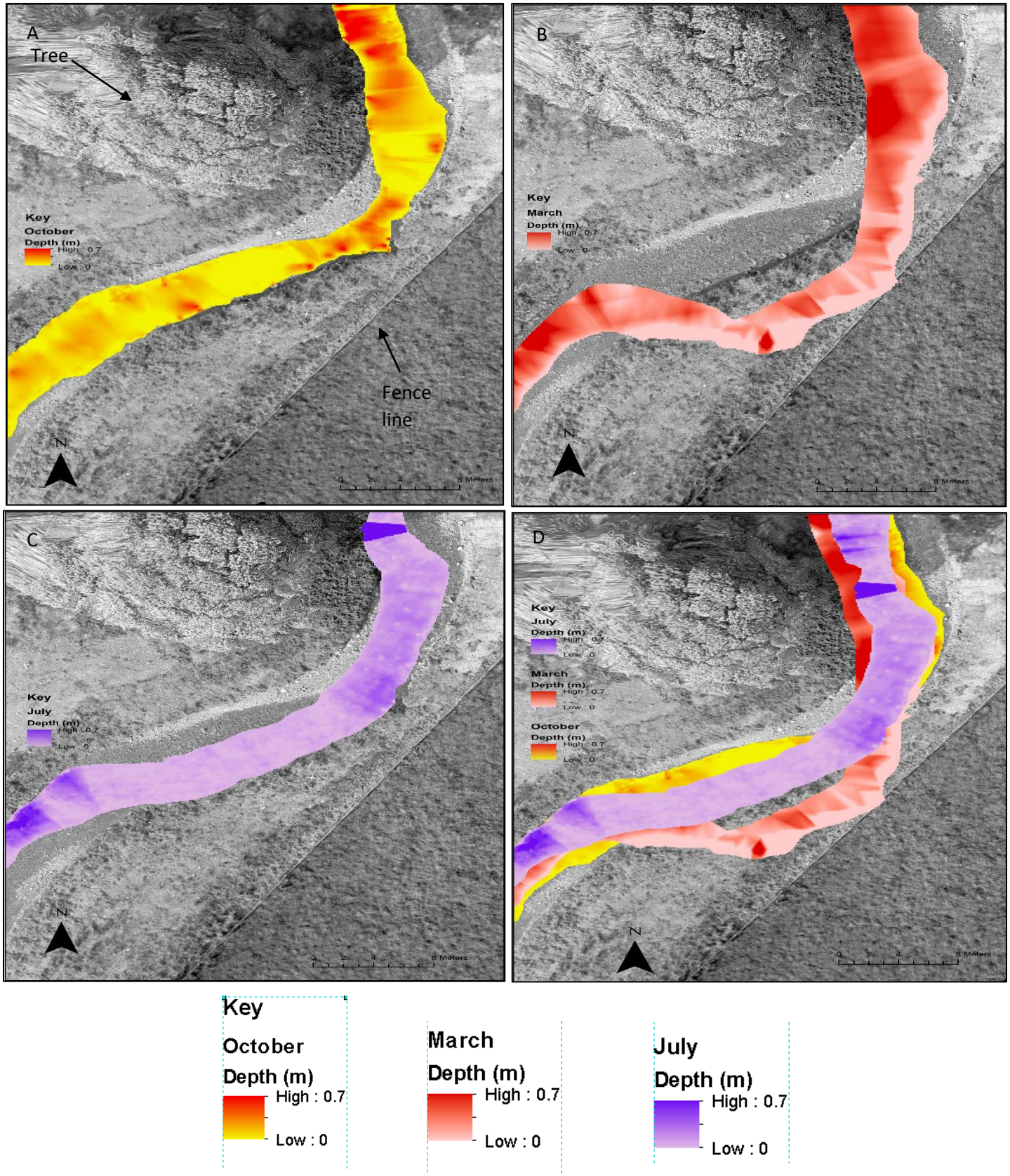

Figure 4.13: Depth and geomorphic variation at a section near the tree for a. October 2014, b. March 2015 and c. July 2015. All channels overlaid are shown in d. October 2014 orthophoto is used as a reference point for all images.

4.4.3 Depth Comparisons

Comparisons between the three surveys indicate and highlight that depth variation is complex and dependent upon a number of deterministic variables that operate on various scales throughout a catchment. Table 4.1 shows the average error associated with the three different field campaigns and indicates that average errors were lowest during the October 2014 survey with a value of 0.029 m. Depth levels on average were highest during the March 2015 survey with an average depth value recorded in the field of 0.36 m. This correlates with the results discussed in Section 4.4.1.2 that indicate the March 2015 campaign had larger depths on average compared to the October 2014 and June 2015 campaigns.

Table 4.1: Average error (between measured and bathymetric), average depth and number of depth points for surveys in October 2014, March 2015 and July 2015.

Survey	Average error (m)	Average depth measured in field (m)	Number of depth points
Oct-14	0.029	0.31	184
Mar-15	0.046	0.36	149
Jul-15	0.039	0.22	80

Figure 4.14 shows these differences in depths in graphical form. The data used is from the refraction correction results discussed earlier. When the October 2014 and March 2015 depths are compared (Figure 4.14a), March 2015 depths can be seen to be generally higher. October 2014 depths can be seen to be higher in a few isolated locations. The far upstream end of the area under investigation has October 2014 depths that are higher than the March 2015 values, while the area immediately before the bridge can be characterised as having October 2014 depths greater than March 2015 depths. The vast majority of the area under investigation (75%) had March 2015 depths that were higher than October 2014 depths (Figure 4.14a). Figure 4.14b shows a comparison of depth values for the March 2015 and July 2015 campaigns. The depth differences were very similar to the comparisons between the October 2014 and March 2015

datasets. March 2015 depths seem to be higher across the majority of the area examined, apart from the true left of the river in the far upstream section and the area before the bridge (Figure 4.14b). Small areas where July 2015 depths were higher can be seen in the middle section. Variable depth differences can be seen when depths are compared for the October 2014 and July 2015 campaigns (Figure 4.14c). This is despite the July 2015 data having the lowest average field recorded depth measurement. Around 60% of the river can be characterised as having depths higher for October 2014, with the remaining 40% having larger July 2015 values.

Data showing the differences in measured and estimated depths can be seen in Figure 4.15. Please note not all the depth measurements in the field as indicated in Table 4.1 were used in bed level validation. The highest R^2 value obtained was with the July 2015 depth corrected data indicating values with this dataset match the trendline derived more closely than both the October 2014 and March 2015 refraction correction data. This is despite the October 2014 data having lower average errors.

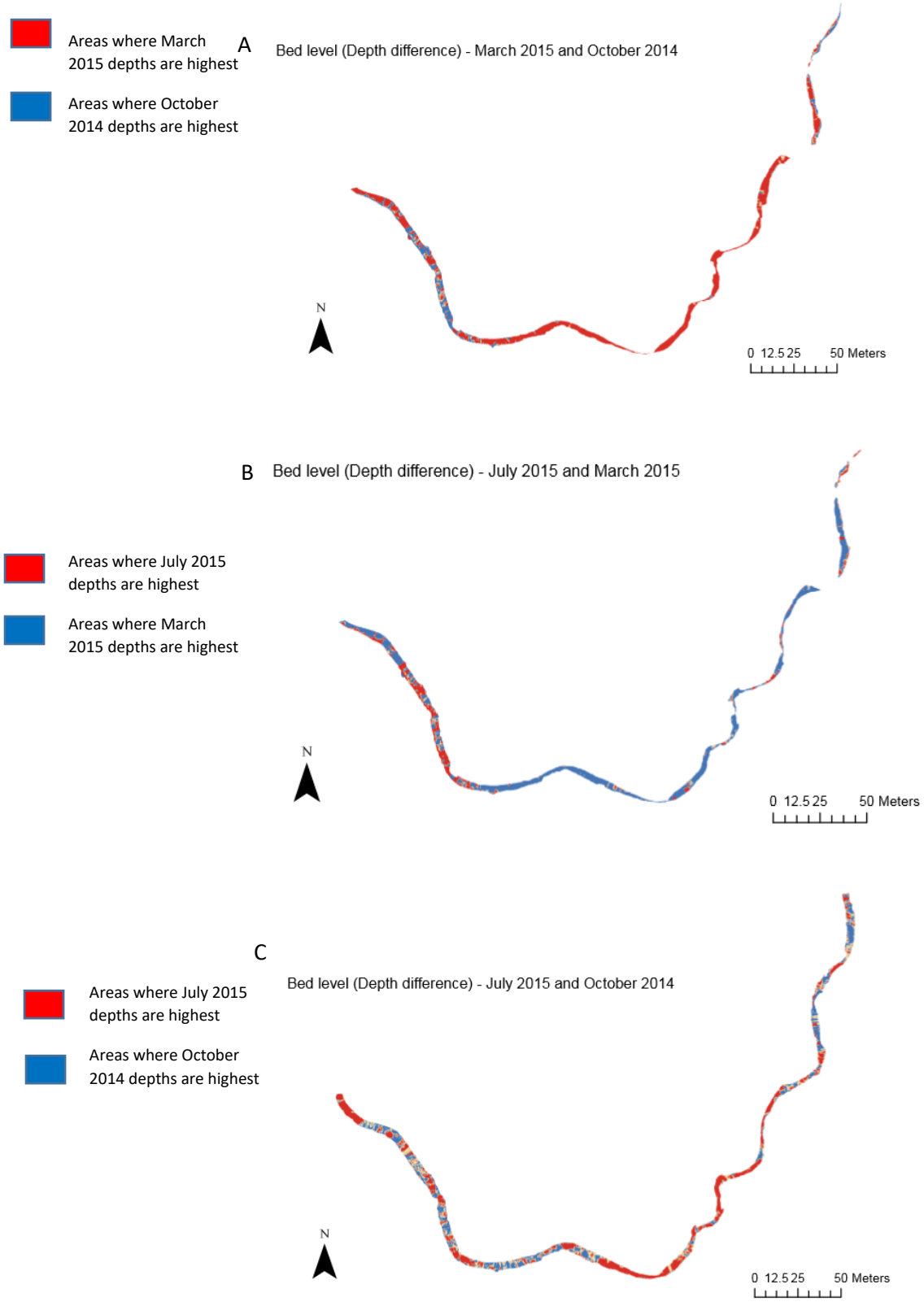

Figure 4.14: Depth differences (derived from corrected bed levels) for a. October 2014 and March 2015, b. March 2015 and July 2015 and c. October 2014 and July 2015.

A

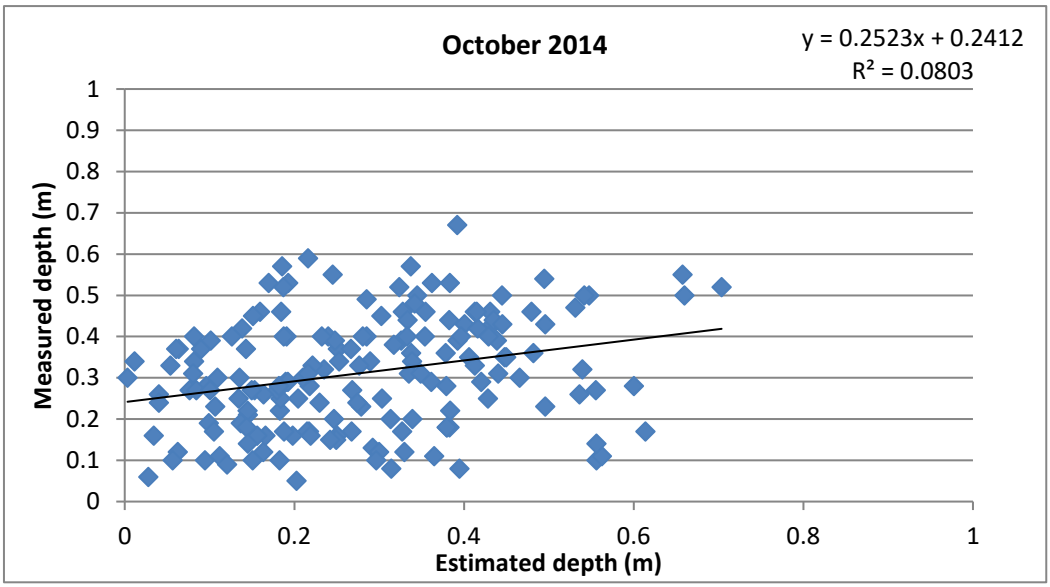

B

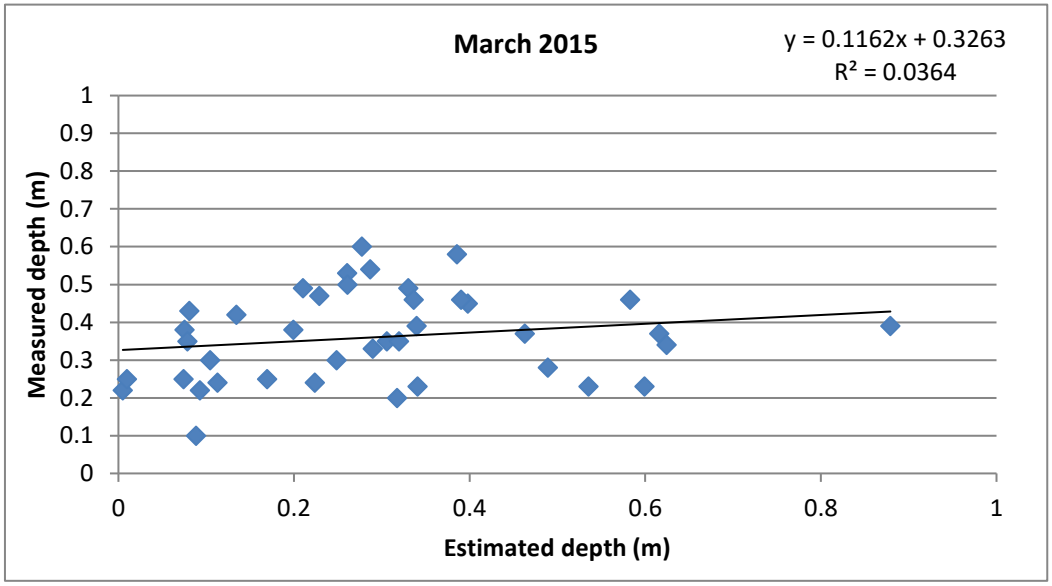

C

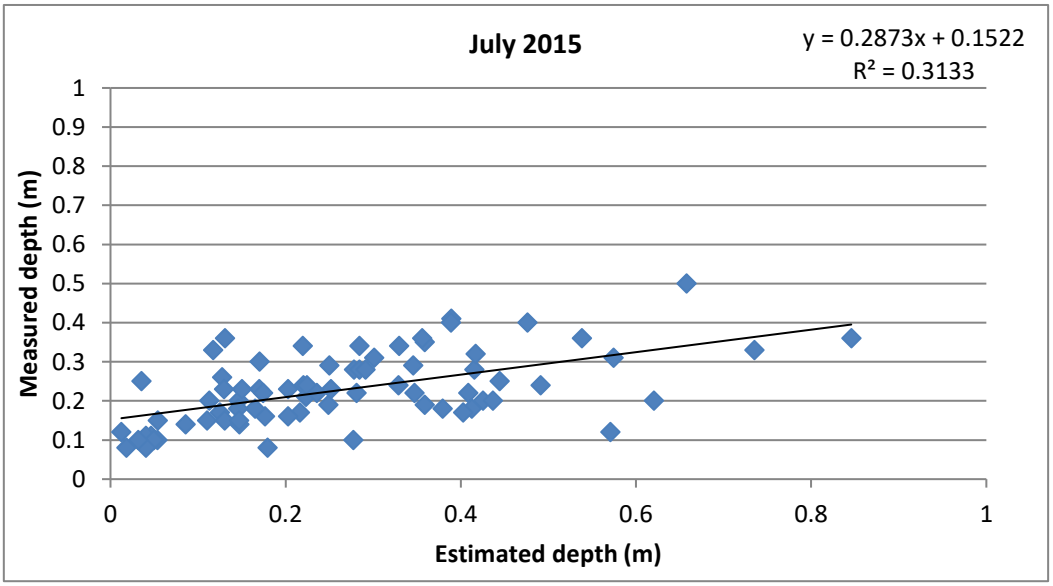

Figure 4.15: Measured depth (m) against estimated depth (m) for a. October 2014, b. March 2015 and c. July 2015.

4.4.4 Corrected DEMs

Dry and wet areas were mosaicked together to produce a corrected DEM which incorporates the full extent of the area under investigation. This was carried out using the procedure discussed in Section 3.6.1. Figure 4.16 shows the corrected DEMs for the three surveys undertaken. These corrected DEMs were used in the DoD and hydraulic modelling analysis and examined to assess their applicability. The influence of depth banding has been discussed throughout this section and can be seen as a reason for unrepresentative depths. Low R^2 values also suggest estimated depths may be a poor indicator of actual depths. Despite this, average errors between the datasets are adequate (Table 4.1).

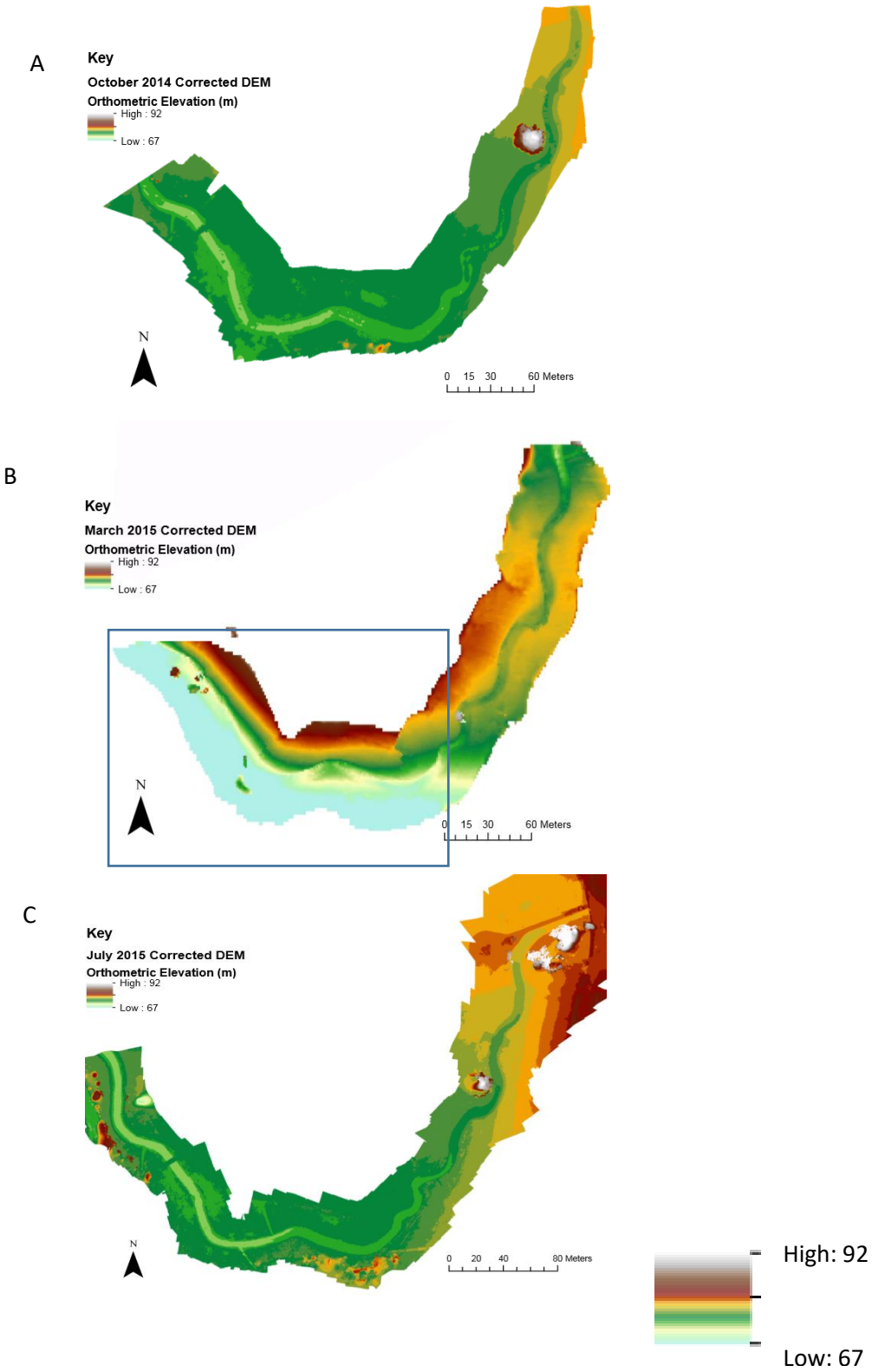

Figure 4.16: Corrected DEMs for a. October 2014, b. March 2015 and c. July 2015. The box in Figure 4.16b shows an area which has larger errors in comparison, this may be due to tree cover and shade. Scale has been enlarged to make viewing clearer, all figures have same scale.

4.4.5 Summary – Bed Level Correction

The March 2015 dataset was seen to be deepest on average which correlates with average measured depths in the field. The refraction correction technique was used to derive bed levels and depths; errors were lowest for the October 2014 values with an average error of 0.029 m. The highest average error was with the March 2015 dataset (0.046 m). A comparison between the three surveys indicates that channel change and adjustment can be of large magnitude. An examination of one area (near the tree) reveals channel change between October 2014 and March 2015 was high and this channel adjustment has been mapped to reveal how depths vary even on relatively small spatial scales. A further analysis of the measured depth differences suggests March 2015 depths generally deepest; smaller and more variable differences can be seen between the October 2014 and July 2015 levels. The issue of depth banding has been discussed and may be promoted by factors such as glare and shade. The bed levels derived from the refraction correction technique were used in subsequent DEM of Difference (DoD) analysis.

4.4.6 Chapter Conclusion

Initial image overlap and Target analysis experiments were conducted on the October 2014 data to assess the best possible conditions for DEM and orthophoto production. A high image overlap, with more targets was concluded as best for inducing improved DEM quality, while the addition of oblique imagery also aided a reduction in errors. SfM data compared adequately with TLS data from both August and October 2014. Differences between SfM-TLS datasets were around 0.04 m (October 2014), while similar differences between the August 2014 and October 2014 data were seen in both the TLS-TLS comparisons and the TLS-SfM comparisons. These errors are across the full extent (excluding wetted area) and thus need to be examined with a degree of caution. Lastly, depths were derived from corrected bed levels

to assess how depth varied between the three surveys. March 2015 depths were generally deepest, while an area of larger magnitude depth and geomorphic change has been examined. Differences between estimated and measured depths are adequate, with March 2015 data having the highest average error. Issues with depth banding which may be induced by environmental characteristics have been discussed.

Chapter 5: DoDs and Hydraulic Modelling

5.1 Introduction

Further data processing techniques were applied to the SfM data to establish how effective and useful it could be in providing information about river change and the processes governing this change. Best quality products were used to first map geomorphic change using the DoD technique (Section 5.2). This would allow patterns of erosion and deposition to be quantified, while allowing an understanding of the frequency and magnitude of such change to be acknowledged. Hydraulic modelling was also examined to assess how SfM products could be used to classify geomorphic units (Section 5.3).

5.2 DEMs of Difference (DoDs)

DoDs (DEMs of difference) allow channel change to be quantified by comparing consecutive elevation models across an area of interest. This technique is very useful as it can give detailed information about the type of processes occurring, while also allowing the frequency and magnitude of such processes to be quantified. Corrected DEMs for October 2014 and June 2015 were used to map patterns of erosion and deposition.

This section is split into two broad sections. First, a DoD examining patterns in erosion and deposition is presented using no MLD for the period between October 2014 and July 2015 (Section 5.2.1). These were chosen as they had the lower error metrics and allowed complete change throughout the monitoring period to be attained. Second, an examination of how change differed under different thresholds of MLD is presented (Section 5.2.2).

5.2.1 Complete DEM Change Between October 2014 and July 2015

The DoD displaying channel change between October 2014 and July 2015 can be seen in Figure 5.1. Figure 5.2 shows the elevation chart that relates to this DoD. Figure 5.1 shows wet areas (channel) and also dry areas (surrounding bars, banks, fields). For the given spatial area under investigation, the majority of the area can be classed as showing net deposition (63%) and the remaining area (37%) can be classed as net erosional (Figure 5.3). The total spatial extent under investigation is 22151 m^2, which equates to 14930 m^2 of deposition and 7221 m^2 of erosion. The largest frequency class of change was between 0.00 and -0.25, where approximately 10500 m^2 can be categorised (Figure 5.2).

Channel change (wetted area) between the two surveys has been measured adequately and Figures 5.4, 5.5 and 5.6 show three examples of where the DoD has accurately mapped DEM change. Bar formation on a meander in the upstream section of the site under examination has been mapped to show deposition over the temporal period (Figure 5.4). Figure 5.5 shows that even smaller features such as gulleys can be mapped and analysed using the DoD technique. Three distinct gulleys can be seen in the July 2015 orthophoto and all have been mapped in the corresponding DoD calculation. Another example showcasing the validity of this technique can be seen in Figure 5.6, where bar formation and fence lines has been mapped on a meander.

To show that change of smaller magnitudes (>1 m) can be mapped accordingly, Figure 5.7 and 5.8 show an erosion and deposition map of the area examined. Bar growth, channel erosion and gulley formation can be mapped and located as shown in the diagrams.

A

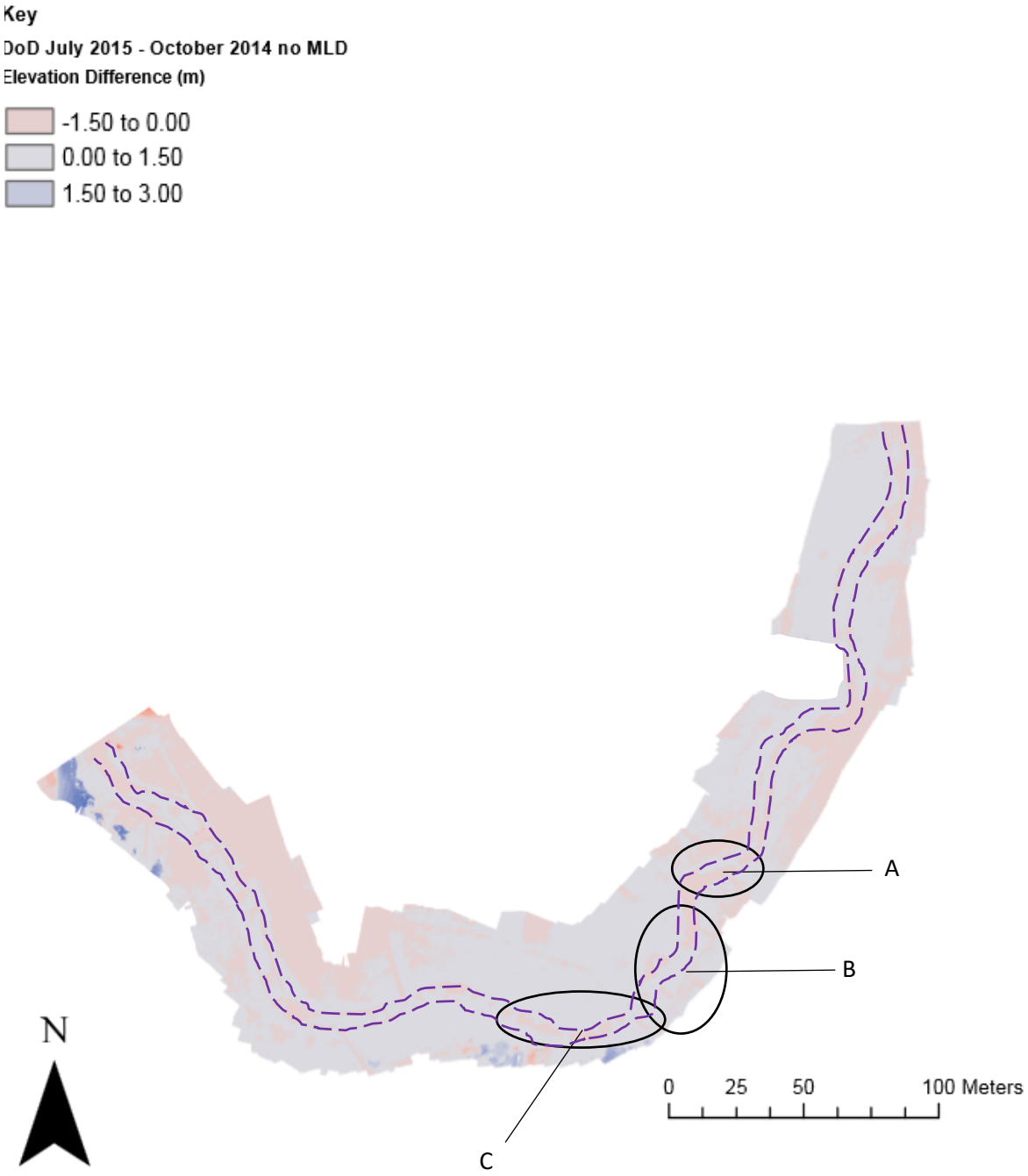
Key
DoD July 2015 - October 2014 no MLD
Elevation Difference (m)
-1.50 to 0.00
0.00 to 1.50
1.50 to 3.00
A
B
C
N
0
25
50
100 Meters

B

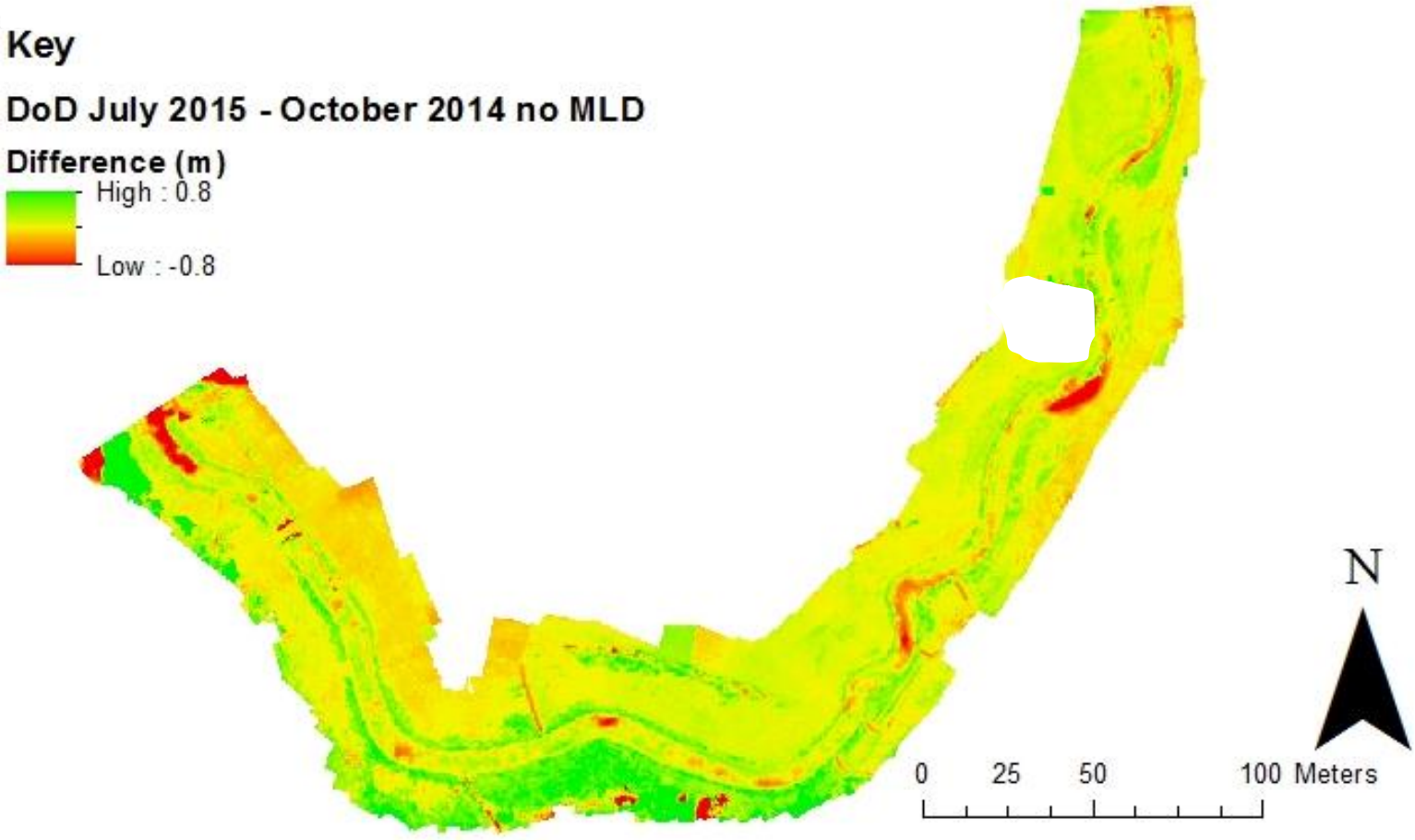

Figure 5.1: A.DoD for October 2014 - July 2015. The locations of change highlighted in Figures 5.4,5,5 and 5.6 are shown by letters a, b and c. River outline shown. Exported in original GCD toolbox format. B. Same data exported showing a scale of ± 0.8m.

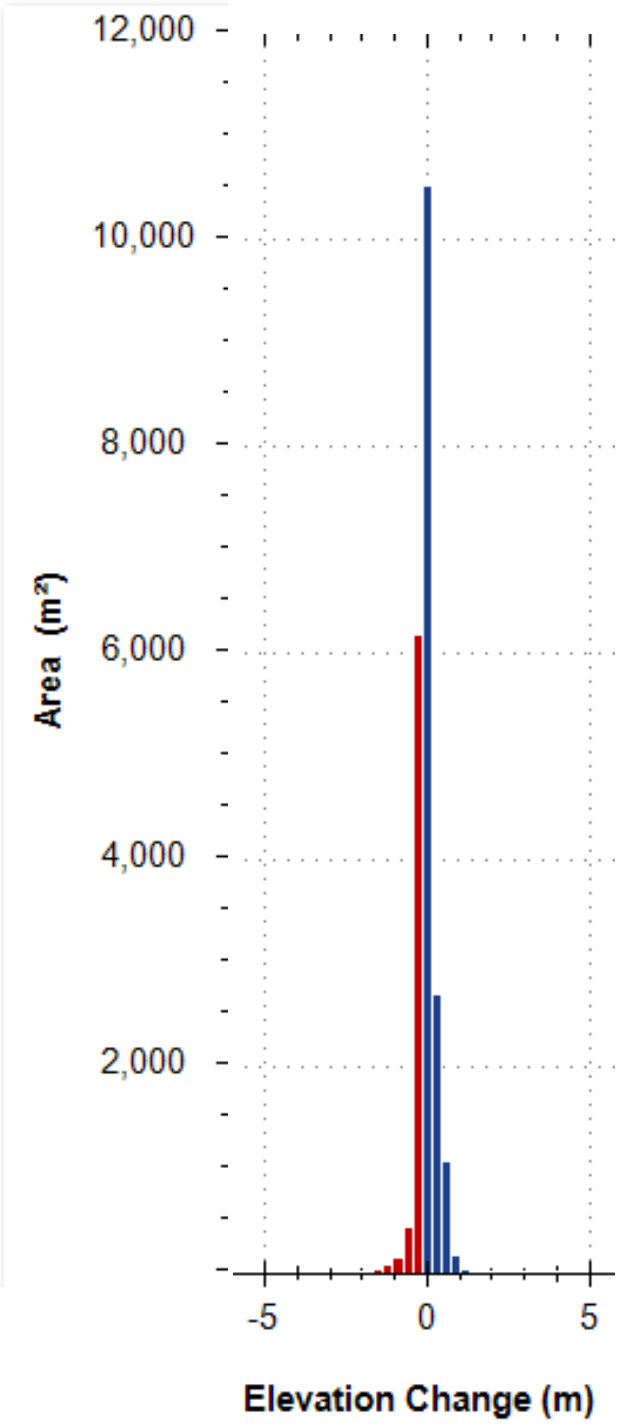

Figure 5.2: Elevation chart for DoD between October 2014 and July 2015.

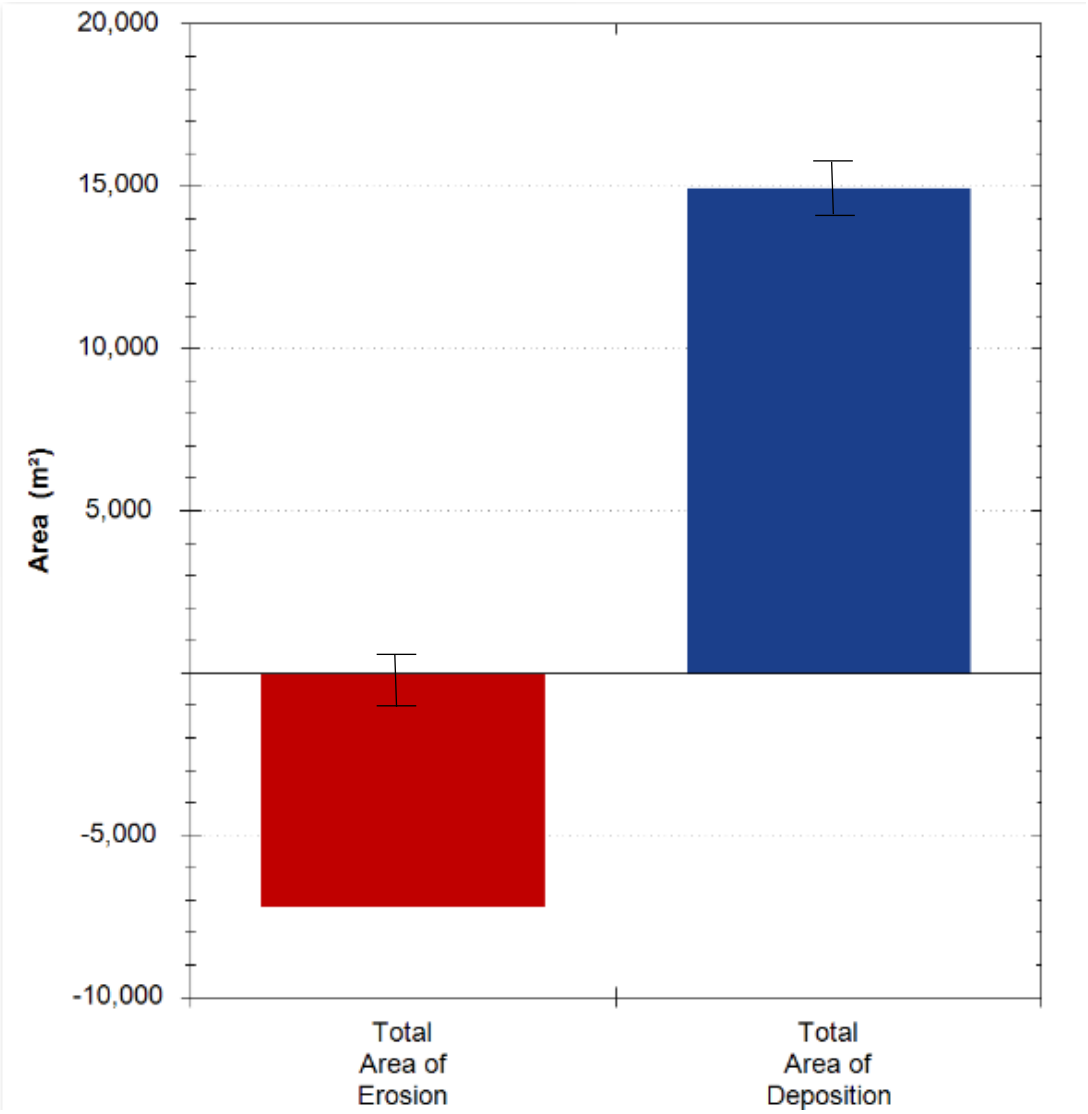

Figure 5.3: Relative areas of erosion and deposition for the DoD between October 2014 and July 2015 with error bars.

A

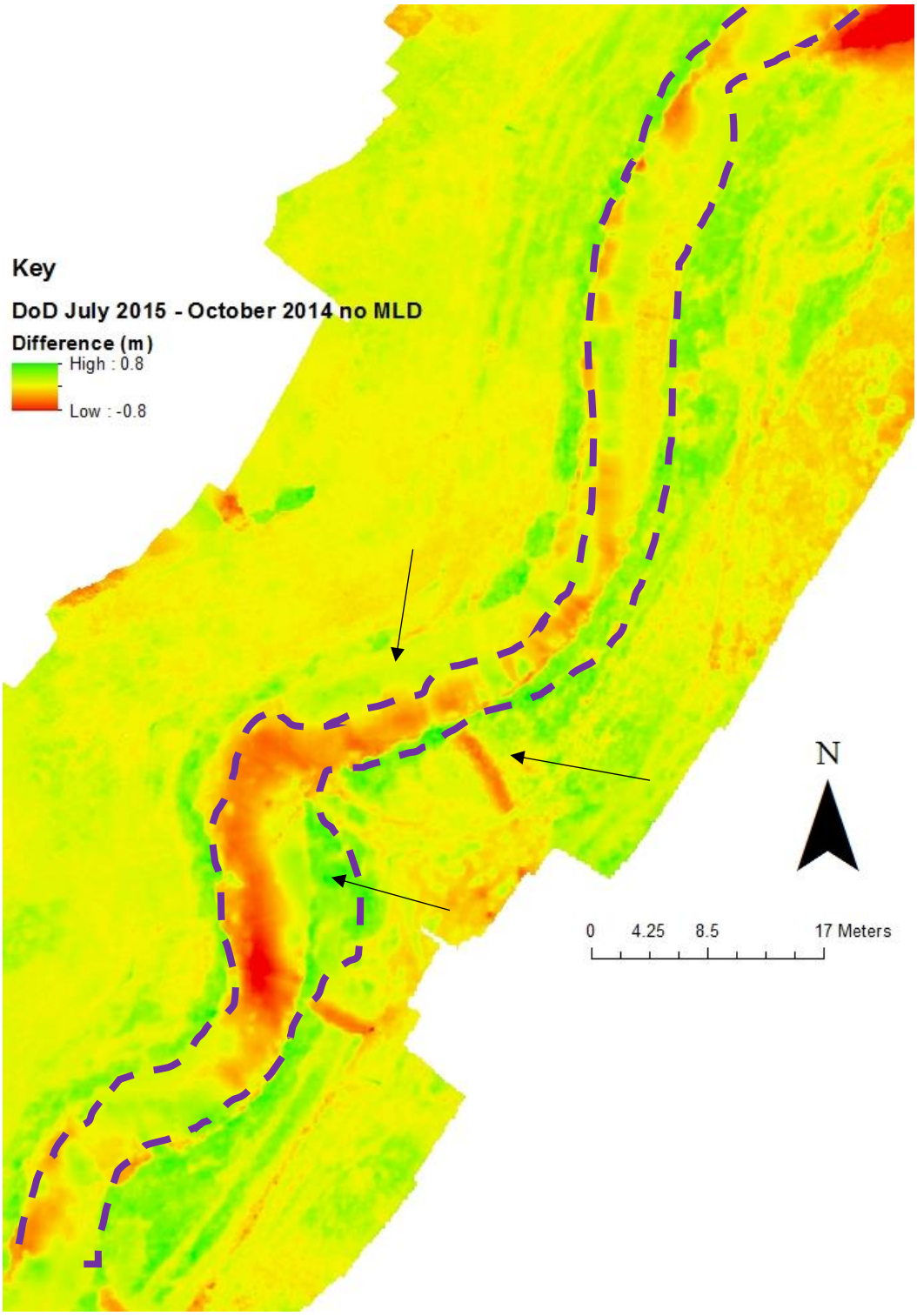
Key
DoD July 2015 - October 2014 no MLD
Difference (m)
High : 0.8
Low : -0.8
N
0
4.25
8.5
17 Meters

B

C

Figure 5.4: DoD change at location A (on Figure 5.1). A. DoD showing areas of erosion and deposition. Bar growth (deposition) and gully formation have been mapped. B. October 2014 orthophoto and c. July 2015 orthophoto to show change in graphical form. River outline shown.

A

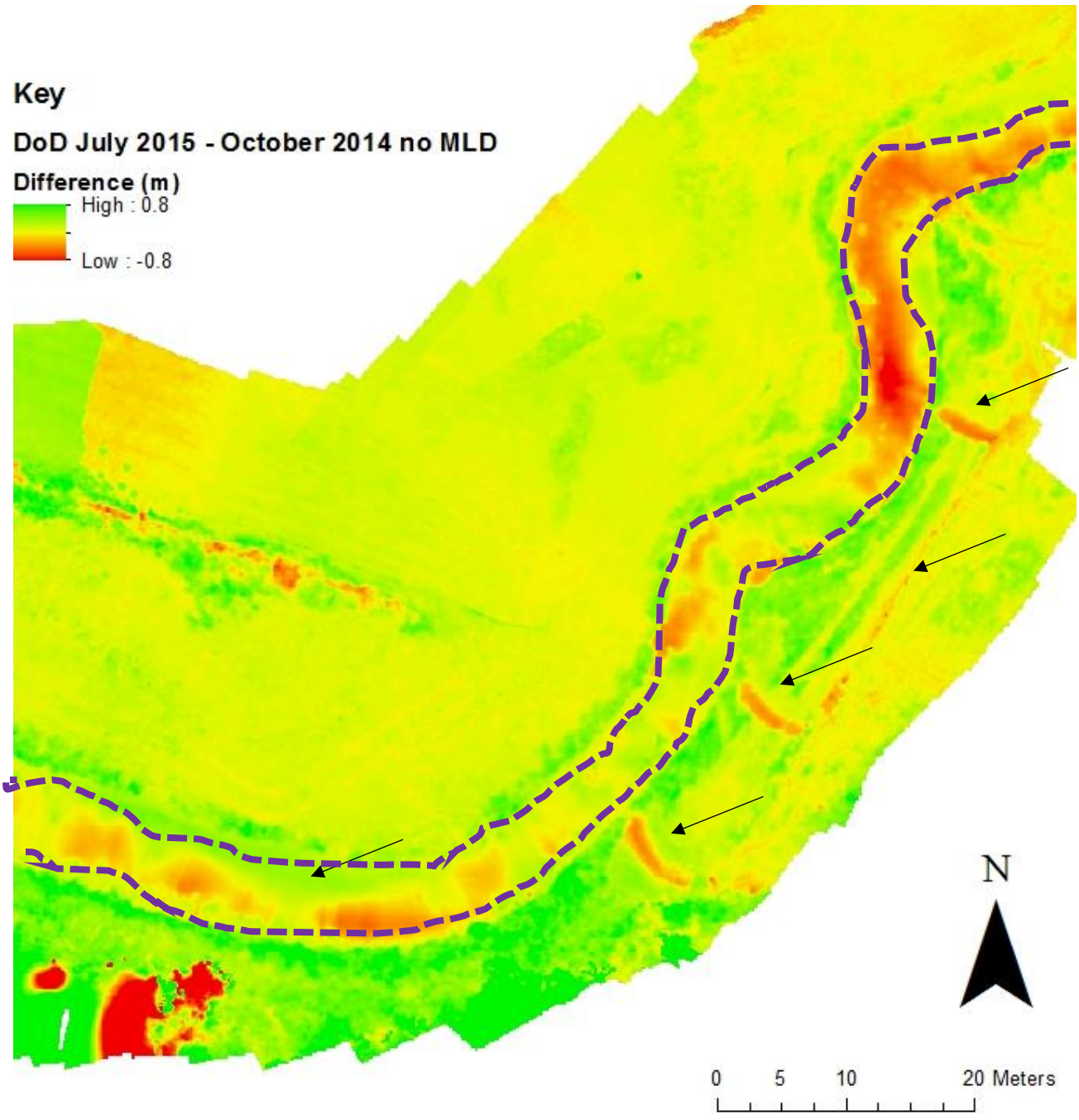
Key
DoD July 2015 - October 2014 no MLD
Difference (m)
High : 0.8
Low : -0.8
N
0
5
10
20 Meters

B

C

Figure 5.5: DoD change at location B (on Figure 5.1). A. DoD showing areas of erosion and deposition. Gully formation, fence line and bar formation/growth have been mapped (black arrows). B. October 2014 orthophoto and c. July 2015 orthophoto to show change in graphical form. River outline shown.

A

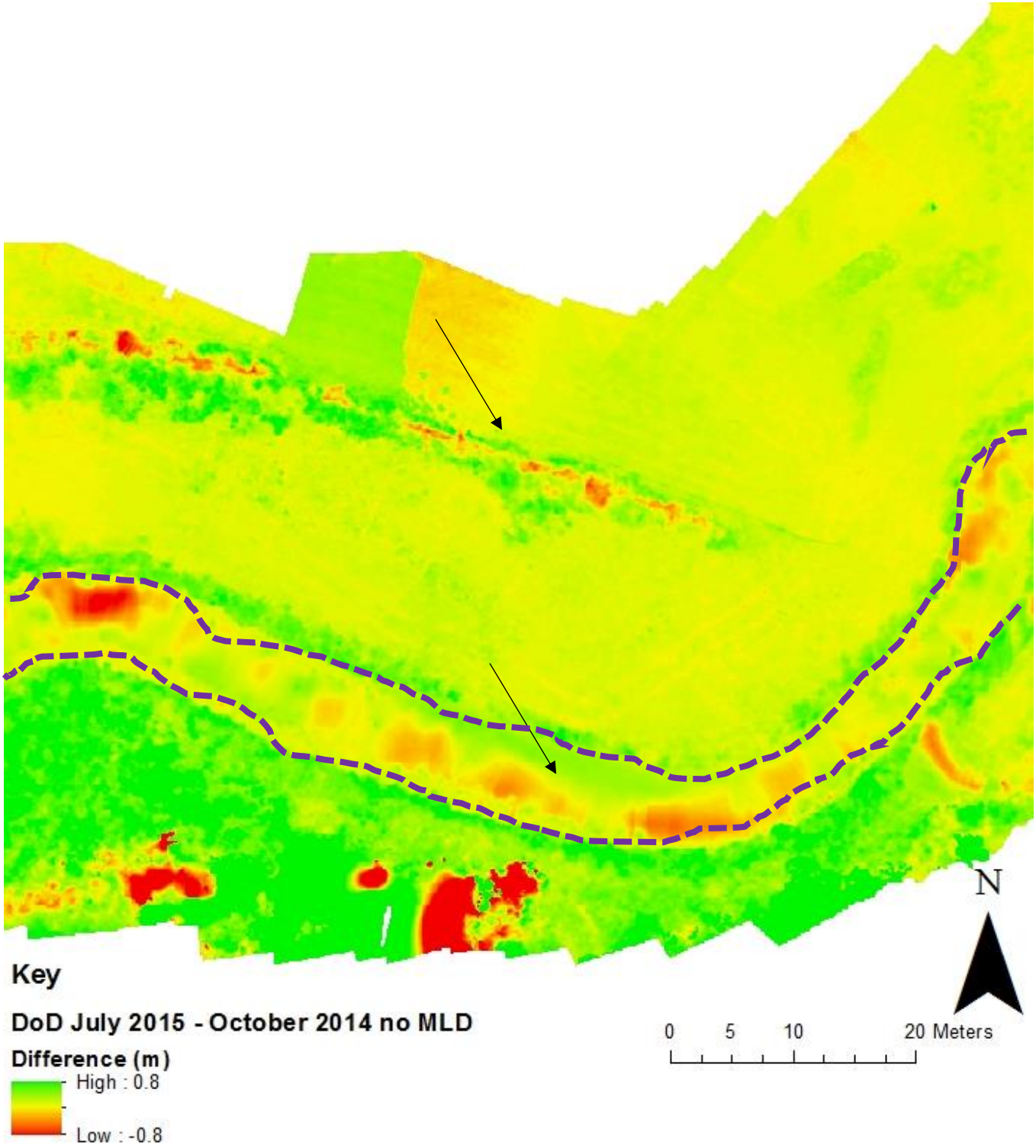
Key
DoD July 2015 - October 2014 no MLD
Difference (m)
High : 0.8
Low : -0.8
N
0
5
10
20 Meters

B

C

Figure 5.6: DoD change at location C (on Figure 5.1). A. DoD showing areas of erosion and deposition. Bar growth and fence line has been mapped (black arrows). B. October 2014 orthophoto and c. July 2015 orthophoto to show change in graphical form. River outline shown.

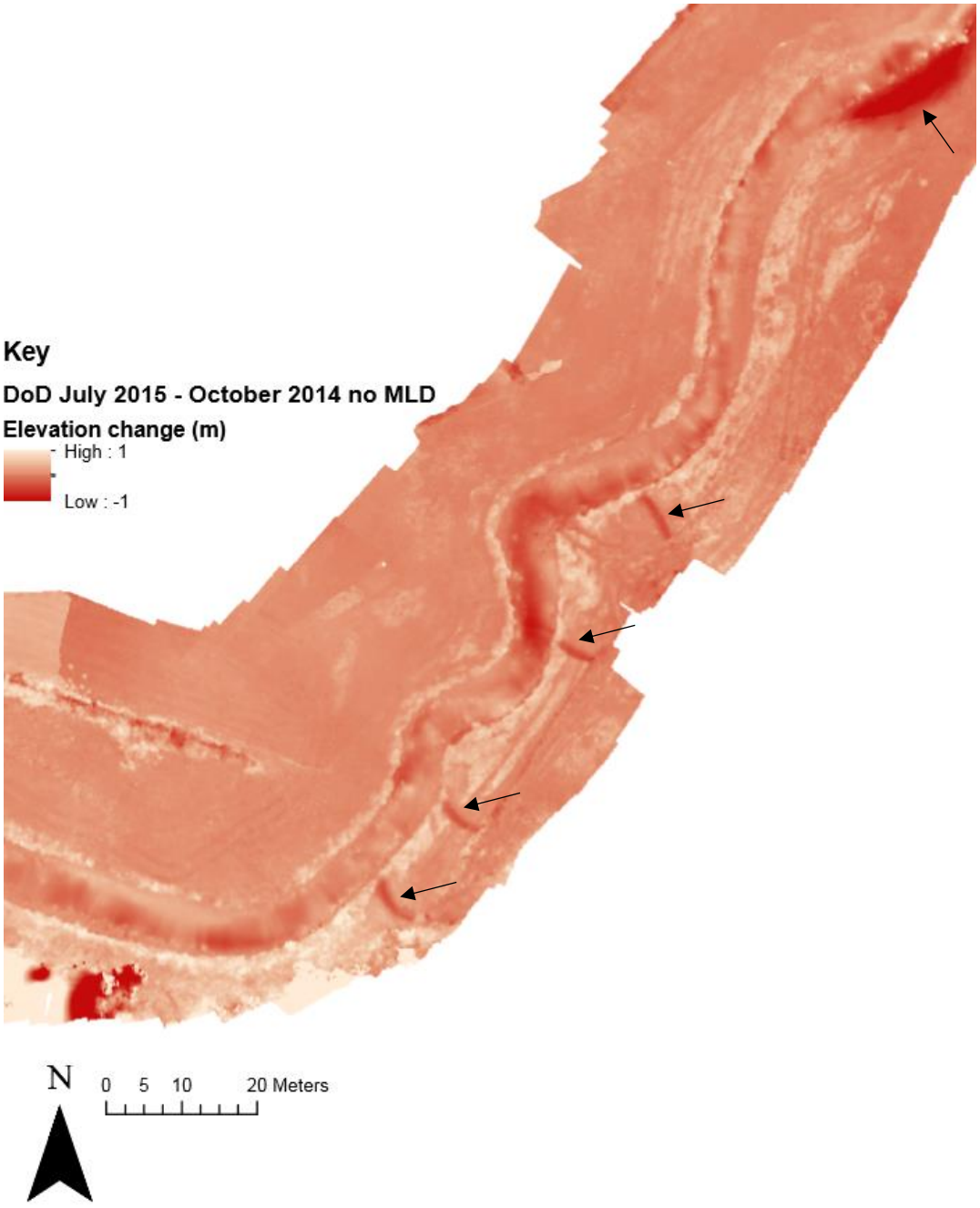

Figure 5.7: Erosion map of the areas examined. Brighter red areas can be associted with a negative change (erosion). Black arrows indicate where gulleys have formed (as discussed in Figure 5.5). Large magntitudes of erosion are also seen in the upstream meander on this diagram (black arrow), this can be matched to an area of river adjustment/change as discussed in Section 4.4.2.

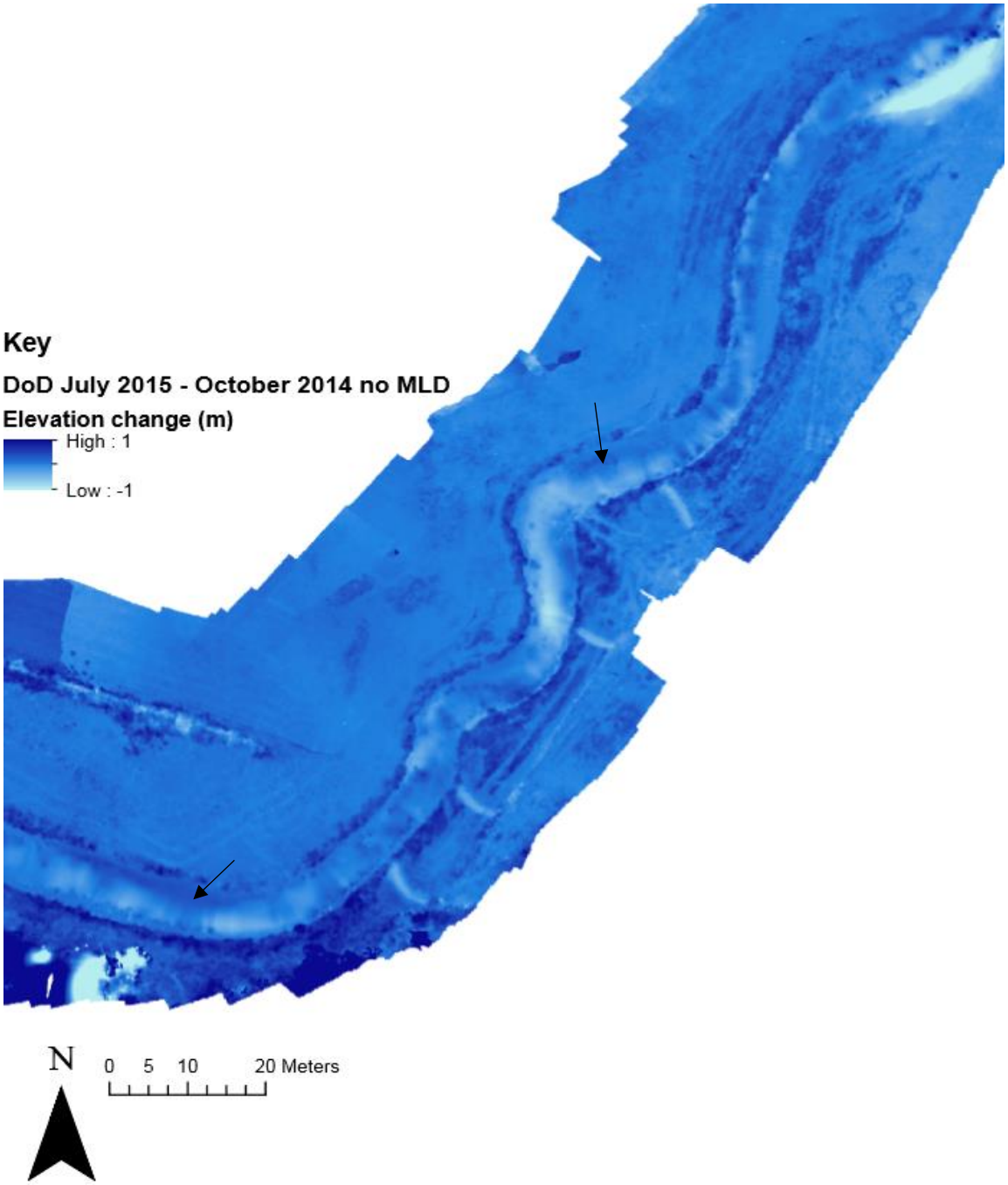

Figure 5.8: Deposition map of the areas examined. Darker blue areas can be associted with a positive change (deposition). Black arrows indicate areas of bar growth (as discussed in Figure 5.4 and 5.6).

5.2.2 Examining Different MLDs

To assess the magnitude of change, different MLD values were examined. These were 0.05 m, 0.20 m, 0.50 m and 1.00 m. The changes observed when differing MLD values are used is summarised in Figures 5.9 and 5.10. The DoDs associated with these differing MLD values can be seen (Figures 5.11, 5.12, 5.13 and 5.14), while elevation charts showing the relative proportion of change in grouped categories for these DoDs can also be viewed in Appendix III. A table showing this data in numerical form can also be seen in Table 5.1.

As expected, the relative area experiencing change at higher MLD values decreased (Figures 5.13 and 5.14). When no MLD value is used, 100% of the area examined experienced change. This decreased to values of 77% (17117 m^2) and 34% (7576 m^2) for MLD's of 0.05 m and 0.20 m respectively. 14% (3029 m^2) of the area experienced change above 0.50 m, while approximately 4% (905 m^2) saw change above 1.0 m. Higher MLD's show that the percentage of erosion compared to deposition increases when larger magnitudes of change are assessed (Figure 5.10). At the 0.20 m level, deposition can be seen to be more prominent, with 62% of the area classed as depositing. However, at higher MLD values of 0.50 and 1.00 m, the relative percentage of area showing erosion increases. 43% and 53% of the area examined showed erosion for the 0.50 and 1.00 m MLD results.

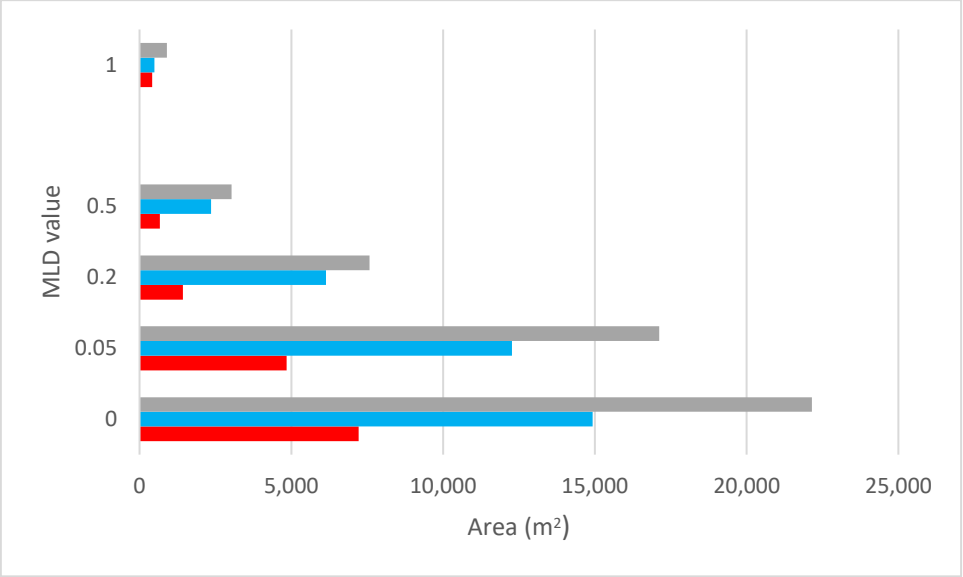

Figure 5.9: Area of change when different MLDs are used. The grey bar shows complete DEM change, while the blue and red bars show deposition and erosion respectively.

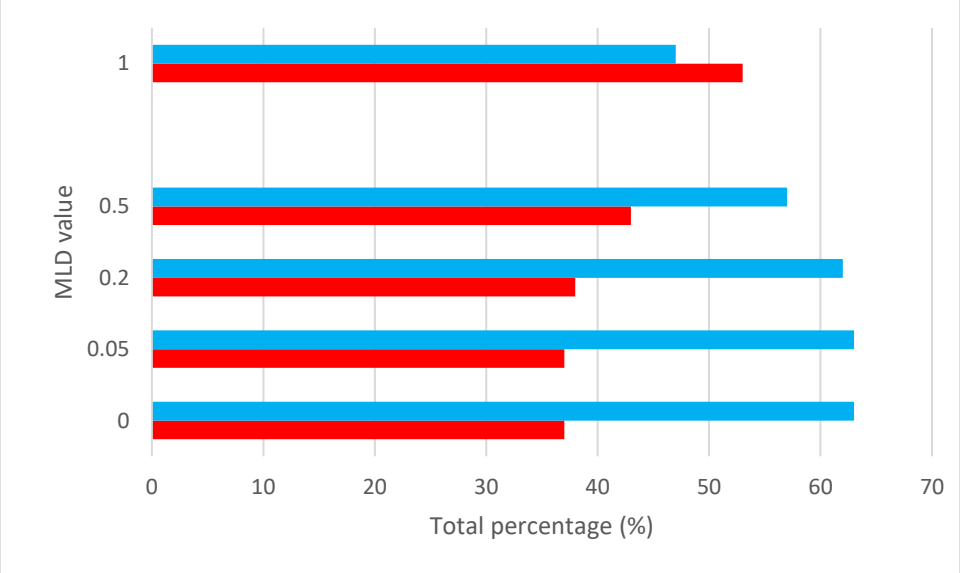

Figure 5.10: Percentages of deposition and erosion when differing MLD values are used. Blue bar shows deposition, while the red bars shows erosion.

Table 5.1: Different MLD values for spatial change.

DoD	Total area of erosion (m^2)	Total area of deposition (m^2)	Total area of detectable change (m^2)	Percentage of area with detectable change (%)	Percentage erosion (%)	Percentage deposition (%)	Percentage imbalance (%)	Percentage net to total volume ratio (%)
no MLD	7,221	14,930	22,151	100	37	63	13	26
0.05 MLD	4,843	12,274	17,117	77	37	63	13	26
0.20 MLD	1,433	6,142	7,576	34	38	62	12	25
0.50 MLD	674	2,355	3,029	14	43	57	7	14
1.00 MLD	413	493	905	4	53	47	-3	-7

The DoD technique has mapped channel change adequately when corresponding orthophotos are compared. The only area of the channel experiencing channel change above 1.0 m is at the upstream meander (Figures 5.13 and 5.14) where channel change has been of the highest magnitude seen throughout the area examined (as discussed in section 4.4.2). This would suggest the DoD technique at higher MLD values has adequately mapped and determined areas where larger magnitudes of change are visible. This area of change can also be seen on the DoDs for the 0.20 and 0.50 m MLD values (Figures 5.12 and 5.13).

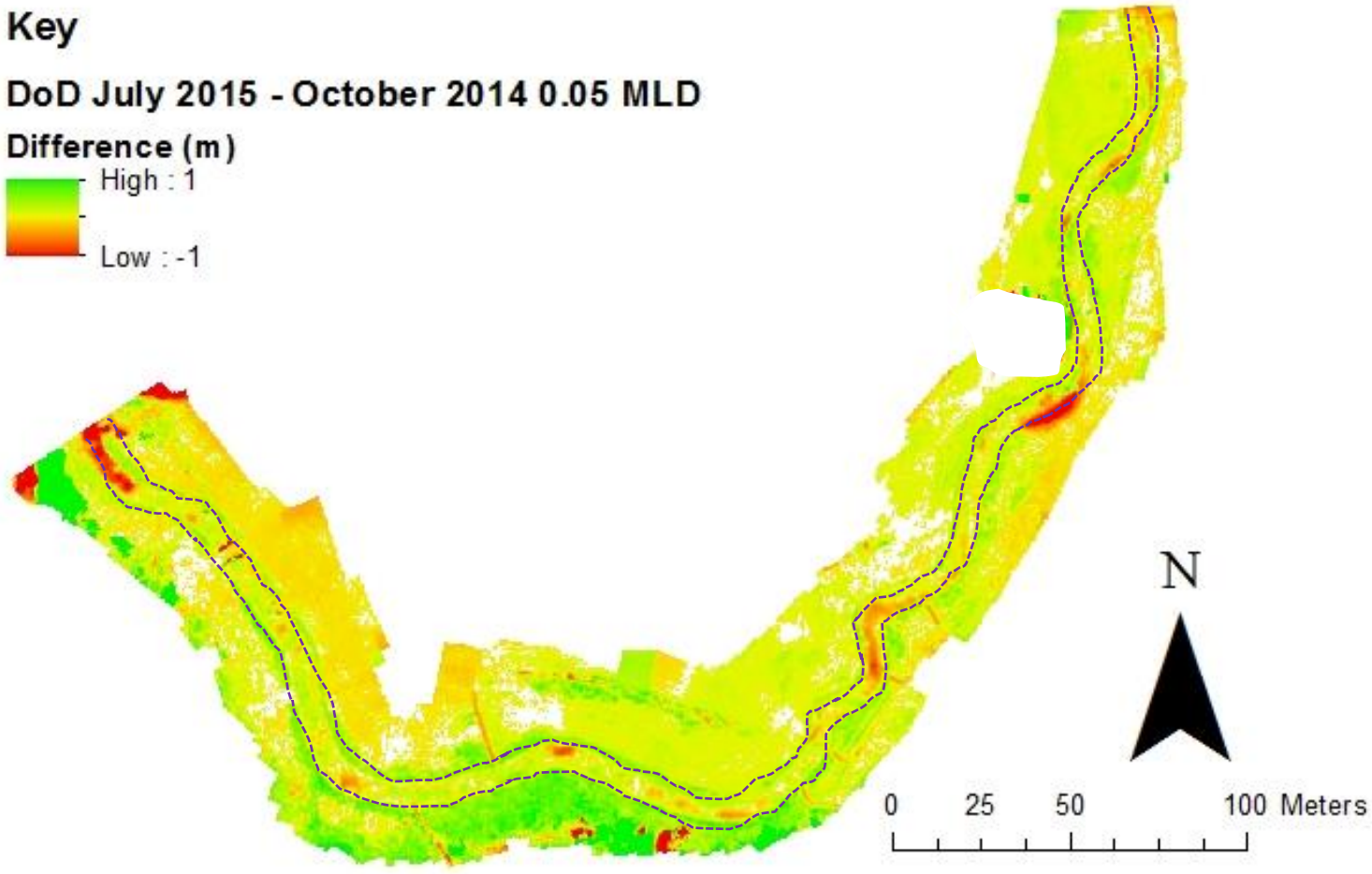

Figure 5.11: DoD for October 2014 and July 2015 at the 0.05 m MLD. See Appendix III for matched elevation chart. River outline shown.

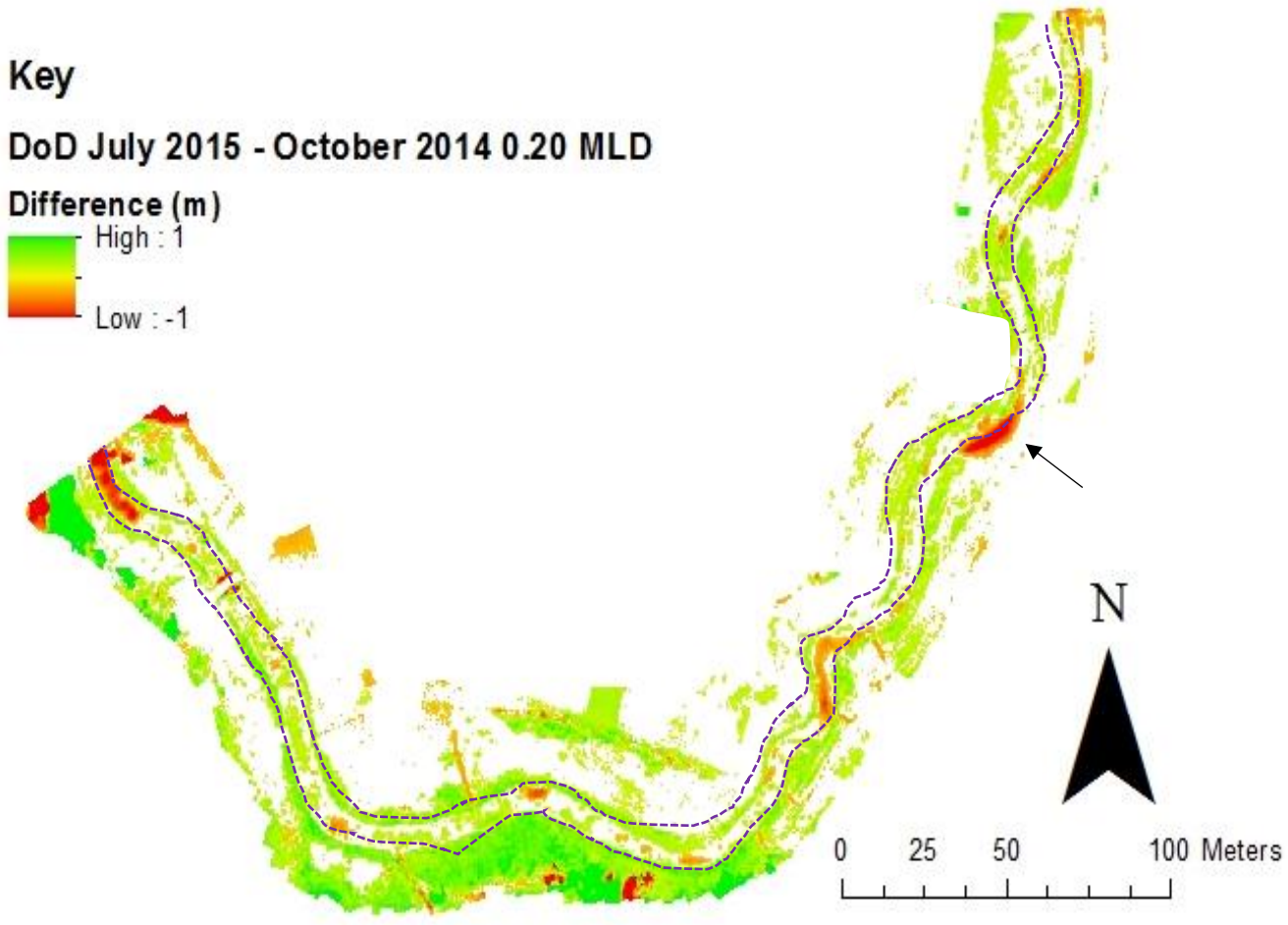

Figure 5.12: DoD for October 2014 and July 2015 at the 0.20 m MLD. See Appendix III for matched elevation chart. The black arrow indicates the area of large erosion near the tree as discussed in Section 4.4.2. River outline shown.

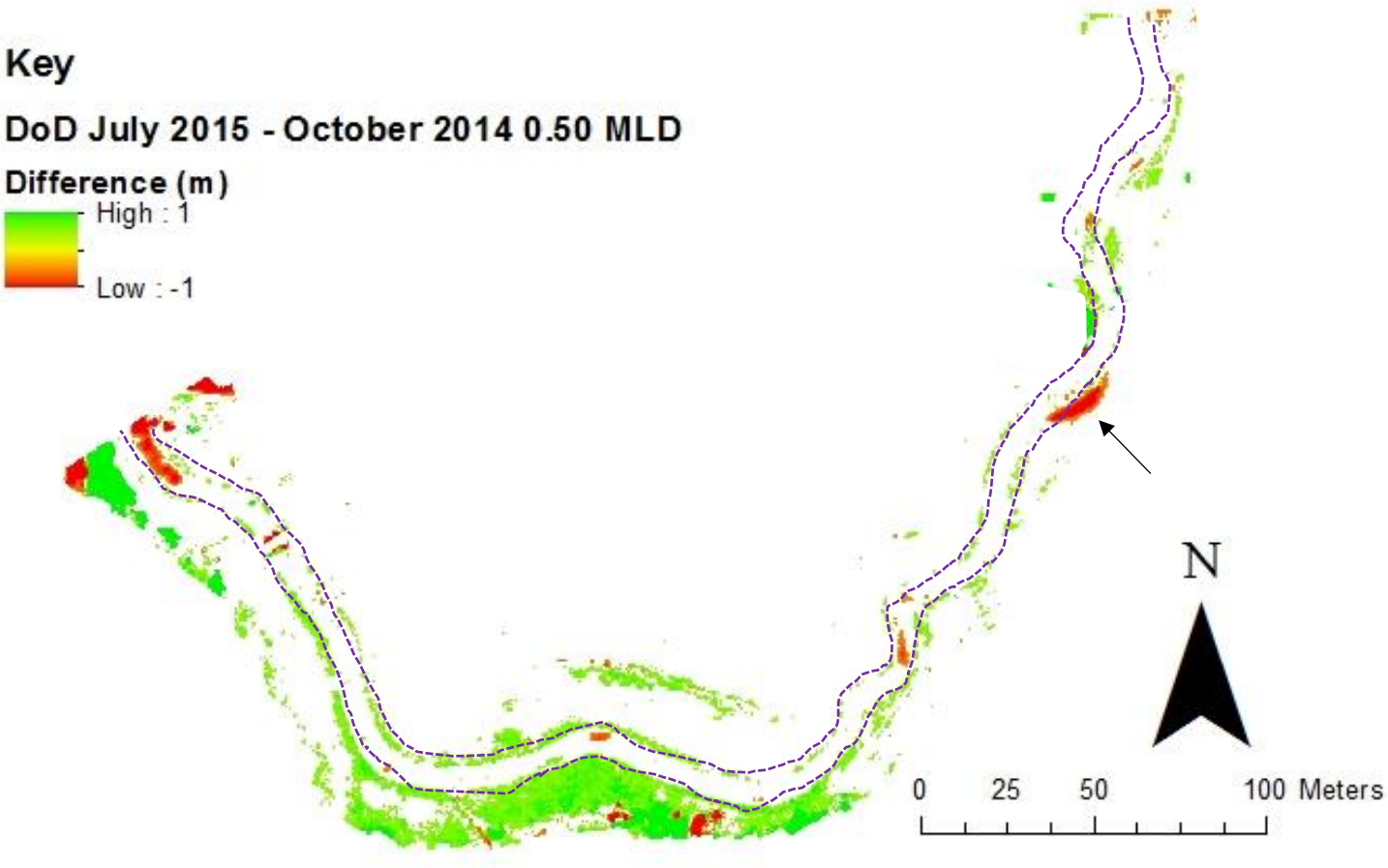

Figure 5.13: DoD for October 2014 and July 2015 at the 0.50 m MLD. See Appendix III for matched elevation chart. The black arrow indicates the area of large erosion near the tree as discussed in Section 4.4.2. River outline shown.

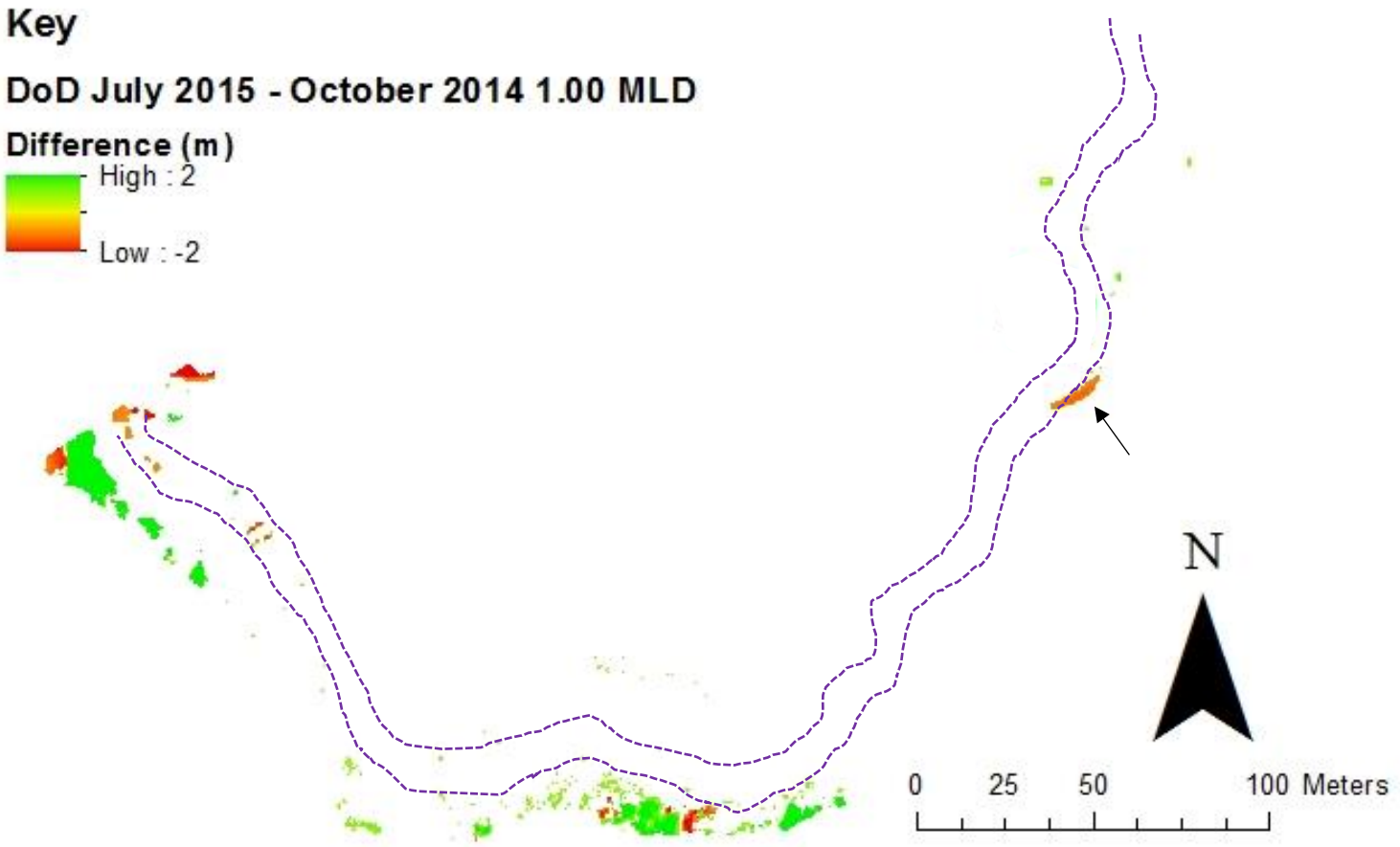

Figure 5.14: DoD for October 2014 and July 2015 at the 1.0 m MLD. Please note change of scales. See Appendix III for matched elevation chart. The black arrow indicates the area of large erosion near the tree as discussed in Section 4.4.2. River outline shown.

5.2.3 Summary

The complete DoD for October 2014 - July 2015 shows the spatial extent that was investigated (dry and wet areas) was mainly depositing. The largest frequency of change was between 0.00 and -0.25 m (deposition) where approximately 10500 m^2 can be classed in this category (Figure 5.2). The DoD examined mapped change precisely with smaller scale features (gullys) visible on the maps produced. The relative proportion of erosion increased as higher MLD values (0.5 and 1.0 m) were examined. 4% of the area examined change above 1.0 m and an area where a large magnitude of erosion has been physically seen has been correlated to the DoD results. This suggests the DoD technique is valid and reliable tool for the analysis of channel and surrounding land change, especially in the context of river restoration efforts. However, caution is required as the influence of tree cover and shade in promoting unrepresentative change may limit the applicability of this technique in other similar river restoration studies, specifically where vegetation cover changes regularly.

5.3 Hydraulic Modelling

Hydraulic modelling was carried out to infer geomorphic units in the Whit Beck data. This process would also validate the SfM outputs produced and determine how effective they could be in a modelling capacity. Initial testing was carried out using the October 2014 dataset by using the optimum conditions discussed in Section 4.2. Further modelling was undertaken using data from July 2015. Table 5.2 shows some of the values used in the hydraulic models created. Flood Modeller software was used in all model outputs. The total flows were selected by examining data in a modelling report for the River Cocker at Low Lorton and Whit Beck at High Lorton (Environment Agency 2013). A 1 in 2-year flood event along this section of the river was modelled to have an approximate flow of 8-13 m^3/s (see Section 3.8). Therefore, the range of selected flows would allow an appreciation of high and low magnitude flows (relative to 1 in 2 years) to be attained.

Table 5.2: The values used in Flood Modeller for the outputs presented.

Simulation length (hours) (model run = steady state)	1
Grid size (m^2)	0.2 x 0.2
Time step (seconds)	1
Roughness value (Manning's)	0.05
Upstream boundary (Total flow m^3/s)	1,2,4 and 6
Downstream boundary (normalised depth / m)	0.005
Number of cells used	68461
Memory usage (per simulation)	671 MB
Solver Scheme	ADI

5.3.1 Total Flow Variability

An assessment of changes in depth and velocity when different total flows are input into the model is presented. Figures 5.15 and 5.16 show depth and velocity variation for flows of 1, 2, 4 and 6 m^3/s using the October 2014 data. An expectation of the data would assume that depth and velocity generally should increase proportionally when larger total flow values are used. Local variation however plays a significant role in determining depth and velocity variation.

5.3.1.1 Depth Variation

Depth outputs using differing total flows are shown in Figure 5.15. Water levels increase as a larger total flow input is used. Deeper channel sections can be seen throughout Whit Beck, particularly in the meandering section (near the tree) and before the near 90° meander. A total flow of 1 m^3/s is likely to be the most realistic output for daily flow variability for October 2014. Flows of 4 m^3/s and 6 m^3/s show very large depths (>0.7 m) throughout the majority of channel area.

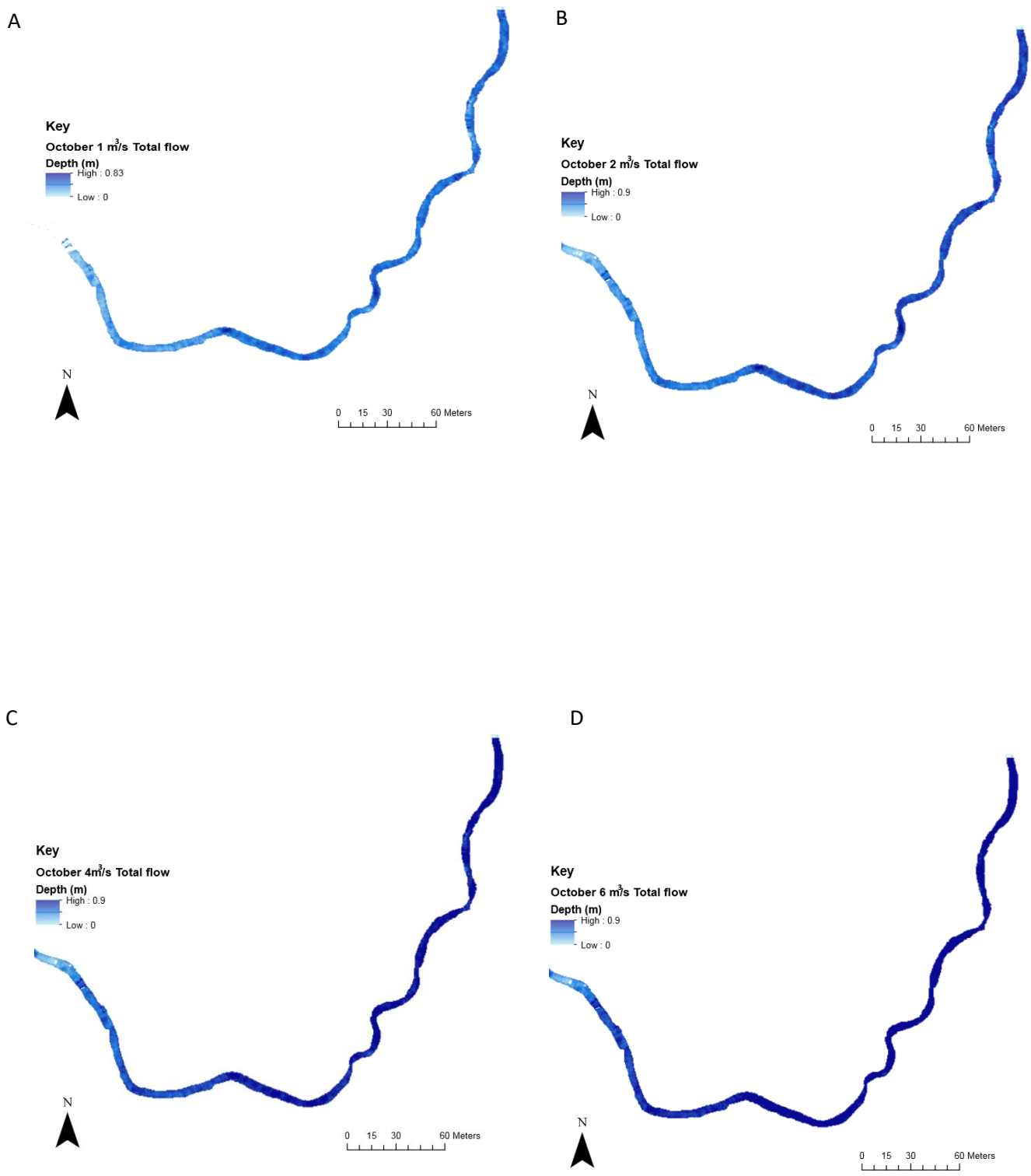

Figure 5.15: Depth varation for different total flow inputs (October 2014 data) a. 1 m^3/s b. 2 m^3/s c. 4 m^3/s and d. 6 m^3/s. All figures have the same scale and north oreintation.

5.3.1.2 Velocity Variation

Figure 5.16 shows velocity outputs for the different flows used. A similar general trend can be noted to depth variation. Velocities generally increase when larger flows are used. 1 m^3/s is probably the most representative output for daily flows in October 2014. Meandering sections can be associated with areas of relatively high and low velocities compared to mean values throughout Whit Beck.

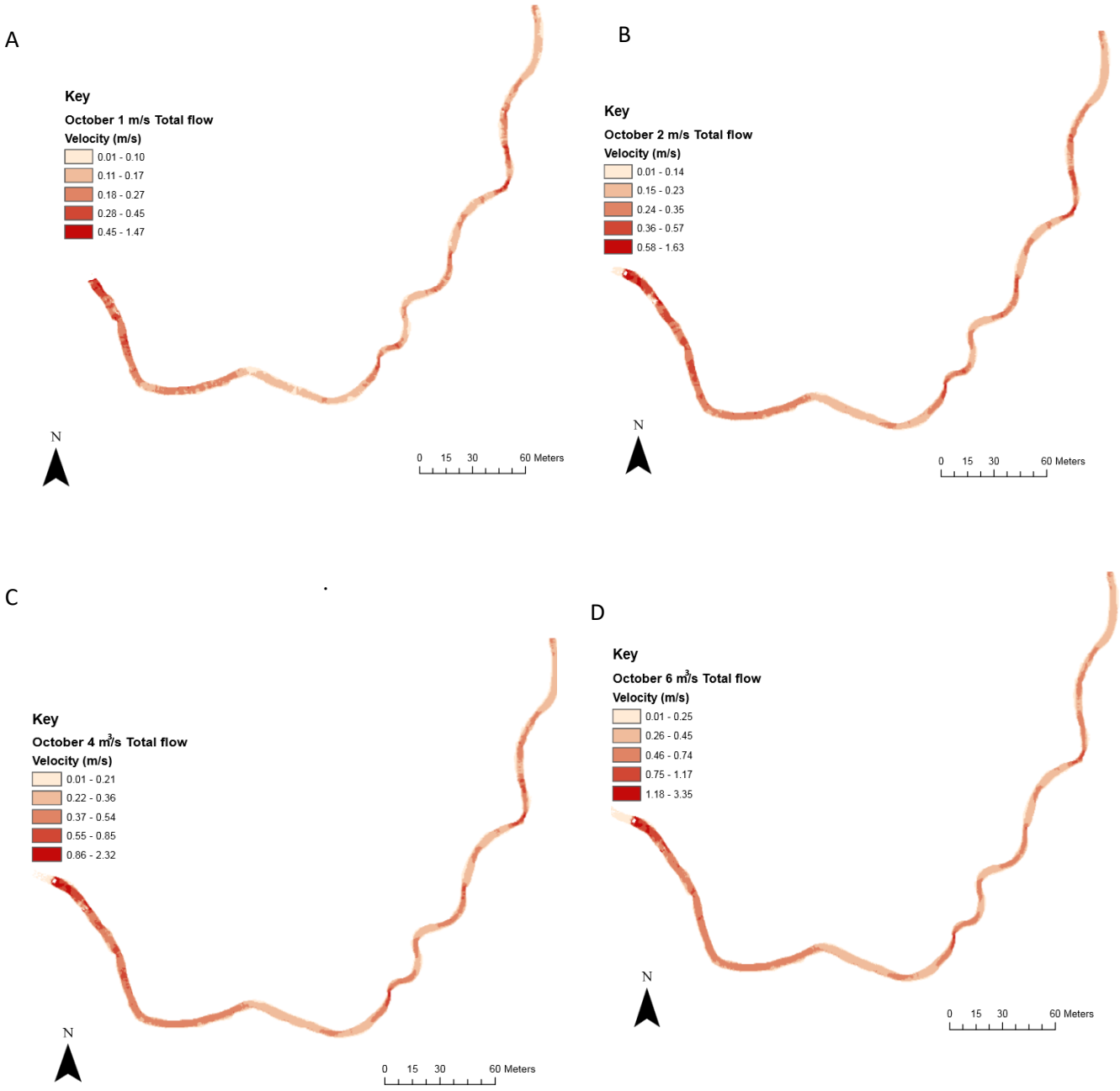

Figure 5.16: Velocity varation for different total flow inputs (October 2014 data) a. 1 m^3/s b. 2 m^3/s c. 4 m^3/s and d. 6 m^3/s All figures have the same scale and north orientation.

5.3.2 Geomorphic Unit Classification

Depth and velocity data can be used to map geomorphic units throughout a channel area. Figure 5.17 shows how different geomorphic units can be classified under different depth and velocity values (Wyrick et al. 2014). This can enable a better understanding and interpretation of the processes within fluvial systems.

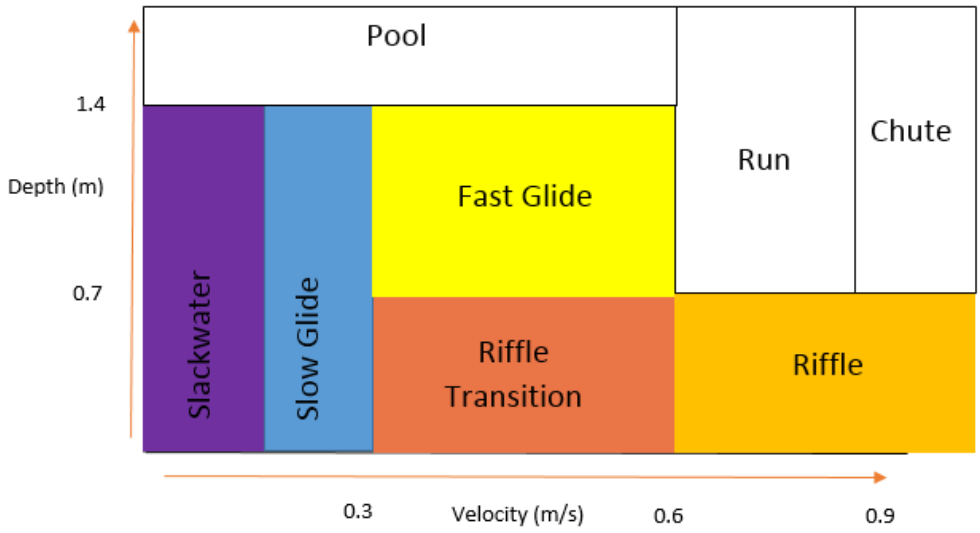

Figure 5.17: A geomorphic unit classification system derived from Wyrick et al. (2014). Coloured units relate to geomorphic units seen along Whit Beck.

5.3.2.1 October 2014 Geomorphic Unit Variability

An appreciation of the different geomorphic units present at three sites along Whit Beck is presented. An input total flow of 1 m^3/s was used and all data is from October 2014. Three sites were chosen which showed a large amount of geomorphic variability (Figure 5.18).

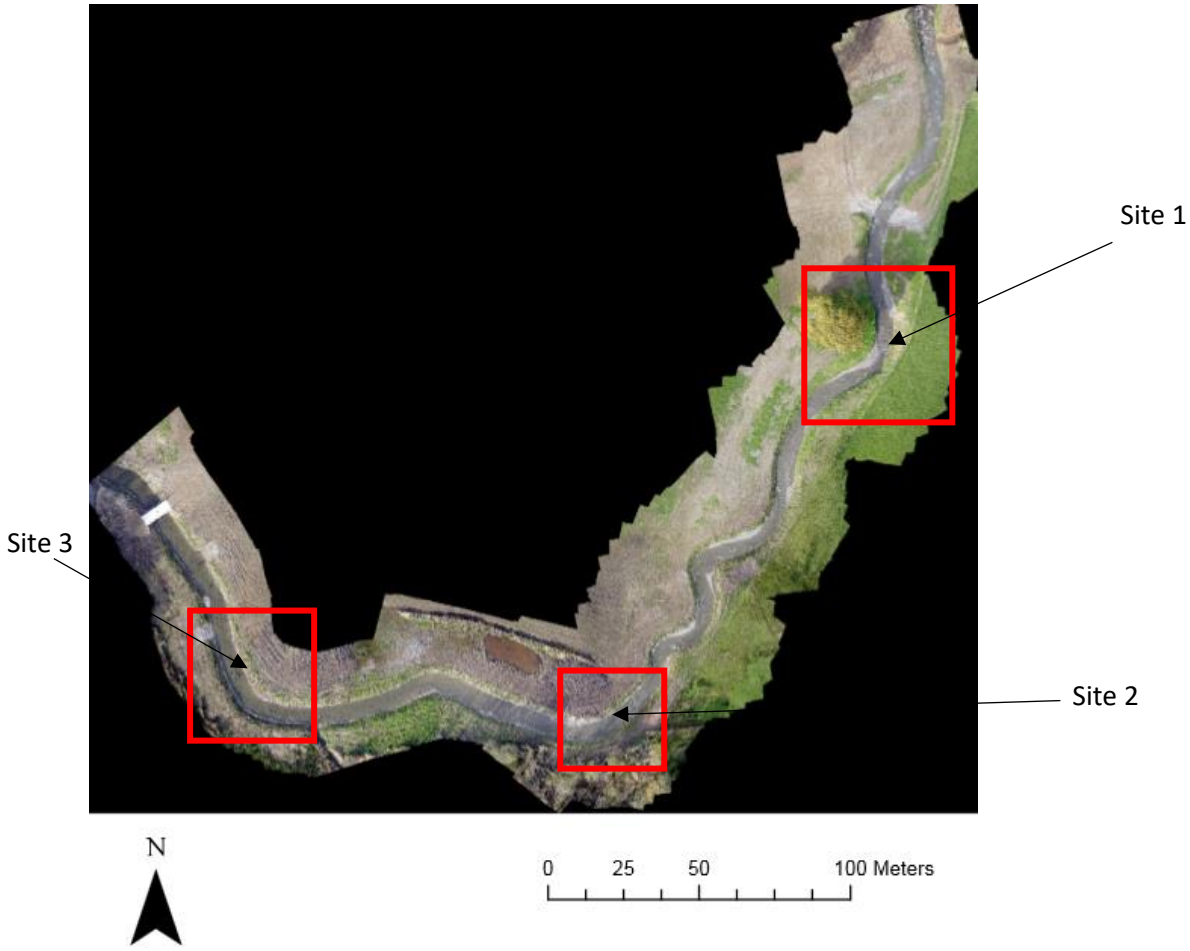

Figure 5.18: An orthophoto showing the three sites used for geomorphic classification under 1 m^3/s total flow input (October 2014).

Figure 5.19 shows geomorphic unit classification for a section of Whit Beck using the graph from Wyrick et al. (2014). Depth and velocity data is shown to demonstrate how geomorphic units are classified. A discussion on the geomorphic units present is presented.

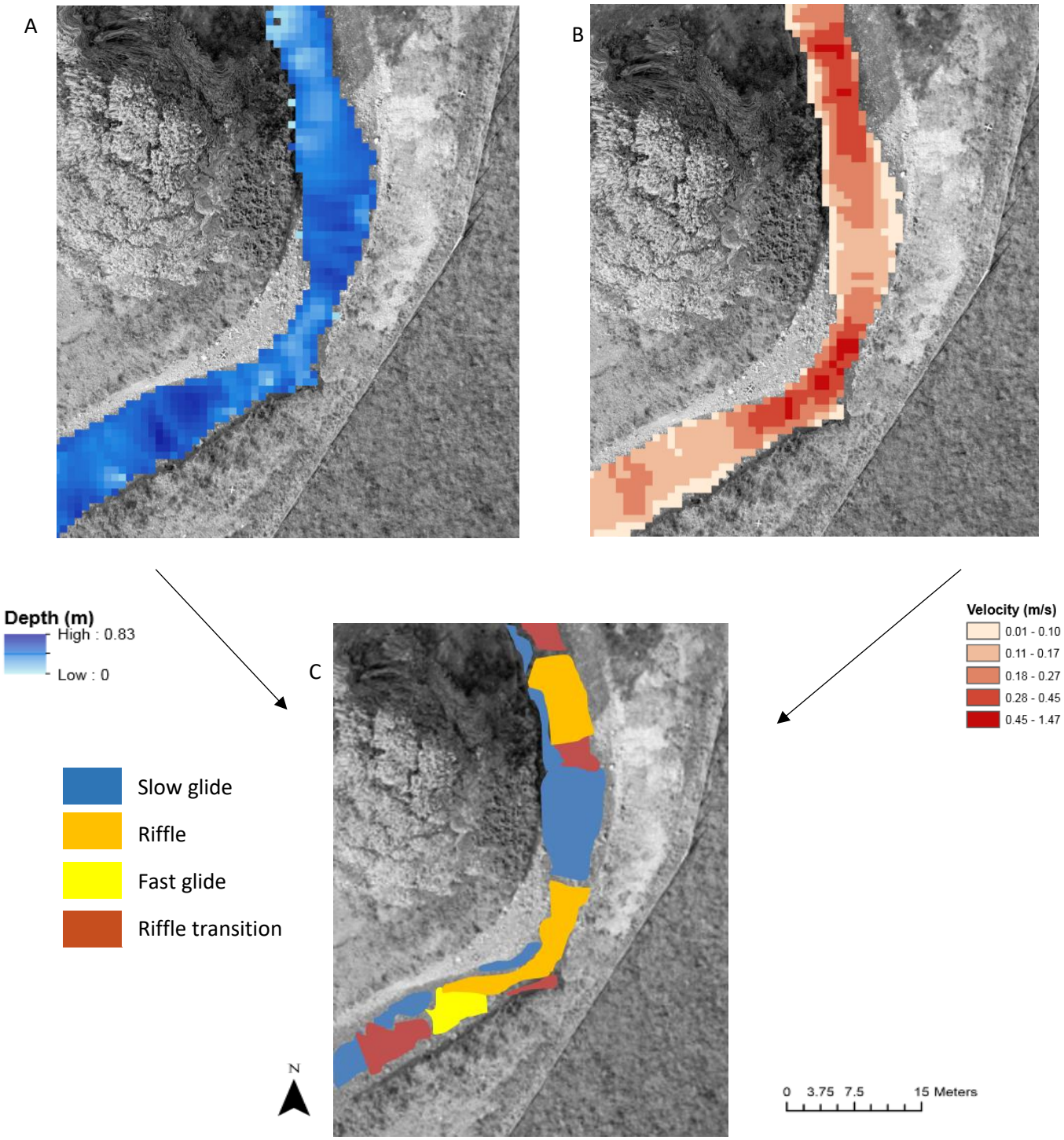

Figure 5.19: Geomorphic unit classification at site 1 for October 2014. a. depths used b. velocities used and c. final classification. This Figure illustrates how units are classed. All figures have the same scale and north orientation.

Site 1 has 4 geomorphic units present (Figure 5.19). Two main riffle areas are seen with a large slow glide area present between them. Riffle transition units seen are usually in close proximity to riffle areas. Site 2 has three units present (Figure 5.20a). A slackwater unit present around the channel boundary can be seen, while the majority of the inner channel area can be classified as a slow glide unit. Riffle transition areas are also present. Four units can be seen at site 3 (Figure 5.20b), the peripheral areas of the channel can be classed as slackwater, while the majority of the inner channel area is slow glide. A riffle unit is also present.

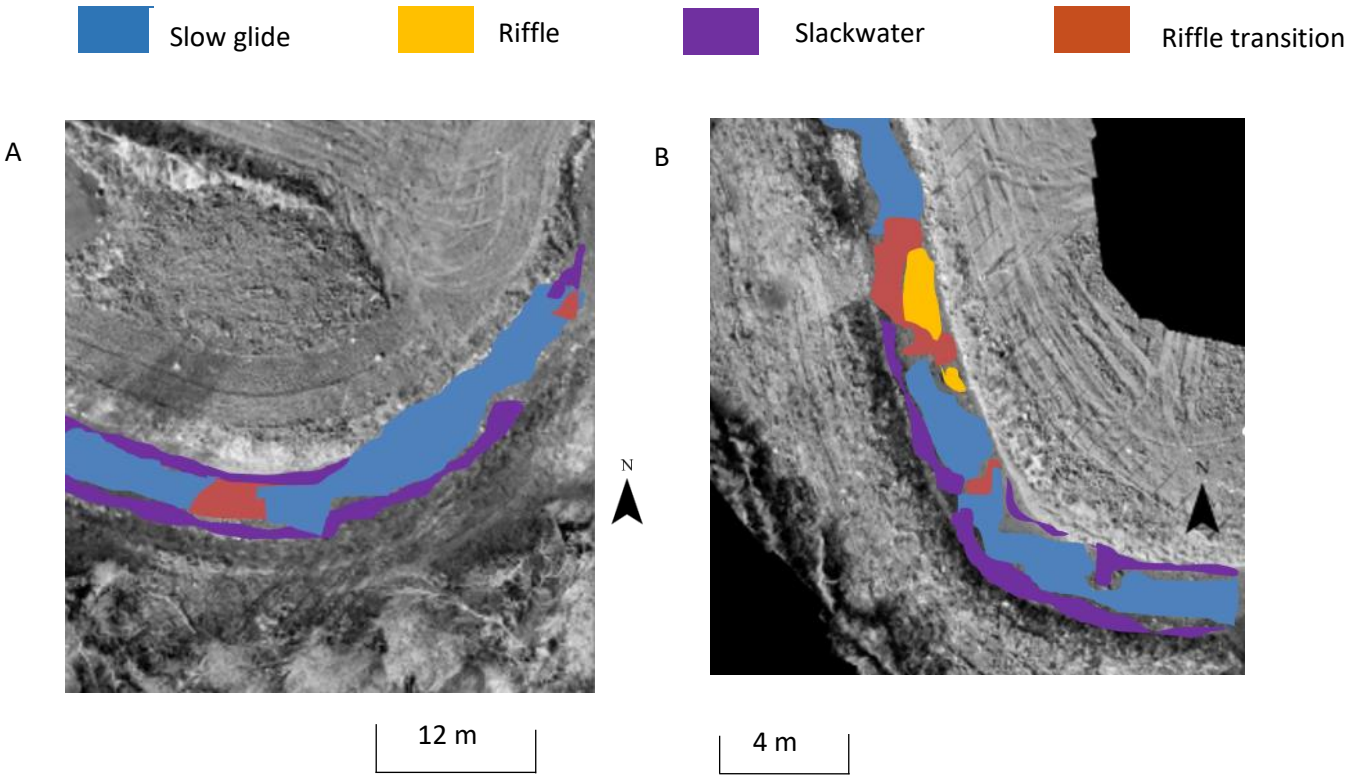

Figure 5.20: Geomorphic units present at sites 2 and 3 (October 2014 modelling) a. Site 2 and b. Site 3.

5.3.2.2 Temporal Variability

Modelled results from July 2015 were compared with October 2014 data to investigate geomorphic unit variability. July 2015 data was chosen as it had the lower combined error compared to the March 2015 dataset and it allowed an assessment of change throughout the entire monitoring period. Figure 5.21 shows the associated depth and velocity at site 1 and the geomorphic units present. Modelled depth data for July 2015 used a flow of 1 m^3/s as input to enable comparison with the October 2014 data.

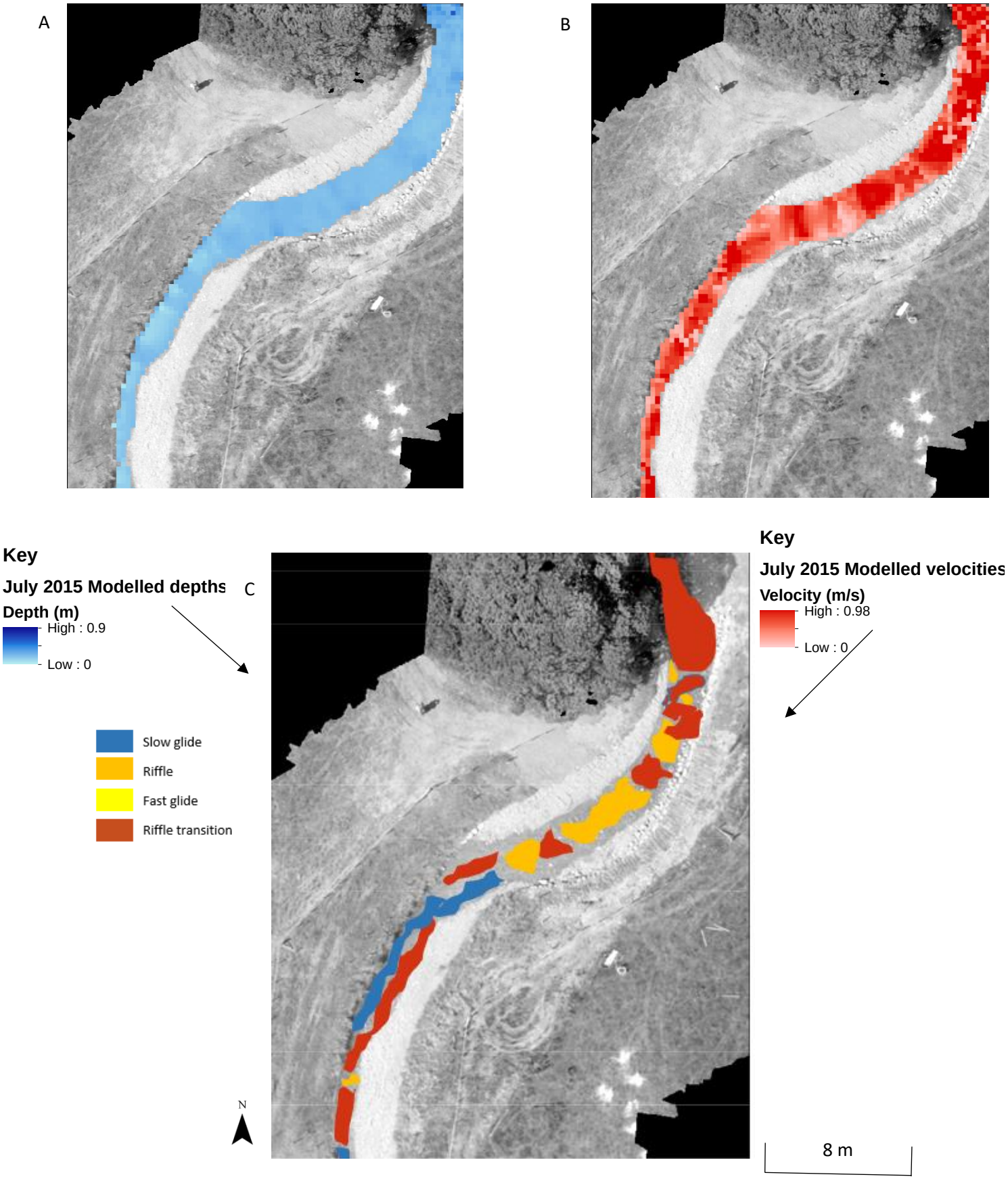

Figure 5.21: An example of how July 2015 geomorphic units were classified. a. depths used, b. velocities used and c. geomorphic units inferred. July orthophoto used. All figures have the same scale and north orientation.

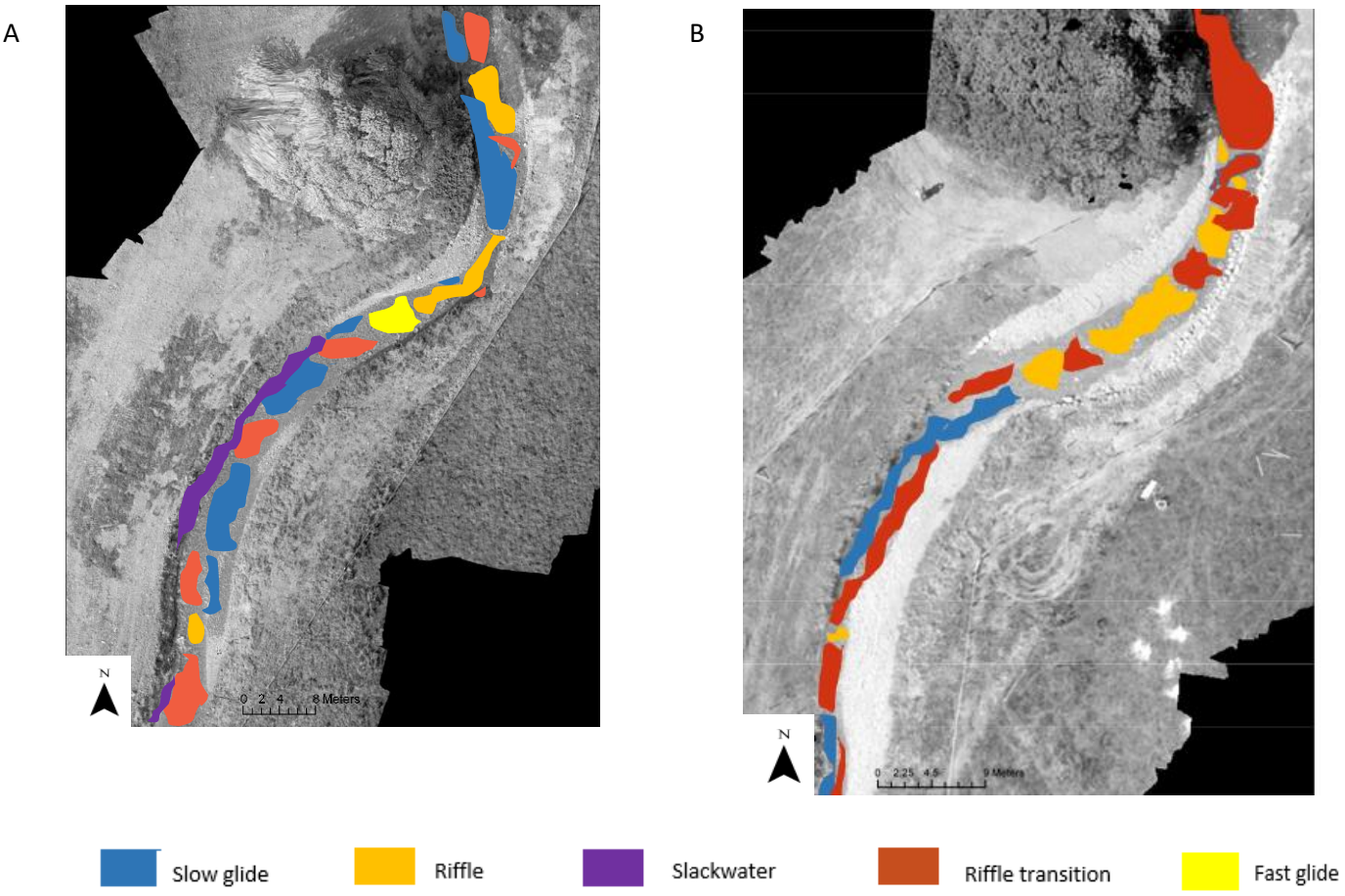

Figure 5.22: Geomorphic units at site 1 for a. October 2014 and b. July 2015. October and July orthophoto used.

Figure 5.22 shows the different geomorphic units associated with site 1 in October 2014 and in July 2015. The majority of the channel in both surveys can be mainly characterised as being slow glide or riffle transition. The riffle area in the mid-section in Figure 5.22 is longer for July 2015, while slackwater areas are visible on the true right of the channel in October 2014.

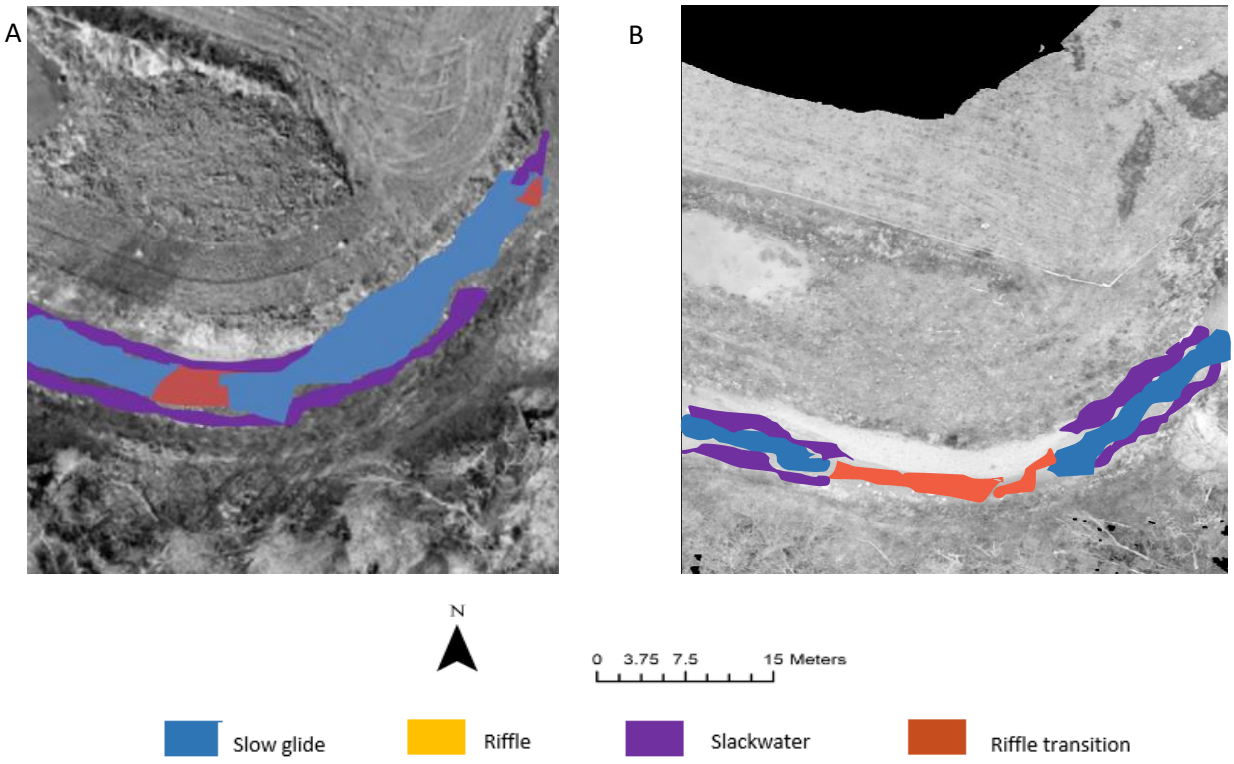

Figure 5.23: Geomorphic unit change at site 2 a. October 2014 and b. July 2015. Same scale and north orientation for both Figures.

At site 2, the same geomorphic units can be seen when both the October 2014 and July 2014 modelled results are compared (Figure 5.23). However, the relative size of the riffle transition unit is larger in July 2015 compared to the October 2014 data. The variation in geomorphic units is less compared to site 1. Inner most areas of the channel can be mainly characterised as being slow glide, while channel edges have lower velocities and are slackwater areas (Figure 5.23).

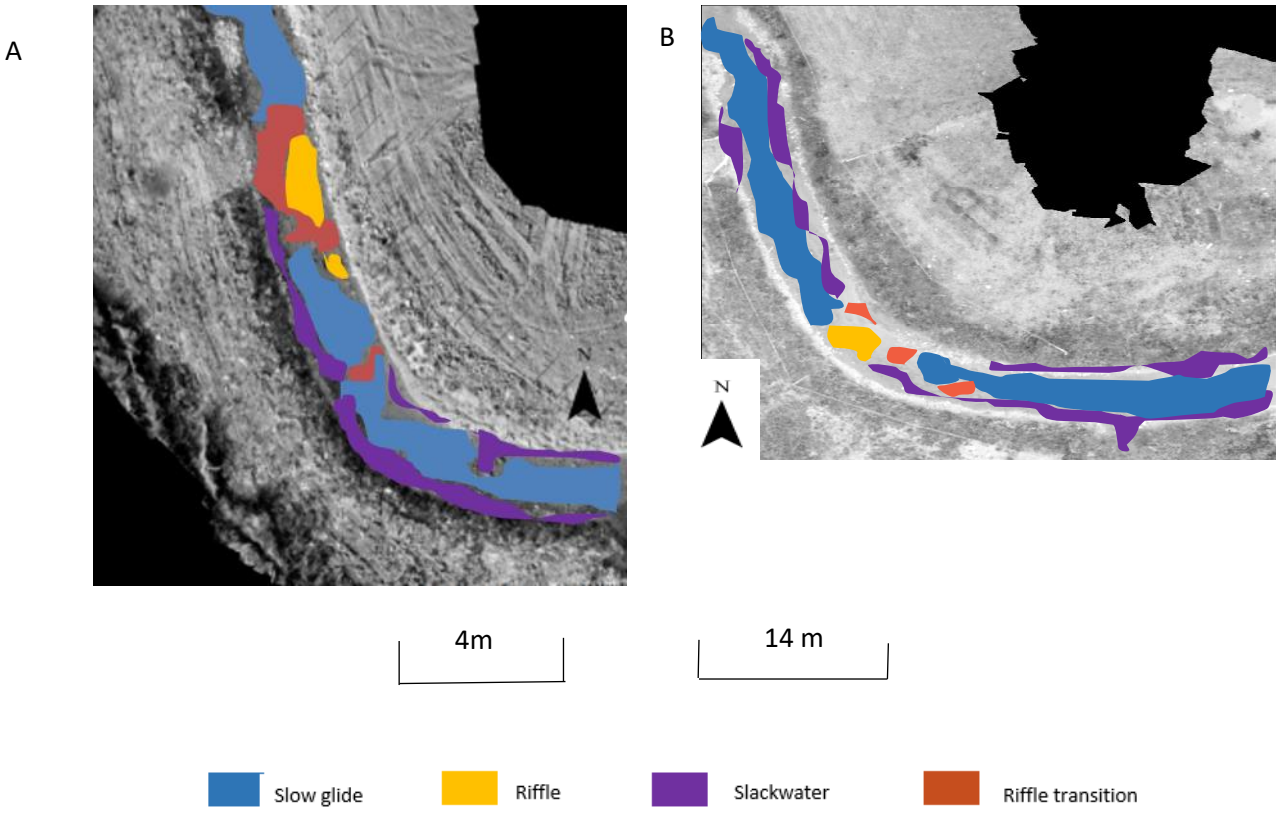

Figure 5.24: Geomorphic unit change at site 3 a. October 2014 and b. July 2015. The July diagram is extended upstream to show riffle migration upstream.

Site 3 shows a similar pattern to observations at site 2 (Figure 5.24). For the upstream section, the innermost channel can be seen to be a slow glide, with channel edges being slackwater areas. Riffle and riffle transition units are apparent in both surveys, with the riffle area larger in October 2014 when compared to July 2015 results. The riffle transition units are also larger and longer in length in October 2014. The relative position of the riffle units also migrates between the two surveys. In October 2014, the riffle (and riffle transition units) are on the true right of the channel. The riffle moves further upstream and into the meander true left side in the July 2015 modelled results.

5.3.3 Modelling Summary

The data presented suggests that SfM data can be used for valid and reliable flow modelling. A range of flow inputs have been used with a total flow of 1 m^3/s suggested to be most realistic for the initial October 2014 modelling. Modelled results can be adequately used to map geomorphic units. By comparing modelled results from two surveys, differences between geomorphic unit structure can be established. Validation using locations of known geomorphic units along with associated velocity and depth data would allow confirmation of the accuracy of this technique.

5.3.4 Chapter Conclusion

In summary, DoD calculations were performed to map patterns of erosion and deposition. The technique suggests that net deposition was more widespread than erosion with 63% of the spatial area examined showing a positive elevation change. Different MLDs were used to see larger values of change and the area of geomorphic change discussed in Section 4.4.2 was mapped and shown to be an erosion "hotspot". Geomorphic change such as bar growth and gulley formation was also mapped suggesting smaller scale features can also be examined adequately. Hydraulic modelling was also carried out on the October 2014 and July 2015 SfM data. From the resulting depth and velocity data (using a 1 m^3/s total flow), geomorphic units were classed and differences between unit structure in October 2014 and July 2015 were examined. The results suggest SfM can be used in a modelling capacity, however validation using actual known units from measured data is required.

6.1 Introduction

In this chapter, error values found along the Whit Beck are compared to similar work in other geomorphic contexts (Section 6.2). The cost of the equipment and software used is also discussed (Section 6.3), while an acknowledgement of the limitations of the methodology used is also provided (Section 6.4). SfM, bathymetric and TLS comparisons are made, while the applicability to certain environments and temporal and spatial resolutions is also examined (Section 6.6). Broader issues are raised including the importance of using UAVs as a tool for communicating geomorphology (Section 6.7).

6.2 Error Comparisons

6.2.1 SfM Errors

In this study, error values for July 2015 were lowest on average with values of -0.00316 m, -0.00364 m and -0.00572 m for the x, y and z axis (pre-correction and validation). Table 6.1 shows all error values for the three surveys undertaken. Different cameras and quadcopters were used to assess if the techniques could be reproduced with different setups. It is suggested that the Panasonic Lumix camera had an input in minimising the errors as this was found to promote best quality results. Table 6.2 shows results from Woodget et al. (2014) (pre-correction and non-submerged) to act as a comparison to the results presented from Whit Beck. Woodget et al. (2014) investigated two rivers, the River Arrow (Worcestershire) and the Coledale Beck (Cumbria). Coledale Beck in particular has very similar characteristics to that of Whit Beck and thus these are suggested to be favourable for comparison.

Table 6.1: Mean error values from this study (pre-correction and validation). All values are for models built using the optimum conditions described.

	Mean error (m)		
	X	Y	Z
October 2014	-0.00350	-0.02120	-0.00310
March 2015	0.01170	0.01590	0.01270
July 2015	-0.00312	-0.00364	-0.00572

Table 6.2: Mean error values from Woodget et al. (2014) (pre correction and validation).

	Mean error (m)		
	River Arrow		
Mean error (m) River Arrow	X	y	Z
May 2013	0.006	-0.001	0.002
June 2013	-0.028	0.008	-0.001
August 2013	0.007	0.007	0.015
Coledale Beck			
July 2013	0.002	-0.001	-0.015

Errors from Woodget et al. (2014) range from between 0.001 and 0.015 m (River Arrow). The majority of errors from this study fall into this range, with March 2015 data showing higher than average error values. When the results are compared to the Coledale Beck, errors are comparative with this study. Z axis errors are highest for both the July 2013 data (Coledale beck) and the July 2015 data (Whit Beck), while both the x and y axes show similar error ranges of between 0.003 m and 0.007 m. Using the previous SfM studies presented in Table 2.1 (Section 2.3), the results presented here are in agreement, most notably with Fonstad et al. (2013) and Smith and Vericat (2015). The latter found errors of between 0.003 m and 0.02 m, specifically in relation to sub-catchment scales, which are similar to error values presented here.

6.2.2 SfM and TLS Comparisons

SfM-TLS differences were 0.041 m (three flight lines) and 0.043 m (one flight line) when the October 2014 SfM data and the October 2014 TLS data were compared (Section 4.2). Work by Smith and Vericat (2015) suggest, that this is a typical range of difference between SfM and TLS data. Differences between the two techniques were found to range between 0.02 m and 0.13 m, while smaller scale analysis (plot scale) suggested smaller errors (less than 0.006 m) were possible. The catchment scale SfM-TLS comparisons made by Smith and Vericat (2015) are of a similar magnitude to the differences discussed for Whit Beck.

Work by Mancini et al. (2013) in a coastal context also found comparable results using an assessment of individual points within DEMs (Figure 6.1). Errors range from up to ± 2 m; however, the majority of differences have smaller error values. Clusters of large differences can be observed as indicated by the red and blue points. Large differences can be seen, however the background level of difference remains relatively small (Figure 6.1).

Similar work by Westoby et al. (2012) found comparable differences (± 2m) when an area of Constitution Hill in Aberystwyth was mapped (Figure 6.2). The majority of the area under investigation has relatively low differences, suggesting that the techniques are comparable. Areas of high differences are shown with the letters A-D. Issues with computer demand (requirements of size and memory) and time for required processing were acknowledged, while the technique of SfM was praised as it allows camera positions to be matched without the input of spatial referencing data (Westoby et al. 2012).

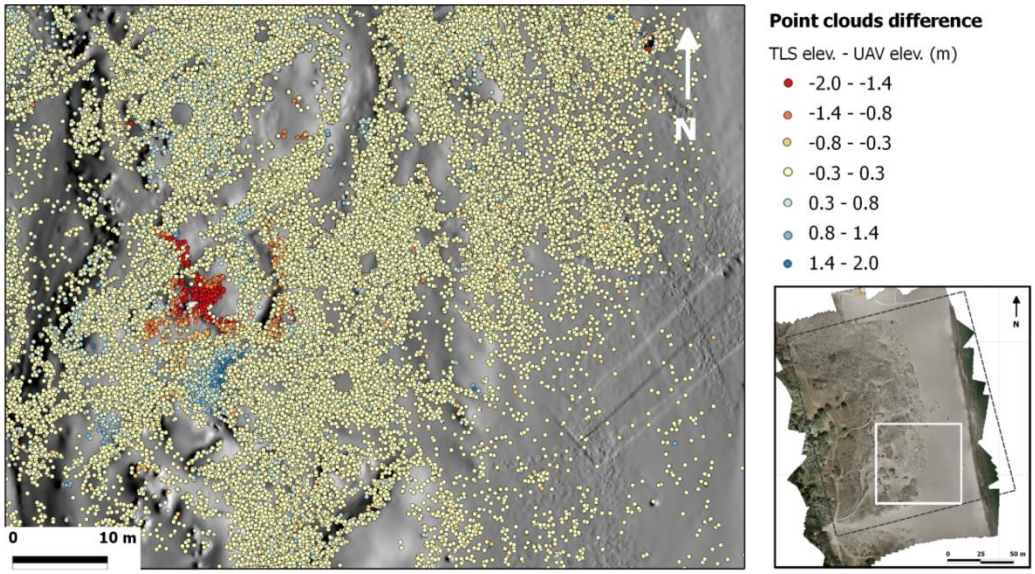

Figure 6.1: An individual point assessment between TLS and SfM. Clusters of high and low differences can be observed with the red and blue points (as indicated), from Mancini et al. (2013). The area shown is Ravenna beach (Italy).

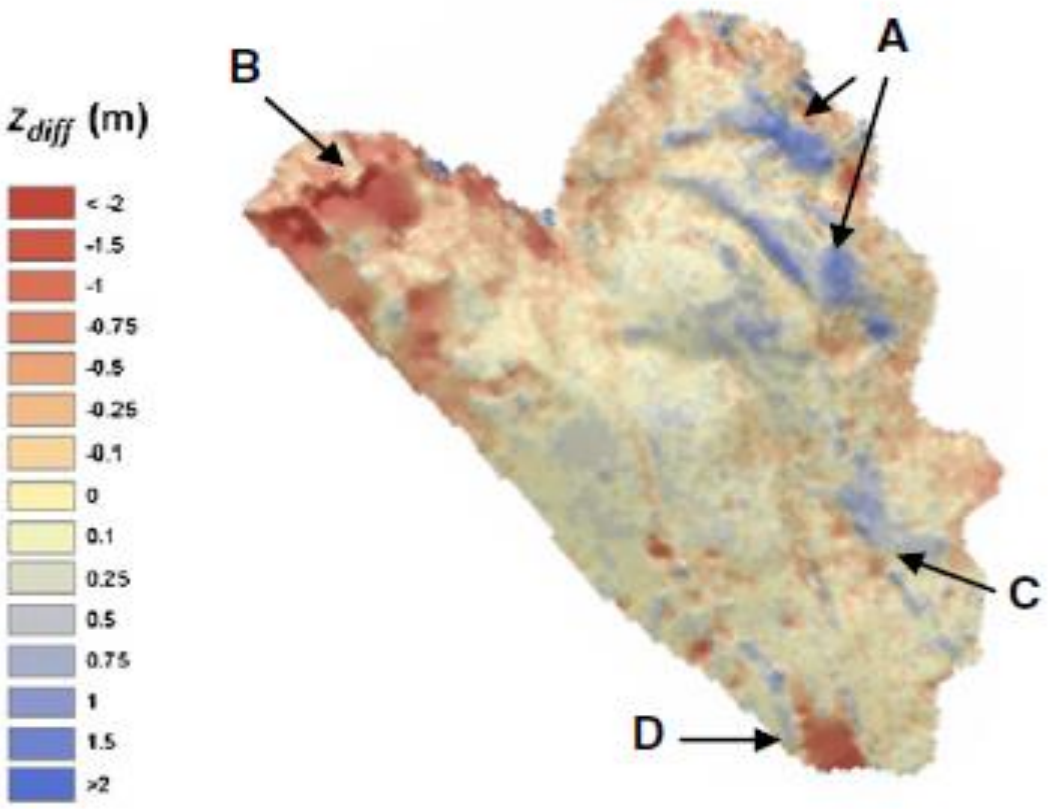

Figure 6.2: The differences observed between TLS and SfM data from Westoby et al. (2012). a, b, c & d relate to areas of positive (red) and negative (blue) change. The area shown is Constitution Hill in Aberystwyth (UK).

Further investigations to understand the reasons for this clustering action is required to fully understand why the differences between SfM-TLS data occur (Piermattei et al. 2015). Although the above examples show that a range of spatial extents and environments can be investigated, similar patterns or trends can be seen.

Other geomorphic surveying methods such as ALS and rtkGPS have been shown to produce data which has closer error statistics to TLS datasets (Passalaqua et al. 2015). Further work is needed if SfM technology is to match the errors seen between these comparisons (Bangen et al. 2014a). The inability to map and compare submerged areas between the two techniques can be seen as a major drawback (Passalacqua et al. 2015). Despite this, SfM offers a spatial and temporal scale for geomorphic investigation which is very similar to that of TLS (Bangen et al. 2014a; Smith and Vericat 2015). In what follows, an evaluation of the SfM technology and the workflows used in this thesis will be presented.

6.2.3 Bathymetric Errors

Studies suggest errors for bathymetric datasets range from between 0.008 m and 0.053 m on average across all axes (Woodget et al. 2014). When the bathymetric errors are examined for Whit Beck, errors (modelled-observed) were 0.0297 m (October 2014), 0.0464 m (March 2015, and 0.0394 m (July 2015) (see Table 4.1, Section 4.3). These are all situated within the range stated by Woodget et al. (2014). Shallower depths have been found to be less favourable to the refraction correction technique, but results from June 2013 (River Arrow) and July 2015 (Whit Beck) suggest the technique can work well in drier months. Despite this, Woodget et al. (2014) found that the refraction correction technique had no beneficial influence over DEMs at Coledale Beck. The shallow depths (below 0.2 m) were suggested as the primary reason for this, while other factors such as shade and glare can also influence the effectiveness of the technique.

6.3 What Is Low Cost?

Although the methodology used was considered low cost, a specific cost threshold cannot be determined as low as this will represent different meanings for different groups of people or organisations. Table 6.3 shows the cost of some of the equipment used in this study. The cost of the quadcopter is much lower than that of the scanning software, and dependent upon the error metrics required for individual studies, SfM use may be applicable to certain tasks and environmental settings. Environmental characteristics can however cause error formation within SfM datasets and issues relating to tree cover, shade, glare and shallow water (refraction correction) have been identified. The initial outlay to buy a quadcopter, along with a licence for usable image processing software such as AgiSoft Photoscan is small in comparison to a terrestrial laser scanner, and this can be seen as a major advantage of the workflow presented.

Table 6.3: Cost of equipment used in this investigation.

Equipment	Cost
Quadcopter (Phantom DJI 2)	£800
Battery	£90
Camera mount	£750
Camera (Panasonic Lumix)	£450
Licence fees	£500 annually (AgiSoft Photoscan educational license for SfM and Cyclone for TLS)
TLS scanner	£50,000

The type of investigation being carried out may help to determine what the definition of low cost is in relation to the specific variables that need to be examined. If monitoring is of long term nature (maybe over a number of years), it might be suggested that acquiring a TLS with higher initial costs may provide better output data in the long term. If the area under investigation is for a shorter temporal period or the variables being examined lend themselves to SfM applicability, it may be more advantageous to use the SfM workflows presented as they provide adequate errors values and have the advantage of being more affordable compared to TLS. For this study, it is assumed that the technology being discussed will mainly be used by environmental consultancies and government organisations and thus the cost of £800 plus a licence fee (and associated camera if needed) is considered to be a relatively low. However, organisations and groups of differing size and financial security (e.g. local action groups, academia) may consider this cost excessive and it must be acknowledged that the technology will not be favourable and usable for every organisation or group. Another important question to be considered is the applicability of the technology for different groups of people and the extent to which it can be used in varying environmental conditions. This technology in theory can be used by people who have had no training and thus this makes it potentially usable by a large number of people. This could allow a new generation of environmental monitoring to be initiated over a variety of different spatial, temporal and geomorphological contexts. In particular, SfM technology could provide the impetus to allow monitoring of landforms across a number of applications, at a low cost in comparison to other methods discussed and at relative ease. The most exciting prospect from this remains the amount of information that can be gathered and obtained from SfM techniques.

The information gathered from monitoring techniques must be incorporated and used in further restoration studies, particularly those aim to improve environmental conditions of rivers without affecting the economic and social security of the area. The analysis of data which

already exists is key for providing a foundation in which further geomorphic studies can be built (Smith et al. 2014a). Different restoration techniques may work better for certain areas and under certain environmental constraints, and determining the best course of action remains of vital significance moving forward. The knowledge gained can only be enhanced by the use and review of suitable technology.

6.4 Limitations of UAVs and SfM

A number of disadvantages associated with the SfM technology need to be addressed in the future to ensure the methodology provides the best opportunity for numerous applications across a wide range of disciplines. The first issue relates to flight restrictions. Figure 6.3 shows some CAA (Civil Aviation Authority) guidelines for the flying of drones. A number of restrictions apply to the flying of UAVs which may restrict the ability to collect appropriate data or make it more difficult to use the technology under specific environmental conditions. For instance, a commercial licence must be gained if the UAV is to be used for commercial activities, so any environmental consultancy that wishes to use the data to make a financial gain must have a commercial licence to fly the quadcopter. This license does not apply to research applications for academic users, however as the technology becomes more widely used and incorporated into environmental monitoring and planning, it can be expected that changes are likely to happen. Flight restrictions on the use of UAVs are likely to become tighter in the future and this may influence the applicability of data collection.

Flight time for the quadcopters used in this investigation was 20 minutes per battery. This will limit the spatial extent over which data can be collected, however the use of more than one battery and portable chargers can limit the effect this can have. Despite this, limited flight time is one of the major drawbacks of UAV technology (Westoby et al. 2012; Piermattei et al. 2015; Bangen et al. 2015a). The longer the flight time, the more data that can be collected which in

turn can provide more information about the catchment or landform being investigated. Examining the wider framework in which knowledge improvement can be fed into a cycle of improving river restoration schemes through better monitoring and knowledge transfer (Section 1.5) is vital if the technology wants to achieve its full potential in the future. The improvement of lithium batteries is therefore of major importance in allowing longer flight times, improved data collection, more knowledge transfer from associated outputs and thus potentially "better" restoration schemes in the future.

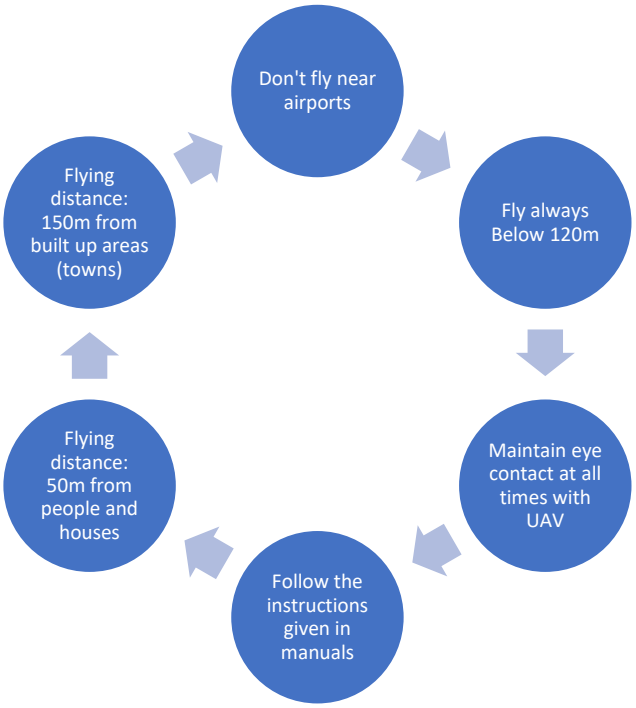

Figure 6.3 Guidelines given out by the CAA, Taken from the CAA (2016).

Another drawback of the technology used is the applicability in certain weather conditions. The majority of quadcopters available cannot be flown in wet or windy conditions. This limits the amount of data collected and therefore the amount of knowledge that can be gained from an area of interest. Flights cannot be carried out in rain which may provide issues specifically in winter periods. This may not be favourable for flood-related applications as winter periods are more likely to experience higher precipitation levels. A wind speed of above 17 mph is also not recommended for flying (Phantom DJI 2), while other quadcopters have other similar wind restrictions applicable to them. The issue with data collection confinement to specific temporal periods which favour certain environmental conditions is that data which is collected may be biased. This therefore may not provide a fair representation of the fluvial processes/environmental formats being observed and lead to poor conclusions and interpretations. The amount of sunshine may also affect the effectiveness of a UAV survey. Glare from reflective surfaces (water) may induce a poor representation of elevation height, which may be a particular issue when river channels are investigated. However, there are glare removal techniques that can be used to help combat this problem and provide better elevation outputs.

A further issue relating to this technology is the computational demand of some image processing software. Although these programs are not difficult to use, data processing can take considerable amounts of time (Rychkov et al. 2012; Westoby et al. 2012). Certain processes may take a number of hours or even days to perform, depending on a number of variables such as image quality, the number of images within a model, and the efficiency of the computer used. The limited number of software applications that can use and apply SfM is also a concern, although the number of appropriate software packages is increasing with time (Westoby et al. 2012).

In summary, it is important to understand that UAV technology has many advantages and an appreciation of both the positive and negative aspects of SfM is required before deciding on its applicability for a specific environmental area. The main disadvantages discussed relate to flight restrictions (flight time and weather conditions), but rapid technological development may result in improved applicability and usage of the technology in future applications (Woodget et al. 2014).

6.5 Evaluating the Effectiveness of Techniques

The applicability of the techniques used in this thesis also needs to be examined. Four different techniques have been used in this study to evaluate the use of SfM data and its wider applicability to a range of different fluvial geomorphic applications. The advantages and disadvantages of these workflows have been discussed in the relevant sections, however a summary of these can be seen in Table 6.4.

Table 6.4: A summary of the advantages and disadvantages of the techniques used in this thesis.

Technique	Section in this thesis	Advantages	Disadvantages and Queries
Comparisons with TLS	Section 4.3	Ability to compare dry areas against a technique of known vertical quality.	Wetted areas cannot be compared as they are not represented well with TLS.
Bathymetry	Section 4.4	Ability to calculate bed levels and depths. Corrected DEMs which fuse together wet and dry areas can be produced.	Errors can be introduced due to glare, shade, tree and vegetation cover and this can cause depth errors. This has been found to work less well in shallower areas.
DoDs	Section 5.2	Geomorphic change between surveys can be examined. This can even be used on smaller features such as gulleys. The use of different MLDs can help understand how the magnitude of change differs.	Influence of vegetation and tree cover can have an effect on the calculations.
Hydraulic modelling	Section 5.3	SfM data can be used for modelling purposes and can deliver data which has the ability to map geomorphic units.	Need for validation of this technique by comparing actual geomorphic unit layout.

To gain an insight into the fundamental post-restoration geomorphic processes and features, a combination of the techniques used could be undertaken. Different techniques will be more favourable to certain geomorphic environments and scales. For instance, DoDs can give information about the present processes occurring along a section of river and on the channel banks, while modelling could be more appropriate for future predictions and responses to climate change. The technique used needs to match the objectives set for each individual research project. The DoD technique has been shown to map the formation of gulleys, which may help promote a better understanding of surface run-off and groundwater saturation. However, the DoD technique may have little success in other geomorphic environments. It may be expected that the DoD technique is less effective in establishing the dominant processes in systems where vegetation levels change frequently for instance. By understanding the relevant advantages and disadvantages of the techniques utilised, it is hoped that better decisions can be made as to when the use of certain techniques is more favourable. This will result in improved data collection, leading to results with appropriate levels of validity and reliability.

6.6 What is the applicability of UAV and SfM Technology Over Differing Spatial and Temporal Scales?

The applicability of the technology to different temporal scales also needs to be considered. Many studies have questioned the temporal aspect of UAV studies and it is suggested that an optimum timeframe which best suits SfM software exists (Tamminga et al. 2014; Smith and Vericat 2015; Piermattei et al. 2015). This will obviously depend on a range of environmental characteristics associated with the area under investigation, and will differ significantly depending on the extent to which data needs to be collected.

The limitations discussed above suggest that a small temporal resolution for data collection through SfM (e.g daily) may be difficult. Issues such as flight time and weather conditions are

likely to limit the temporal resolution of surveys, except in specific, fortuitous circumstances. The technology cannot be used to monitor change on an hourly or daily basis in a coherent and reliable manner and thus larger temporal scales must be used. Morphological change on weekly intervals is more likely to be able to be monitored effectively and accurately given the current limitations of the software. If there is a need for a shorter temporal interval (repeat surveys), it is unlikely that the technology can be used effectively and efficiently.

Smith and Vericat (2015) found that the accuracy and error formation within SfM results varied over different spatial extents. SfM becomes less accurate over larger areas and optimum areas of investigation have been suggested to be in the region of around 10-20 m when patterns of soil erosion were analysed. This suggests the use of the technique outlined in this investigation is vulnerable to error inducement, specifically when larger spatial scales are examined. However, optimum spatial extents for different types of investigation are expected. Smith and Vericat (2015) do suggest that rapidly changing environments such as rivers provide the best chance for the software to be used effectively. The importance of validation within the results is also vital and cannot be ignored (Smith and Vericat 2015). It is difficult to assess the true optimum working conditions for the technology discussed given the complexity of natural environments. Figure 6.4 shows the spatial extent (and spatial resolution) to which it has been suggested a variety of topographic survey methods can be utilised. It has been suggested that TLS and SfM have an almost exact overlap (Figure 6.4) within a spatial system with areas of up to tens of km reportedly effective to survey and 100 to 100,000 points/ m^2 being suggested as typical spatial resolutions. These are high spatial resolutions compared to other topographical survey techniques. Other techniques such as ALS allow larger spatial extents to be examined. This can be seen as a drawback of the SfM technology but improvements in flight time and weather resistance are likely to improve this.

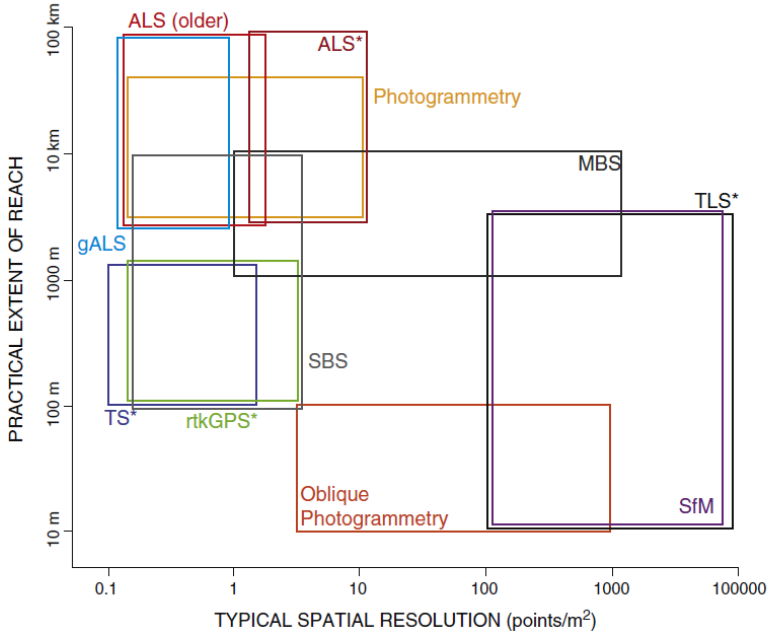

Figure 6.4: The spatial extent over which it has been suggested different topographic surveys work. SfM is shown in purple. Figure adapted from Bangen et al. (2015a).

6.7 Communicating Geomorphology: Promoting Geomorphology In A Wider Context

The use of UAVs in monitoring geomorphological landforms and assessing the magnitude and frequency of processes can have wider benefits to the science of geomorphology as a whole. The methodology discussed can interact with and may initiate a "new generation" of geomorphologists and may have great potential for conveying intricate scientific discussion into wider groups of people within society.

Gregory et al. (2014) discuss the issues and challenges associated with presenting and discussing geomorphic science in an ever increasing social-media friendly world. Software such as Twitter, Facebook and LinkedIn are promoted as new pathways through which new groups of people can engage with geomorphology. A shift from conventional forms of teaching and learning from desk or lecture type presentations, to a more holistic incorporation of a range

of methods, which allow students or other groups of people (within academia and consultancies) to participate in a new way of knowledge sharing is required. Some would suggest that there is a real need for academic and environmental consultancy groups to change and partake in these new modes of communication to promote geomorphic understanding. The use of UAVs and other novel technology has the potential to be a primary promoter of river restoration monitoring and other geomorphic research. It can be viewed in the same way as other communicating software, in which it allows science to be applied and engaged with new groups of people. The use of UAVs is becoming more widespread and can be used for a range of different purposes, specifically in relation to leisure activities. Geomorphological research should embrace this new "craze of UAVs" and connect research to the more widespread use of the technology within society. There is a specific need for collaboration between geomorphology and the arts, where data can be presented more favourably to non-specialists (Tooth et al. 2016). Geomorphology can become more accessible to wider groups of people in a fun and enjoyable manner, while promoting the transfer of knowledge between researchers and public bodies. The potential is large; however, organisations must act to ensure the full benefit of this opportunity is realised (Viles 2015).

It is important to acknowledge that although knowledge transfer through new modes of communication and techniques is vital in inducing a growing community of shared knowledge, there are however potential issues. It is fine to increase dialogue between different organisations and share information, however there is a real danger of academic projects and environmental consultancies losing their identity and rigour by engaging in work which benefits a range of parties. A cycle of continual progression and integration of new technologies is required to maintain development (Figure 6.5). This is one of the challenges outlined by Gregory et al. (2014). Knowledge transfer is integral in promoting better and improved restoration schemes, but if the number of people who can carry out geomorphic investigations

increases due to new and novel procedures, the importance of certain individuals and groups may be reduced. This is of major concern, specifically when geomorphology becomes more transmitted through social media and other more transnational means. The perfect response is to have a mix of new engaging technologies which help share knowledge throughout society, but also allow academic and consultancy institutions to maintain a clear sense of purpose within the larger geomorphological community. This balance in itself is constantly changing, as are the organisations which have to move forward in promoting new communication methods. UAV technology provides a great opportunity to help stimulate the growth of the science of geomorphology and to help share knowledge between different groups of people. It is however important that institutions remain professional and maintain a sense of authority.

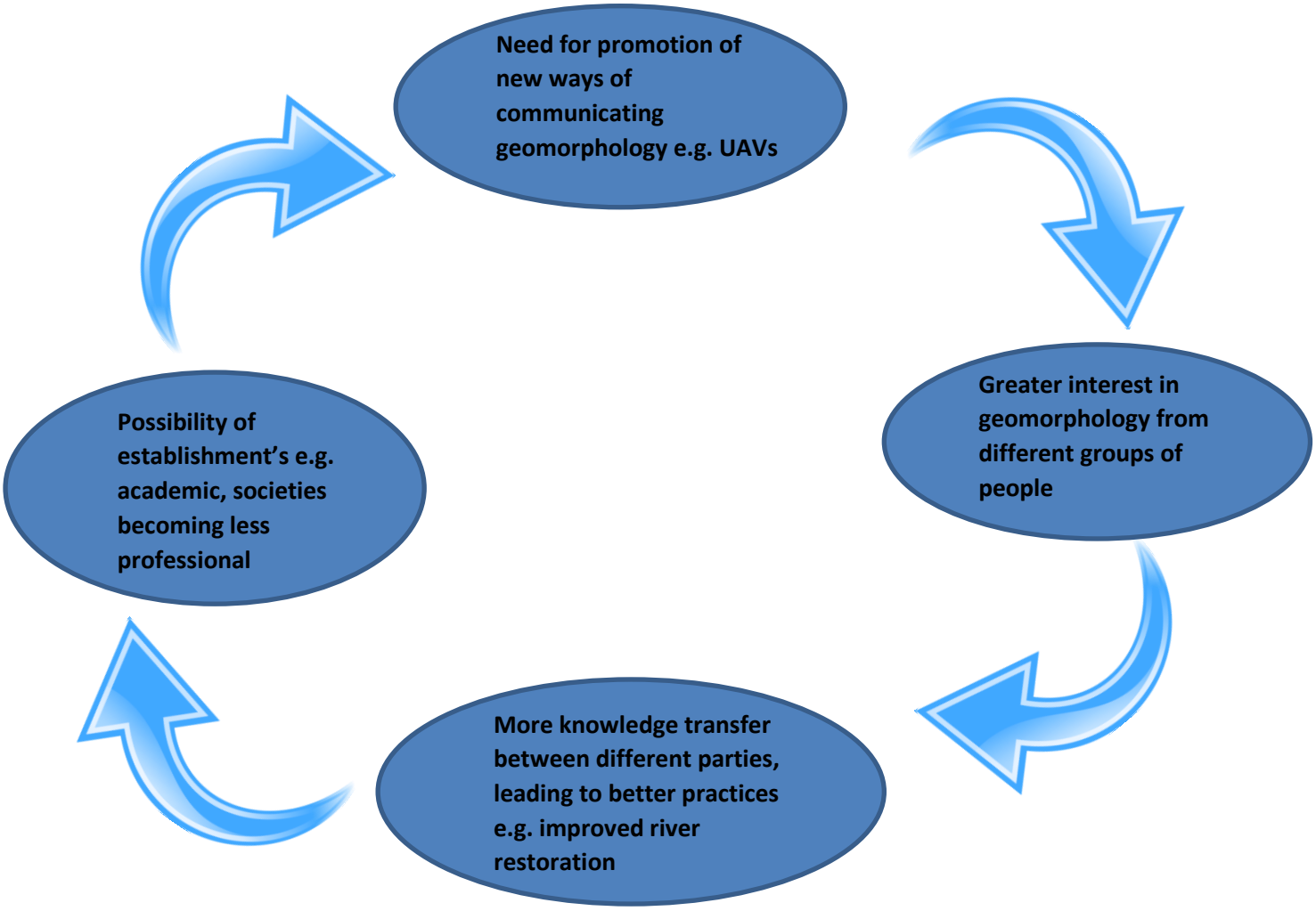

Figure 6.5: Showing how the promotion of new technologies can be seen as a cycle which allows a greater transfer of geomorphic knowledge within the wider geomorphic community.

6.8 Conclusion: Is SfM Technology The Way forward?

The use of UAVs and SfM has been discussed and the efficiency of the technology and technique will differ significantly depending on the environmental characteristics of the survey being carried out. It is important to appreciate that not one technique of topographical survey will fit the individual needs of every site, and different techniques and procedures will work better under differing scenarios (Bangen et al. 2015a). The applicability of SfM depends on the requirements of the job and thus it is difficult to evaluate all possible needs that the software may require.

Despite this, a "check list" can be produced which allows the technology to be evaluated under certain criteria (Table 6.5). The technology can produce high quality products that enable GIS related tasks to be carried out. Studies have suggested optimum spatial and temporal scales for the use of SfM technology. The growing importance of acquiring new information to improve river restoration for future generations and the geomorphic community as a whole provides a platform for SfM to develop, however improvements must be made if the technology is to become imbedded fully in future geomorphic change investigations (Smith and Vericat 2015). The growth of drivers such as WFD can be seen as other important factors which may provide the impetus for further development in this technology. Improvements to the limitations outlined in previous sections can only allow the techniques utilized to improve and provide a foundation upon which the science of geomorphology can be highlighted to a wider audience in the future (Gregory et al. 2014). The potential is vast and ensuring the technology is maximised to its best capabilities is crucial for future use and development.

Table 6.5: A summary of the UAV/SfM technology.

Variable	Criteria met for monitoring of River Restoration	Notes and discussion with relation to this study
Low cost	✓	UAVs are relatively low cost in comparison to TLS costs. An appreciation of what is low cost must be acknowledged.
Applicability – spatial and temporal	✓	More work needs to be completed to fully understand the appropriate spatial and temporal scales. SfM is applicable to a large variety of spatial and temporal scales and offers a unique methodology as it is very similar to the scales that can be used with TLS. For the purposes of monitoring Whit Beck, the technology used has delivered adequate results.
Applicability – different groups of people	✓	The applicability to a large number of people is key in promoting geomorphology and specifically river restoration. The technology is becoming more usable within society and the geomorphic and hydrological community must embrace this change.
Errors and reliability over different contexts	✓	Errors are of a low magnitude, and comparable with TLS outputs. Similar work stated similar error statistics (Woodget et al. 2014).
Ability to perform GIS tasks	✓	TLS (raster calculations), bathymetric, DoDs and hydraulic modelling were all carried out on the SfM outputs.
Easy to use	✓	No training is required (non-commercial), however computer demands may be an issue.
Limitations/ issues with data collection	✗	The technology does have a number of limitations that have yet to be fully addressed.
Can improvements be made?	✓	Improvements are the most important aspect in future use of this technology. Physical improvements to UAVs would allow a better spatial and temporal dynamic to be evaluated, while further studies in understanding error formation would be advantageous.

SfM errors from Whit Beck compare in magnitude to those stated in other similar studies, most notably Woodget et al. (2014). The TLS differences observed also correlate closely to SfM-TLS comparisons by Mancini et al. (2013) in coastal geomorphology and Westoby et al. (2012) in hillslope geomorphology. Understanding the pathways by which these differences occur and determining ways to improve SfM errors in relation to other topographical surveying methods is important for future growth of the technology (Piermattei et al. 2015). One of the major advantages of SfM is the low cost aspect of the technology when compared to other topographical methods, most notably TLS. Although TLS errors are lower on average, given the relative cost, many advantages in using SfM can be seen. Wider questions still need to be asked about the applicability of the technology, especially on small temporal scales (daily) and large spatial scales (tens of km's), however a similar spatial-temporal window of applicability to that of TLS can be seen. The importance of UAVs as a tool for communicating geomorphology to a wider audience of people cannot be underestimated and this provides the opportunity for a "new generation of geomorphologists" to be developed. More widely, understanding river restoration from a social perspective can aid our understanding of the physical format of many fluvial systems. A holistic approach which allows knowledge gain and transfer through novel technologies and techniques can only benefit future river restoration projects. The cycle of providing new knowledge through the testing of new methodologies is vital in the promotion of improved river restoration (Smith et al. 2014a).

Chapter 7: Conclusions and Future Perspectives

7.1 Summary of findings

The main aim of this study was to evaluate UAV and SfM technology in monitoring of post-restoration fluvial activity. A number of techniques were used which aimed to examine the effectiveness and applicability of SfM data, while explore the possible limitations of this methodology at the current time. It was found that a high image overlap and an increased number of targets is likely to have a positive influence in reducing error formation. The July 2015 data had the lowest combined errors suggesting this was the best set-up to promote highest quality products. TLS data compares adequately with differences of around 0.04 m, regardless of the number of flight lines used in the formation of DEMs. A refraction correction technique was also carried out and similar errors were reported to Woodget et al. (2014).

Further data processing methods have been applied to the data to assess how SfM products can be used for monitoring of post-restoration fluvial dynamics. A DoD was carried out between the October 2014 and July 2015 datasets to assess DEM change over the period under investigation. Patterns of erosion and deposition can be mapped and larger magnitude changes can be highlighted when differing MLDs are used. Issues with changing vegetation cover and shadow effects are highlighted. Hydraulic modelling of data also allowed geomorphic units to be inferred from modelled depth and velocity data. The modelling results show SfM data has the potential to be used in a modelling capacity when the correct input parameters are utilised.

The relative low cost of the technology compared to other geomatics techniques can be seen as a major advantage, especially when compared to TLS. The applicability of the technology to different geomorphic environments is also seen as positive, while a similar spatial and temporal window of applicability can be acknowledged. It is suggested that future work tries to broaden

this spatial and temporal window further in order to make the technology more applicable to differing needs.

The easy-to-use nature of the methodology discussed also provides another advantage over other techniques. No training or licence is required (i.e. if the use is non-commercial) and this makes the techniques discussed available to a larger group of people. Geomorphology as a whole needs to become more socially involved, as discussed by Gregory et al. (2014), and UAVs provide the platform in which new ideas about the discipline can be projected and incorporate many different groups of society. Limitations are apparent however, and will need to be addressed in future work. The influence of vegetation, glare and shadow on certain workflows have been discussed, while flight time and weather resistance are two major issues preventing the wider applicability of the technology. It is hoped that with further technological development, the use of UAVs can grow, while the precision and accuracy of products can also be improved.

The technology has an important role in knowledge transfer and can be used effectively to help manage and assess river restoration techniques. From a wider geomorphic perspective, the technology has many applications, as rates of geomorphic change can be mapped effectively. The importance of external drivers in promoting the use of the techniques presented cannot be underestimated, specifically in future contexts. Drivers such as the WFD (Water Framework Directive) are likely to ensure improvement in river restoration schemes is of key significance moving forward, suggesting new low cost approaches may be seen as the way forward. The result of the EU referendum may however provide some uncertainty.

7.2 Future Perspectives

A number of limitations have been identified when using the UAV and SfM workflows presented and improvements to the technology in the future are likely to increase the wider applicability of the techniques. Nine key areas that need to be addressed in the future are shown in Table 7.1, while timeframes for the implementation of the strategies have been suggested.

Table 7.1: Nine pathways to improve SfM use in the future.

Way to improve future use of SfM	**When should it be done by? (short, medium, long term) As a guide: Short term - <2 yrs. Medium term - 2 - 5 yrs. Long term - >5 yrs.**	**By who?**
Understand the parameters and influence of parameters e.g image overlap, shade cover	Short-medium	Academics, environmental consultancies
Identify the most important and deterministic parameters on DEM quality	Short-medium	Academics, environmental consultancies
Understand when SfM use is most favourable	Short-medium	Academics, environmental consultancies
Improve UAVs - flight time, weather resistance	Short-medium	Engineers, environmental consultancies
Improve computer software to aid image processing	Short-medium	Academics, engineers
Promote the technology to a wider audience of people, specifically in water management and monitoring field	Short-medium	Academics, environmental consultancies, governments
Determine most appropriate environmental contexts for uses and focus efforts and resources on them	Medium-long	Academics, environmental consultancies
Promote a culture of improved river restoration which incorporates all applicable pockets of society by using UAVs as a tool for knowledge transfer and gain	Long	Academics, engineers, environmental consultancies, governments
Use legislation such as WFD and CWA to provide impetus for new technology	Long	Academics, environmental consultancies, governments, engineers

First, further work is required to establish the importance of different variables such as GCPs image overlap and surface textures. The variable analysis presented here concluded that higher image overlaps provided a reduction in error values, while an increased number of targets was likely to have a positive impact on results. There is a multitude of different variables which have not been examined (e.g effects of slope, turbidity, glare, shadow, vegetation, light levels, calibration process in image processing) and further experimentation of variables is vital to promote best quality product formation. By understanding the mechanisms behind the results obtained, a better knowledge of data quality can be established. Data quality is likely to vary significantly depending on the scale under investigation and this must also be examined further (Smith and Vericat 2015). Determining the most important influences on DEM quality is equally important, and frameworks should be used to guide future workflows. It is important the academics and environmental consultancies share knowledge and work together to identify gaps in our understanding. SfM will not be applicable to all investigations and thus an understanding of when best to use a specific geomatics technique is beneficial. The creation of "best use" criteria could be an important step in determining which topographical techniques fit the different niches of geomorphic enquiries and environments.

Improvements to the UAVs are likely to increase potential usage. Table 7.2 shows some areas where UAVs could improve in the future. Flight restrictions limit the spatial extent to which data can be collected, while weather conditions confine flights to specific times, which may influence results and produce outputs which are favourable to specific environmental characteristics. Improvements to UAVs potentially could increase the practicality of flights; this would ensure larger spatial and temporal extents can be investigated.

Table 7.2: Some areas where UAVs could be improved in the future.

Battery life	Increasing the battery life is likely to allow a larger spatial extent to be covered.
Battery weight	Reducing the weight of the battery may improve flight times and weather resistance.
Weather resistance	Increasing the weather resistance is vital to improve applicability in wet and windy environments.
Weightload and stability	Reducing the weight of the quadcopter is likely to improve flight times.
Safety	Increasing the number of safety options on UAVs will promote the use of them within wider society. e.g fly-back, blade control.
Price	Although the cost in comparison to TLS is low, reductions in cost are likely to make the technology more affordable for a wider range of people.

Improvements to the computer programs which process the imagery would also be beneficial, although even at this current time, an improvement in the number of available programs is apparent. Programs which could process data quickly and efficiently are likely to promote the use of this technology. Dependent upon the amount and type of imagery, processing times currently are good (most DEMs could be created under a day if a batch process is requested), however improvements could still be made. A longer term aim is to promote a culture of improved river restoration through better use of UAV and SfM technology. This ideally should incorporate all stakeholders and use the technology as a tool to help transfer knowledge between differing groups of people. This will need adequate collaboration and funding in order to maximise potential benefits, while particular focus is required in order to ensure knowledge gained is translated to improved projects on the ground.

An "order of priority" should be formed which highlights the key geomorphological landscapes in which SfM has the largest opportunity to impact positively on. Further studies in all areas of geomorphology are integral if this knowledge is to be gained, while promoting the use of SfM to a wider audience of people also has to be a priority. The use of legislation such as the WFD in the EU can be seen as a catalyst in promoting the use of new technologies and allows

an opportunity for new partnerships and knowledge pathways to be formed, despite the uncertainty associated with the EU referendum.

This remains an unanswered question at the current time. The UK voted to leave the EU and questions remain as to how and when this process will be initiated. The future of EU funding is not clear and no clear distinct strategy has been put forward to show how river restoration will be manged if the UK leaves the EU. From a positive perspective, the UK would have more control over river restoration projects and their implementation and thus funding could be adequately managed. More funding and resources could be placed into the restoration community and a specific need for cross-disciplinary knowledge transfer from all stakeholders could be addressed. However, if the UK leaves the EU, other areas of the economy which receive more public attention and engagement may be prioritised for funding (e.g NHS, immigration). This may leave less money available for environmental concerns, specifically river restoration. To some extent, fluvial geomorphologists have a key role to play in ensuring river restoration remains an important issue within scientific communities and wider general audiences. Therefore, UAVs and other techniques which can be used by a range of different people have an increased importance in promoting the need for monitoring of rivers, and more widely other geomorphic landscapes to showcase the significance of geomorphology as a whole. The result of the EU referendum has cast doubt over the direction of river restoration in the UK. The importance of drivers such as the WFD may become less significant in the coming years and other catalysts may be required to provide further impetus in ensuring river restoration remains of importance outside the geomorphic community. Alongside, changing hydroclimates (Appendix I) and a growing need for monitoring, the EU referendum result remains one of the major uncertainties about how river management and monitoring in the UK moves forward.

In summary, the technology has enormous potential in offering high resolution accurate topographic datasets for low cost and over a spatial and temporal scale similar to that of TLS. This applicability will only grow in the future as improvements are made to UAVs and the computer programs which process the imagery. Furthermore, UAVs have an important role in communicating geomorphology to a wider audience of people and can help bring together different groups of people in order to promote best practice for river restoration projects and wider geomorphological proposals. This can help drive a culture of constant improvements in the design, implementation and monitoring of restoration schemes and this can only help propel the discipline further in the future. The EU referendum result may cause uncertainty about the influence of drivers such as the WFD in UK river restoration going forward and fresh impetus may be required in future years to ensure the discipline receives the attention it deserves from all corners of society. Fluvial geomorphologists have a critical role to play in promoting new methodologies which enable river restoration to remain a key focus in the years ahead.

Reference list

Andersen, J., Refsgaard, J.C., Jensen, K.H., (2001). Distributed hydrological modelling of the Senegal River Basin - model construction and validation. Journal of Hydrology. 247 (3), 200-214.

Arya, S., Mount, D.M., Netanyahu, N.S., Silverman, R. and Wu, A.Y., (1998). An optimal algorithm for approximate nearest neighbour searching fixed dimensions. Journal of the ACM *(JACM)*, *45*(6), 891-923.

Ashmore, P., (2015). Towards a sociogeomorphology of rivers. Geomorphology, 251, 149-156.

Avian, M., Kellerer-Pirklbauer, A., Bauer, A., (2009). LiDAR for monitoring mass movements in permafrost environments at the cirque Hinteres Langtal, Austria, between 2000 and 2008. Natural Hazards and Earth System Science. 9 (4),1087-1094.

Bangen, S.G., Wheaton, J.M., Bouwes, N., Bouwes, B., Jordan, C., (2014a). A methodological intercomparison of topographic survey techniques for characterizing wadeable streams and rivers. Geomorphology. 206,343-361.

Bangen, S., Wheaton, J., Bouwes, N., Jordan, C., Volk, C., Ward, M.B., (2014b). Crew variability in topographic surveys for monitoring wadeable streams: a case study from the Columbia River Basin. Earth Surface Processes and Landforms. 39 (15),2070-2086.

Barry, R. G.; Chorley R.J. (2009) Atmosphere, weather and climate. Routledge: New York.

Beechie, T.J., Sear, D.A., Olden, J. D., Pess, G.R., Buffington, J.M., Moir, H., Roni, P., Pollock, M.M., (2010). Process based principles for restoring river ecosystems. BioScience. 60 (3), 209-222.

Brasington, J., Langham, J., Rumsby, B., (2003). Methodological sensitivity of morphometric estimates of coarse fluvial sediment transport. Geomorphology. 53 (3), 299-316.

Brasington, J., Rumsby, B.T., McVey, R.A., (2000). Monitoring and modelling morphological change in a braided gravel-bed river using high resolution GPS-based survey. Earth Surface Processes and Landforms. 25 (9),973-990.

Brasington, J., Vericat, D., Rychkov, I., (2012). Modelling river bed morphology, roughness, and surface sedimentology using high resolution terrestrial laser scanning. Water Resources Research, 48 (11), 1-18.

Brown, M. and Lowe, D.G., (2007). Automatic panoramic image stitching using invariant features. International journal of computer vision, *74*(1), 59-73.

Brown, R.A., Pasternack, G.B., (2014). Hydrologic and topographic variability modulate channel change in mountain rivers. Journal of Hydrology. 510, 551-564.

Buchanan, B.P., Walte, M.T., Nagle, G.N., Schneider, R.L., (2010). Monitoring and assessment of a river restoration project in central New York. River Restoration and Applications, 27.

Cairns Jr, J., (1991). The need for integrated environmental systems management. Integrated environmental management, 5-20.

Caruso, B.S., (2006). Project river recovery: restoration of braided gravel-bed river habitat in New Zealand's high country. Environmental Management, 37 (6), 840-861.

Chin, A., Gregory, K.J., (2005). Managing urban river channel adjustments. Geomorphology, 69 (1), 28-45.

Clarke, L., Field, J. (2015) Geomorphological techniques. British Society for Geomorphology. London, UK. ISSN:2047-0371.

Dufour, S., Piégay, H., (2009). From the myth of a lost paradise to targeted river restoration: forget natural references and focus on human benefits. River research and applications, 25 (5), 568-581.

Eden, S., Tunstall, S.M., Tapsell, S.M., (2000). Translating nature: river restoration as nature-culture. Environment and Planning *D*, 18 (2), 257-274.

Emery, S.B., Perks, M.T., Bracken, L.J., (2013). Negotiating river restoration: The role of divergent reframing in environmental decision-making. Geoforum, 47, 167-177.

England, J., Skinner, K.S., Carter, M.G., (2008). Monitoring, river restoration and the Water Framework Directive. Water and Environment Journal, 22 (4), 227-234.

Fabris, M., Pesci, A., (2005). Automated DEM extraction in digital aerial photogrammetry: precisions and validation for mass movement monitoring. Annals of Geophysics. 48 (6), 973-988.

Fischler, M.A. and Bolles, R., RC (1987): Random sample consensus: a paradigm for model fitting with application to image analysis and automated cartography. Readings in computer vision: issues, problems, principles, and paradigms,726-740.

Flood Modeller (2016) Hydraulic modelling software for 1D and 2D uses. Data available from: https://www.floodmodeller.com/en-gb

Fonstad, M.A., Dietrich, J.T., Courville, B.C., Jensen, J.L., Carbonneau, P.E., (2013). Topographic structure from motion: a new development in photogrammetric measurement. Earth Surface Processes and Landforms. 38 (4), 421-430.
Fornaciai, A., Behncke, B., Favalli, M., Neri, M., Tarquini, S., Boschi, E., (2010). Detecting short-term evolution of Etnean scoria cones: a LIDAR-based approach. Bulletin of volcanology. 72 (10), 1209-1222.

Förstner, W., (1986). A feature based correspondence algorithm for image matching. International Archives of Photogrammetry and Remote Sensing, *26*(3), pp.150-166.

Frissell, C.A., Liss, W.J., Warren, C.E., Hurley, M.D., (1986). A hierarchical framework for stream habitat classification: viewing streams in a watershed context. Environmental management. 10 (2), 199-214.

Furukawa, Y., Curless, B., Seitz, S.M. and Szeliski, R., (2010), June. Towards internet-scale multi-view stereo. In Computer Vision and Pattern Recognition (CVPR), 2010 IEEE Conference *on* (1434-1441). IEEE.

Furukawa, Y. and Ponce, J., (2010). Accurate, dense, and robust multiview stereopsis. IEEE transactions on pattern analysis and machine intelligence, *32*(8),1362-1376.

Gilvear, D.J., Casas‐Mulet, R., Spray, C.J., (2012). Trends and issues in delivery of integrated catchment scale river restoration: lessons learned from a national river restoration survey within Scotland. River Research and Applications, 28 (2), 234-246.

Gómez-Gutiérrez, Á., de Sanjosé-Blasco, J.J., de Matías-Bejarano, J., Berenguer-Sempere, F., (2014). Comparing two photo-reconstruction methods to produce high density point clouds and DEMs in the corral del Veleta Rock Glacier (Sierra Nevada, Spain). Remote Sensing. 6 (6), 5407-5427.

Grabowski, R.C., Surian, N., Gurnell, A.M., (2014). Characterizing geomorphological change to support sustainable river restoration and management. Wiley Interdisciplinary Reviews: Water. 1 (5) 483-512.

Graf, W.L., (1996). 18 Geomorphology and Policy for Restoration of Impounded American Rivers: What is' Natural?'. In The Scientific Nature of Geomorphology*:* Proceedings of the 27th Binghamton Symposium in Geomorphology, Held 27-29 September, 1996 (Vol. 27, 443). John Wiley & Sons.

Gregory, K.J., Lane, S.N., Lewin, J., Ashworth, P.J., Downs, P.W., Kirby, M.J., 1Viles, H.A., (2014). Communicating geomorphology: global challenges for the twenty‐first century. Earth Surface Processes and Landforms, 39 (4), 476-486.

Hackney, C., Clayton, A., (2015) Unmanned Aerial Vehicles (UAVs) and their application in geomorphic mapping. Geomorphological techniques. British Society for Geomorphology. London, UK.

Harris, C. and Stephens, M., (1988), August. A combined corner and edge detector. In Alvey vision conference (Vol. 15, No. 50, 0-5244).

Heritage, G.L., Milan, D.J., Large, A.R. Fuller, I.C., (2009). Influence of survey strategy and interpolation model on DEM quality. Geomorphology, 112 (3), 334-344.

Hobbs P. R. N., Gibson A., Jones L., Pennington C., Jenkins G., Pearson S., Freeborough K. (2010). Monitoring coastal change using terrestrial LiDAR. Geological Society, London, Special Publications, 345.

Hugenholtz, C.H., Whitehead, K., Brown, O.W., Barchyn, T.E., Moorman, B.J., LeClair, A., Riddell, K., Hamilton, T., (2013). Geomorphological mapping with a small unmanned

aircraft system (SUAS): feature detection and accuracy assessment of a photogrammetrically-derived digital model. Geomorphology. 194, 16-24.

Jähnig, S.C., Lorenz, A.W., Hering, D., Antons, C., Sundermann, A., Jedicke, E. Haase, P., 2011. River restoration success: a question of perception. Ecological Applications, 21(6), 2007-2015.

James, M.R., Robson, S., (2014). Mitigating systematic error in topographic models derived from UAV and ground-based image networks. Earth Surface Processes and Landforms. 39 (10),1413-1420.

James, M.R., Robson, S. (2012) Straightforward reconstruction of 3D surfaces and topography with a camera: accuracy and geoscience application. Journal of Geophysical Research. 117 F03017

Javernick, L., Brasington, J., Caruso, B. (2014) Modelling the topography of shallow braided rivers using structure from motion photogrammetry. Geomorphology. 213 166-182.

Knighton, D., (1998). Fluvial forms and processes. London. Edward Arnold.

Lane, S.N., Westaway, R.M., Murray Hicks, D., (2003). Estimation of erosion and deposition volumes in a large, gravel-bed, braided river using synoptic remote sensing. Earth Surface Processes and Landforms. 28 (3),249-271.

Large, A., Mayes, W.M., Newson, M.D., Parkin, G., (2007). Using long-term monitoring of fen hydrology and vegetation to underpin wetland restoration strategies. Applied Vegetation Science, 10 (3), 417-428.

Lave, R., (2009). The controversy over Natural Channel Design: substantive explanations and potential avenues for resolution. Journal of the American Water Resources Association 45 (6), 1519–1532.

Lave, R., (2014). Freedom and constraint: Generative expectations in the US stream restoration field. Geoforum, 52, 236-244.

Lave, R., (2016). Stream restoration and the surprisingly social dynamics of science. Wiley Interdisciplinary Reviews: Water, 3 (1), 75-81.

Lave, R., Doyle, M., Robertson, M., (2010). Privatizing stream restoration in the U.S. Social Studies of Science. 40 (5), 677–703.

Leeks, G.J., Lewin, J.,Newson, M.D., (1988). Channel change, fluvial geomorphology and river engineering: The case of the Afon Trannon, Mid-Wales. Earth Surface Processes and Landforms, 13 (3), 207-223.

Lewin, J., Weir, M.J.C., (1977). Morphology and recent history of the Lower Spey. The Scottish Geographical Magazine, 93 (1), 45-51.

Lourakis, M.I. and Argyros, A.A., (2009). SBA: A software package for generic sparse bundle adjustment. ACM Transactions on Mathematical Software *(TOMS)*, *36*(1), 2.

Lowe, D.G., (2004). Distinctive image features from scale-invariant keypoints. International journal of computer vision, *60*(2), 91-110.

Lucas, B.D., Kanade, T., (1981), August. An iterative image registration technique with an application to stereo vision. In IJCA. Vol. 81 674-679.

Lucieer, A., de Jong, S., Turner, D., (2013). Mapping landslide displacements using Structure from Motion (SfM) and image correlation of multi-temporal UAV photography. Progress in Physical Geography. 105, 2354-2366.

Major J.J., Dzurisin D., Schilling S.P., Poland M.P., (2009). Monitoring lava-dome growth during the 2004-2008 Mount St. Helens, Washington, eruption using oblique terrestrial photography. Earth and Planetary Science Letters. 286,243-254.

Mancini, F., Dubbini, M., Gattelli, M., Stecchi, F., Fabbri, S., Gabbianelli, G., (2013). Using unmanned aerial vehicles (UAV) for high-resolution reconstruction of topography: the structure from motion approach on coastal environments. Remote Sensing, 5 (12), 6880-6898.

Marcus, W.A., Fonstad, M.A., (2010). Remote sensing of rivers: the emergence of a subdiscipline in the river sciences. Earth Surface Processes and Landforms. 35 (15),1867-1872.

McMillan, A.A., (2002). Onshore Quaternary geological surveys in the 21st century—a perspective from the British Geological Survey. Quaternary science reviews. 21 (8),889-899.

McMillan, H.K., Brasington, J., (2008). End-to-end flood risk assessment: A coupled model cascade with uncertainty estimation. Water Resources Research. 44 (3), 1-14.

Micheletti, N., Chandler, J., Lane, S. (2015) SfM Photogrammetry. Geomorphological techniques. British Society for Geomorphology. London, UK.

Milan, D.J., Heritage, G.L., Large, A.R., Fuller, I.C., (2011). Filtering spatial error from DEMs: Implications for morphological change estimation. Geomorphology, 125 (1), 160-171.

Morandi, B., Piégay, H., Lamouroux, N., Vaudor, L., (2014). How is success or failure in river restoration projects evaluated? Feedback from French restoration projects. Journal of environmental management, 137, 178-188.

Neal, R.A., Phillips, I.D., (2011). Winter daily precipitation variability over Cumbria, Northwest England. Theoretical and applied climatology, 106 (1-2), 245-262.

Newson, M., Large, A.R., (2006). 'Natural 'rivers, 'hydromorphological quality'and river restoration: a challenging new agenda for applied fluvial geomorphology. Earth Surface Processes and Landforms, 31 (13), 1606-1624.

Nield JM, Chiverrell RC, Darby SE, Leyland J, Vircavs LH, Jacobs B. (2012). Complex spatial feedbacks of tephra redistribution, ice melt and surface roughness modulate ablation on tephra covered glaciers. Earth Surface Processes and Landforms. 38 (1), 95-102.

O'neal MA, Pizzuto JE., (2011). The rates and spatial patterns of annual riverbank erosion revealed through terrestrial laser-scanner surveys of the South River, Virginia. Earth Surface Processes and Landforms. 36, 695-701.

Palmer, M., Allan, J.D., Meyer, J., Bernhardt, E.S., (2007). River restoration in the twenty-first century: data and experiential knowledge to inform future efforts. Restoration Ecology, 15 (3), 472-481.

Passalacqua, P., Belmont, P., Staley, D.M., Simley, J.D., Arrowsmith, J.R., Bode, C.A., Crosby, C., DeLong, S.B., Glenn, N.F., Kelly, S.A., Lague, D., (2015). Analyzing high resolution topography for advancing the understanding of mass and energy transfer through landscapes: A review. Earth-Science Reviews, 148, 174-193.

Pérez, M., Aguera, F., Carvajal, F., (2013). Low cost surveying using an unmanned aerial vehicle. International Archives of the Photogrammetry, Remote Sensing and Spatial Information Science. 40, 311-315.

Piégay, H., Gregory, K.J., Bondarev, V., Chin, A., Dahlstrom, N., Elosegi, A., Gregory, S.V., Joshi, V., Mutz, M., Rinaldi, M.,Wyzga, B., (2005). Public perception as a barrier to introducing wood in rivers for restoration purposes. Environmental Management, 36 (5), 665-674.

Piermattei, L., Carturan, L., Guarnieri, A., (2015). Use of terrestrial photogrammetry based on structure from motion for mass balance estimation of a small glacier in the Italian Alps. Earth Surface Processes and Landforms. 40 (13), 1791-1802.

Popov IV. (1962). Application of morphological analysis to the evaluation of the general channel deformations of the River Ob. Soviet Hydrology. 3 267-324.

Resop J., Hession W.,(2010). Terrestrial Laser Scanning for Monitoring Streambank Retreat: Comparison with Traditional Surveying Techniques. Journal of Hydraulic Engineering, 136,794-798.

Rinaldi, M., Piégay, H., Surian, N. (2011) Geomorphological Approaches for River Management and Restoration in Italian and French Rivers, in Stream Restoration in Dynamic Fluvial Systems (eds A. Simon, S. J. Bennett and J. M. Castro), American Geophysical Union, Washington, D. C. doi: 10.1029/2010GM000984

Rosnell, T., Honkavaara, E., (2012). Point cloud generation from aerial image data acquired by a quadcopter type micro unmanned aerial vehicle and a digital still camera. Sensors, 12 (1), 453-480.

Rychkov, I., Brasington, J., Vericat, D., (2012). Computational and methodological aspects of terrestrial surface analysis based on point clouds. Computers & Geosciences, 42, 64-70.

Schnabel, R., Wahl, R. and Klein, R., (2007), June. Efficient RANSAC for point-cloud shape detection. In Computer graphics forum (Vol. 26, No. 2, 214-226). Blackwell Publishing Ltd.

Seidl, R., Stauffacher, M., (2013). Evaluation of river restoration by local residents. Water Resources Research, 49 (10),7077-7087.

Smith, B., Clifford, N.J., Mant, J., (2014a). Analysis of UK river restoration using broad-scale data sets. Water and Environment Journal. 28 (4), 490-501.

Smith, B., Clifford, N.J., Mant, J., (2014b). The changing nature of river restoration. *Wiley* Interdisciplinary Reviews: Water. 1 (3), 249-261.

Smith, M. (2015) Data acquisition of elevation data: TLS. Geomorphological techniques. British Society for Geomorphology. London, UK.

Smith, M.W., Vericat, D., (2015). From experimental plots to experimental landscapes: topography, erosion and deposition in sub-humid badlands from Structure-from-Motion photogrammetry. Earth Surface Processes and Landforms. 40 (12),1656-1671.
Snavely, N., Seitz, S.M., Szeliski, R., (2006). Photo Tourism: exploring photo collections in 3D. ACM transactions on graphics. 25 (3), 835-846.

Snavely, N., Seitz, S.M., Szeliski, R., (2008). Modeling the world from internet photo collections. International Journal of Computer Vision. 80 (2),189-210.

Tadaki, M., Brierley, G., Cullum, C., (2014). River classification: theory, practice, politics. Wiley Interdisciplinary Reviews: Water, 1 (4), 349-367.

Tamminga, A., Hugenholtz, C., Eaton, B., Lapointe, M. (2014) Hyper spatial remote sensing of channel reach morphology and hydraulic fish habitat using an unmanned aerial vehicle (UAV): A first assessment in the context of river research and management. River Research and Applications. 31 (3), 371-391.

Tooth, S., Viles, H.A., Dickinson, A., Dixon, S.J., Falcini, A., Griffiths, H.M., Hawkins, H., Lloyd-Jones, J., Ruddock, J., Thorndycraft, V.R., Whalley, B., (2016). Visualizing geomorphology: improving communication of data and concepts through engagement with the arts. Earth Surface Processes and Landforms. DOI: 10.1002/esp.3990 – in publication

Van Der Wal D., Pye K., Neal A., (2002). Long-term morphological change in the Ribble Estuary, northwest England. Marine Geology. 189, 249-266.

Vericat, D., Brasington, J., Wheaton, J., Cowie, M., (2009). Accuracy assessment of aerial photographs acquired using lighter-than-air blimps: low-cost tools for mapping river corridors. River Research and Applications. 25 (8), 985-1000.

Vericat, D., Smith, M.W., Brasington, J., (2014). Patterns of topographic change in sub-humid badlands determined by high resolution multi-temporal topographic surveys. Catena, 120,164-176.

Viles, H., (2016). Technology and geomorphology: Are improvements in data collection techniques transforming geomorphic science? Geomorphology, 270, 121-133.

Westoby, M.J., Brasington, J., Glasser, N.F., Hambrey, M.J., Reynolds, J.M., (2012). 'Structure-from-Motion' photogrammetry: A low-cost, effective tool for geoscience applications. Geomorphology. 179, 300-314.

Wheaton, J.M., Brasington, J., Darby, S.E., Sear, D.A., (2010). Accounting for uncertainty in DEMs from repeat topographic surveys: improved sediment budgets. Earth Surface Processes and Landforms. 35 (2), 136-156.

Wheaton, J.M., Fryirs, K.A., Brierley, G., Bangen, S.G., Bouwes, N., O'Brien, G., (2015). Geomorphic mapping and taxonomy of fluvial landforms. Geomorphology. 248, 273-295.

Wilcock, P.R., (2012). Stream Restoration in Gravel-Bed Rivers. Gravel-Bed Rivers: Processes, Tools, Environments, 135-149.

Williams, R.D., (2012). DEMs of difference. Geomorphological Techniques (Online Edition), edited by LE Clarke, British Society for Geomorphology.

Williams, R.D., Brasington, J., Hicks, M., Measures, R., Rennie, C.D., Vericat, D., (2013). Hydraulic validation of two-dimensional simulations of braided river flow with spatially continuous aDcp data. Water Resources Research. 49 (9), 5183-5205.

Williams, R.D., Brasington, J., Vericat, D., Hicks, D.M., (2014). Hyperscale terrain modelling of braided rivers: fusing mobile terrestrial laser scanning and optical bathymetric mapping. Earth Surface Processes and Landforms. 39 (2), 167-183.

Williams, R.D., Rennie, C.D., Brasington, J., Hicks, D.M., Vericat, D., (2015). Linking the spatial distribution of bed load transport to morphological change during high-flow events in a shallow braided river. Journal of Geophysical Research: Earth Surface. 120 (3), 604-622.

Wohl, E., Lane, S.N., Wilcox, A.C., (2015). The science and practice of river restoration. Water Resources Research, 51(8), 5974-5997.

Woodget, A.S., Carbonneau, P.E., Visser, F., Maddock, I.P., (2014). Quantifying submerged fluvial topography using hyperspatial resolution UAS imagery and structure from motion photogrammetry. Earth Surface Processes and Landforms. 40 (1), 47-64.

Woolsey, S., Capelli, F., Gonser, T.O.M., Hoehn, E., Hostmann, M., Junker, B., Paetzold, A., Roulier, C., Schweizer, S., Tiegs, S.D., Tockner, K., (2007). A strategy to assess river restoration success. Freshwater Biology. 52 (4), 752-769.

Wyrick, J.R., Senter, A.E., Pasternack, G.B., (2014). Revealing the natural complexity of fluvial morphology through 2D hydrodynamic delineation of river landforms. Geomorphology. 210,14-22.

Data Download References

Airscapes Imagery (2016) Data available from: http://www.airscapes.co.uk

British Geological Survey (2016) Data available from http://www.bgs.ac.uk/data/home.html?src=topNav

Civil Aviation Authority (2016) Data available from http://dronesafe.uk/wp-content/uploads/2016/11/Dronecode.pdf

Derwent Catchment Flood Management Plan (2009) Data available from: https://www.gov.uk/government/uploads/system/uploads/attachment_data/file/289419/Derwent_Catchment_Flood_Management_Plan.pdf

DigiMap (2016) Data available from: http://digimap.edina.ac.uk

Environment Agency (2013) River Cocker at Low Lorton and Whit Beck at High Lorton – modelling report (contact EA).

Environment Agency (2016) Data download available from: https://data.gov.uk/publisher/environment-agency

Geomorphic Change Detection (2016) by Joe Wheaton, Data available from: http://gcd.joewheaton.org/

GoogleEarth (2016) Data available from: https://www.google.com/earth/

Land use map (2007) by the Centre for Ecology and Hydrology (2007), Data available from: http://www.ceh.ac.uk/services/land-cover-map-2007

Metoffice (2016), Data available from: http://www.metoffice.gov.uk

Natural England (2016) Data available from: http://www.gis.naturalengland.org.uk/pubs/gis/GIS_register.asp

OneGeology (2016) Data available from: http://www.onegeology.org

Photoscan (2016) Data available from: http://www.agisoft.com/forum/index.php?topic=89.0

South Cumbria Rivers Trust (2016) Data available from: http://www.theriverstrust.org/riverstrusts/south_cumbria.html

Spider financial (2016) Data Available from: http://www.spiderfinancial.com/support/documentation/numxl/reference-manual/descriptive-stats/mae

StatisticsHowTo (2016) Data available from: http://www.statisticshowto.com/rmse/

West Cumbria Rivers Trust (2016) Data available from: http://westcumbriariverstrust.org/projects

World Weather Online (2016) Data available from: http://www.worldweatheronline.com

Whit Beck News Articles

Whit Beck pre-restoration, BBC (2014)
http://www.bbc.co.uk/news/uk-england-cumbria-28890122
Whit Beck, ITV (2016)
http://www.itv.com/news/border/update/2015-07-20/west-cumbrian-river-flows-for-the-first-time-in-decades/

Appendix I: Comparing Rainfall in The Two Catchments - Changing Hydroclimates?

This brief summary of rainfall in Cumbria in 2015 is included to show the importance of monitoring, specifically in relation to a changing climate. The diverse topography, geology and land use within the two locations presents a range of complex variables which in turn may induce and promote a diverse range of geomorphology and fish habitat (and population). Rainfall is a significant factor which will influence the hydrological characteristics of both restoration schemes. It plays a deterministic role in many of the processes governing the hydrological characteristics within channels and on floodplains, so to expand on the information already presented, a brief comparison of rainfall dynamics is presented.

All catchments within Cumbria for the last year (2015) have experienced exceptionally high rainfall levels as characterised by data from the Environment Agency (2016) and the Met Office (2016). More rainfall (as a percentage) has been recorded in the Eden catchment over the last 12 months than in the Derwent catchment. This goes against the mean annual rainfall values for Furness Abbey and Skirwith presented in earlier sections. Rainfall in the Eden catchment was 147% as a percentage of expected values for 2015, while the Derwent catchment had a rainfall percentage of 139% above expected values. This pattern can be observed when the rainfall totals for the last 6 months, 3 months and December 2015 are examined. Figure 1 highlights the key rainfall values for all Cumbrian catchments; however, our focus here is on the Derwent and Eden. December 2015 was an exceptionally wet month for both catchments, with both having precipitation values 300% above expected values.

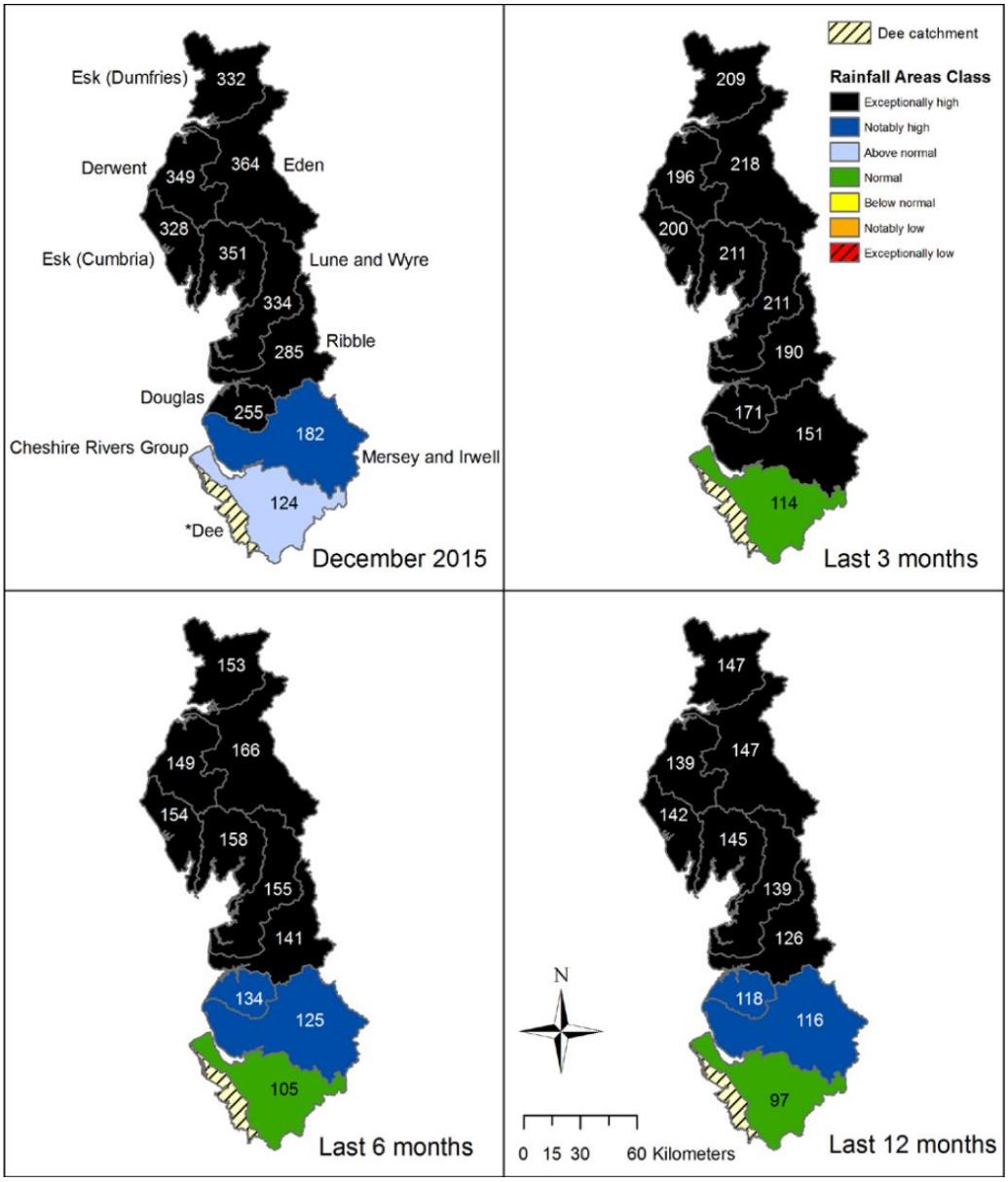

Figure 1: Rainfall data for all Cumbrian catchments. Values are percentages of expected values. A 100% value would mean the observed value matched the expected value. Data sourced from the Environment Agency (2016) and the Met Office (2016). Data is for the year 2015, e.g last 6 months relate to the months of July 2015 – December 2015.

When rainfall values per month in 2015 are examined, the magnitude of the values reached becomes highlighted (Figure 2). In 2015, the Derwent catchment experienced 7 months where rainfall was above the expected value and 5 months where it was below. December 2015 had the highest positive difference with a value of 349%, while other positive months included January, February, March, May, July and November. The largest negative difference from

expected values was seen in September 2015 with a value of 38%. The Eden shows a remarkably similar pattern. Seven months can be characterised as being above expected values and December is again the wettest month with a value of 364%. Other particularly high value months include November and May. Five months have rainfall lower than expected, with September having the largest negative difference.

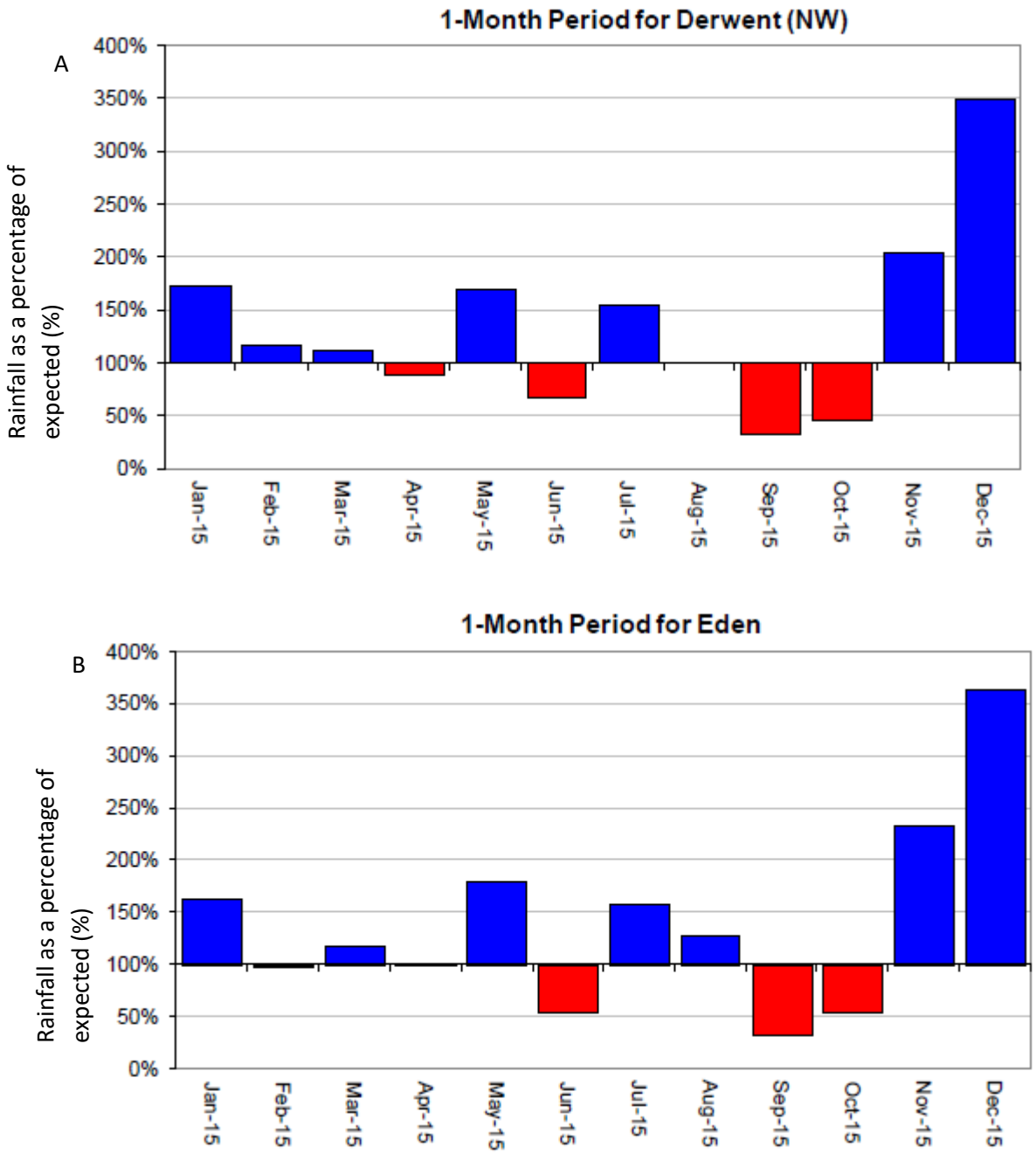

Figure 2: Rainfall totals per month as a percentage of expected values. A. Derwent B. Eden. Data sourced from the Environment Agency (2016) and the Met Office (2016).

Appendix I

Rainfall and river flow are evidently very closely linked hydrological components within a catchment, thus river flow is likely to fluctuate similarly when rainfall variability is examined. This is despite the vast range of variables interacting within hydrological mechanisms in a catchment. River flow in both the Derwent and Eden catchments generally match expected values if the months of November and December are ignored (Figure 3).

For the Derwent, flow was characterised as normal in March, April, June, July and August. River flow for October 2015 was exceptionally low and matches the low rainfall totals observed for the month (Figure 3). River flow increases dramatically in November 2015 with values starting at exceptionally low and then increasing sharply to a flow of above 90 m^3/s for December 2015. The lower boundary for a notably high flow on the Derwent in November is 40 m^3/s and this emphasises the magnitude of the river flow discussed. A very similar pattern can be observed for the Eden. River flow was classified as normal for all months between March and October except for May and August. Notably high flows of 60 m^3/s can be observed in May, while values higher than 49 m^3/s are seen in August. October, as seen on the Derwent had low river flows which were followed by extremely high flows in both November and December. Flow in December peaked at 325 m^3/s, with the higher boundary of a notably high flow being 150 m^3/s.

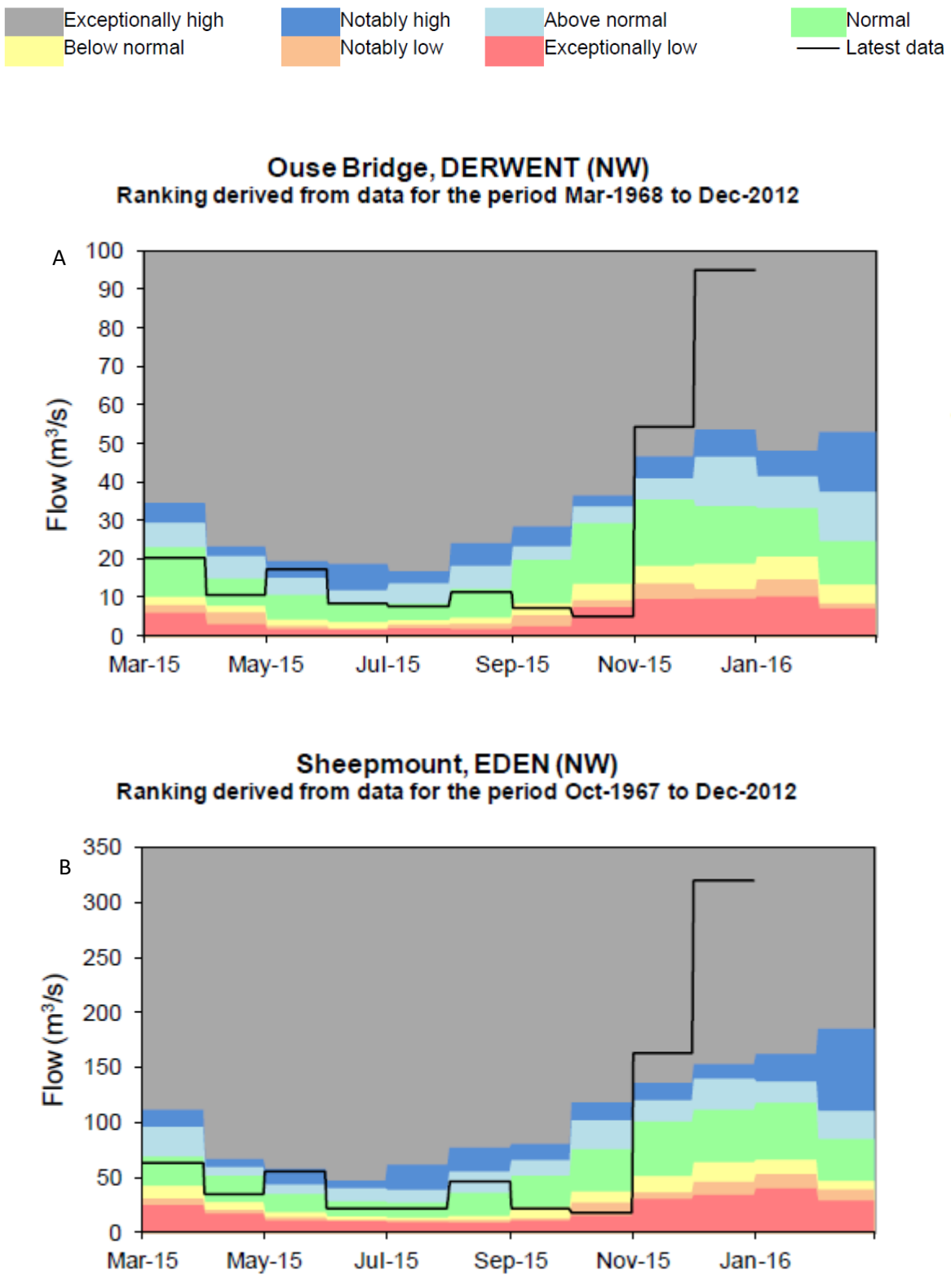

Figure 3: River flow for A. Derwent and B. Eden for months in 2015. Data sourced from the Environment Agency (2016) and the Met Office (2016).

Appendix I

The values presented give an overview of rainfall and river flow within both catchments in 2015. It is important to acknowledge that 2015 in the north west of England was a very wet year with very high rainfall and river flow values across many catchments. The purpose of this brief summary was to give an indication of how two important hydrological variables differed within the two respective catchments. The values presented may support the notion that future hydroclimates may be more wet, suggesting proportional increases in precipitation and river discharge may be possible. The monitoring of rivers (through the techniques and methodology outlined) will become more important as flood risk increases due to "more sustained wetter periods" which will become increasingly unpredictable. Fluvial geomorphologists have an important part to play in examining past, present and future hydrological data in order to promote best practice solutions which promote "healthy" river systems and aid our understanding of the complexity of river dynamics.

Appendix II: Error Values and Statistics

Table 1: Rounded Ground Control Point errors with no validation for image overlap experiments (Figure 4.3).

Model		Approximate Image Overlap (%)											
	Error (m)	60			70			80			90		
	M1	X	Y	Z	X	Y	Z	X	Y	Z	X	Y	Z
		0.076	0.096	0.024	-0.008	-0.003	0.037	0.001	-0.013	-0.009	0.006	-0.002	-0.003
	M2	X	Y	Z	X	Y	Z	X	Y	Z	X	Y	Z
		0.001	0.011	0.026	0.001	-0.002	-0.054	0.007	-0.015	0.008	0.029	-0.001	-0.004
	M3	X	Y	Z	X	Y	Z	X	Y	Z	X	Y	Z
		0.004	-0.023	-0.009	0.007	-0.017	0.001	0.006	-0.018	-0.008	-0.003	-0.021	-0.003

Appendix II

Table 2: Rounded MAE for image overlap experiments (Figure 4.4).

Model		Approximate Image Overlap (%)			
	MAE (m)	60	70	80	90
	M1	0.011	0.073	0.005	0.003
	M2	0.071	0.036	0.007	0.002
	M3	0.006	0.004	0.003	0.006

Table 3: Rounded RMSE for image overlap experiments (Figure 4.4).

Model		Approximate Image Overlap (%)			
	RMSE (m)	60	70	80	90
	M1	0.118	0.092	0.015	0.015
	M2	0.451	0.230	0.003	0.081
	M3	0.107	0.007	0.074	0.098

Table 4: Rounded STDEV error for image overlap experiments (Figure 4.4).

Model		Approximate Image Overlap (%)			
	STDEV error	60	70	80	90
	M1	0.104	0.275	0.077	0.055
	M2	0.325	0.190	0.085	0.043
	M3	0.080	0.062	0.065	0.081

Table 5: Rounded Ground Control Point Errors for Target experiments (Figure 4.5).

Number of GCPs	Mean error (m)		
	X	Y	Z
6	0.0349	0.0196	-0.1590
9	0.0372	-0.0306	-0.0269
12	0.0356	-0.0220	-0.0061
15	0.0276	0.01850	-0.0076
18	0.0237	-0.0186	-0.0059
21	0.0217	-0.0136	-0.0074
24	0.0179	-0.0251	-0.0059
27	0.0119	-0.0166	-0.0094
30	0.0077	-0.0194	-0.0159
33	0.0054	-0.0188	-0.0144

Table 6: Rounded MAE, RMSE and STDEV for Target experiments (Figure 4.6). 10 error validation targets were used for each statistic, number of GCP's relate to the targets used in model formation.

Number of GCP's	MAE (m)	RMSE (m)	STDEV error
6	0.0386	-0.200	0.205
9	0.0082	-0.043	0.095
12	0.0056	0.0186	0.078
15	0.0047	0.0037	0.071
18	0.0042	0.0092	0.068
21	0.0036	0.0021	0.061
24	0.0054	-0.040	0.075
27	0.0038	0.0462	0.063
30	0.0044	-0.096	0.067
33	0.0038	0.099	0.065

Table 7: Error values using Ground Control Points for the three UAV surveys.

	Mean error (m)		
	X	Y	Z
October 2014	-0.00350	-0.02120	-0.00310
March 2015	0.01170	0.01590	0.01270
July 2015	-0.00312	-0.00364	-0.00572

Appendix III: DoD elevation charts

(match DoD figures) - Figures 5.11- 5.14

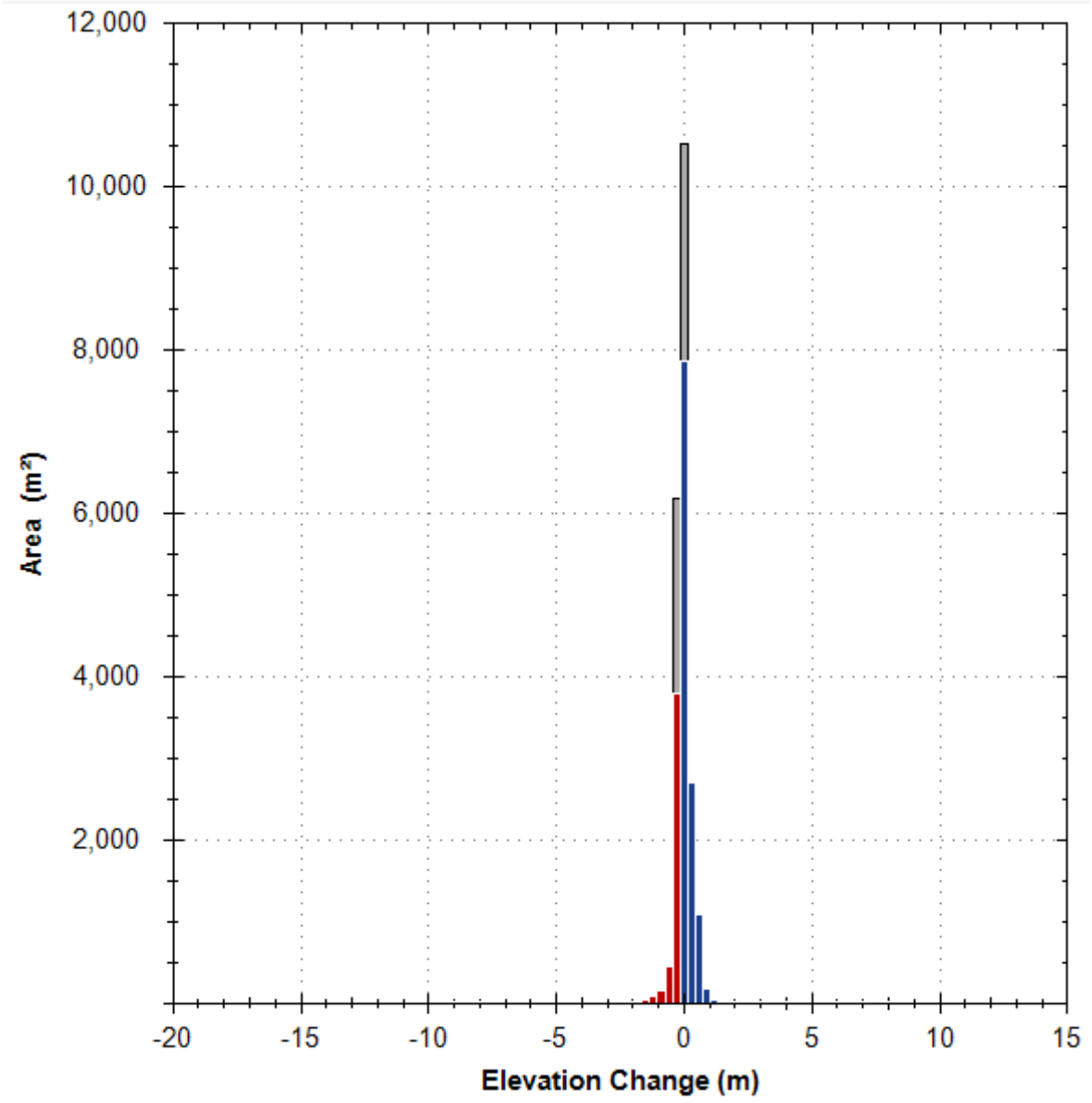

Figure 1: Elevation chart for 0.05 m MLD DoD (October 2014 – July 2015). Blue bars indicate a positive change (deposition), while red bars indicate a negative change (erosion). The grey bars indicate change which is below the MLD investigated and thus is excluded from this DoD.

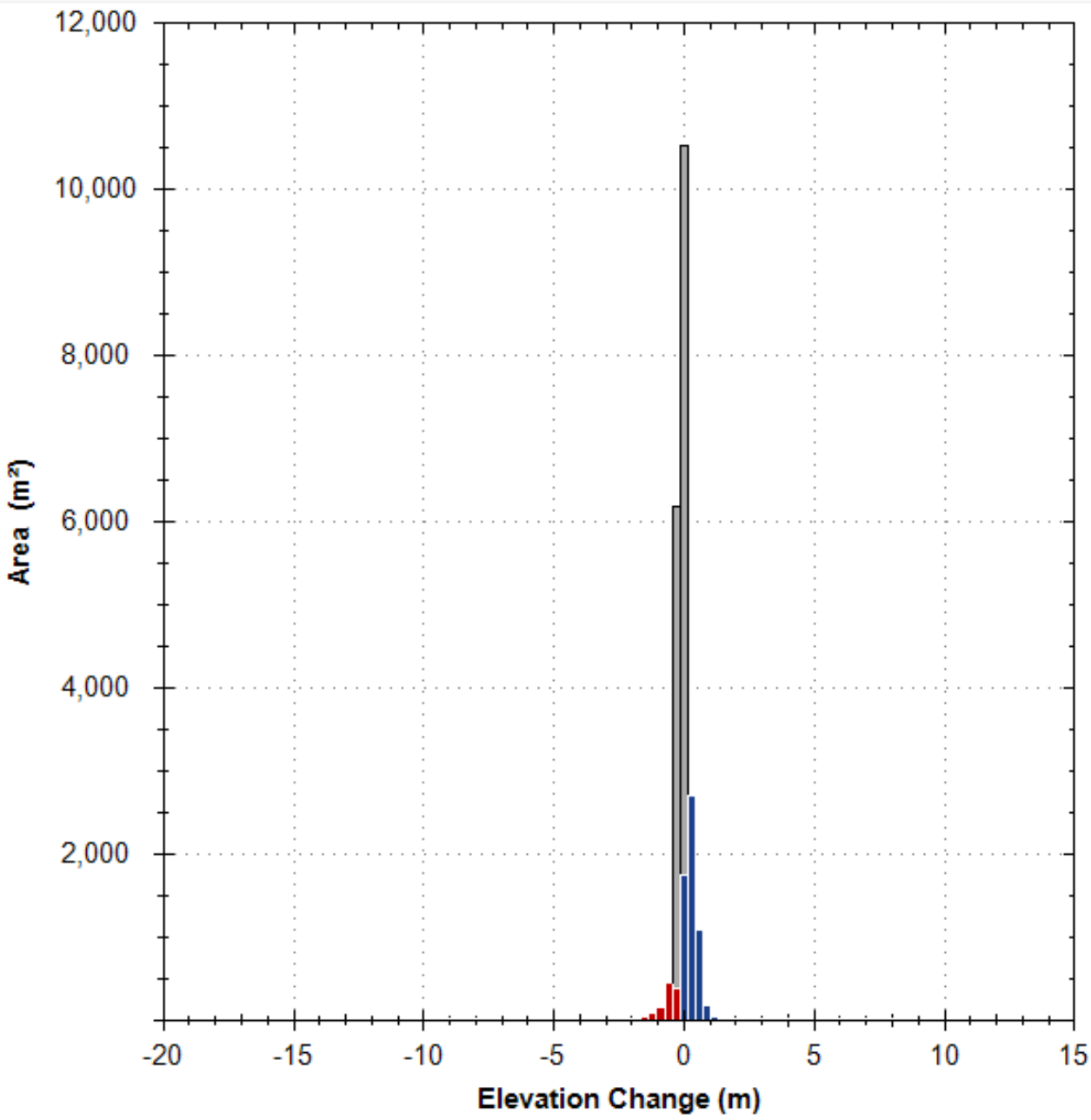

Figure 2: Elevation chart for 0.20 m MLD DoD (October 2014 – July 2015). Blue bars indicate a positive change (deposition), while red bars indicate a negative change (erosion). The grey bars indicate change which is below the MLD investigated and thus is excluded from this DoD.

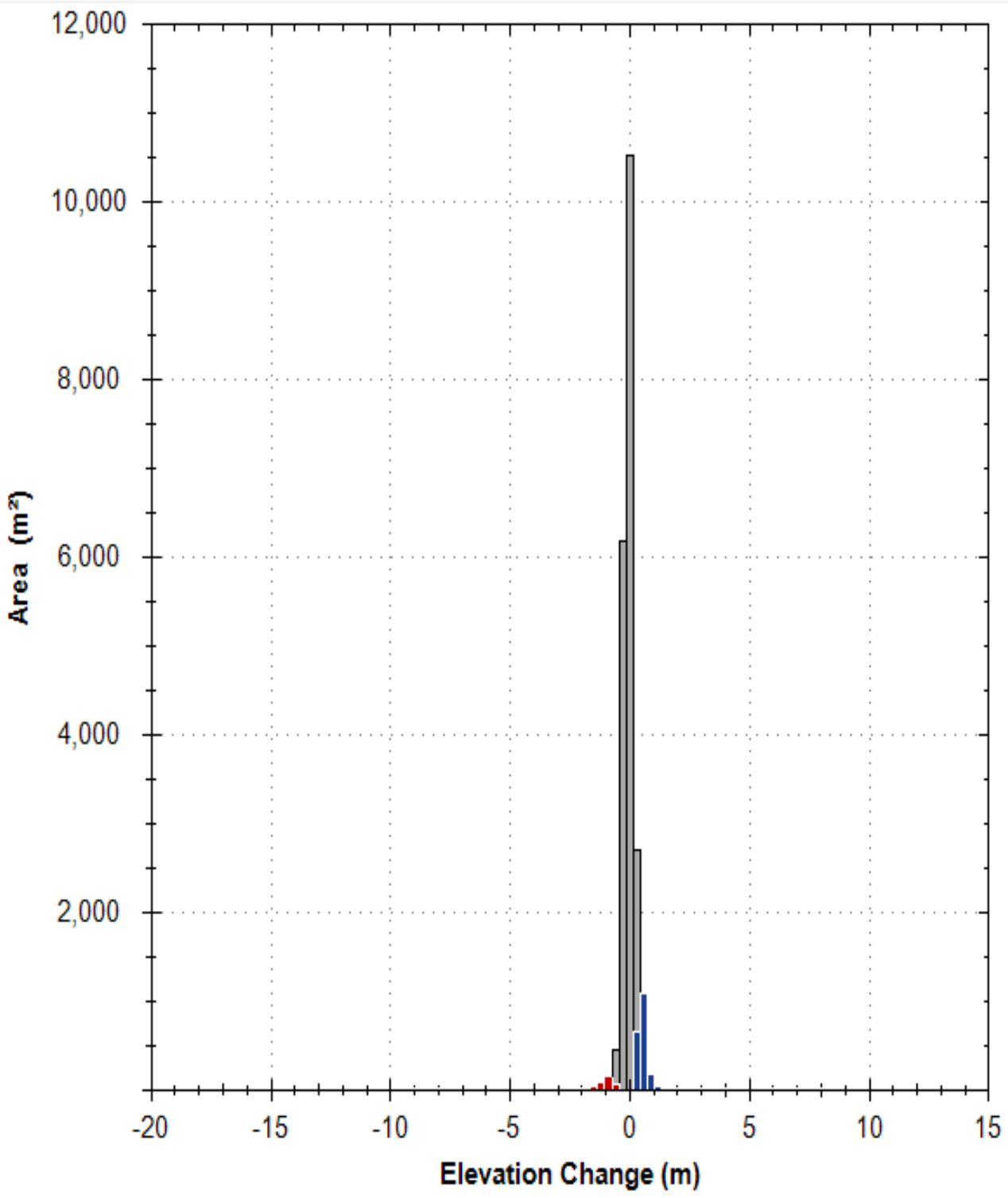

Figure 3: Elevation chart for 0.50 m MLD DoD (October 2014 – July 2015). Blue bars indicate a positive change (deposition), while red bars indicate a negative change (erosion). The grey bars indicate change which is below the MLD investigated and thus is excluded from this DoD.

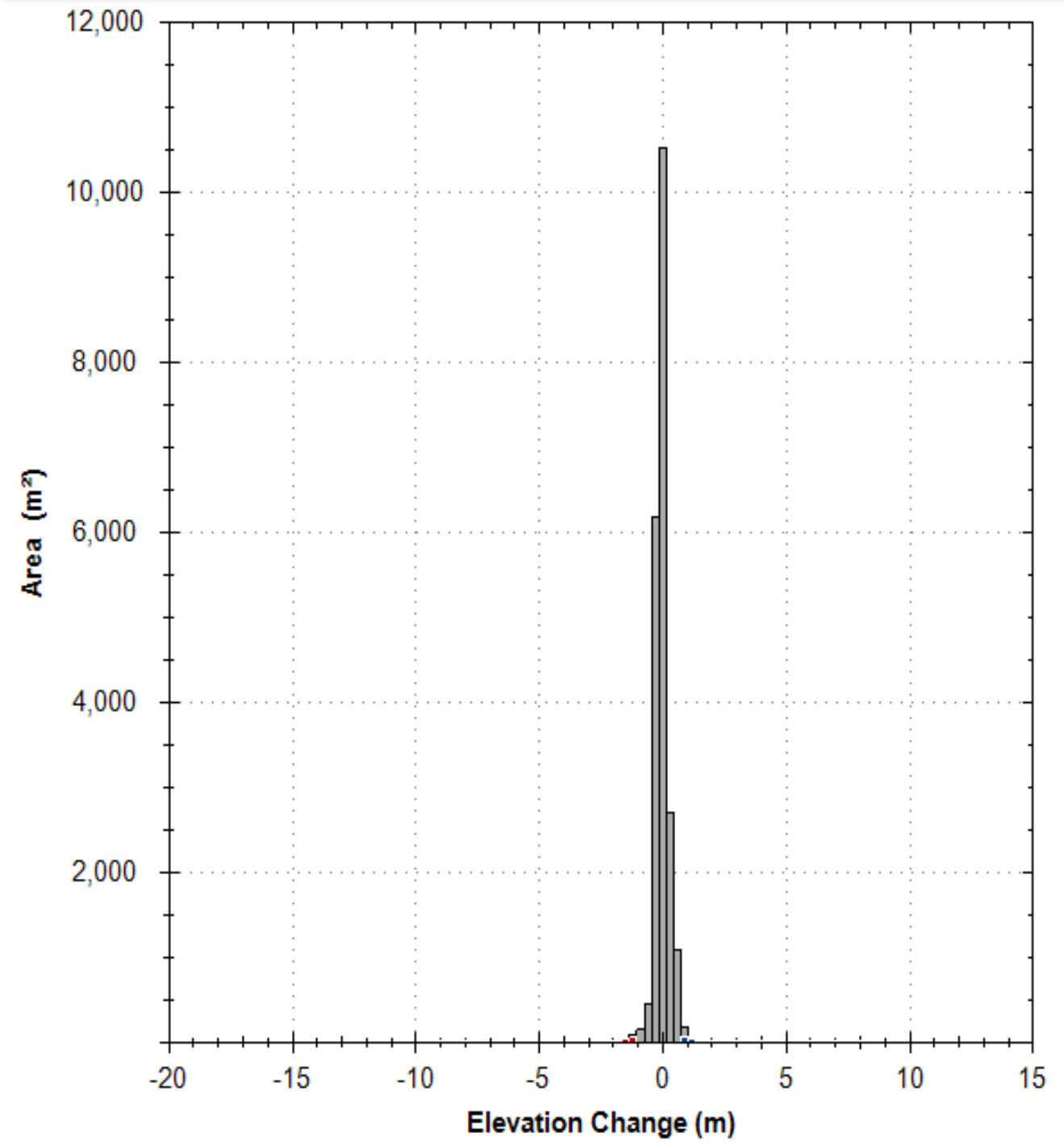

Figure 4: Elevation chart for 0.10 m MLD DoD (October 2014 – July 2015). Blue bars indicate a positive change (deposition), while red bars indicate a negative change (erosion). The grey bars indicate change which is below the MLD investigated and thus is excluded from this DoD.